SANDIA REPORT

SAND2012-10416
Unlimited Release
Printed December 2012

Renewable Source Controls for Grid Stability

Raymond H. Byrne, Ryan T. Elliott, Jason C. Neely, César A. Silva-Monroy, David A. Schoenwald, and Lisa L. Grant

Prepared by
Sandia National Laboratories
Albuquerque, New Mexico 87185 and Livermore, California 94550

Sandia National Laboratories is a multi-program laboratory managed and operated by Sandia Corporation, a wholly owned subsidiary of Lockheed Martin Corporation, for the U.S. Department of Energy's National Nuclear Security Administration under contract DE-AC04-94AL85000.

Approved for public release; further dissemination unlimited.

Sandia National Laboratories

Issued by Sandia National Laboratories, operated for the United States Department of Energy by Sandia Corporation.

NOTICE: This report was prepared as an account of work sponsored by an agency of the United States Government. Neither the United States Government, nor any agency thereof, nor any of their employees, nor any of their contractors, subcontractors, or their employees, make any warranty, express or implied, or assume any legal liability or responsibility for the accuracy, completeness, or usefulness of any information, apparatus, product, or process disclosed, or represent that its use would not infringe privately owned rights. Reference herein to any specific commercial product, process, or service by trade name, trademark, manufacturer, or otherwise, does not necessarily constitute or imply its endorsement, recommendation, or favoring by the United States Government, any agency thereof, or any of their contractors or subcontractors. The views and opinions expressed herein do not necessarily state or reflect those of the United States Government, any agency thereof, or any of their contractors.

Printed in the United States of America. This report has been reproduced directly from the best available copy.

Available to DOE and DOE contractors from
U.S. Department of Energy
Office of Scientific and Technical Information
P.O. Box 62
Oak Ridge, TN 37831

Telephone: (865) 576-8401
Facsimile: (865) 576-5728
E-Mail: reports@adonis.osti.gov
Online ordering: http://www.osti.gov/bridge

Available to the public from
U.S. Department of Commerce
National Technical Information Service
5285 Port Royal Rd
Springfield, VA 22161

Telephone: (800) 553-6847
Facsimile: (703) 605-6900
E-Mail: orders@ntis.fedworld.gov
Online ordering: http://www.ntis.gov/help/ordermethods.asp?loc=7-4-0#online

SAND2012-10416
Unlimited Release
Printed December 2012

Renewable Source Controls for Grid Stability

Raymond H. Byrne, Ryan T. Elliott, Jason C. Neely,
César A. Silva-Monroy, David A. Schoenwald and Lisa L. Grant
Sandia National Laboratories
Energy Storage and Transmission Analysis Department
MS 1140, P.O. Box 5800
Albuquerque, NM 87185-1140
email: rhbyrne@sandia.gov

Abstract

The goal of this study was to evaluate the small signal and transient stability of the Western Electricity Coordinating Council (WECC) under high penetrations of renewable energy, and to identify control technologies that would improve the system performance. The WECC is the regional entity responsible for coordinating and promoting bulk electric system reliability in the Western Interconnection. Transient stability is the ability of the power system to maintain synchronism after a large disturbance while small signal stability is the ability of the power system to maintain synchronism after a small disturbance. Transient stability analysis usually focuses on the relative rotor angle between synchronous machines compared to some stability margin. For this study we employed generator speed relative to system speed as a metric for assessing transient stability. In addition, we evaluated the system transient response using the system frequency nadir, which provides an assessment of the adequacy of the primary frequency control reserves. Small signal stability analysis typically identifies the eigenvalues or modes of the system in response to a disturbance. For this study we developed mode shape maps for the different scenarios. Prony analysis was applied to generator speed after a 1.4 GW, 0.5 second, brake insertion at various locations. Six different WECC base cases were analyzed, including the 2022 light spring case which meets the renewable portfolio standards. Because of the difficulty in identifying the cause and effect relationship in large power system models with different scenarios, several simulations were run on a 7-bus, 5-generator system to isolate the effects of different configurations. Based on the results of the study, for a large power system like the WECC, incorporating frequency droop into wind/solar systems provides a larger benefit to system transient response than replacing the lost inertia with synthetic inertia. From a small signal stability perspective, the increase in renewable penetration results in subtle changes to the system modes. In general, mode frequencies increase slightly, and mode shapes remain similar. The system frequency nadir for the 2022 light spring case was slightly lower than the other cases, largely because of the reduced system inertia. However, the nadir is still well above the minimum load shedding frequency of 59.5 Hz. Finally, several discrepancies were identified between actual and reported wind penetration, and additional work on wind/solar modeling is required to increase the fidelity of the WECC models.

keywords: transient stability, small signal stability, renewable energy, power system stability.

Acknowledgment

This research was sponsored by the U.S. Department of Energy, Office of Electricity Delivery and Energy Reliability. The authors would like to thank Gil Bindewald for his oversight of this effort. Dr. Dan Trudnowski and Dr. Matt Donnelly provided invaluable feedback throughout the project. Dr. Trudnowski shared MATLAB® Prony code that was adapted to generate the Prony results presented in this study. Abraham Ellis provided advice on industry practices throughout the length of the project and kept the project team up to date on the activities of the WECC Renewable Energy Modeling Task Force, which he chairs.

© 2012 The MathWorks, Inc. MATLAB® and Simulink® are registered trademarks of The MathWorks, Inc. See www.mathworks.com/trademarks for a list of additional trademarks. Other product or brand names may be trademarks or registered trademarks of their respective holders.

Sandia National Laboratories is a multi-program laboratory managed and operated by Sandia Corporation, a wholly owned subsidiary of Lockheed Martin Corporation, for the U.S. Department of Energy's National Nuclear Security Administration under contract DE-AC04-94AL85000.

Contents

Abstract 3

Acknowledgement 4

Table of Contents 5

List of Figures 7

List of Tables 9

Nomenclature 13

1 Introduction 15
- 1.1 Review of Control Approaches for Wind and Solar . . . 17
- 1.2 Report Organization . . . 19

2 Methodology 19
- 2.1 WECC Scenarios . . . 19
- 2.2 Metrics . . . 20
  - 2.2.1 Frequency Nadir . . . 20
  - 2.2.2 Generator Speed . . . 20
  - 2.2.3 Prony Analysis . . . 20

3 Transient Response: 7-Bus, 5-Generator System 24
- 3.1 Sensitivity to Generation Type . . . 25
- 3.2 Sensitivity to System Inertia . . . 27
- 3.3 Sensitivity to Generation Headroom . . . 29
- 3.4 Sensitivity to Wind Generation . . . 30

4 Transient Response: WECC 36
- 4.1 Comparison of 2022 and 2012 Cases . . . 36
- 4.2 High Renewables Penetration, 2022 Light Spring Case . . . 37
- 4.3 Generator Speeds . . . 38

5 Small Signal Stability: 6-Bus, 4-Generator System 42
- 5.1 Wind Generation Effects on Inter-area Mode . . . 43
- 5.2 Effect of Wind Controls on Inter-area Mode . . . 44

6 Small Signal Stability: WECC 47
- 6.1 Modes of Oscillation Excited by a Chief Joseph Brake Insertion . . . 48
  - 6.1.1 0.23 to 0.29 Hz, North-South Mode . . . 49
  - 6.1.2 0.34 to 0.47 Hz, Alberta-B.C. Mode . . . 55
  - 6.1.3 Sporadically Observed Modes . . . 62
- 6.2 Small Signal Stability Conclusions . . . 68
  - 6.2.1 Mode Shape Considerations . . . 68
  - 6.2.2 Damping Ratio as a Function of Renewable Energy Penetration . . . 68

7 Summary and Conclusions 71

References 73

Appendix A - Statistics for the 2012 and 2022 WECC Base Cases 75

Appendix B - Monitored Generators 93

Appendix C - Generator Models and Circuit Parameters, 7-bus, 5-Generator System 94

Appendix D - Prony Analysis 96

Appendix E - Prony Analysis, Low Damping Signals 207

Appendix F - Frequency Nadir 218

Appendix G - Transient Stability: Generator Speeds 220

List of Figures

1 Western Electricity Coordinating Council (WECC) area. 15
2 Location of monitored generators. 21
3 Location of disturbances. 22
4 7-Bus, 5-Generator example system 24
5 7-Bus, 5-Generator system: Sensitivity of the system frequency response to generation type. 26
6 7-Bus, 5-Generator system: Sensitivity of generator controls to generation type showing total difference between generator input and output powers. 26
7 7-Bus, 5-Generator system: Sensitivity of inter-area oscillations to generation type. 27
8 7-Bus, 5-Generator system: Relative generator speed errors with respect to generation type. 27
9 7-Bus, 5-Generator example system: System frequency response for generator inertia varied (± 25%,± 50%). 28
10 7-Bus, 5-Generator example system: System frequency transient response for two headroom cases. 30
11 7-Bus, 5-Generator example system: Investigation of wind penetration 32
12 7-Bus, 5-Generator example system: Investigation of wind penetration in system dominated by hydro generation. 33
13 7-Bus, 5-Generator example system: Investigation of wind penetration in system dominated by coal generation. 34
14 7-Bus, 5-Generator example system: Investigation of wind penetration in system dominated by gas generation. 35
15 WECC system frequency response to a double Palo Verde trip at $t = 10$ seconds. Six WECC scenarios: 2012 heavy summer, 2012 heavy winter, 2012 light summer, 2022 heavy winter, 2022 light summer, and 2022 light spring. The 2022 light spring meets the renewable portfolio standards. 36
16 2022 light spring WECC system frequency response to a double Palo Verde trip at $t = 10$ seconds. Five scenarios: 2022 light spring, 2022 light spring with type 3/4 wind replaced with **genrou**, 2022 light spring with type 3/4 wind replaced with **genrou** (no governor response), 2022 light spring with type all wind replaced with **genrou**, and 2022 light spring with type all wind replaced with **genrou** (no governor response). 38
17 Maximum speed error relative to system speed. 1.4 GW Chief Joseph brake insertion for 0.5 seconds. 41
18 6-Bus, 4-Generator test system. 43
19 Generator power simulation results for 6-bus, with 4 with all-thermal generation and replacing GEN3 with a type 4 wind plant. 44
20 Generator speed simulation results for 6-bus, with 4 with all-thermal generation and replacing GEN3 with a type 4 wind plant. 44
21 Prony analysis of GEN1-GEN4 speed for the all-thermal case and replacing GEN3 with a type 4 wind plant. 45
22 Prony analysis of GEN2-GEN4 speed for the all-thermal case and replacing GEN3 with a type 4 wind plant. 45
23 Generator power simulation results for 6-bus, with 4 with type 4 wind GEN3 with droop control and inertial emulation. 46
24 Generator speed simulation results for 6-bus, with 4 with type 4 wind GEN3 with droop control and inertial emulation. 46
25 Prony analysis of GEN1-GEN4 speed when replacing GEN3 with a type 4 wind plant with droop control and inertial emulation. 46
26 Prony analysis of GEN2-GEN4 speed when replacing GEN3 with a type 4 wind plant with droop control and inertial emulation. 47

27 Relationship between marker color and residue angle. 48
28 2012 heavy summer, 0.23 Hz inter-area oscillation mode. 50
29 2012 light summer, 0.24 Hz inter-area oscillation mode. 51
30 2012 heavy winter, 0.24 Hz inter-area oscillation mode. 52
31 2022 heavy winter, 0.24 Hz inter-area oscillation mode. 53
32 2022 light summer, 0.29 Hz inter-area oscillation mode. 54
33 2012 heavy summer, 0.35 Hz inter-area oscillation mode. 56
34 2012 light summer, 0.40 Hz inter-area oscillation mode. 57
35 2012 heavy winter, 0.35 Hz inter-area oscillation mode. 58
36 2022 heavy winter, 0.39 Hz inter-area oscillation mode. 59
37 2022 light summer, 0.47 Hz inter-area oscillation mode. 60
38 2022 light spring, 0.46 Hz inter-area oscillation mode. 61
39 2012 heavy winter, 0.56 Hz inter-area oscillation mode. 63
40 2012 heavy winter, 0.68 Hz inter-area oscillation mode. 64
41 2012 heavy summer, 0.60 Hz inter-area oscillation mode. 65
42 2012 light summer, 0.88 Hz inter-area oscillation mode. 66
43 2022 heavy winter, 0.79 Hz inter-area oscillation mode. 67
44 2012 light summer, 1.4 GW Chief Joseph brake, 0.5 seconds. Lightly damped modes from Prony analysis. 70
45 Maximum speed error relative to system speed. 1.4 GW Chief Joseph brake insertion for 0.5 seconds. 221
46 Maximum speed error relative to system speed. 1.4 GW brake insertion on the El Dorado bus for 0.5 seconds. 222
47 Maximum speed error relative to system speed. 1.4 GW brake insertion on the Hemingway bus for 0.5 seconds. 223
48 Maximum speed error relative to system speed. 1.4 GW brake insertion on the Midway bus for 0.5 seconds. 224
49 Maximum speed error relative to system speed. Double Palo Verde trip. Note that the remaining Palo Verde generator was not considered because of the close proximity to the contingency. 225

List of Tables

1 WECC scenarios . . . 19
2 Initial steady state generator and load power levels in the 7-bus, 5-generator model. Convention: generators are sourcing and loads are sinking. . . . 25
3 Generator parameters for headroom analysis. Case 1 is a 60% reduction in headroom. Case 2 is an 80% reduction in headroom. . . . 29
4 WECC system frequency response to a double Palo Verde trip at $t = 10$ seconds. Frequency nadir and time of nadir. . . . 37
5 Key statistics for the 2012 and 2022 WECC Base Cases. Additional statistics are found in Appendix D. . . . 37
6 Generators with maximum relative speed . . . 40
7 Frequency and damping of the dominant mode in the 2022 light spring case . . . 69
8 2012 heavy summer power generated by conventional units. . . . 76
9 2012 heavy summer power generated by renewable units. . . . 77
10 2012 heavy winter power generated by conventional units. . . . 78
11 2012 heavy winter power generated by wind and solar. . . . 79
12 2012 light summer power generated by conventional units. . . . 80
13 2012 light summer power generated by wind and solar. . . . 81
14 2022 heavy winter power generated by conventional units. . . . 82
15 2022 heavy winter power generated by wind and solar. . . . 83
16 2022 light summer power generated by conventional units. . . . 84
17 2022 light summer power generated by wind and solar. . . . 85
18 2022 light spring power generated by conventional units. . . . 86
19 2022 light spring power generated by wind and solar. . . . 87
20 Metrics for 2012 WECC Base Cases . . . 88
21 Metrics for 2022 WECC Base Cases . . . 89
22 2012 heavy winter, total generation: 147,171 MW, renewable generation: 699 MW. . . . 90
23 2012 heavy summer, total generation: 185,246 MW, renewable generation: 1,358 MW. . . . 90
24 2012 light summer, total generation: 120,097 MW, renewable generation: 973 MW. . . . 91
25 2022 heavy winter, total generation: 182,460 MW, renewable generation: 2,276 MW. . . . 91
26 2022 light spring, total generation: 120,583 MW, renewable generation: 18,124 MW. . . . 92
27 2022 light summer, total generation: 146,670 MW, renewable generation: 10,032 MW. . . . 92
28 Summary of monitored generators. . . . 93
29 7-bus, 5-generator system line voltages. . . . 95
30 7-bus, 5-generator system line parameters. . . . 95
31 2012 heavy summer, 1.4 GW at Chief Joseph brake, 0.5 sec . . . 97
31 2012 heavy summer, 1.4 GW at Chief Joseph brake, 0.5 sec . . . 98
31 2012 heavy summer, 1.4 GW at Chief Joseph brake, 0.5 sec . . . 99
32 2012 heavy summer, 1.4 GW at El Dorado bus, 0.5 sec . . . 99
32 2012 heavy summer, 1.4 GW at El Dorado bus, 0.5 sec . . . 100
32 2012 heavy summer, 1.4 GW at El Dorado bus, 0.5 sec . . . 101
33 2012 heavy summer, 1.4 GW at Hemingway Bus, 0.5 sec . . . 101
33 2012 heavy summer, 1.4 GW at Hemingway Bus, 0.5 sec . . . 102
33 2012 heavy summer, 1.4 GW at Hemingway Bus, 0.5 sec . . . 103
34 2012 heavy summer, 1.4 GW at Midway bus, 0.5 sec . . . 103
34 2012 heavy summer, 1.4 GW at Midway bus, 0.5 sec . . . 104
34 2012 heavy summer, 1.4 GW at Midway bus, 0.5 sec . . . 105
35 2012 heavy summer, double Palo Verde trip . . . 105
35 2012 heavy summer, double Palo Verde trip . . . 106

35 2012 heavy summer, double Palo Verde trip . . . 107
35 2012 heavy summer, double Palo Verde trip . . . 108
36 2012 heavy winter, 1.4 GW at Chief Joseph brake, 0.5 sec . . . 109
36 2012 heavy winter, 1.4 GW at Chief Joseph brake, 0.5 sec . . . 110
36 2012 heavy winter, 1.4 GW at Chief Joseph brake, 0.5 sec . . . 111
37 2012 heavy winter, 1.4 GW at El Dorado bus, 0.5 sec . . . 111
37 2012 heavy winter, 1.4 GW at El Dorado bus, 0.5 sec . . . 112
37 2012 heavy winter, 1.4 GW at El Dorado bus, 0.5 sec . . . 113
38 2012 heavy winter, 1.4 GW at Hemingway Bus, 0.5 sec . . . 113
38 2012 heavy winter, 1.4 GW at Hemingway Bus, 0.5 sec . . . 114
38 2012 heavy winter, 1.4 GW at Hemingway Bus, 0.5 sec . . . 115
39 2012 heavy winter, 1.4 GW at Midway bus, 0.5 sec . . . 115
39 2012 heavy winter, 1.4 GW at Midway bus, 0.5 sec . . . 116
39 2012 heavy winter, 1.4 GW at Midway bus, 0.5 sec . . . 117
40 2012 heavy winter, double Palo Verde trip . . . 117
40 2012 heavy winter, double Palo Verde trip . . . 118
40 2012 heavy winter, double Palo Verde trip . . . 119
41 2012 light summer, 1.4 GW at Chief Joseph brake, 0.5 sec . . . 120
41 2012 light summer, 1.4 GW at Chief Joseph brake, 0.5 sec . . . 121
41 2012 light summer, 1.4 GW at Chief Joseph brake, 0.5 sec . . . 122
42 2012 light summer, 1.4 GW at El Dorado bus, 0.5 sec . . . 122
42 2012 light summer, 1.4 GW at El Dorado bus, 0.5 sec . . . 123
42 2012 light summer, 1.4 GW at El Dorado bus, 0.5 sec . . . 124
43 2012 light summer, 1.4 GW at Hemingway Bus, 0.5 sec . . . 124
43 2012 light summer, 1.4 GW at Hemingway Bus, 0.5 sec . . . 125
44 2012 light summer, 1.4 GW at Midway bus, 0.5 sec . . . 126
44 2012 light summer, 1.4 GW at Midway bus, 0.5 sec . . . 127
45 2012 light summer, double Palo Verde trip . . . 128
45 2012 light summer, double Palo Verde trip . . . 129
45 2012 light summer, double Palo Verde trip . . . 130
46 2022 heavy winter, 1.4 GW at Chief Joseph brake, 0.5 sec . . . 131
46 2022 heavy winter, 1.4 GW at Chief Joseph brake, 0.5 sec . . . 132
46 2022 heavy winter, 1.4 GW at Chief Joseph brake, 0.5 sec . . . 133
47 2022 heavy winter, 1.4 GW at El Dorado bus, 0.5 sec . . . 133
47 2022 heavy winter, 1.4 GW at El Dorado bus, 0.5 sec . . . 134
47 2022 heavy winter, 1.4 GW at El Dorado bus, 0.5 sec . . . 135
48 2022 heavy winter, 1.4 GW at Hemingway Bus, 0.5 sec . . . 135
48 2022 heavy winter, 1.4 GW at Hemingway Bus, 0.5 sec . . . 136
48 2022 heavy winter, 1.4 GW at Hemingway Bus, 0.5 sec . . . 137
49 2022 heavy winter, 1.4 GW at Midway bus, 0.5 sec . . . 137
49 2022 heavy winter, 1.4 GW at Midway bus, 0.5 sec . . . 138
49 2022 heavy winter, 1.4 GW at Midway bus, 0.5 sec . . . 139
50 2022 heavy winter, double Palo Verde trip . . . 139
50 2022 heavy winter, double Palo Verde trip . . . 140
50 2022 heavy winter, double Palo Verde trip . . . 141
51 2022 light summer, 1.4 GW at Chief Joseph brake, 0.5 sec . . . 142
51 2022 light summer, 1.4 GW at Chief Joseph brake, 0.5 sec . . . 143
52 2022 light summer, 1.4 GW at El Dorado bus, 0.5 sec . . . 143
52 2022 light summer, 1.4 GW at El Dorado bus, 0.5 sec . . . 144
52 2022 light summer, 1.4 GW at El Dorado bus, 0.5 sec . . . 145

53 2022 light summer, 1.4 GW at Hemingway Bus, 0.5 sec . . . 145
53 2022 light summer, 1.4 GW at Hemingway Bus, 0.5 sec . . . 146
53 2022 light summer, 1.4 GW at Hemingway Bus, 0.5 sec . . . 147
54 2022 light summer, 1.4 GW at Midway bus, 0.5 sec . . . 147
54 2022 light summer, 1.4 GW at Midway bus, 0.5 sec . . . 148
54 2022 light summer, 1.4 GW at Midway bus, 0.5 sec . . . 149
55 2022 light summer, double Palo Verde trip . . . 149
55 2022 light summer, double Palo Verde trip . . . 150
55 2022 light summer, double Palo Verde trip . . . 151
56 2022 light spring, 1.4 GW at Chief Joseph brake, 0.5 sec . . . 152
56 2022 light spring, 1.4 GW at Chief Joseph brake, 0.5 sec . . . 153
57 2022 light spring, 1.4 GW at El Dorado bus, 0.5 sec . . . 153
57 2022 light spring, 1.4 GW at El Dorado bus, 0.5 sec . . . 154
57 2022 light spring, 1.4 GW at El Dorado bus, 0.5 sec . . . 155
58 2022 light spring, 1.4 GW at Hemingway Bus, 0.5 sec . . . 156
58 2022 light spring, 1.4 GW at Hemingway Bus, 0.5 sec . . . 157
59 2022 light spring, 1.4 GW at Midway bus, 0.5 sec . . . 157
59 2022 light spring, 1.4 GW at Midway bus, 0.5 sec . . . 158
59 2022 light spring, 1.4 GW at Midway bus, 0.5 sec . . . 159
59 2022 light spring, 1.4 GW at Midway bus, 0.5 sec . . . 160
60 2022 light spring, double Palo Verde trip . . . 160
60 2022 light spring, double Palo Verde trip . . . 161
60 2022 light spring, double Palo Verde trip . . . 162
61 2022 light spring (Note 1), 1.4 GW at Chief Joseph brake, 0.5 sec . . . 163
61 2022 light spring (Note 1), 1.4 GW at Chief Joseph brake, 0.5 sec . . . 164
62 2022 light spring (Note 1), 1.4 GW at El Dorado bus, 0.5 sec . . . 164
62 2022 light spring (Note 1), 1.4 GW at El Dorado bus, 0.5 sec . . . 165
62 2022 light spring (Note 1), 1.4 GW at El Dorado bus, 0.5 sec . . . 166
63 2022 light spring (Note 1), 1.4 GW at Hemingway Bus, 0.5 sec . . . 167
63 2022 light spring (Note 1), 1.4 GW at Hemingway Bus, 0.5 sec . . . 168
64 2022 light spring (Note 1), 1.4 GW at Midway bus, 0.5 sec . . . 168
64 2022 light spring (Note 1), 1.4 GW at Midway bus, 0.5 sec . . . 169
64 2022 light spring (Note 1), 1.4 GW at Midway bus, 0.5 sec . . . 170
65 2022 light spring (Note 1), double Palo Verde trip . . . 170
65 2022 light spring (Note 1), double Palo Verde trip . . . 171
65 2022 light spring (Note 1), double Palo Verde trip . . . 172
65 2022 light spring (Note 1), double Palo Verde trip . . . 173
66 2022 light spring (Note 2), 1.4 GW at Chief Joseph brake, 0.5 sec . . . 174
66 2022 light spring (Note 2), 1.4 GW at Chief Joseph brake, 0.5 sec . . . 175
67 2022 light spring (Note 2), 1.4 GW at El Dorado bus, 0.5 sec . . . 176
67 2022 light spring (Note 2), 1.4 GW at El Dorado bus, 0.5 sec . . . 177
68 2022 light spring (Note 2), 1.4 GW at Hemingway Bus, 0.5 sec . . . 178
68 2022 light spring (Note 2), 1.4 GW at Hemingway Bus, 0.5 sec . . . 179
69 2022 light spring (Note 2), 1.4 GW at Midway bus, 0.5 sec . . . 179
69 2022 light spring (Note 2), 1.4 GW at Midway bus, 0.5 sec . . . 180
69 2022 light spring (Note 2), 1.4 GW at Midway bus, 0.5 sec . . . 181
70 2022 light spring (Note 2), double Palo Verde trip . . . 182
70 2022 light spring (Note 2), double Palo Verde trip . . . 183
70 2022 light spring (Note 2), double Palo Verde trip . . . 184
71 2022 light spring (Note 3), 1.4 GW at Chief Joseph brake, 0.5 sec . . . 185

71 2022 light spring (Note 3), 1.4 GW at Chief Joseph brake, 0.5 sec . . . 186
72 2022 light spring (Note 3), 1.4 GW at El Dorado bus, 0.5 sec . . . 187
72 2022 light spring (Note 3), 1.4 GW at El Dorado bus, 0.5 sec . . . 188
73 2022 light spring (Note 3), 1.4 GW at Hemingway Bus, 0.5 sec . . . 188
73 2022 light spring (Note 3), 1.4 GW at Hemingway Bus, 0.5 sec . . . 189
73 2022 light spring (Note 3), 1.4 GW at Hemingway Bus, 0.5 sec . . . 190
74 2022 light spring (Note 3), 1.4 GW at Midway bus, 0.5 sec . . . 190
74 2022 light spring (Note 3), 1.4 GW at Midway bus, 0.5 sec . . . 191
74 2022 light spring (Note 3), 1.4 GW at Midway bus, 0.5 sec . . . 192
75 2022 light spring (Note 3), double Palo Verde trip . . . 192
75 2022 light spring (Note 3), double Palo Verde trip . . . 193
75 2022 light spring (Note 3), double Palo Verde trip . . . 194
75 2022 light spring (Note 3), double Palo Verde trip . . . 195
76 2022 light spring (Note 4), 1.4 GW at Chief Joseph brake, 0.5 sec . . . 196
76 2022 light spring (Note 4), 1.4 GW at Chief Joseph brake, 0.5 sec . . . 197
77 2022 light spring (Note 4), 1.4 GW at El Dorado bus, 0.5 sec . . . 198
77 2022 light spring (Note 4), 1.4 GW at El Dorado bus, 0.5 sec . . . 199
78 2022 light spring (Note 4), 1.4 GW at Hemingway Bus, 0.5 sec . . . 200
78 2022 light spring (Note 4), 1.4 GW at Hemingway Bus, 0.5 sec . . . 201
79 2022 light spring (Note 4), 1.4 GW at Midway bus, 0.5 sec . . . 201
79 2022 light spring (Note 4), 1.4 GW at Midway bus, 0.5 sec . . . 202
79 2022 light spring (Note 4), 1.4 GW at Midway bus, 0.5 sec . . . 203
80 2022 light spring (Note 4), double Palo Verde trip . . . 203
80 2022 light spring (Note 4), double Palo Verde trip . . . 204
80 2022 light spring (Note 4), double Palo Verde trip . . . 205
80 2022 light spring (Note 4), double Palo Verde trip . . . 206
81 Summary of low damping signals . . . 207
81 Summary of low damping signals . . . 208
81 Summary of low damping signals . . . 209
81 Summary of low damping signals . . . 210
81 Summary of low damping signals . . . 211
81 Summary of low damping signals . . . 212
81 Summary of low damping signals . . . 213
81 Summary of low damping signals . . . 214
81 Summary of low damping signals . . . 215
81 Summary of low damping signals . . . 216
81 Summary of low damping signals . . . 217
82 Frequency Nadir for Different Stimulus . . . 218

Nomenclature

AGC Automatic Generation Control

BPA Bonneville Power Administration

BL Base load, refers to baseload conventional generation that is set to run at constant output power

COI California-Oregon Intertie

CU Conventional generating unit

GW Gigawatt, 10^9 watts

GR Governor responsive, refers to generation that is equipped with a governor control system

Hz Hertz, units are cycles per second

MVA Megavolt amperes, 10^6 volt-amperes

MVAr Megavolt amperes reactive, 10^6 volt-amperes reactive

MW Megawatt, 10^6 watts

NG No governor, refers to generation that is not equipped with a governor control system

PDCI Pacific DC Inertie

PSLF General Electric's Positive Sequence Load Flow program employed for power system transient simulation

PSS Power System Stabilizer

WECC Western Electricity Coordinating Council

WWSIS Western Wind and Solar Integration Study

This page intentionally left blank.

1 Introduction

The main objective of this study was to evaluate the effects of increased renewable penetration on the small signal and transient stability of the Western Electricity Coordinating Council (WECC). The WECC is the regional entity responsible for coordinating and promoting bulk electric system reliability in the Western Interconnection. The Western Interconnection, shown in Figure 1, encompasses the western United States, British Columbia, Alberta, and parts of northern Mexico. Since the WECC base cases do not contain any

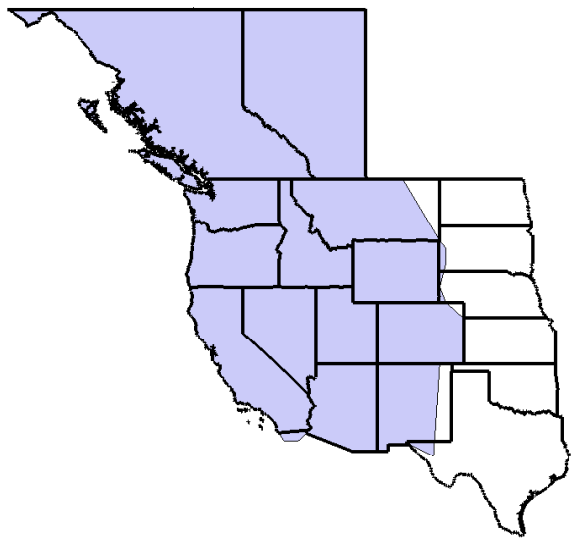

Figure 1: Western Electricity Coordinating Council (WECC) area.

solar models (solar is often modeled as a negative load or as a wind plant), this effort has focused on the effect of wind penetration in the WECC. From a perspective of replaced inertia and lost governor response, the results of this study apply equally to high penetrations of wind and solar.

Transient stability is the ability of the power system to maintain synchronism after a large disturbance. Examples of severe disturbances include loss of generation, loss of a large load, or a transmission system fault. If the angular separation between machines in the system grows too large, the system will lose synchronism and protective relaying will begin to trip. Factors which influence transient stability are [1]:

- Generator loading
- Generator output during the fault
- Fault clearing time
- Post-fault transmission system reactance
- Generator reactance
- Generator inertia
- Generator internal voltage magnitude
- Speed and design of the excitation system
- Design of the power system stabilizer
- Load composition

A lower reactance increases peak power and reduces initial rotor angle. The higher the inertia, the slower the rate of change in angle.

Because some classes of wind and solar generation provide no system inertia, and displace traditional generation with inertia, there is a concern that high renewable penetration might lead to transient stability issues. The most practical method to investigate transient stability of large power systems is through time-domain simulations [1]. For this study we employed General Electric's Postive Sequence Load Flow (PSLF) software. A double Palo Verde loss, which is a worst-case contingency for the WECC, served as the stimulus for the transient stability analysis. In order to better isolate the cause and effect relationship for different parameter changes, simulations were also run on 7-bus, 5-generator system. Likewise, the stimulus for this analysis was a loss of generation.

Rotor angle provides a direct measure of transient stability. For this study we employed generator speed relative to system speed. In addition, the frequency nadir metric proposed in [2] was used to evaluate the system transient response. Frequency nadir measures the system's disturbance rejection performance. Generator frequency, speed ω, and angle, δ, are related by

$$\omega = \frac{d\delta}{dt} \ \text{(p.u.)}, \quad f = 60\omega \ \text{(Hz)} \tag{1}$$

$$\frac{d\omega}{dt} = \frac{d^2\delta}{dt^2} \tag{2}$$

Accelerations in rotor angle result in a change in generator speed. While the nadir of the system frequency is a direct measure of the adequacy of the primary frequency control reserves, it also provides insight into the transient stability of the system. By also looking at generator speed, which is the derivative of rotor angle, we gain additional information about the transient stability of the system. Generators that have large speed differences from system speed, and thus large angle differences, are more prone to transient instability.

Small signal stability is the ability of the power system to maintain synchronization in the face of small disturbances. Small signal instability is often the result of insufficient damping of system oscillations [1]. In order to investigate the small signal stability of the WECC, we again employed PSLF to simulate different scenarios. A resistive brake insertion for 0.5 seconds at various locations (Chief Joseph, El Dorado, Hemingway, and Midway) provided the stimulus to the system. Generator speeds were monitored at 23 locations distributed throughout the WECC. Prony analysis was applied to the generator speeds to identify system modes. Then, mode shape maps of the WECC were developed for several different scenarios, including a case which meets the renewable portfolio standards. These maps provide insight into potential future mode shape changes as a result of increased renewable penetration. A 6-bus, 4 generator system was also analyzed to provide insight into the effects of increased renewable penetration on small signal stability. These results include scenarios with two additional wind control mechanisms: frequency droop and synthetic inertia. Frequency droop is a control output proportional to the local frequency error while synthetic inertia is a control output proportional to the time rate of change (derivative) of local frequency.

Previous studies that have investigated high renewable penetration in the western U.S. include the Western Wind and Solar Integration Study (WWSIS) [3]. This study analyzed the power system operated by the WestConnect group which includes utilities in Arizona, Colorado, Nevada, New Mexico, and Wyoming (California was not included because it had completed a renewable integration study). The primary objective of this effort was to identify and quantify any system performance or operational problems with respect to load following, regulation, and operation during low load periods. The frequency response of the three U.S. interconnections was explored in [4]. For the WECC analysis, this study utilized the 2012 light winter base case as a starting point. The base case was modified to reduce the load to 80 GW and to convert all wind turbine models to type 3 (doubly-fed asynchronous induction generator with voltage control and reactive power). The maximum wind generation in this study was 9 GW, and the system frequency nadir was recorded for 6 different scenarios.

The influences of distributed generation and renewable energy on transient stability are explored in [5]. This paper employs a test power network with two synchronous generators connected to a distribution network with distributed generation and a wind farm. The wind was modeled as a doubly-fed induction generator, and their simulation results showed a slight improvement in transient stability with the combination of distributed generation and wind.

An assessment of the WECC mode shapes as a function of topology changes appears in [6]. This study considered 277 "N-1" contingencies involving the loss of a 500 kV transmission line. A modified version of the 2009 heavy summer WECC operating case was employed. The California-Oregon Intertie (COI) flow was increased and several transmission lines were tripped to yield a low-damping case for the study. This analysis focused on the North-South inter-area mode. The study found that for most scenarios, the mode shapes do not change significantly. The exception was changes in the BC hydro tie lines which resulted in a significant change in mode shape.

A reduced-order transient-simulation model of the WECC, termed the "minniWECC", was utilized in [7] to estimate the observability of inter-area oscillations. The WECC model was reduced to 34 generators, 171 lines and transformers, 19 load buses, and 2 DC lines. This study evaluated the performance of real-power injection, reactive power injection, and series compensation devices for system-wide damping control applications. The effort focused on the North-South mode and the British Columbia mode since they have the greatest impact on COI oscillations.

Baseline damping and mode shape estimates derived from Pacific DC Inertie (PDCI) probing are summarized in [8]. This research identified the following four major inter-area modes of interest:

1. The North-South mode nominally near 0.25 Hz
2. The Alberta mode nominally near 0.4 Hz
3. The British Columbia mode near 0.6 Hz
4. The Colstrip mode nominally near 0.8 Hz

Other modes exist in the system, but these four are observed most often. This is especially true in the northern half of the system. The North-South and Alberta modes are the most widely observed and widespread. This, combined with their lower frequency makes them the most troublesome. Historically, the Alberta interconnection has the strongest influence on the North-South and Alberta modes. When Alberta is not connected, these two modes combine to form a single mode at approximately 0.32 Hz (near the middle of the two modes).

The transient and small signal stability of power systems with increased penetration of doubly fed induction generators (DFIGs) is discussed in [9]. This study employed the DSATools package developed by Powertech Labs, Inc. to study a large test system representing the Midwestern portion of the U.S. interconnection. The small signal analysis evaluated the eigenvalue sensitivity with respect to inertia. For the transient stability analysis, the maximum post-fault angle separation of any two generators in the system, δ_{max}, was assessed by calculating the transient stability index (TSI).

$$TSI = \frac{360 - \delta_{max}}{360 + \delta_{max}}, \quad -100 < TSI < 100 \tag{3}$$

This study identified both detrimental and beneficial impacts from an increased DFIG penetration.

1.1 Review of Control Approaches for Wind and Solar

In recent years, the U.S. and other nations have begun preparing for electric power system operation in which non-dispatchable renewable resources such as wind and solar photovoltaic achieve a high degree of penetration in the electric power grid. As these renewable resources start proliferating, one can start to see an increased role for these resources in the control functions of the grid. Indeed, this study is focused

on the potential benefits and pitfalls of employing wind and solar as control systems on the power grid. Traditionally, dynamic control of active power and frequency to regulate and stabilize the grid has been primarily implemented through the action of synchronous generators directly coupled to the network at 60 Hz. When compared to traditional turbine-driven synchronous generators, renewable generation, such as wind and photovoltaic sources, result in very different electromechanical dynamics to the grid. The intermittency of renewable sources has received wide attention in the research literature. This study has instead focused on the distinctions between renewables and traditional generation that are most relevant to the dynamics of control. Some of these key distinctions are: (1) renewable sources are typically not "naturally" synchronous sources, locked to the 60 Hz grid frequency; (2) renewable sources couple to the grid indirectly, through power electronic devices (e.g. inverters); (3) individual renewable sources are typically much smaller in MW capacity, and therefore larger numbers of individual units contribute collectively.

Many existing renewable based control approaches seek to encourage renewable generation to behave as much like traditional machines as possible (e.g. "synthetic inertia"). This approach is widely reflected in research literature and on the part of the major wind turbine vendors. These references propose supplemental controls that attempt to mimic the inertial characteristics inherent to the physics of traditional synchronous machines (e.g., [10], [11], [12], [13], [14]).

The trend toward a high degree of renewable resource penetration, illustrate that the opportunity exists for renewable resources to play a large role in grid power system control. Renewable generation can be viewed as a new class of control "actuators," and these new classes of generators have very different bandwidth and saturation limits than those associated with traditional turbine-generators. In addition, high bandwidth, time synchronized Phasor Measurement Units (PMUs), combined with improved algorithms and computational hardware, enable more sophisticated state feedback optimal control designs. In [15], the authors demonstrate that a renewable generator controller using just one remote PMU measurement, along with standard locally measured quantities, can significantly improve the quality of its control action. The authors employ an optimal control based design to tailor the dynamics of the commands to the specific characteristics of bandwidth and actuation limits. Indeed, the authors argue that renewable resource based controllers can in some instances perform much better than merely "mimicking" the system inertia of a more traditional turbine-based generator. In this study, inertial emulation or "synthetic inertia" is analyzed both for its merits as well as its potential drawbacks.

Existing research [16] has recognized that storage as a supplement could be used to reduce drive train stress in a wind turbine. In this case, the power output of the battery is used to extend the bandwidth of the wind turbine's actuation. That is, viewed as an actuator in the frequency domain, the Bode plot of the wind turbine has a low pass filter transfer characteristic, from the commanded power change as actuator input, to the achieved change in electrical power as actuator output. This suggests that a supplemental control action, whether from a battery or other source, is to extend the effective frequency range of actuation [8]. With suitable sizing of the battery relative to the cut-off frequency, a band limited, predominantly high-pass control design inherently respects the charge/discharge limits of the battery.

If an inverter-coupled generation source directly substitutes for a synchronous machine generation source, without compensating control, this reduces the inertial response to supply/demand mismatch in the grid. Several studies have looked at the impact of this reduction in system inertia due to the increasing penetration of wind generation on grid frequency regulation (e.g., [12], [17], [18]). As the penetration of wind is expected to grow significantly in the coming decades, researchers and vendors have improved their designs to allow these technologies to better contribute to grid frequency regulation and stability. Most of the solutions proposed to date seek to mimic the inherent inertial response of traditional synchronous generators; i.e., they add a control loop that incrementally feeds or draws active power in response to a decline or rise in the rate of change of system frequency. The control power required by this proposed additional loop comes from varying the mechanical input power to a wind turbine, or by drawing/feeding additional active power from/to the grid through the rotor side [19].

The issues associated with photovoltaic generation are similar. For maximum efficiency at different

levels of isolation, the voltage output must be allowed to vary over a range of values to track the maximum power output point. The power electronic converters that couple directly to the solar panel are typically designed to keep the module at its maximum efficiency by regulating the DC voltage at its terminals; a further step of power electronic conversion then takes the DC power output of multiple panels and converts it to AC voltages and current at the grid interface point. The physics of this production process do not involve any rotating sources, and offers no significant short-term energy storage mechanism analogous to the inertia of a traditional synchronous generator (for more details see [20]).

1.2 Report Organization

This report is organized as follows. Section 2 provides an overview of the methodology applied to arrive at the study findings. This includes a description of the various scenarios and metrics. Section 3 reviews transient response results for a 7-bus, 5-generator system as various parameters are changed. It is easier to visualize the cause and effect relationship of parameter changes on a small system. Section 4 presents transient response results for six different WECC base cases, including the 2022 light spring case which meets the renewable portfolio standards. Small signal stability results for a 6-bus, 4-generator system are summarized in Section 5 and results for the WECC follow in Section 6. The key results are summarized in Section 7. The appendices contain additional details of the study results.

2 Methodology

This section reviews the methodology applied to arrive at the study findings. This includes a summary of the WECC base cases and a description of the study metrics. The metrics employed in this study are: system frequency nadir, generator speed, and Prony analysis of generator speed.

2.1 WECC Scenarios

Six different WECC base cases were analyzed in this study: 2012 heavy summer, 2012 light summer, 2022 light spring, 2012 heavy winter, 2022 light summer, and 2022 heavy winter. The "heavy" cases represent heavy system loading that typically occurs in the late afternoon. The "light" cases represent light system loading that typically occurs in the middle of the night. The season refers to the time of year. The generation statistics for each case are summarized in Table 1. More detailed statistics broken down by WECC area are found in Appendix A. The 2022 light spring case meets the renewable portfolio standards for the region, and is the most pertinent for this analysis because it has the highest penetration of renewables and a light load. This is the case with the most inertia from synchronous generation replaced by renewable generation with no inertia.

Year	**Description**	**Total Generation** (MW)	**Renewable Generation** (MW)	**Percent Renewables** (%)
2012	Heavy summer	185,246	1,358	0.73
2012	Heavy winter	147,170	699	0.47
2012	Light summer	120,097	973	0.81
2022	Light spring	120,583	18,124	15.03
2022	Light summer	146,670	10,032	6.84
2022	Heavy winter	182,460	2,276	1.25

Table 1: WECC scenarios

2.2 Metrics

Several methods were employed to study and describe the transient and small signal stability of the WECC system. For transient stability we employed generator speed relative to system speed. Generator speed, which is the derivative of rotor angle, provides a direct assessment of transient stability. System speed is defined as the MVA base weighted average of all generator speeds. Large deviations with respect to system speed indicate large angle changes with respect to the average system angle. For small signal stability we developed mode shape maps to visualize system oscillations. In addition, the appendices contain mode shape data in tabular form. These tables provide detailed information on the damping at each monitored generator in response to the system stimulus. The system transient response was evaluated using the system frequency nadir proposed by [2]. Frequency nadir is a direct measure of the adequacy of the primary frequency control reserves and provides some insight into the transient stability of the system.

2.2.1 Frequency Nadir

The frequency nadir of the system frequency is defined as the minimum system frequency in response to a disturbance. The system frequency for the purposes of this study is defined as the MVA base weighted average of the speed of all synchronous generators in the system. While this metric is suitable for simulation studies with access to all generator speeds, it is not practical for analyzing real disturbance where only limited data is available. The definition used in this study is consistent with the definition in the CAISO Frequency Response Study [21].

$$\omega_{system} = \frac{\sum_{i=1}^{N} MVA_i \omega_i}{\sum_{i=1}^{N} MVA_i} \quad \text{(p.u.)} \tag{4}$$

$$f_{system} = 60 \cdot \omega_{system} \quad \text{(Hz)} \tag{5}$$

where MVA_i is the MVA base rating for the ith machine, ω_i is the speed of the ith machine, and N is the number of synchronous generators in the system. Since the speed is per unit (p.u.), the system frequency is the MVA base weighted average speed times 60.

2.2.2 Generator Speed

Twenty three representative generators geographically distributed in the WECC were monitored and analyzed in this study. A map of the monitored generator locations appears in Figure 2. More detailed information on the monitored generators appears in Appendix B. Speed relative to the system speed, which is defined in Equation 4, was employed to assess the transient stability of the monitored generators. Speed deviations relative to system speed provide some insight into the transient stability. Generators with large speed excursions have large angle excursions. The maximum speed, e_{max}, was defined as

$$e_{max} = \max\left(|\omega_{gen}(t) - \omega_{sys}(t)|\right), \quad t \in (t_0,\ t_f) \tag{6}$$

This definition is equivalent to the L_1 norm. In this study, we identified generators with large speed excursions for each of the base cases and each of the disturbances. These generators are more prone to transient instability. For the small signal stability calculations, Prony analysis (discussed in the next section) was applied to the speed of the monitored generators.

2.2.3 Prony Analysis

Prony analysis is a method for fitting a linear model to measured data. While this approach was developed in the late 1700's, only in the last 20 years has it been applied to the analysis of power systems [22, 23, 24].

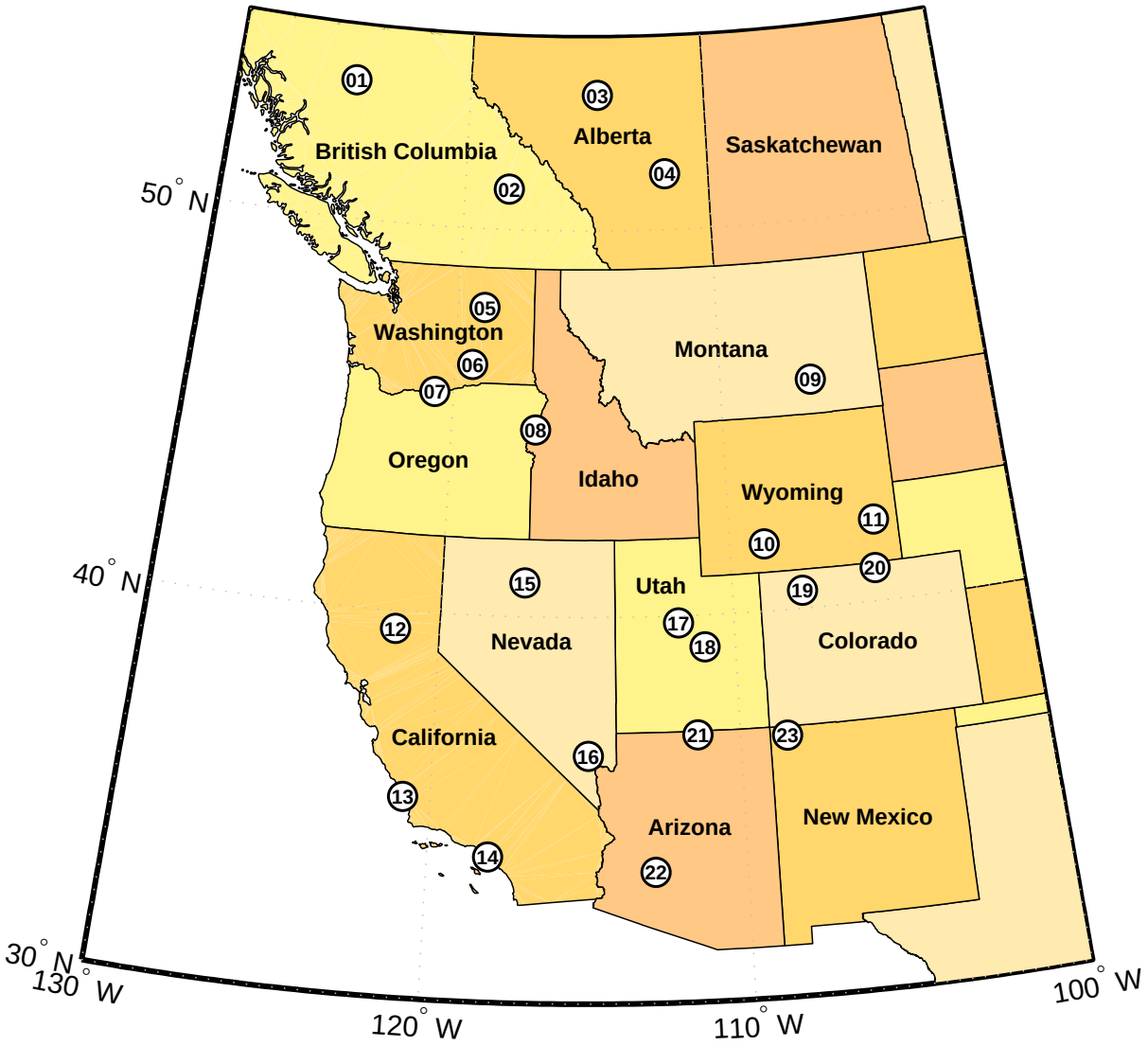

Marker Number	Plant Name	Marker Number	Plant Name
01	Kemano Power Station	13	Diablo Canyon Power Plant
02	Revelstoke Dam	14	Haynes Generating Station
03	Sundance Power Plant	15	North Valmy Generating Station
04	Sheerness Generating Station	16	Silverhawk Generating Station
05	Grand Coulee Dam	17	Currant Creek Power Plant
06	Columbia Generating Station	18	Hunter Power Plant
07	John Day Dam	19	Craig Generating Station
08	Brownlee Dam	20	Rawhide Energy Station
09	Colstrip Power Plant	21	Navajo Generating Station
10	Jim Bridger Power Plant	22	Palo Verde Generating Station
11	Laramie River Generating Station	23	San Juan Generating Station
12	Edward Hyatt Power Plant		

Figure 2: Location of monitored generators.

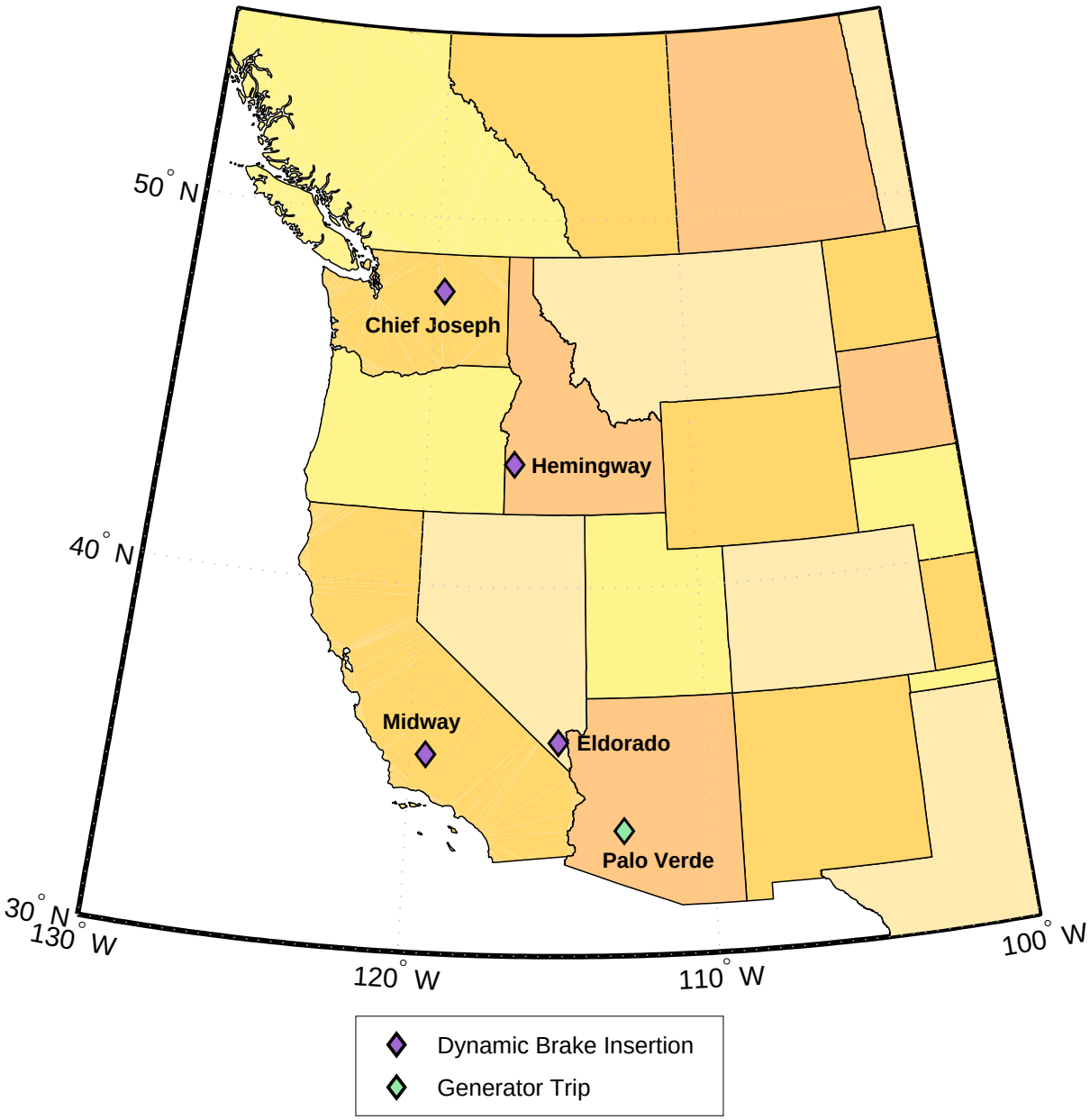

Figure 3: Location of disturbances.

Prony analysis assumes that a signal $y(t)$ is modeled by

$$y(t) = \sum_{i=1}^{n} B_i e^{\lambda_i t} \tag{7}$$

where $B_i \in \mathbb{C}$ is the residue for the continuous-time pole $\lambda_i \in \mathbb{C}$, $\lambda_i \neq \lambda_j, \;\; i \neq j$. The order of the model is n. The objective of Prony analysis is to identify the residues, poles, and n that result in a least squares fit to the measured data [8]. For a discrete-time system, with a constant sample period T seconds, the system model is given by

$$y(kT) = \sum_{i=1}^{n} B_i z_i^k, \;\; k = 0, \; \ldots, \; N-1 \tag{8}$$

where $z_i = e^{\lambda_i T}$ is the discrete-time pole. The characteristic equation of y is given by

$$d(z) = 1 - \left(a_1 z^{-1} + \; \ldots \; + a_n z^{-n}\right) \tag{9}$$

The three steps in solving for the discrete time poles and residue are:

1. Assuming a model order n, solve for the coefficients of the characteristic polynomial by solving the auto-regressive sequence using the measured data, y_m,

   $$y_m(kT) = a_1 y_m((k-1)T) + \; \ldots \; + a_n y_m((k-n)T) \tag{10}$$

   This step is referred to as the linear prediction (LP) problem [25].

2. Calculate the roots of the characteristic equation which are the poles of the discrete-time system.

3. Solve for the residues, B_i, using the measured data and discrete time poles.

   $$y_m(kT) = \sum_{i=1}^{n} B_i z_i^k, \;\; k = 0, \; \ldots, \; N-1 \tag{11}$$

   Equation (11) constructs a Vandermonde matrix, so this step is referred to as the Vandermonde problem.

Given K data points of measured data, the highest order model fit is $n = floor(K/2)$. A selection of n less than this value will result in an over-determined problem. The true model order is often unknown, and even when it is known, a higher order is chosen to improve the numerical robustness of the linear prediction and Vandermonde steps. An example of a process for selecting the model order based on the Akaike information criteria is described in [26]. For this analysis, the model order n was defined as

$$n = round(K/2) - 11 \tag{12}$$

The modes of interest were then selected based on the energy relative to the dominant mode.

So far, the discussion of Prony analysis has focused on the single-input, single-output system model. A Prony method for the single-input, multiple output case is described in [27]. For the analysis in this report, the single-input, single-output Prony analysis approach was employed. To identify system modes, a clustering algorithm was applied to the modes identified in each generator speed signal. For each mode, the relative energy for each participating generator was defined as

$$Relative\ energy = \frac{Mode\ energy\ for\ generator\ i}{Maximum\ observed\ energy} \tag{13}$$

$$Mode\ energy = \sum_{i=1}^{N} x_i^2 \tag{14}$$

where x_i is the ith sample of the time series of the mode of interest.

The next section discusses transient stability results for a 7-bus, 5-generator system.

3 Transient Response: 7-Bus, 5-Generator System

The purpose of this section is to isolate parameters/characteristics that affect system transient response and then consider them in the context of increased penetration of renewable generation. Modern wind turbines (e.g. type 3 and type 4) and solar inverters do not provide the inertia of traditional synchronous generation, nor do they typically provide a frequency droop function (e.g. governor response). In order to mitigate the loss of inertia and governor response, two different control schemes were evaluated: frequency droop and synthetic inertia. Frequency droop is a control output proportional to the local frequency error. Synthetic inertia is a control output proportional to the time rate of change (derivative) of the local frequency. In the event of a transient, both schemes require the renewable device to source or sink additional power. Several schemes have been proposed to enable frequency droop and synthetic inertia. These include: curtailment, energy storage, or drawing from the blade inertia (only applicable to wind). This report focuses on the performance improvement from the addition of the control law and not on the source of the additional energy.

The transient stability of a large power system is a function of numerous parameters. In order to provide insight into how different parameters affect transient stability, it is useful to first look at a simple system. Specifically, the 7-bus, 5-generator system shown in Figure 4 was employed. The initial steady state power levels of each generator and load are summarized in Table 2. A table listing bus voltages and line reactances is given in Appendix C. For each simulation, the generator GEN5 is disabled at $t = 10$ seconds. The total generation at $t = 0$ is 2,531 MW and the loss of GEN5 corresponds to a 1.98% loss of total generation. The system is then simulated for an additional 80 seconds to better capture the steady state response.

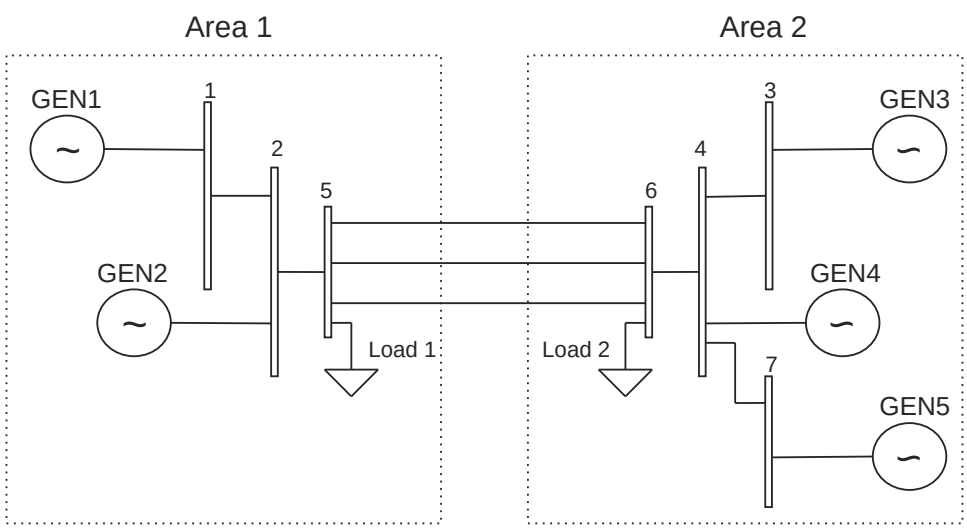

Figure 4: 7-Bus, 5-Generator example system

Four categories of generation were considered with this system: (1) hydro (COULEE plant settings), (2) coal (COLSTRIP 4 plant settings), (3) gas (HAYNES plant settings), and (4) wind (type 4) generation. Parameters that affect the transient response include: the system inertia, the generator/governor/PSS mix, the amount of generator headroom, and the fraction of generators with governor response. To illustrate the effect of each of these parameters on transient response, the following scenarios were simulated with the 7-bus, 5-generator system:

- Sensitivity to generation type: Generators configured to be all hydro, all coal, or all gas
- Sensitivity to system inertia: Generators configured to be all hydro, all coal, or all gas with inertia varied ($\pm$ 50%, $\pm$ 25%)

Name	MVAbase (MVA)	Real Power (t=0) (MW)	Reactive Power (t=0) (MVAr)
GEN1	1000	900	179.5
GEN2	500	400	200
GEN3	900	531	-20.1
GEN4	900	650	423
GEN5	100	50	-50
Load1	NA	1000	250
Load2	NA	1500	250

Table 2: Initial steady state generator and load power levels in the 7-bus, 5-generator model. Convention: generators are sourcing and loads are sinking.

- Sensitivity to generation headroom: Generators configured to be all coal, and headroom is reduced by 60% and 80%
- Sensitivity to Wind generation: Generators are first configured to be all hydro, all coal, or all gas; then GEN3 is adjusted for loss of governor control and a change to wind generation with and without additional power compensation (e.g. frequency droop and synthetic inertia)

The PSLF models for each generator type are listed in Appendix C. Each of the models is from the 2022 light spring WECC case with the exception of the COULEE hydro model. The WECC model was unstable in the small system, so the governor parameters were replaced with the PSLF default values. The choice of a coal generator as the baseline model for the headroom study was arbitrary. The goal was to keep all scenario parameters fixed and only change one parameter at a time to isolate the effect of the change.

3.1 Sensitivity to Generation Type

The transient response of a power system is highly dependent on the generation mix. Variables include the inertia, the speed of the governor response, the speed of the excitation response, and the speed of the power system stabilizer. For this study, "typical" hydro, coal and gas plants were tested with the same disturbance: loss of GEN5 (1.98% of total generation). The simulation results were then considered with respect to system frequency response, total system power, individual generator speed response, and inter-area oscillation. The plant models are based on the WECC models for the following generators:

- Coal plant: Colstrip generator 4
- Gas plant: Haynes generator 1
- Hydro plant: Coulee generator 1. Note, the system was unstable with the governor model from the WECC base case. Therefore, it was replaced with the default governor settings.

It is convenient to begin the investigation with system frequency response; the simulation results are found in Figure 5. In particular, it is noted that there is a significant difference in frequency nadir for the three types of generation. The coal plant system has the highest nadir frequency (59.9262 Hz), the gas plant system is the middle case (59.9110 Hz), and the hydro plant system has the lowest nadir frequency (59.8854 Hz). A severe frequency deviation with loss of generation is often associated with insufficient system inertia; however, the hydro, coal, and gas generation systems have inertia constants of $H = 4.78$ *sec*, $H = 3.70$ *sec*, and $H = 4.05$ *sec* respectively. Hydro generation, having the larger inertia,

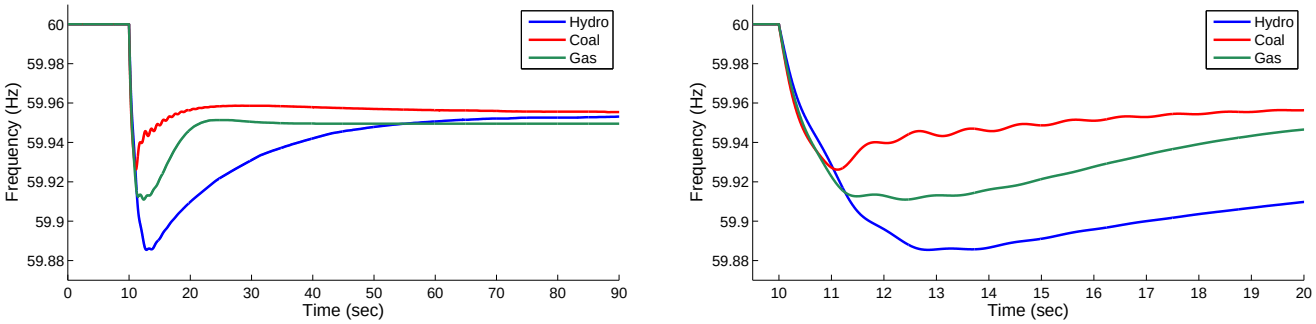

(a) System frequency for each generator type.

(b) System frequency for each generator type, close-up of the transient.

Figure 5: 7-Bus, 5-Generator system: Sensitivity of the system frequency response to generation type.

suffers the greatest frequency deviation. Similarly, coal generation, having the smallest inertia constant, has the smallest drop in frequency. This disparity is due to several factors including but not limited to rate limits on valves and actuators as well as governor/exciter/PSS settings that manage the power flow into and out of the generator. The sum total of these effects result in a power difference across the rotating machines.

To illustrate the effect of total power management on system frequency response, it is helpful to compute the total power into and out of the generators. For mechanical power in p_{mech}, electrical power out p_{gen}, and total power loss p_{loss}, the rotor speed increases when $p_{mech} - p_{gen} - p_{loss} > 0$ and decreases when $p_{mech} - p_{gen} - p_{loss} < 0$, and the rate of this increase/decrease is inversely proportional to the inertial constant H. This *power difference* is given in Figure 6 for each generator type. Specifically, the quantity $p_{mech} - p_{gen} - p_{loss}$ is summed across all four generators. In this case, p_{loss} is estimated as $p_{loss} = P_{mech}(t = 0) - P_{gen}(t = 0)$ for each generator. It is noted that, after the transient, the coal generators have the fastest response (in *power in - power out*), followed by the gas generators and then the hydro generators. Although system inertia plays a role in the frequency response, the power management characteristics of the above described generators dominate in determining their respective transient responses. However, the role of inertia is not neglected herein; system inertia is relevant to our analysis and will be studied in the next section.

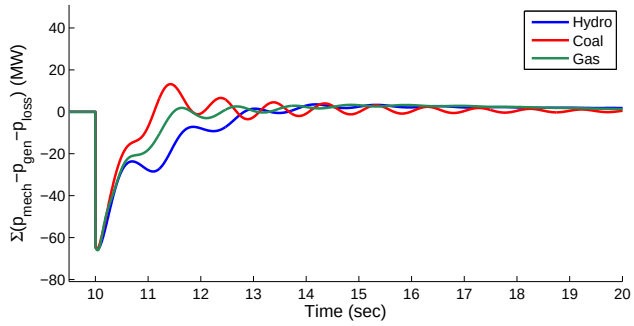

Figure 6: 7-Bus, 5-Generator system: Sensitivity of generator controls to generation type showing total difference between generator input and output powers.

In addition to system frequency response, there are inter-area oscillations as well as individual generator relative speed effects. To investigate the inter-area oscillations that result from disabling GEN5, the difference $\omega_{area1} - \omega_{area2}$ was computed for each generation type. In this case, *Area 1* is the area including GEN1 and GEN2, and *Area 2* is the area including GEN3, GEN4, and GEN5. The results are shown in Figure 7. The relative speed error was computed in per unit $(\omega_{gen} - \omega_{sys})$ for each generator and generator

type; then, to best compare these systems to one another, the $max_{gen}(|\omega_{gen} - \omega_{sys}|)$ was computed with each generation type. The results are consolidated in Figure 8.

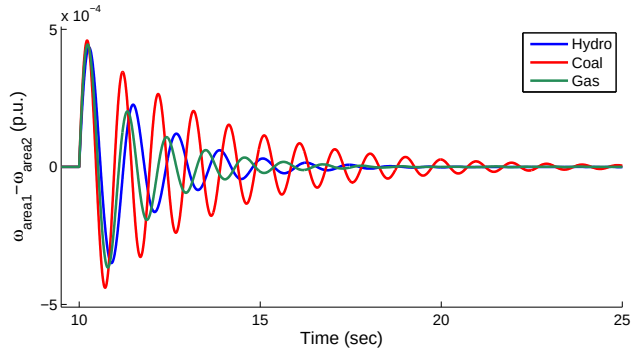

Figure 7: 7-Bus, 5-Generator system: Sensitivity of inter-area oscillations to generation type.

.

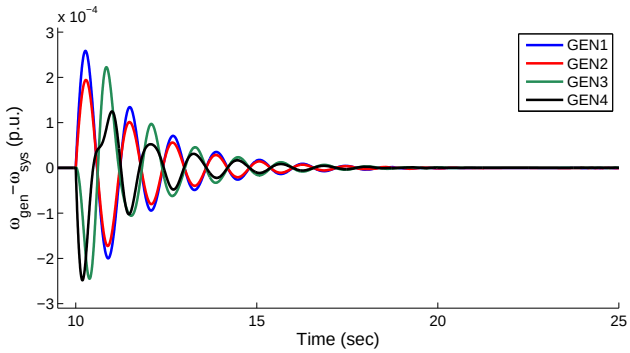

(a) Hydro generation.

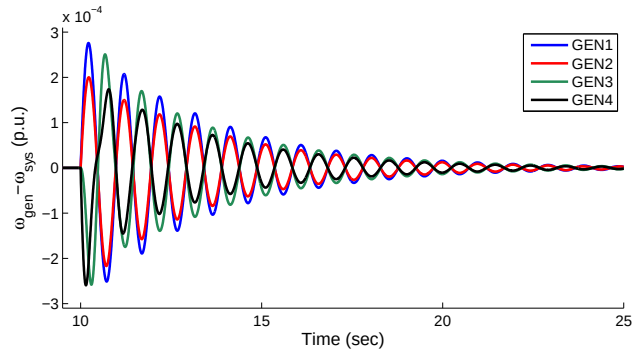

(b) Coal generation.

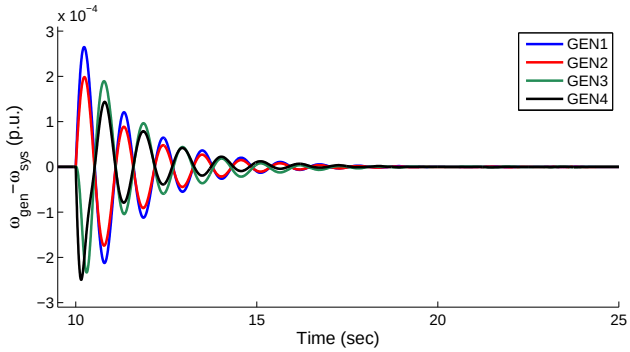

(c) Gas generation.

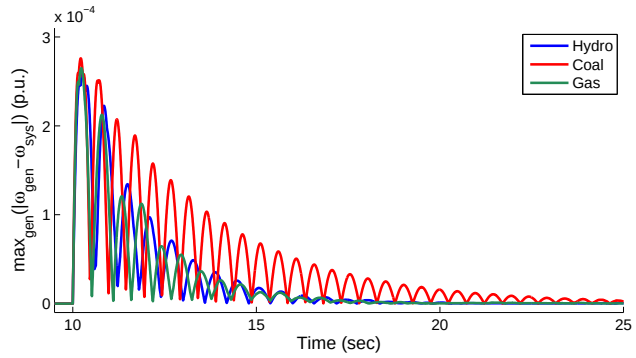

(d) Comparison of Max error.

Figure 8: 7-Bus, 5-Generator system: Relative generator speed errors with respect to generation type.

It is noted, depending on plant characteristics (e.g. inertia, governor speed, PSS settings, etc.), it is possible to obtain different results. The important point is that plant characteristics and generation mix have a significant effect on the system frequency nadir after a transient.

3.2 Sensitivity to System Inertia

To illustrate the effect of system inertia on transient response, the 7-bus, 5-generator system was configured with each plant modeled after a typical hydro, coal, or gas plant. Simulations were conducted as the inertia

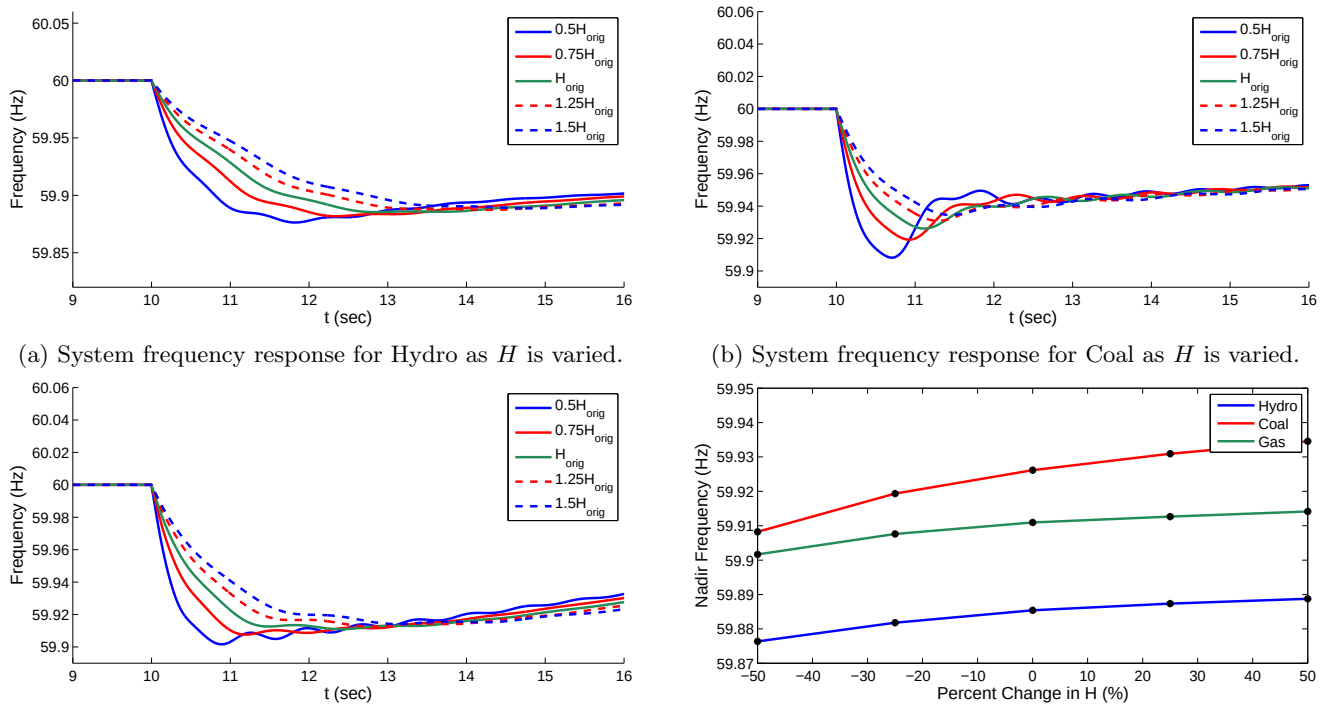

(a) System frequency response for Hydro as H is varied.

(b) System frequency response for Coal as H is varied.

(c) System frequency response for Gas as H is varied.

(d) System frequency nadir as H is varied.

Figure 9: 7-Bus, 5-Generator example system: System frequency response for generator inertia varied ($\pm$ 25%,$\pm$ 50%).

of each generator was varied relative to the nominal value, H_0,

$$H \in \{0.5H_0,\ 0.75H_0,\ H_0,\ 1.25H_0,\ 1.5H_0\} \tag{15}$$

The results are shown in Figure 9. The the rate of change of the system frequency after the disturbance is inversely proportional to system inertia. The higher the system inertia, the slower the drop in system frequency. For each generation type, the frequency nadir is the lowest (largest deviation) for the case with the least system inertia. It is noted, however, that in the case of hydro and gas generation, the close-up plots in Figure 9 reveal the lower inertia systems recover more quickly. In both cases, between $13 < t < 14$ the lower inertia cases overtake the higher inertia cases in system frequency. This is because the governor/exciter/PSS settings are the same in each case, and the resulting power difference is better capable of accelerating the generator with less inertia. This may be true of the coal case as well, but due to system frequency oscillations, this is not as easily observed.

The sensitivity of the system frequency nadir to system inertia is also found in Figure 9 for each generation type. As stated in the previous section, it is noted that hydro has the lower frequency nadir (greater deviation), gas is the middle case, and coal has the higher frequency nadir (lower deviation). It is further noted that the coal generation frequency nadir appears to have greater sensitivity to percent changes in inertia than gas or hydro. Stated more directly, coal generation shows the greatest relative improvement for increase in inertia than the others. To explain this, we consider the dynamic equation for a generator rotor speed

$$\dot{\omega} = \frac{d\omega}{dt} = \frac{p_{mech} - p_{gen} - p_{loss}}{\omega H} \tag{16}$$

where for the purposes of this discussion, all quantities are in per unit. As mentioned previously, the frequency nadir is proportional to the system inertia. To infer the effect of inertia on dynamic response, we compute the partial derivative

$$\frac{\partial \dot{\omega}}{\partial H} = -\frac{p_{mech} - p_{gen} - p_{loss}}{\omega H^2} \tag{17}$$

Since H^2 appears in the denominator of equation 17, the sensitivity of $\dot{\omega}$ to changes in H is greatest when H is small. Since H is smallest for the coal generation system used herein, the results in Figure 9(d) are consistent with the above equations.

It should be noted that although this set of simulations only varied inertia, inertia and governor response are related. For a system with lower inertia, depending on the characteristics of the system, it might be possible to tune the governor so that the frequency nadir is unaffected. With less inertia, the initial drop will be faster, but the governor will be faster, so the nadir stays the same. However, if the characteristics of the governor are held constant and inertia is varied, the rate of change in system frequency and the nadir are both a function of inertia.

3.3 Sensitivity to Generation Headroom

The transient stability of a power system is affected by the amount of governor response headroom. For this example, the same 7-bus, 5-generator system is employed, with a total pre-contingency generation of 2,531 MW. Two different scenarios were simulated. For both cases, the total available generation after the contingency, a loss of GEN5, is greater than the pre-contingency power generation. The maximum generator output, MWcap, for each scenario is summarized in Table 3.

Generator Name	**MVAbase (MVA)**	**Pgen (t=0) (MW)**	**Nominal MWcap (MW)**	**Case 1 MWcap (MW)**	**Case2 MWcap (MW)**
GEN1	1000	900	1000	940	920
GEN2	500	400	500	440	420
GEN3	900	532	900	678	605
GEN4	900	650	900	750	700
GEN5	100	50	GEN5 is turned off at $t = 10$ sec		

Table 3: Generator parameters for headroom analysis. Case 1 is a 60% reduction in headroom. Case 2 is an 80% reduction in headroom.

The results for these simulations are shown in Figure 10. For the first case of reduced headroom, the headroom of all generators was reduced by 60%, but no generators were limited in their output during the experiment. In this case, it is noted that there is no discernible difference in the max speed error from the two cases; a reduced headroom does not appear to impact the ability of the generators to synchronize to one another. However, the system frequency nadir is 2.8 mHz lower: 59.9234 Hz instead of 59.9262 Hz and the system frequency settles to a 7.6 mHz lower value in the steady state: 59.9478 Hz instead of 59.9554 Hz (estimated using the value at the end of the simulation).

For the second headroom case, the headroom of all generators was reduced by 80%, but no generators were limited in their output during the experiment. Again, there was no discernible difference in the max speed error from the two cases. However, in this case, the change in system nadir frequency was 4.9 mHz: 59.9213 Hz instead of 59.9262 Hz. In addition, the reduction in headroom had a greater impact on system frequency, reducing the steady state value by at least 10.5 mHz: 59.9449 Hz instead of 59.9554 Hz (estimated using the value at the end of the simulation). These two examples illustrate how a reduction in governor responsive headroom reduces the system frequency nadir with all other parameters held constant.

While there is a noticeable reduction in frequency nadir with reduced governor headroom, the effect on transient stability is minimal. There is not a significant difference in generator speeds for the two cases in

Figure 10.

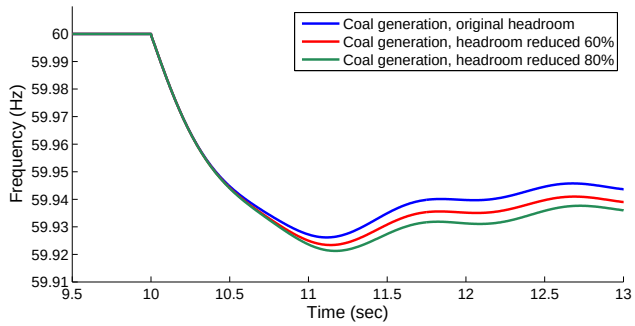

(a) System frequency, nominal, 60% reduction in headroom, and 80% reduction in headroom.

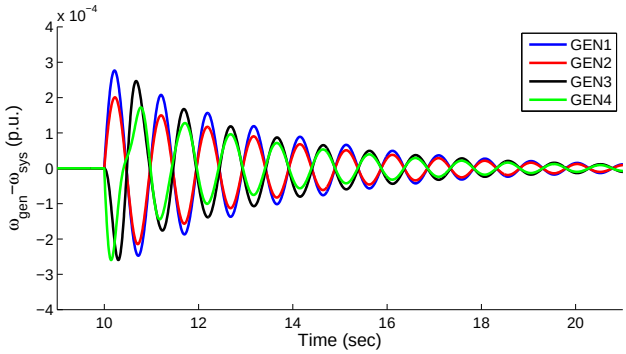

(b) Case 1, relative speed errors, 60% reduction in headroom.

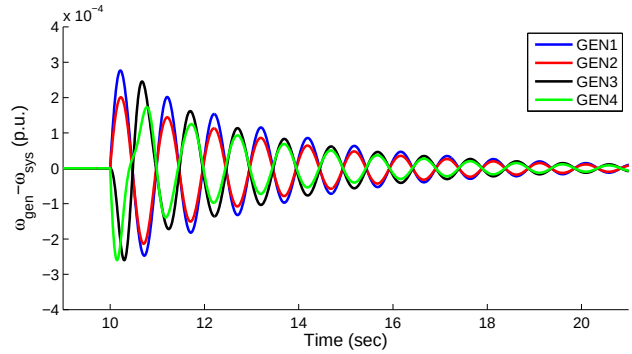

(c) Case 1, relative speed errors, 80% reduction in headroom.

Figure 10: 7-Bus, 5-Generator example system: System frequency transient response for two headroom cases.

3.4 Sensitivity to Wind Generation

This section explores the effect of wind generation on transient response. The following scenarios were simulated to highlight the effects of governor response, wind penetration, and wind control algorithms. Each of these simulations was performed with base conventional generation being all hydro, all coal, and all gas.

- The baseline case is 100 % coal, gas, or hydro generation
- The GEN3 governor is disabled
- GEN3 is replaced with a type 4 wind generator
- GEN3 is replaced with a type 4 wind generator with frequency droop (275 kW/mHz)
- GEN3 is replaced with a type 4 wind generator with frequency droop (275 kW/mHz) and inertial emulation (100 kW·sec/mHz)

The results are summarized in Figure 11 and are seen to be consistent across generation types. The baseline case is given for 100% coal, gas, or hydro generation, shown in each plot by the solid blue line. When the governor on GEN3 is disabled, the response of the system as a whole is diminished resulting in a lower frequency nadir and a lower steady state frequency. In the third case, GEN3 is replaced by a type 4 wind generator, thus removing GEN3's inertia from the system; the system frequency drops furthest but

recovers to the same steady-state frequency as in the second case. In the fourth case, an additional power signal is applied to the output of the wind generator. This power signal is given by

$$p_{GEN3} = P_{ref} + K_d(f_0 - f_{bus3}) \tag{18}$$

where $f_0 = 60$ Hz, f_{bus3} is the frequency observed at bus 3, and the control gain K_d is 275 kW/mHz. The addition of this term results in a response that resembles *droop* control. In this case, it is noted that the system frequency nadir is mitigated and that the steady-state frequency is very nearly that of the first scenario. In the fifth and final case, the additional power signal is augmented to include an inertial emulation term that responds to oppose the time rate of change in the frequency as bus 3 as follows

$$p_{GEN3} = P_{ref} + K_d(f_0 - f_{bus3}) - K_i \frac{df_{bus3}}{dt} \tag{19}$$

where K_i is 100 kW·sec/mHz. To justify the inertial emulation term in equation 19, we consider again the dynamic equation 16. After some manipulation, the generator power is determined to be

$$p_{gen} = p_{mech} - p_{loss} - H\omega\dot{\omega} \tag{20}$$

where $H\omega\dot{\omega}$ is the per unit power sourced (or sinked) when decelerating (accelerating) the rotating mass of the generator. Since the type 4 wind turbine interfaces through the grid, the effect of this term must be emulated.

With the addition of an inertial emulation term, we observe some additional improvement in the system frequency nadir, but the improvement is minimal. However, this inertial emulation term is key to mitigating the oscillation of generators with respect to one another following a transient. To study this, we once again consider the relative speed error in per unit ($\omega_{gen} - \omega_{sys}$) for each generator, generator type and scenario. The results for wind penetration in a system dominated by hydro generation are given in Figure 12. For the first experiment where all generation is hydro (with governor control), the speed errors display a balanced response to the stimulus; GEN1 and GEN2 swing together, and GEN3 and GEN4 swing together with approximately the same magnitude. When the governor on GEN3 is disabled, the response can be seen to differ only slightly. However, in the third scenario, wherein GEN3 becomes a type 4 wind generator, the speed errors of the remaining three generators become asymmetrical. Specifically, the oscillation of GEN4 becomes disproportionately large as the inertia of Area 2 has been reduced. In the fourth case, where a control mimicking droop compensation is added to the wind generator, a slight reduction in the magnitude of the oscillations is observed, but the asymmetry persists. However, in the fifth case, wherein inertial emulation is included with the wind generator, the oscillations are mitigated substantially and better distributed across the three generators. This test is repeated for systems having coal and gas conventional generation; these results are given in Figures 13,14. One notes the same principle results as those shown in Figure 12; the oscillatory energy of GEN4 becomes disproportionately large when GEN3's inertia is removed from Area 2, but the oscillatory energy of GEN4 can be mitigated by adding inertial emulation to the wind turbine controls. The effect of wind generation on inter-area modes is investigated more thoroughly in Chapter 5.

It is noted that the additional controls on the wind generator potentially require some energy storage. This storage may be the rotational inertia of the wind turbine blades or some additional electrochemical (i.e. battery) or electromechanical (i.e. flywheel) energy storage system working in concert with the wind generator. Alternatively, the controls could be used to manage wind generator headroom. This would require the wind turbine to operate in steady-state at a suboptimal operating point, likely above the maximum power point tip-speed ratio. When additional energy was needed, the wind turbine could claim additional energy by decelerating the turbine blades and falling back to an operating point that generates more power.

Herein, K_d and K_i were selected empirically; however, these terms may be determined through analysis and are expected to scale with generation. For example, based on these experiments we may choose to

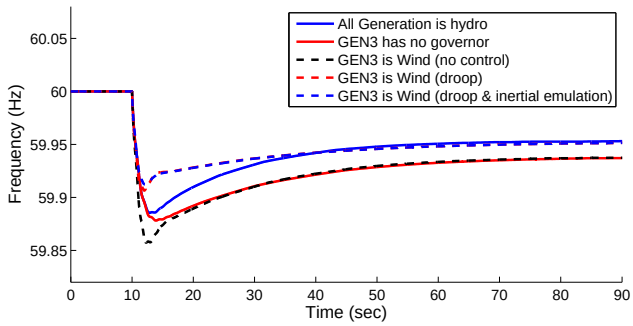

(a) System frequency transient response, hydro generation.

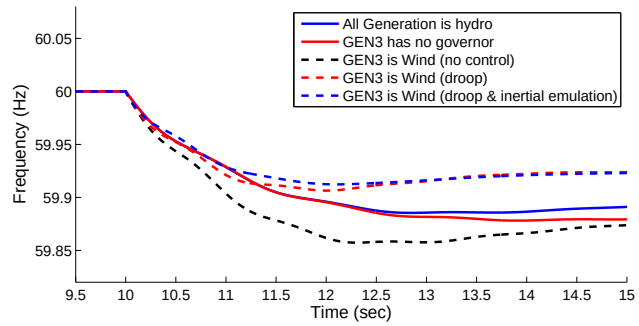

(b) System frequency transient response, first 3 seconds after the transient, hydro generation.

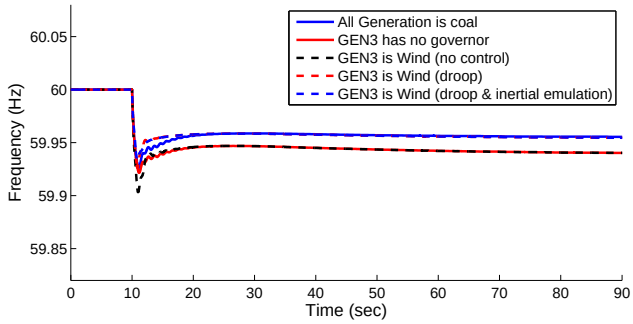

(c) System frequency transient response, coal generation.

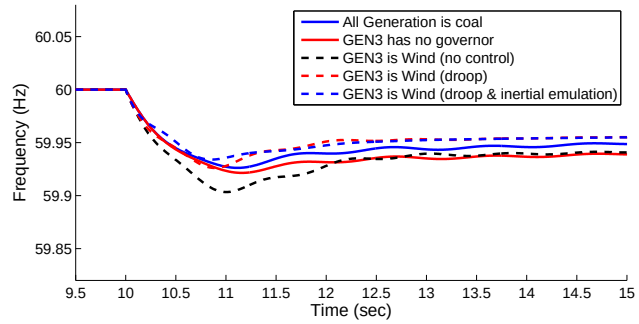

(d) System frequency transient response, first 3 seconds after the transient, coal generation.

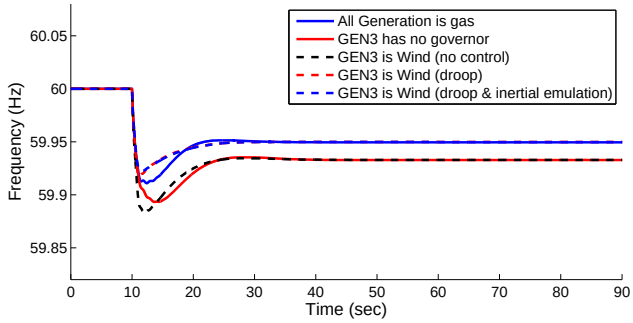

(e) System frequency transient response, gas generation.

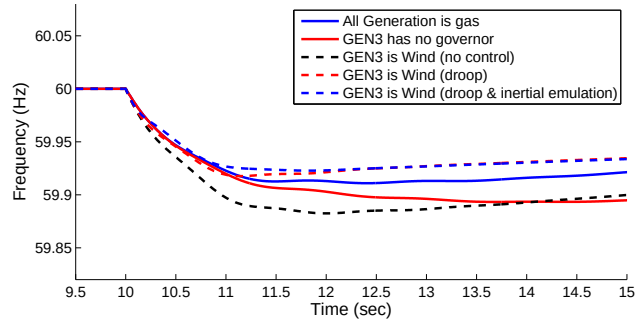

(f) System frequency transient response, first 3 seconds after the transient, gas generation.

Figure 11: 7-Bus, 5-Generator example system: Investigation of wind penetration

compute K_d to be $K_d = P_{max} \cdot 30.6\text{kW/mHz}$. Thus, to respond to a 100 mHz frequency drop for five minutes would require the addition of 30.6 MW/2.55 MW-hr of energy storage to the grid for each 1 GW of installed wind generation. Likewise, this same analysis may be applied to scaling K_i (although the energy requirements will be substantially less). Specifically, after equating $H\omega\dot{\omega}$ and $K_i\frac{df}{dt}$ (with the proper application of per unit conversion), one finds that $K_i = \frac{H_{em}P_{max}}{60}$ where K_i is in kW/mHz, the emulated inertia H_{em} is in seconds, and maximum generator output P_{max} is in MW.

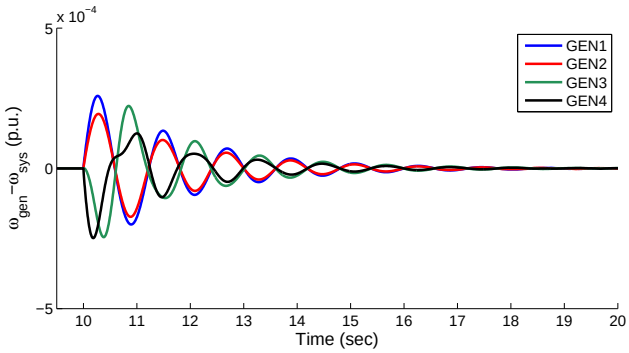

(a) Relative generator speed errors: GEN3 is hydro generation.

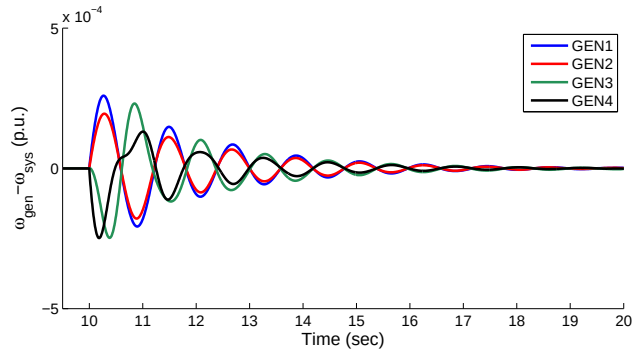

(b) Relative generator speed errors: GEN3 is hydro generation with disabled governor.

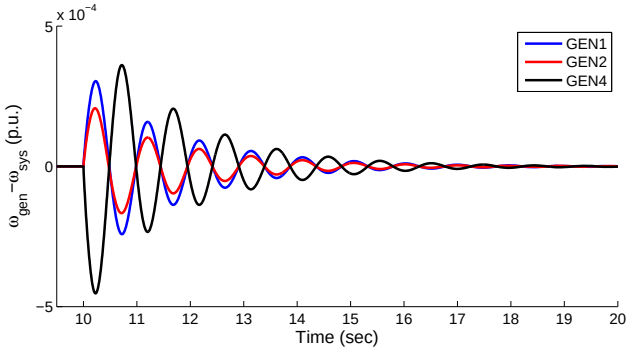

(c) Relative generator speed errors: GEN3 is wind generation.

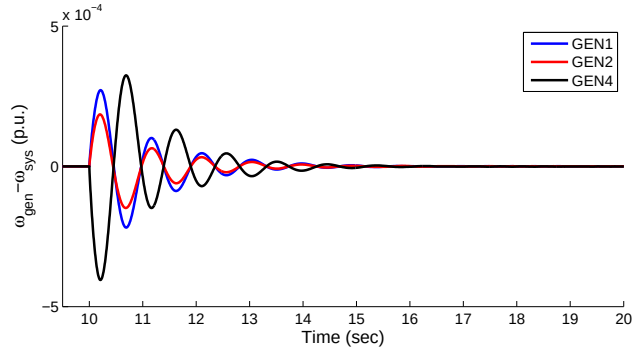

(d) Relative generator speed errors: GEN3 is wind generation with droop.

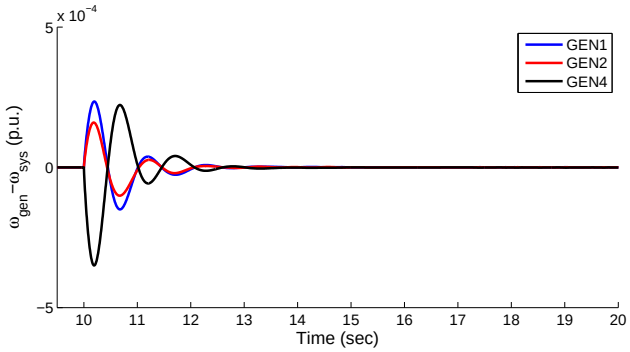

(e) Relative generator speed errors: GEN3 is wind generation with droop and inertial emulation.

Figure 12: 7-Bus, 5-Generator example system: Investigation of wind penetration in system dominated by hydro generation.

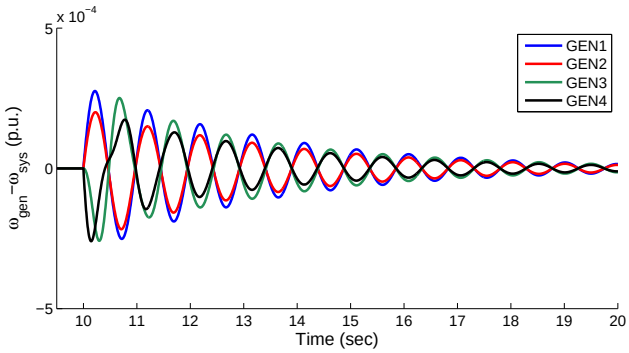

(a) Relative generator speed errors: GEN3 is coal generation.

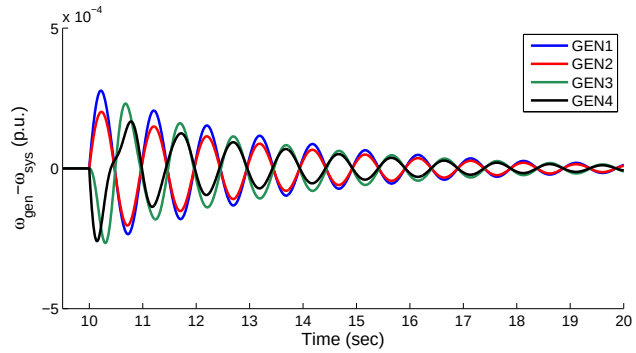

(b) Relative generator speed errors: GEN3 is coal generation with disabled governor.

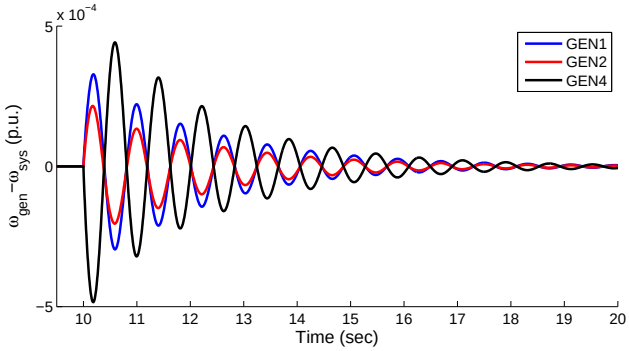

(c) Relative generator speed errors: GEN3 is wind generation.

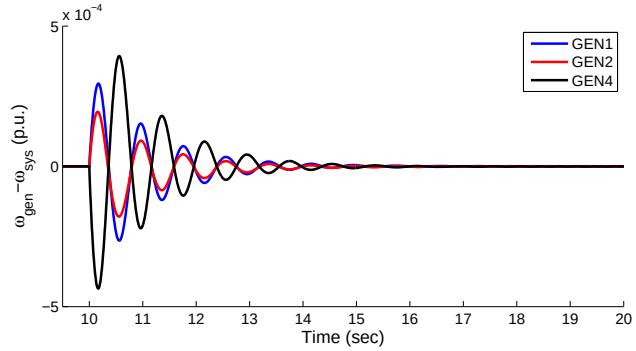

(d) Relative generator speed errors: GEN3 is wind generation with droop.

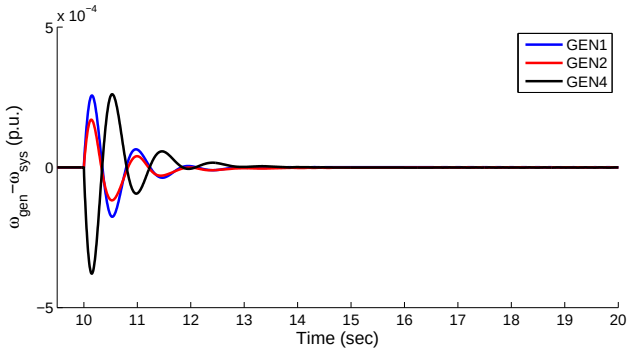

(e) Relative generator speed errors: GEN3 is wind generation with droop and inertial emulation.

Figure 13: 7-Bus, 5-Generator example system: Investigation of wind penetration in system dominated by coal generation.

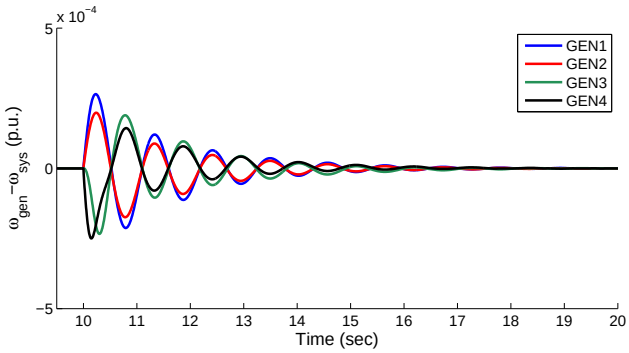

(a) Relative generator speed errors: GEN3 is gas generation.

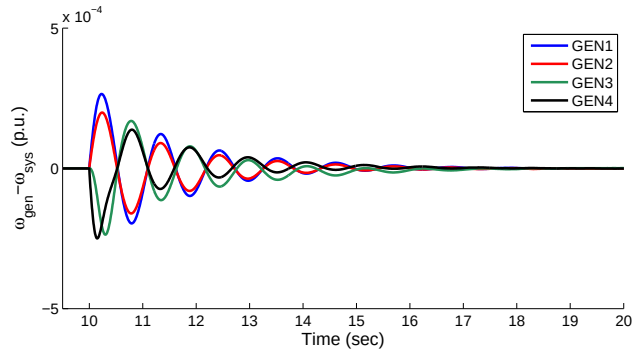

(b) Relative generator speed errors: GEN3 is gas generation with disabled governor.

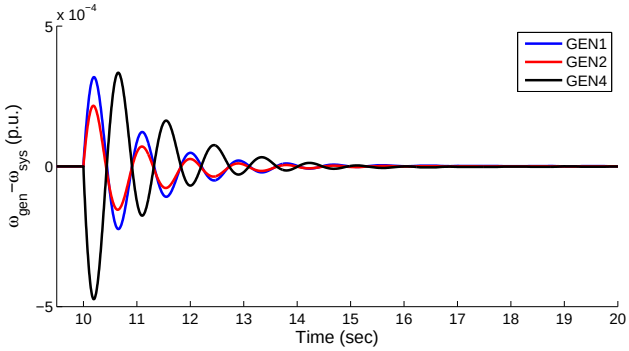

(c) Relative generator speed errors: GEN3 is wind generation.

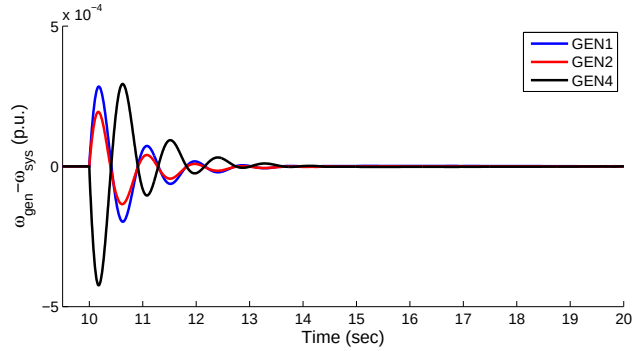

(d) Relative generator speed errors: GEN3 is wind generation with droop.

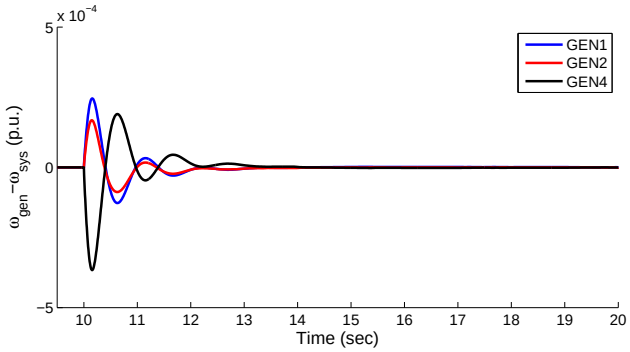

(e) Relative generator speed errors: GEN3 is wind generation with droop and inertial emulation.

Figure 14: 7-Bus, 5-Generator example system: Investigation of wind penetration in system dominated by gas generation.

4 Transient Response: WECC

In this section the transient response results are presented for six different WECC base cases. The stimulus for each simulation is a double Palo Verdo loss (approximately 2.8 GW of generation), which is a worst case contingency for the WECC. The metrics for comparing the cases are: the system frequency nadir and the generator speed relative to the system speed. The next section reviews the results for all cases while the subsequent section focuses on the 2022 light spring high renewables case.

4.1 Comparison of 2022 and 2012 Cases

Figure 15 contains the WECC system frequency response to a double Palo Verde trip for the six cases studied. The system frequency nadir for each case is also summarized in Table 4. The 2022 light spring case has the lowest nadir, while the 2022 heavy winter case has the highest nadir. For all cases, the frequency nadir is well above the highest load shedding frequency of 59.5 Hz that is commonly implemented in the WECC [4]. While there is a difference in renewable generation between these two cases, the fraction of renewable generation is not the cause of the lower nadir. The dominant factor is the size of the disturbance relative to the total generation. The total generation for the 2022 light spring case is 120 GW while the total generation for the 2022 heavy winter case is 185 GW. The corresponding loss of generation for the 2022 light spring case is 2.33% of total generation compared to 1.51% of total generation for the 2022 heavy winter case. The governor headroom has a secondary contribution. The second best (highest) nadir is the 2012 heavy summer case. Here the contingency is also a smaller fraction of generation (1.5%), but there is less governor headroom (12.8 GW versus 18.6 GW) which explains the slightly poorer performance. The difference between the two worst cases, 2022 light spring and 2012 light summer, can be explained by the reduced system inertia in the 2022 light spring case from the high wind penetration. Both of these cases have roughly the same total generation, 120 GW, and the 2022 light spring case has more governor headroom, 18 GW versus 15 GW. Section 3.2 illustrated the effect of system inertia on frequency nadir. The next section uses the 2012 light spring case to quantify the effects of additional inertia versus additional governor responsive headroom.

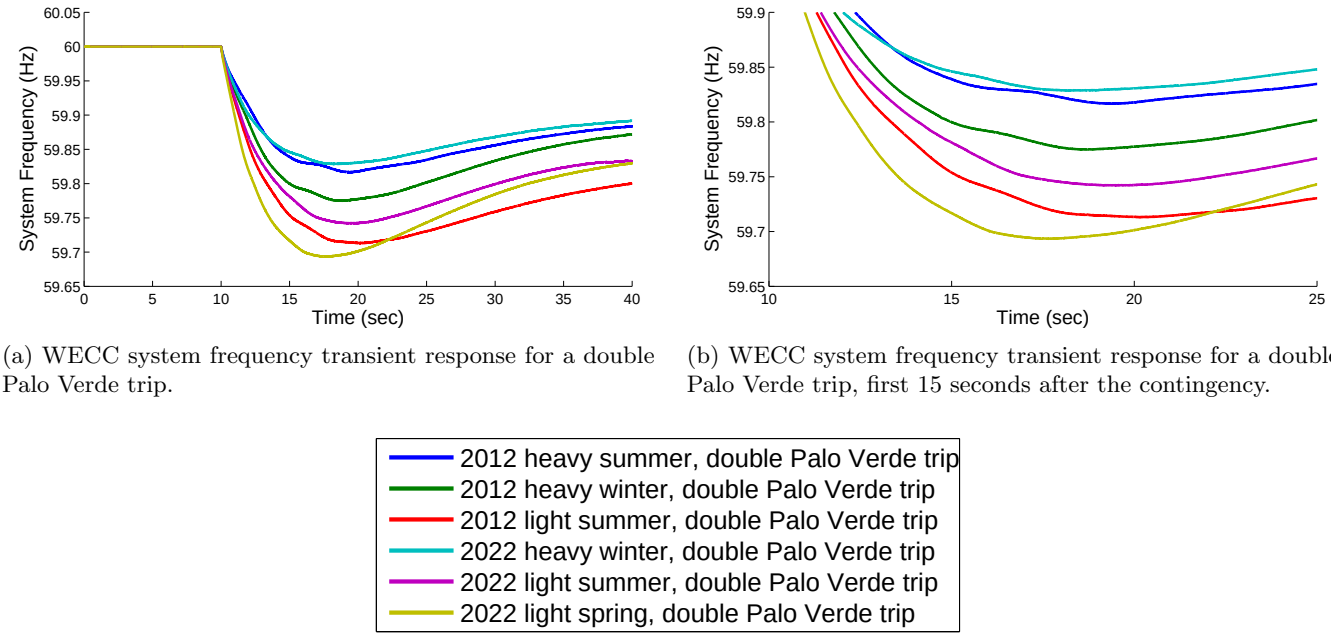

(a) WECC system frequency transient response for a double Palo Verde trip.

(b) WECC system frequency transient response for a double Palo Verde trip, first 15 seconds after the contingency.

Figure 15: WECC system frequency response to a double Palo Verde trip at $t = 10$ seconds. Six WECC scenarios: 2012 heavy summer, 2012 heavy winter, 2012 light summer, 2022 heavy winter, 2022 light summer, and 2022 light spring. The 2022 light spring meets the renewable portfolio standards.

WECC case	Nadir (Hz)	Time (sec)
2012 heavy summer	59.817	19.4
2012 heavy winter	59.775	18.9
2012 light summer	59.713	20.2
2022 heavy winter	59.829	18.2
2022 light summer	59.742	19.8
2022 light spring	59.693	17.7

Table 4: WECC system frequency response to a double Palo Verde trip at $t = 10$ seconds. Frequency nadir and time of nadir.

	2012			2022		
Quantity	**Heavy Summer**	**Heavy Winter**	**Light Summer**	**Heavy Winter**	**Light Summer**	**Light Spring**
Total PGEN (MW)	185,246	147,171	120,097	182,460	146,670	120,583
Wind/Solar PGEN (MW)	1,358	699	973	2,276	10,032	18,124
GR Headroom (MW):	12,788	13,478	15,142	18,634	17,835	17,976

Table 5: Key statistics for the 2012 and 2022 WECC Base Cases. Additional statistics are found in Appendix D.

4.2 High Renewables Penetration, 2022 Light Spring Case

In order to quantify the contribution of system inertia and governor response to system frequency nadir in the WECC 2022 light spring case, the following scenarios were simulated:

1. 2012 light spring case
2. 2012 light spring case, all type 3/4 wind turbines converted to **genrou** models
3. 2012 light spring case, all type 3/4 wind turbines converted to **genrou** models, no governor response
4. 2012 light spring case, all wind turbines converted to **genrou** models
5. 2012 light spring case, all wind turbines converted to **genrou** models, no governor response

With so many differences between the various WECC cases, the six scenarios listed above isolate the effect of lost inertia and governor response on the system frequency nadir. The first case serves as the baseline. The second case replaces the type 3 and 4 wind turbines with an equivalent synchronous generator, the **genrou** model, with governor response. The **genrou** model is the most prevalent type in the WECC base case models by power and generates approximately half of the total power. It describes a solid rotor generator represented by equal mutual inductance rotor modeling [28]. The default PSLF parameterts were used for the generator, exciter, power system stabilizer, and governor. The maximum output was set to 117.6% of the power generated to provide reasonable headroom. The third case disables the governor response on the generators that replaced the wind. The type 2 and 3 wind turbines were kept because they provide some system inertia. The fourth case replaces all wind turbines with an equivalent synchronous

generator with governor response. The last case disables the governor response on the generators that replaced the wind. The transient response for each scenario is shown in Figure 16.

In all scenarios the frequency nadir was well above the load shedding frequency of 59.5 Hz. Scenarios 2 and 4 exhibit the highest frequency nadir. Both of these cases have more governor responsive headroom than the baseline WECC case. The highest nadir is with type 1/2 wind turbines in the system while the type 3/4 turbines have been replaced with synchronous machines. The lowest frequency nadir is the case with all wind replaced with synchronous generators without governor response. There is little difference between the baseline WECC case and the two scenarios where wind is replaced with synchronous generator without governor response. These simulations show that governor response has a larger effect on the system frequency nadir compared to system inertia. This is consistent with the results for a 7-bus, 5-generator system discussed in Section 3.

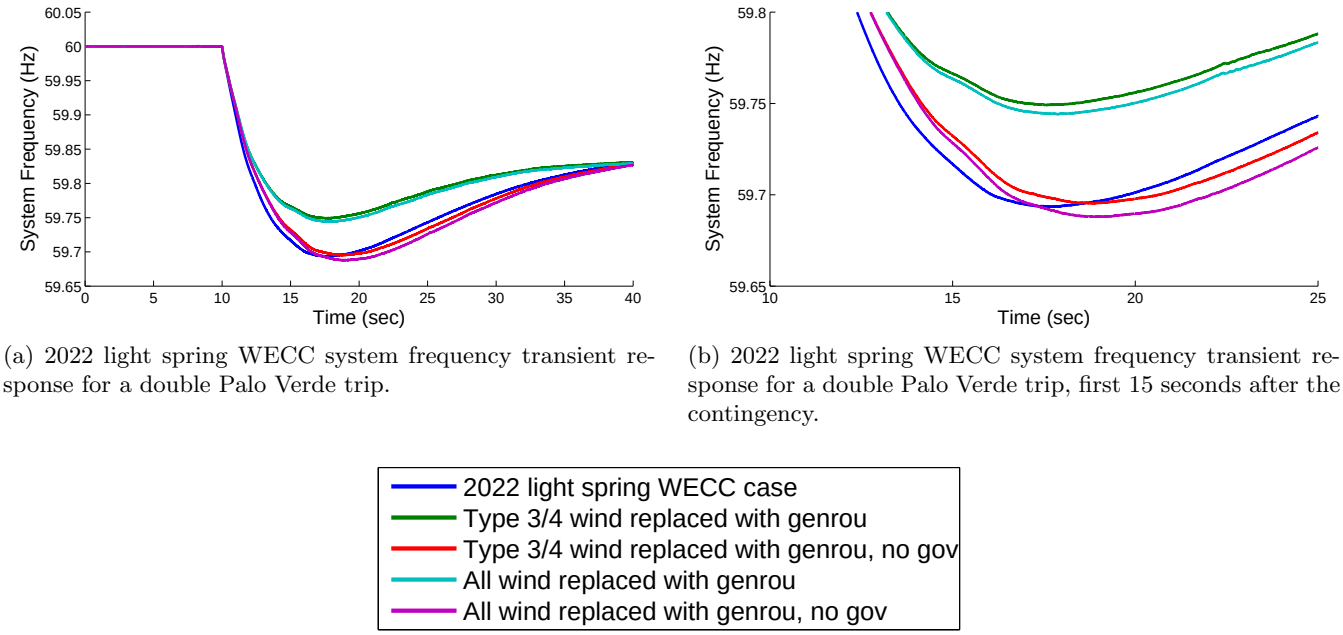

(a) 2022 light spring WECC system frequency transient response for a double Palo Verde trip.

(b) 2022 light spring WECC system frequency transient response for a double Palo Verde trip, first 15 seconds after the contingency.

Figure 16: 2022 light spring WECC system frequency response to a double Palo Verde trip at $t = 10$ seconds. Five scenarios: 2022 light spring, 2022 light spring with type 3/4 wind replaced with **genrou**, 2022 light spring with type 3/4 wind replaced with **genrou** (no governor response), 2022 light spring with type all wind replaced with **genrou**, and 2022 light spring with type all wind replaced with **genrou** (no governor response).

4.3 Generator Speeds

Transient stability is the ability of the power system to maintain synchronism after a large disturbance. Typically, a transient stability analysis looks at the relative rotor angle between a pair of generators to make sure that the maximum excursion meets some stability margin. In a large power system like the WECC, there are a combinatorially large number of generator pairs. Therefore, for this analysis we analyzed the maximum speed excursion of the monitored generators relative to the system speed. The system speed is the MVA base weighted average of all synchronous generators in the system. Therefore, the relative speed error provides insight into which generators are speeding up or slowing down more relative to the system average. Since relative angle is the integral of relative speed, large speed excursions correlate with large angle excursions. For each test case, the four generators with the largest magnitude relative speed were identified. This is equivalent to the L_1 norm.

$$e_{max} = \max\left(|\omega_{gen}(t) - \omega_{sys}(t)|\right), \quad t \in (t_0,\ t_f) \tag{21}$$

This information is summarized in Table 6 and time series plots for each scenario appear in Appendix H. The **Gen 1** column corresponds to the generator with the maximum relative speed error. Similarly, **Gen 2**, **Gen 3**,and **Gen 4** have the 2nd, 3rd, and 4th largest magnitude errors.

A large contributor to the size of the speed oscillations is the size and location of the disturbance. Therefore, the remaining Palo Verde generator was excluded from consideration for the double Palo Verde contingency. This effect explains why for each stimulus there are one or two generators that are always at the top of the list. A more interesting observation is generators that are always on the list, regardless of the scenario or disturbance. These generators are more prone to large speed and angle swings as the result of a disturbance. Kemano is most prevalent, and this is consistent with its grid topology. It is at the end of a long set of transmission lines.

Year	WECC Case	Stimulus	Gen 1	Gen 2	Gen 3	Gen 4
2012	heavy summer	Chief Joseph Brake	Kemano	Grand Coulee	Columbia	Colstrip
2012	heavy winter	Chief Joseph Brake	Kemano	Grand Coulee	Colstrip	Columbia
2012	light summer	Chief Joseph Brake	Kemano	Grand Coulee	Revelstoke	Columbia
2022	heavy winter	Chief Joseph Brake	Kemano	Grand Coulee	Revelstoke	Colstrip
2022	light summer	Chief Joseph Brake	Grand Coulee	Kemano	Columbia	Revelstoke
2022	light spring	Chief Joseph Brake	Grand Coulee	Kemano	Colstrip	Columbia
2022	light spring (Note 1)	Chief Joseph Brake	Grand Coulee	Kemano	Columbia	Colstrip
2022	light spring (Note 2)	Chief Joseph Brake	Kemano	Grand Coulee	Columbia	Colstrip
2022	light spring (Note 3)	Chief Joseph Brake	Kemano	Grand Coulee	Columbia	Colstrip
2022	light spring (Note 4)	Chief Joseph Brake	Kemano	Grand Coulee	Columbia	Colstrip
2012	heavy summer	El Dorado Bus	Silverhawk	Navajo	Kemano	Sundance
2012	heavy winter	El Dorado Bus	Silverhawk	Navajo	Kemano	Haynes
2012	light summer	El Dorado Bus	Silverhawk	Navajo	Kemano	Sundance
2022	heavy winter	El Dorado Bus	Silverhawk	Navajo	Haynes	Kemano
2022	light summer	El Dorado Bus	Silverhawk	Navajo	Sundance	Kemano
2022	light spring	El Dorado Bus	Silverhawk	Navajo	Sundance	Kemano
2022	light spring (Note 1)	El Dorado Bus	Silverhawk	Navajo	Sundance	Kemano
2022	light spring (Note 2)	El Dorado Bus	Silverhawk	Navajo	Sundance	Kemano
2022	light spring (Note 3)	El Dorado Bus	Silverhawk	Navajo	Sundance	Kemano
2022	light spring (Note 4)	El Dorado Bus	Silverhawk	Navajo	Sundance	Kemano
2012	heavy summer	Hemingway Bus	Brownlee	Hunter	Jim Bridger	Currant Creek
2012	heavy winter	Hemingway Bus	Brownlee	Hunter	Jim Bridger	North Valmy
2012	light summer	Hemingway Bus	Brownlee	Kemano	Hunter	Jim Bridger
2022	heavy winter	Hemingway Bus	Brownlee	Jim Bridger	Hunter	Currant Creek
2022	light summer	Hemingway Bus	Brownlee	Jim Bridger	North Valmy	Kemano
2022	light spring	Hemingway Bus	Brownlee	Jim Bridger	Hunter	Kemano
2022	light spring (Note 1)	Hemingway Bus	Brownlee	Jim Bridger	Hunter	Kemano
2022	light spring (Note 2)	Hemingway Bus	Brownlee	Jim Bridger	Hunter	Kemano
2022	light spring (Note 3)	Hemingway Bus	Brownlee	Jim Bridger	Hunter	Kemano
2022	light spring (Note 4)	Hemingway Bus	Brownlee	Hunter	Jim Bridger	Kemano
2012	heavy summer	Midway Bus	Diablo Canyon	Kemano	Sundance	Rawhide
2012	heavy winter	Midway Bus	Diablo Canyon	Haynes	Kemano	Edward Hyatt
2012	light summer	Midway Bus	Diablo Canyon	Rawhide	Kemano	Laramie River
2022	heavy winter	Midway Bus	Diablo Canyon	Haynes	Rawhide	Kemano
2022	light summer	Midway Bus	Diablo Canyon	Rawhide	Sundance	Edward Hyatt
2022	light spring	Midway Bus	Diablo Canyon	Rawhide	Laramie River	Sundance
2022	light spring (Note 1)	Midway Bus	Diablo Canyon	Rawhide	Haynes	Sundance
2022	light spring (Note 2)	Midway Bus	Diablo Canyon	Rawhide	Haynes	Laramie River
2022	light spring (Note 3)	Midway Bus	Diablo Canyon	Haynes	Rawhide	Sundance
2022	light spring (Note 4)	Midway Bus	Diablo Canyon	Rawhide	Haynes	Laramie River
2012	heavy summer	Double Palo Verde	Sundance	Sheerness	San Juan	Kemano
2012	heavy winter	Double Palo Verde	San Juan	Silverhawk	Sundance	Diablo Canyon
2012	light summer	Double Palo Verde	Sundance	Sheerness	Kemano	San Juan
2022	heavy winter	Double Palo Verde	San Juan	Sundance	Sheerness	Navajo
2022	light summer	Double Palo Verde	Sundance	Sheerness	San Juan	Kemano
2022	light spring	Double Palo Verde	Sundance	San Juan	Navajo	Silverhawk
2022	light spring (Note 1)	Double Palo Verde	San Juan	Navajo	Sundance	Silverhawk
2022	light spring (Note 2)	Double Palo Verde	San Juan	Navajo	Sundance	Silverhawk
2022	light spring (Note 3)	Double Palo Verde	San Juan	Navajo	Sundance	Silverhawk
2022	light spring (Note 4)	Double Palo Verde	San Juan	Navajo	Sundance	Silverhawk

Table 6: Generators with maximum relative speed

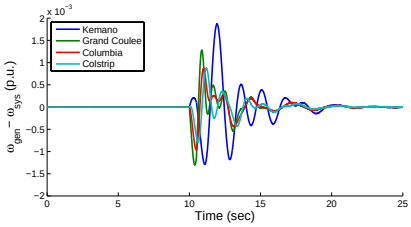

(a) 2012 heavy summer.

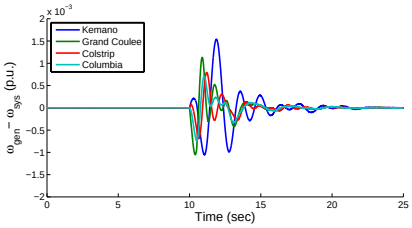

(b) 2012 heavy winter.

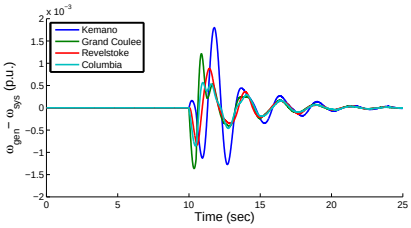

(c) 2012 light summer.

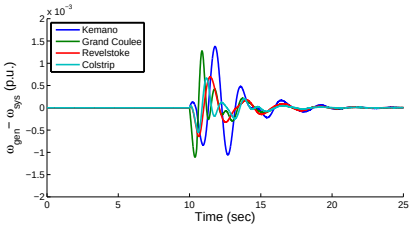

(d) 2022 heavy winter.

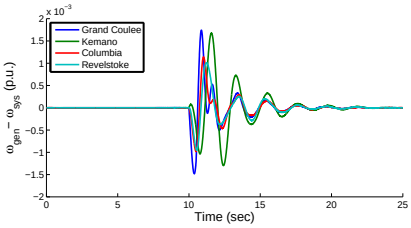

(e) 2022 light summer.

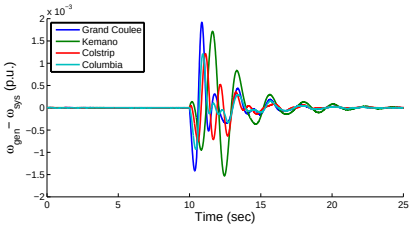

(f) 2022 light spring.

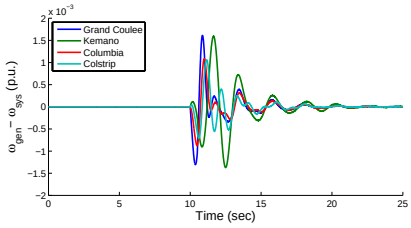

(g) 2022 light spring, all type 3/4 wind replaced with **genrou** with governor response.

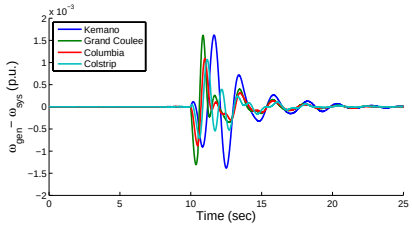

(h) 2022 light spring, all type 3/4 wind replaced with **genrou**, no governor response.

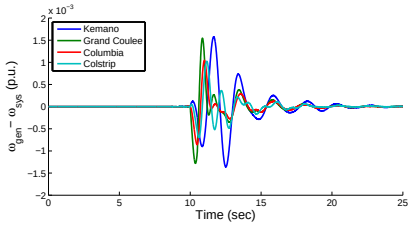

(i) 2022 light spring, all wind replaced with **genrou** with governor response.

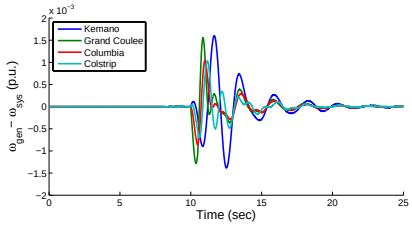

(j) 2022 light spring, all wind replaced with **genrou**, no governor response.

Figure 17: Maximum speed error relative to system speed. 1.4 GW Chief Joseph brake insertion for 0.5 seconds.

5 Small Signal Stability: 6-Bus, 4-Generator System

Small signal stability refers to the ability of a power system to maintain synchronism in the face of small disturbances. Small disturbances are those which perturb the system in a way that the system can be described through the use of linear equations. Two main types of oscillations are observed when a small disturbance arises: local oscillations and inter-area oscillations. These oscillations, also known as modes, are categorized based on the interaction between generators.

Local modes occur when electrically close generators or groups of generators oscillate against each other within an area. These electrically close generators are interconnected by impedances that are small in comparison to impedances involved in the inter-area transmission of power. Local modes can be caused by inadequate tuning of control systems such as generator exciters and are generally observed at frequencies higher than 1 Hz.

Inter-area modes occur when groups of electrically distant generators swing against each other. The interconnection between these electrically distant areas present impedances values much larger (e.g., 10 times) than the impedances connecting the generators within each area. Inter-area modes generally occur across heavily loaded or weak transmission paths at frequencies between 0.1 and 1 Hz.

Local damping conditions of either local or inter-area oscillations can result in service interruptions in the electric grid. However, because inter-area modes occur across large geographic regions covered by multiple balancing authorities, they are more difficult to detect than local modes. When inter-area mode damping is insufficient and a small disturbance arises, the magnitude of the oscillations between areas can increase over time and lead to a break out of the interconnection. Then, a mismatch between load and generation within local areas is caused by the interruption of power imports and/or exports. An example of such behavior is the August 10, 1996 WECC blackout that interrupted service to over 7 million customers in the western United States. Currently, Phasor Measurement Unit (PMU) data is analyzed to detect low damping conditions. However, as the power system changes, mainly due to the introduction of renewable portfolio standards in several western states, the nature of these inter-area oscillations also changes.

The result presented in this section is a prelude to effects observed in simulation for a future WECC configuration having greater wind penetration. Specifically, in a following section, the impact of increased wind penetration on the mode frequency and mode shape of inter-area oscillations in the 2022 Light Spring base case will be studied. Although a reduced system inertia is considered a problem, the resulting increase in mode frequency may in fact be a benefit. In particular, it is noted that the first swing angular deviation is affected both by the severity of the relative rotor speed error and by the modal frequency. For a dominant damped modal frequency of f_m in Hertz, a damping coefficient of ζ, the relative rotor speed error, $\Delta\omega_i$, is approximated as

$$\Delta\omega_i \approx Ae^{-\zeta\omega_0 t}\sin(2\pi f_m t), \quad \text{(radians/sec)} \tag{22}$$

where A is in radians/sec,

$$\omega_0 = \frac{2\pi f_m}{\sqrt{1-\zeta^2}} \tag{23}$$

is the undamped frequency in radians/sec and the stimulus is assumed to begin at $t_0 = 0$. The first swing angular deviation, $\Delta\delta_i$, is approximated by integrating equation (22) from $t_0 = 0$ to $t = \frac{1}{4f_m}$ as follows

$$\Delta\delta_i\left(\frac{1}{4f_m}\right) \approx \frac{A}{(2\pi f_m)^2 + (\zeta\omega_0)^2}\left(2\pi f_m - \zeta\omega_0 e^{-\frac{\zeta\omega_0}{4f_m}}\right), \quad \text{(radians)} \tag{24}$$

It is noted, however, that $\Delta\delta_i$ is not maximized at $t = \frac{1}{4f_m}$ but rather at $t = \frac{1}{2f_m}$ for this approximation, giving the result

$$\Delta\delta_i\left(\frac{1}{2f_m}\right) \approx \frac{A2\pi f_m}{(2\pi f_m)^2 + (\zeta\omega_0)^2}\left(1 + e^{-\frac{\zeta\omega_0}{2f_m}}\right), \quad \text{(radians)} \tag{25}$$

Thus the relative rotor angle deviation may be reduced either by a reduction in A, an increase in damping ζ, an increase in the modal frequency f_m, or an increase in the dominant undamped frequency ω_0. Clearly,

f_m and ω_0 are closely related. An increase in f_m can result from either an increase in ω_0 and/or a decrease in damping ζ. However, the sensitivity of f_m to changes in ζ tends to be small for small values of ζ.

In this section we present an analysis of inter-area oscillations using a 6-bus 4-generator model with generators grouped in two areas. This system was modified to show the effects of renewable energy penetration on inter-area modes. Conclusions from this 6-bus test system provide insight into behaviors observed in larger power systems.

5.1 Wind Generation Effects on Inter-area Mode

The inter-area mode in the 6-bus 4-generator small test system shown in Figure 18 was simulated with a fault at bus 5 in order to excite the inter-area mode. The fault was applied at 10 seconds and it is cleared after 0.1 seconds at 10.1 seconds. To determine the effects of wind generation in the inter-area mode, the simulation was first performed for a system where all 4-generators are thermal plants. Then, GEN3 is replaced with a type 4 wind plant and the simulation is performed again.

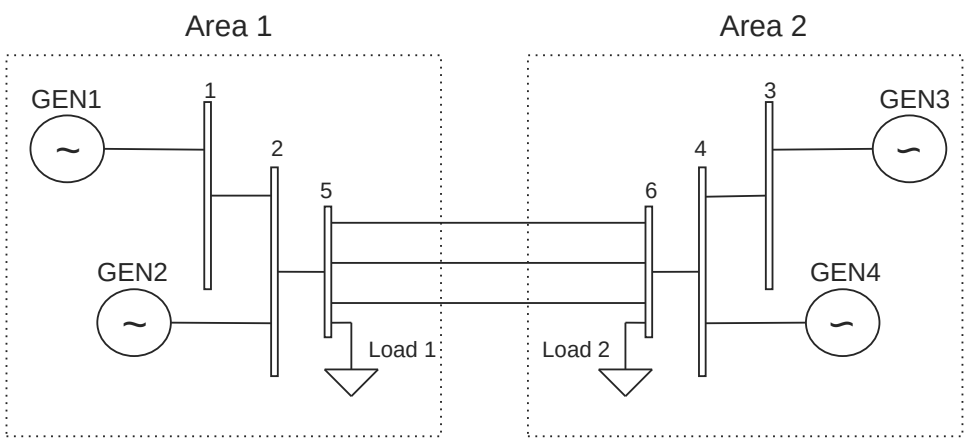

Figure 18: 6-Bus, 4-Generator test system.

Note that the only difference between the 6-Bus system here presented and the 7-Bus system presented previously is that GEN5 and bus 7 that connects it to the system are not present in the 6-Bus system. Recall that in the transient stability simulation GEN5 was lost. In such case, the 7-bus system and the 6-bus system are identical. We will refer to GEN1 and GEN2 as being located in *Area 1* and GEN3 and GEN4 as being located in *Area 2*.

Figure 19 shows output power results of the simulations with all-thermal generation and when GEN3 is replaced with a type 4 wind plant. When a fault is applied at bus 5, there is an instantaneous reduction in electrical load which creates a mismatch between electrical and mechanical torques. Generator speeds increase due to this mismatch and the moment of inertia of each synchronous machine increases. Simulation results showing the effects of changing GEN3 from a thermal plant into a type 4 wind plant on generator speeds are shown in Figure 20. Once the fault is cleared after 0.1 seconds, the balance between mechanical and electrical torques is reestablished and generators decelerate. Electrically close generators decelerate at a similar rate, while generators separated by large impedances decelerate at different rates. Thus, two areas are formed and inter-area oscillations take place.

Figure 20(a) shows generators in Area 1 oscillating together. Generators in Area 2 also oscillate together but are in anti-phase to generators in Area 1. This is the inter-area mode. In this example, the inter-area mode dies down after 15 seconds approximately, which in a real power system would be considered poor damping. Simulation results for generator speeds when GEN3 is replaced with a type 4 wind plant are shown in Figure 21(b). Since type 4 wind generators are asynchronous machines with a power electronics interface to the grid, speed from GEN3 does not appear in this figure. In this case, generators in area 1 oscillate against GEN4 (shown in red) located in Area 2. When comparing these results with the all-thermal generation case, three effects can be identified from the addition of wind are discovered: (i) the amplitude

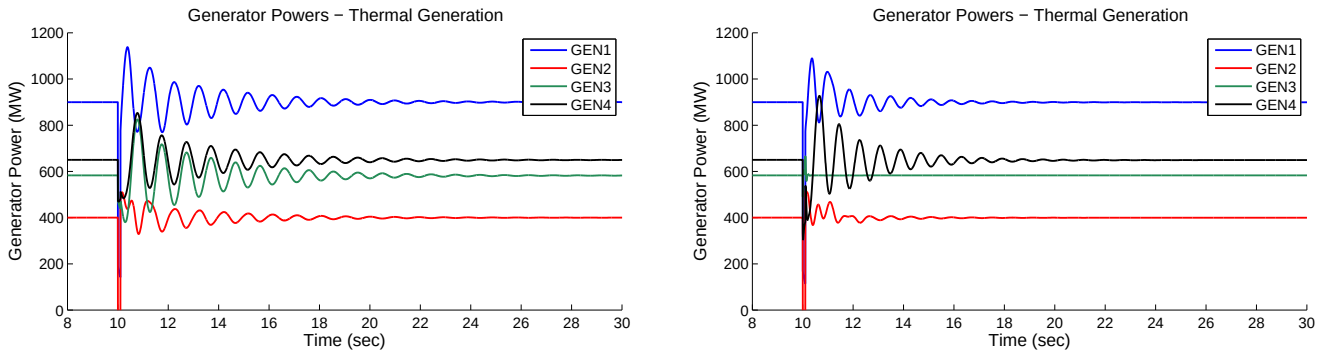

(a) All-thermal generation.

(b) GEN3 replaced with a type 4 wind plant.

Figure 19: Generator power simulation results for 6-bus, with 4 with all-thermal generation and replacing GEN3 with a type 4 wind plant.

of GEN4 oscillations has increased; (ii) the amplitude of the oscillations seen in generation located in Area 1 has decreased; and (iii) inter-area oscillations take less time to die down, or in other words, there is an improvement on damping.

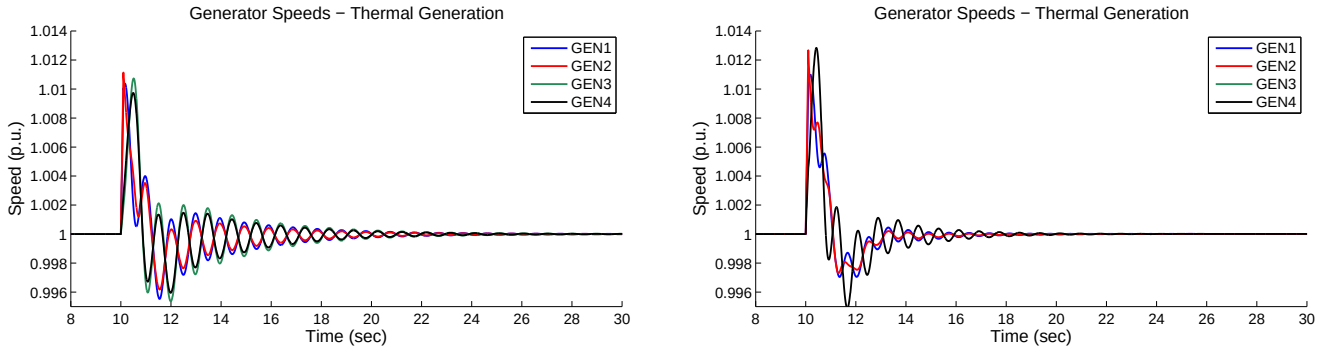

(a) All-thermal generation.

(b) GEN3 replaced with a type 4 wind plant.

Figure 20: Generator speed simulation results for 6-bus, with 4 with all-thermal generation and replacing GEN3 with a type 4 wind plant.

Prony analysis was employed to determine the frequency and damping of the inter-area oscillations in both cases, with all-thermal generation and when GEN3 is replaced with a wind plant. Results of Prony analysis on the difference of speeds between GEN1 and GEN4 are shown in Figure 21. The time axis have been set such that the disturbance occurs at time $t = 0$. Results of Prony analysis on the difference of speeds between GEN2 and GEN4 are shown in Figure 22.

Prony results from 21 and 22 show that the frequency of inter-area oscillations increased from 1.03 Hz to 1.24 Hz when wind replaces conventional generation causing a reduction in inertia. Additionally, the damping of inter-area oscillations decreases slightly. This might be a side effect of the change in frequency since power system stabilizers tend to be better at damping oscillations at higher frequencies.

5.2 Effect of Wind Controls on Inter-area Mode

Wind controls were described in Section 3.4. The first type of control uses frequency feedback with proportional gain to emulate droop control. The second type of control adds a term proportional to the differential of the (local) frequency to improve the inertia of the system. In this section we discuss the effects of these two control schemes on the inter-area mode observed in the 6-buses, 4-generator system.

The same fault at bus 5 is applied to the system. Figure 23 presents the simulation results corresponding

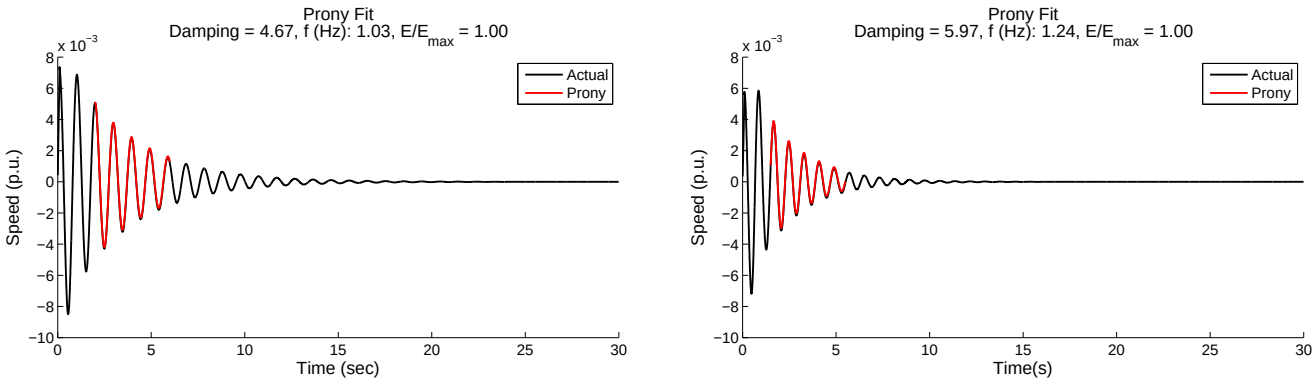

(a) All-thermal generation.

(b) GEN3 replaced with a type 4 wind plant.

Figure 21: Prony analysis of GEN1-GEN4 speed for the all-thermal case and replacing GEN3 with a type 4 wind plant.

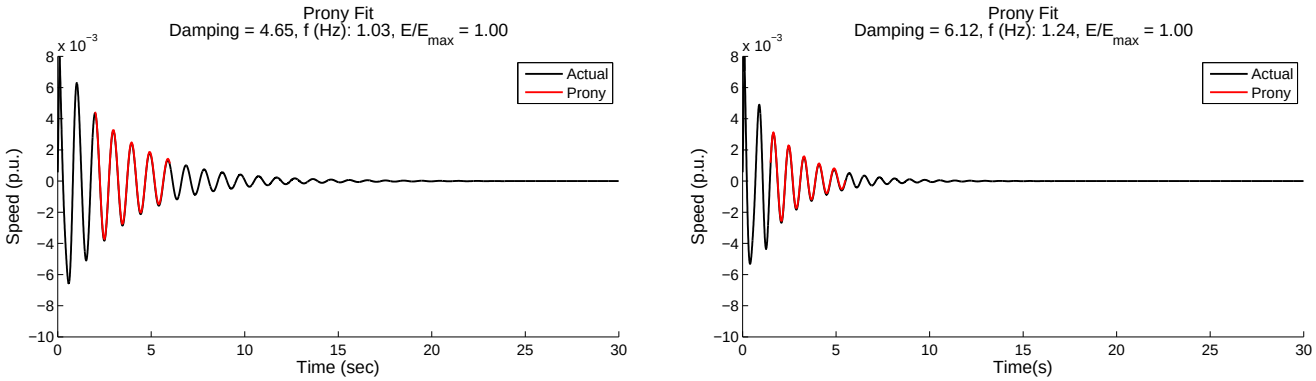

(a) All-thermal generation.

(b) GEN3 replaced with a type 4 wind plant.

Figure 22: Prony analysis of GEN2-GEN4 speed for the all-thermal case and replacing GEN3 with a type 4 wind plant.

to the output power of the different generators in the system. In the case where GEN3 has droop control, its output power is reduced as a response to a higher than nominal frequency. This in turn reduces the ripple in the output power of other generators in the system when compared to the results seen in Figure 19. When GEN3 is equipped with droop control and inertial emulation, the magnitude of the ripple in the output power of other generators is even further reduced. This is the result of GEN3 better counteracting frequency deviations thanks to the derivative term in the control scheme.

Simulation results of generator speeds are depicted in Figure 24. Speed of GEN3 does not appear in the plot because the wind plant is an asynchronous generator connected to the grid via power electronics, hence its frequency differs from that of the grid. When droop control is added to GEN3, oscillations of other generators are reduced. The first speed swing of GEN4 is reduced from 1.012 to 1.01 p.u. which indicates an increase of synchronizing torque in the system. The oscillations in both areas are completely damped after 6 seconds, which indicates an increase of damping torque in the system. When inertial emulation is added, the initial speed swing of GEN4 is further reduced to less than 1.009 p.u. and the oscillations in both areas are completely damped after 4 seconds.

Prony analysis was performed on the generator speed signals in order to compare the damping and frequency of the inter-area mode. The results for Prony on GEN1-GEN4 speed are shown in Figure 25 for the cases where droop control and inertial emulation was present in the wind plant. In the case where droop control was added, the inter-area mode damping increased from 6.12% to 11.55%, at approximately the same frequency as in the wind plant with no controls. In the case where inertial emulation was also

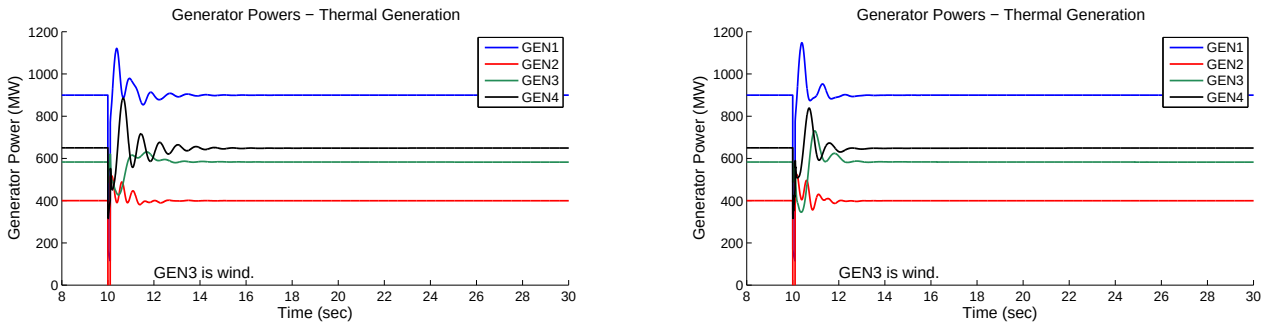

(a) GEN3 has droop control.

(b) GEN3 has droop control and inertial emulation.

Figure 23: Generator power simulation results for 6-bus, with 4 with type 4 wind GEN3 with droop control and inertial emulation.

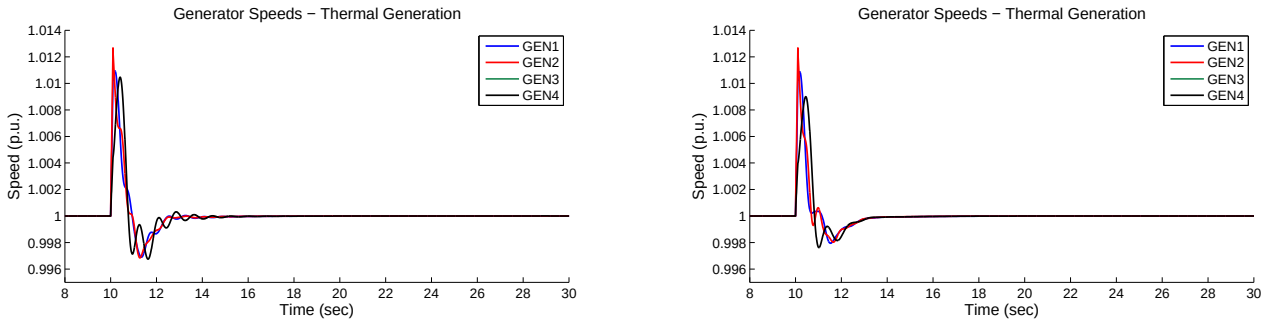

(a) GEN3 has droop control.

(b) GEN3 has droop control and inertial emulation.

Figure 24: Generator speed simulation results for 6-bus, with 4 with type 4 wind GEN3 with droop control and inertial emulation.

available in the wind plant, a dramatic increase in the damping of the inter-area mode was observed to approximately 33%.

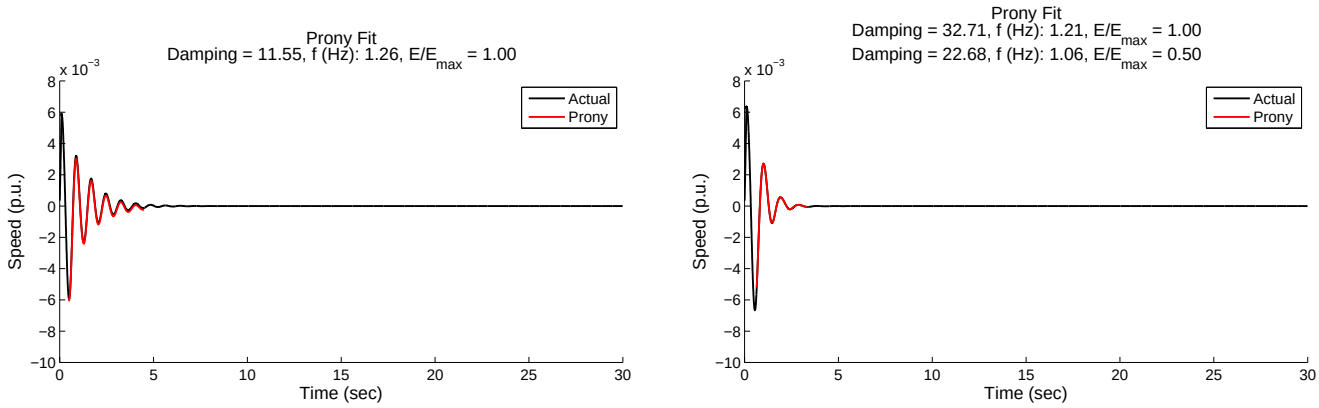

(a) GEN3 has droop control.

(b) GEN3 has droop control and inertial emulation.

Figure 25: Prony analysis of GEN1-GEN4 speed when replacing GEN3 with a type 4 wind plant with droop control and inertial emulation.

Prony analysis of GEN2-GEN4 speeds in Figure 26 shows that when GEN3 has droop control the

damping of the inter-area mode doubles from the case where no controls are present in the wind plant, confirming the results from the Prony analysis performed on GEN1-GEN4 speeds. The frequency of the mode does not change significantly. Prony results for the case where GEN3 has droop control and inertial emulation shows similar results, for the mode at 1.26 Hz. However, other modes are observed. This seems to be a numerical artifact due to the short duration of the oscillations.

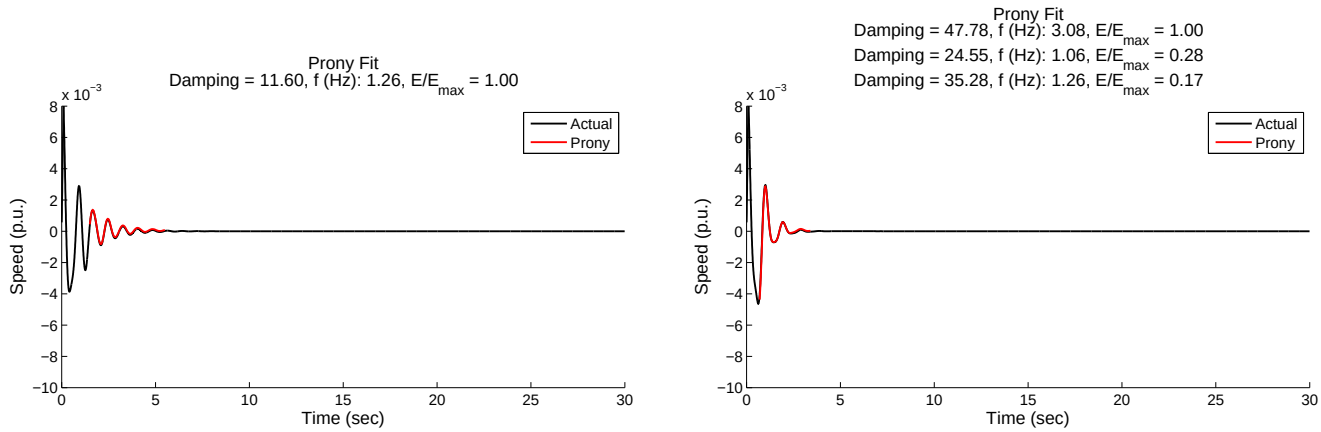

(a) GEN3 has droop control.

(b) GEN3 has droop control and inertial emulation.

Figure 26: Prony analysis of GEN2-GEN4 speed when replacing GEN3 with a type 4 wind plant with droop control and inertial emulation.

In conclusion, wind generation with a power electronics based interface to the grid, such as type 3 and 4 wind turbines, does not have a negative effect on the damping of inter-area modes. The frequency of the oscillations increases from the all thermal generation case and because control systems found in generators such as power system stabilizers are good at damping higher frequency oscillations, damping of the inter-area modes in our test system seems to increase slightly. When droop control and inertial emulation are part of the wind plant, simulation results show that damping and synchronizing torque in the system improve.

6 Small Signal Stability: WECC

To study the impact of increased renewable energy penetration on small signal stability in the WECC, PSLF was used to simulate the insertion of the Chief Joseph Dynamic Brake. The Bonneville Power Administration (BPA) installed the 1.4 GW braking resistor at Chief Joseph Dam in 1974 to improve the first swing stability of the system [29]. To simulate the insertion of the dynamic brake, an EPCL script based on the WECC routine *alldyns.p* was developed which inserted a purely resistive shunt at a selected bus. At the beginning of the dynamic simulation the system was allowed to operate unperturbed for 10 seconds to provide it sufficient time to reach steady state. The shunt was inserted for a period of 0.5 seconds, and following its removal the dynamic simulation continued for another 30 seconds. To observe the effect of disturbance location on the excitation of inter-area oscillation modes, the dynamic brake insertion was simulated at four locations: Chief Joseph Dam, El Dorado Substation, Midway Substation, and Hemingway Substation. The latter three locations were selected because they are important substations connected to the 500 kV transmission system. Figure 3 illustrates the locations of the dynamic brake insertions.

Prony analysis is an effective tool for estimating the modal content of power system oscillations from measured ringdowns [27]. In this study, Prony's method was used to fit a linear combination of exponential terms to the portion of each monitored generator speed signal following the removal of the resistive brake. The employed method assumed the system to be single-input, single-output (SISO) with distinct eigenvalues. For a given mode of oscillation, this system identification technique yields frequency and

damping estimates that vary across ringdowns [30]. To account for this effect, a centroid-based clustering algorithm was used to group complex exponential terms according to frequency. Each cluster was treated as a distinct mode of oscillation, and the maximum residue magnitude of each mode was normalized to one to allow for comparison of relative participation. When each term of the linear combination is expressed as a damped sinusoid, the magnitude of the residue corresponds to one half the amplitude of the sinusoid. The calculated damping ratios were expressed as a percentage and recorded in the mode summary tables.

The Prony analysis described above generates a large volume of data, and one of the challenges of this study was to present the results in a form that allows one to quickly obtain the important information. To address that challenge, a map was created for each mode displaying a marker at the location of each of the 23 monitored generators. For a particular generation unit, the area of the marker is proportional to the magnitude of the residue. The magnitude of the residue represents how much, if at all, a generation unit participates in a given mode of oscillation. The color of the marker is indicative of the angle of the residue. When a term of the linear combination from Prony's method is expressed as a sinusoid, its phase angle corresponds to the residue angle. The mode shape maps do not display information about the damping ratio of the modes. This information is presented in tabular form in Appendix D.

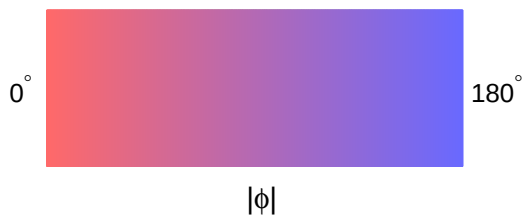

Figure 27: Relationship between marker color and residue angle.

The color of the map markers was calculated, or mixed, using a custom function written in MATLAB® . The function maps the absolute value of the residue angle onto a color spectrum between red and blue. If the residue angle is zero degrees, the marker color is a shade of pure red. Conversely, if the residue angle is 180 degrees, the marker color is a shade of pure blue. For all other angles, the function mixes the shades of red and blue to arrive at a shade of purple which is more red for angles near zero degrees, and more blue for angles near 180 degrees. Marker color remains constant in the event of a sign change because the input of the function is the absolute value of the angle. For example, residue angles of -10 degrees and 10 degrees both produce the same marker color. By convention the generation unit with the largest residue magnitude is selected to be the angle reference for the mode, so its marker color is pure red. Please see Figure 27 for a visual depiction of the relationship between marker color and residue angle.

6.1 Modes of Oscillation Excited by a Chief Joseph Brake Insertion

There were two modes of oscillation excited by a Chief Joseph Brake Insertion in which a large number of generators participated, and the mode shape remained consistent across cases. Classically, mode shape is defined by the right eigenvector of a mode of oscillation, which includes the residue magnitude and angle [30]. In the context of this report, it also refers to the geographical distribution of the participating generation units. For both mode shapes, the frequency of oscillation varied slightly across cases. For instance, the frequency of oscillation of one of the modes migrated from 0.23 Hz in the 2012 heavy summer case to 0.29 Hz in the 2022 light summer case. Notably, no mode of oscillation with a frequency in this range was observed in the 2022 light spring case which features the highest penetration of renewable energy. The other most prevalent mode of oscillation was observed in a frequency range between 0.35 Hz and 0.47 Hz. It is challenging to pinpoint precisely which factors determine the frequency migration of a mode across WECC base cases; however, the primary differences between the cases are the loading condition and generation mix, so it is likely that these factors play a role.

In addition to those previously mentioned, other inter-area oscillation modes were observed sporadically. These modes were not excited across a majority of cases, nor did they possess a consistent, predictable mode shape. The sporadically observed modes can be loosely grouped into three categories. The defining characteristic of the first category is that Kemano, in northern British Columbia, oscillates against other units in the system. The observed frequency of oscillation for this mode varied between 0.56 Hz and 0.72 Hz. The defining characteristic of the second category is that Colstrip in Montana oscillates against other units in the system. This mode was observed at a frequency of 0.79 Hz in the 2022 heavy winter case. The defining characteristic of the third category is that units in the American Pacific Northwest oscillate against other units in the system. In some cases, the mode appeared to be driven by Brownlee on the Oregon-Idaho border, and in other cases it appeared to be driven by the units in Washington.

6.1.1 0.23 to 0.29 Hz, North-South Mode

For the 0.23 Hz to 0.29 Hz mode, the generators with the largest amplitude of oscillation are located at the Sheerness and Sundance Generating Stations in Alberta. Depending on the loading condition and generation mix, either or both of the monitored generators in British Columbia can participate as well. For this mode, the oscillations of the generators in Alberta and British Columbia are in phase. Geographically, the units which have a phase angle near zero are located north of the 45th parallel, which tracks the border between Montana and Wyoming. The one exception to this rule occurs in the 2022 light summer case in which the monitored generator at North Valmy in Nevada has a phase angle of approximately 31 degrees. In terms of absolute deviation, the phase angle of the monitored unit at North Valmy is closer to that of the reference than the monitored unit at Colstrip, which has a phase angle of approximately -33 degrees.

The generators which participate in this mode that are most out of phase with the units in Alberta are located primarily in Utah, Arizona, and Colorado. This mode can be described, roughly speaking, as generators in Alberta oscillating against units in the states which meet at Four Corners region of the American Southwest. Although these are two key areas involved in the oscillation mode, in various cases, generators in every state/province in the WECC region participate. The characteristics of this mode which vary from one case to the next are the frequency of oscillation, the units which participate, and the location of the generators which are most out of phase with the reference.

In the 2012 heavy summer case, this mode shape is observed at a frequency of 0.23 Hz, which is the lowest for any of the WECC base cases. This case also has the highest loading and generation of any of the cases, with slightly more than 185 GW of power produced. In this case, Revelstoke Dam in British Columbia participates in the mode, but Kemano does not. This means that the insertion of the Chief Joseph Brake did not excite an oscillation near 0.23 Hz at Kemano. The generator with the largest per unit oscillation amplitude was Sundance, which means that it serves as the angle reference for the mode. The generator which is most out of phase with the reference is located at Craig Station in western Colorado. Of the units which are approximately 180 degrees out of phase with the reference, Currant Creek and Hunter in Utah have the largest amplitude. The units which do not participate in this mode for this case are Kemano, Coulee, Hyatt, and North Valmy.

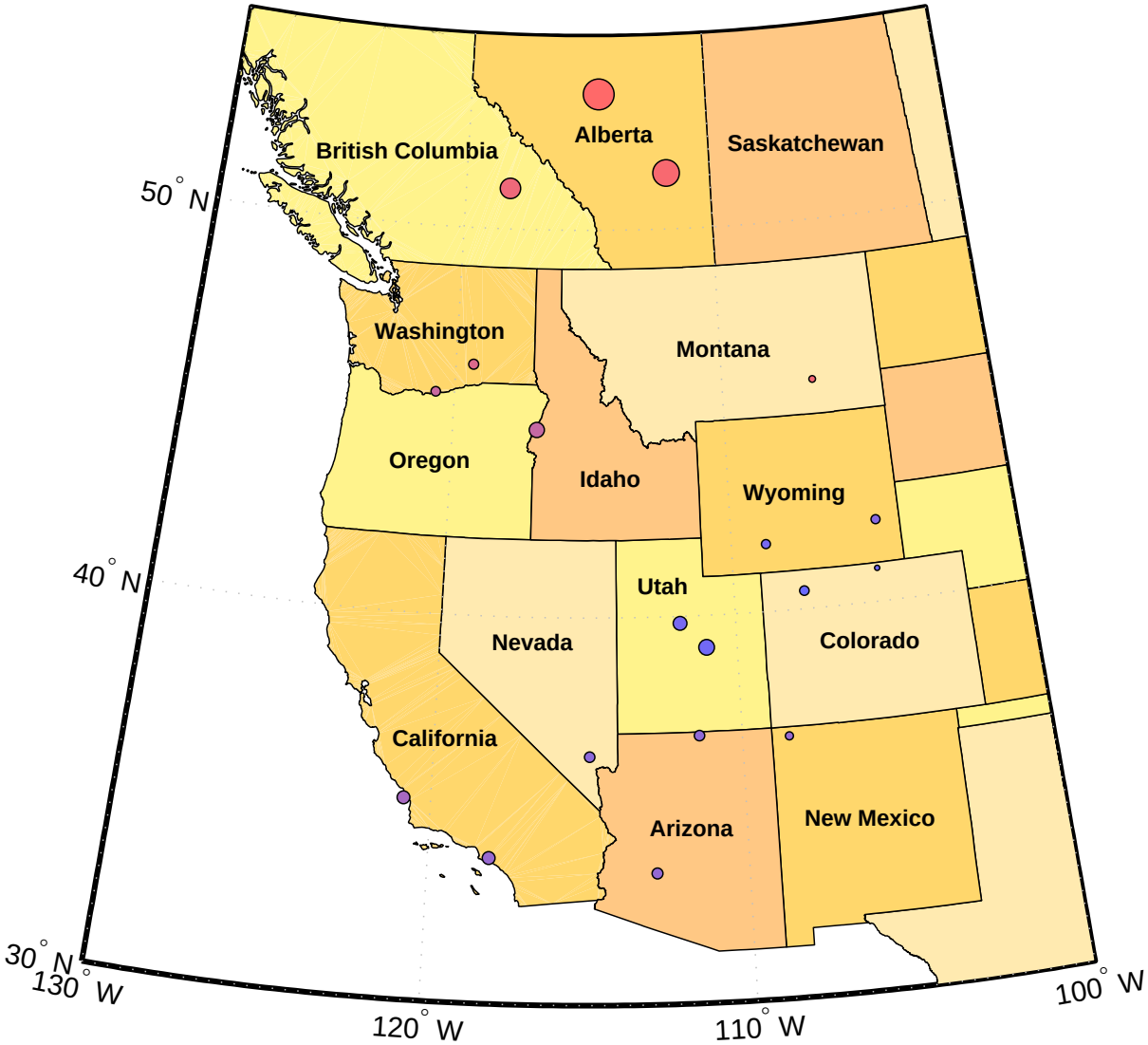

Figure 28: 2012 heavy summer, 0.23 Hz inter-area oscillation mode.

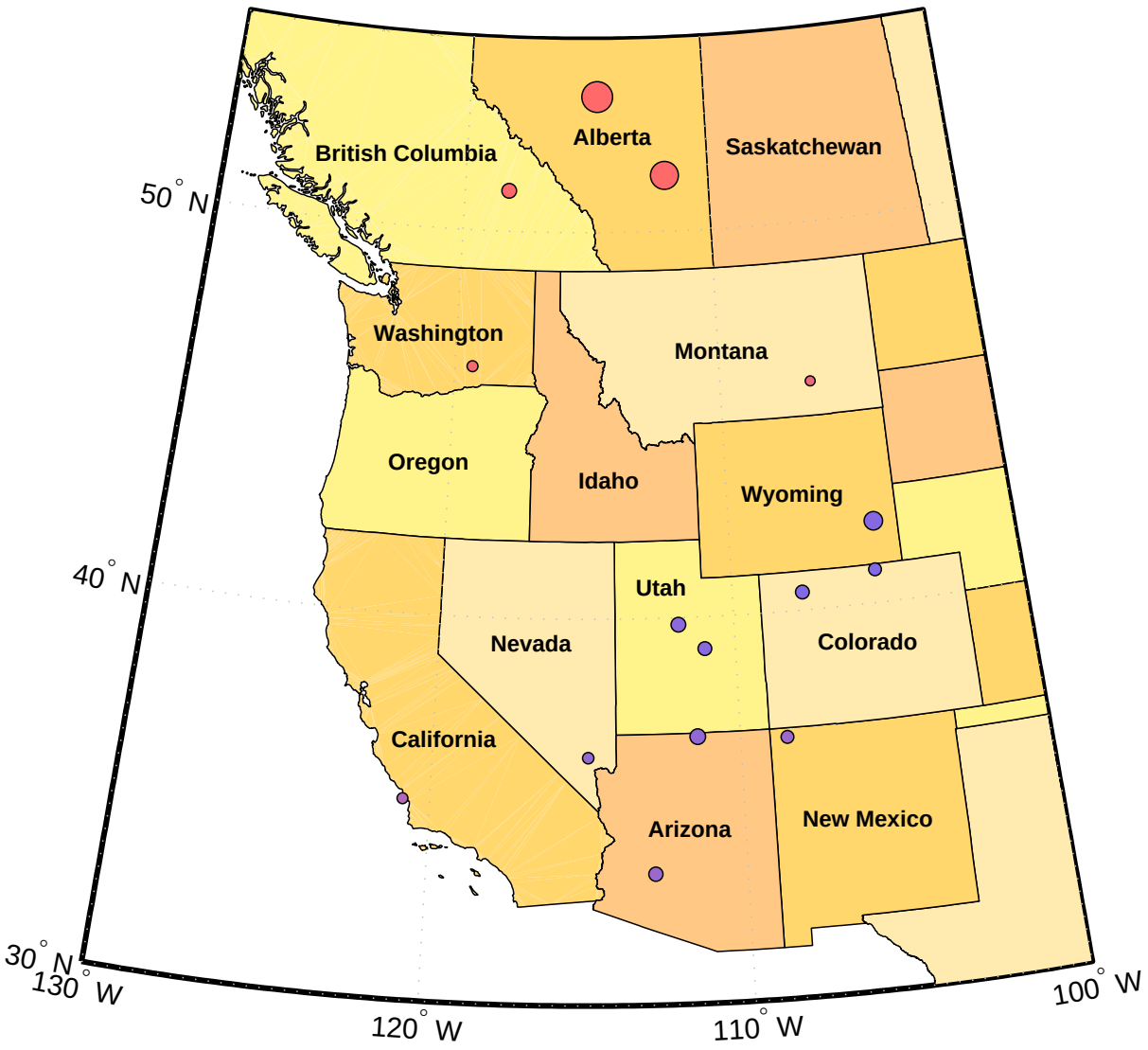

Figure 29: 2012 light summer, 0.24 Hz inter-area oscillation mode.

In the 2012 light summer case, this mode shape is observed at a frequency of 0.24 Hz, which is the frequency at which this mode is most commonly observed. The loading and generation in this case are much lighter than in the 2012 heavy summer case, with slightly more than 120 GW of power produced. Although the difference in loading between the 2012 heavy and light summer cases is greater than 60 GW, the frequency at which this mode oscillates changed by only 0.01 Hz. This implies that changes in system loading alone are not sufficient to explain the observed variation in frequency across cases. It should be noted that the installed wind generation capacity varies minimally between the 2012 heavy and light summer cases.

Again, Revelstoke Dam participates in the mode, but Kemano does not. The generator which is most out of phase with the reference is Rawhide in northern Colorado; however, no generator is more than 147 degrees out of phase with the reference. Of the units that are out of phase with the reference, Laramie, Navajo, and Currant Creek have the largest amplitude.

Figure 30: 2012 heavy winter, 0.24 Hz inter-area oscillation mode.

As in the 2012 light summer case, in 2012 heavy winter this mode shape is observed at a frequency of 0.24 Hz. Notably, no units in Washington, Oregon, Idaho, or Montana participate in this mode for this case. This may be related to the fact that Revelstoke does not oscillate at a frequency near 0.24 Hz; however, more analysis would be required to determine whether or not there is a relationship between the participation of Revelstoke and the oscillation of generators in the American Pacific Northwest.

An interesting characteristic of the 0.24 Hz mode for this case is that the average amplitude of oscillation for the generators south of the 45th parallel is larger than for any of the previously discussed base cases. Recall that Prony's method was performed on the per unit rotor speed signal of each generator, and that the magnitudes of the residues were normalized such that the largest value was equal to one. Therefore, Figure 30 demonstrates that the amplitude of oscillation for the generators in the southern half of the region is larger with respect to that of the generators in Canada than in the other WECC base cases.

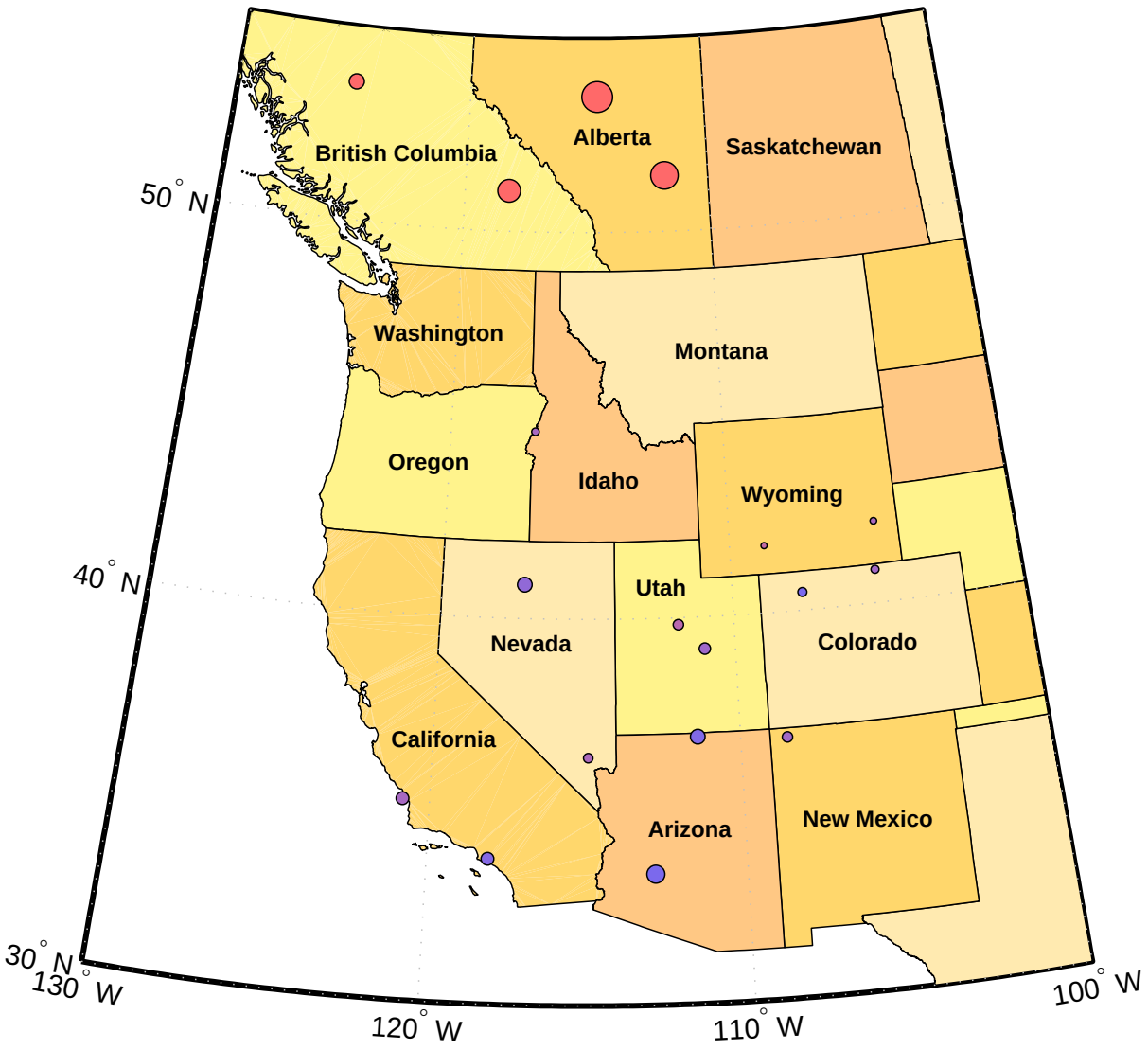

Figure 31: 2022 heavy winter, 0.24 Hz inter-area oscillation mode.

The primary difference between the mode shape depicted in Figure 31 for the 2022 heavy winter case and those presented for the 2012 base cases is that both generating stations in British Columbia, Kemano and Revelstoke, participate. In the 2012 base cases the generators in British Columbia were not observed to participate together. Another characteristic of this mode shape that sets it apart from previous cases is that the generation units that are most out of phase with the reference are located in Arizona, not Utah and Colorado.

Compared with the 2012 heavy winter case, in the 2022 heavy winter case there are a greater number of generation units which participate in the 0.24 Hz mode, which indicates a greater amount of energy at that frequency. In the 2022 heavy winter case, every monitored generator south of the 45th parallel besides Hyatt participates in the mode. Generally, when comparing inter-area oscillations excited by the same disturbance, as the number of generators in an area which oscillate at a particular frequency increases, the average amplitude of oscillation of those generators tends to decrease. A comparison of Figures 30 and 31 illustrates that effect.

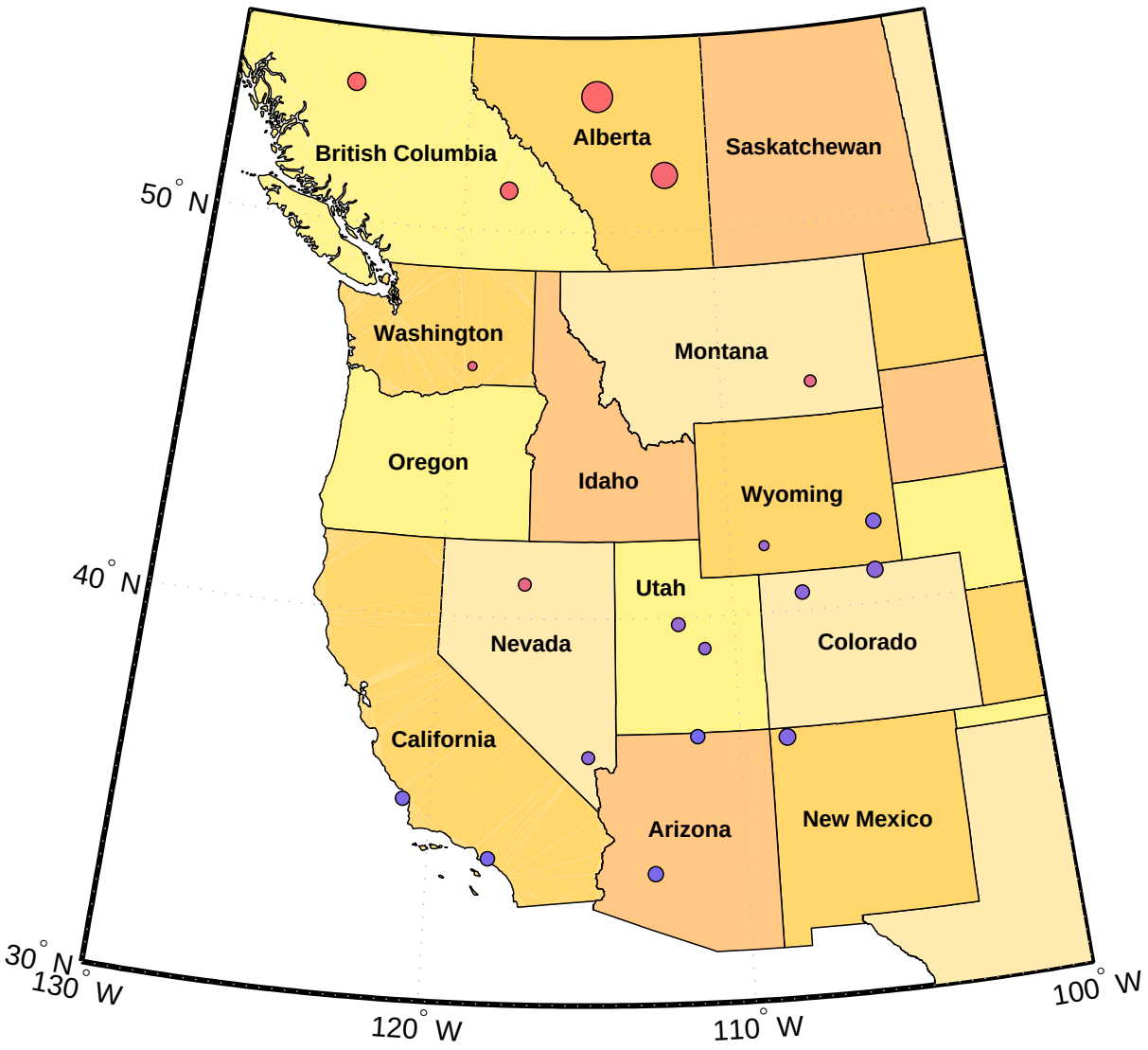

Figure 32: 2022 light summer, 0.29 Hz inter-area oscillation mode.

In the 2022 light summer case, the mode shape in Figure 32 is observed at a frequency of 0.29 Hz. As the frequency of a mode increases, the duration of the oscillation's first swing decreases. In general, this is beneficial from the perspective of first swing stability because the system is more likely to maintain sychronism. Modal frequency is influenced not only by loading condition and generation mix, but also by transmission infrastructure, particularly the impedance between areas.

Compared with the mode shape for 2012 light summer case presented in Figure 29, the mode shape for the 2022 light summer case shows that four additional units participate: Kemano in Canada; and North Valmy, Bridger, and Haynes in the US. At approximately 31 degrees, the phase angle of the 0.29 Hz oscillation at North Valmy is closer to the phase angle of Sundance in Alberta than to that of Silverhawk in southern Nevada. Therefore, the two units in Nevada oscillate against one another, and belong to different geographic regions of the mode.

6.1.2 0.34 to 0.47 Hz, Alberta-B.C. Mode

Characteristically, in the 0.34 to 0.47 Hz mode, the oscillations of the generators in Alberta and British Columbia are out of phase. For this reason, the mode has in the past been referred to as the Alberta-B.C. mode [8]. In practice, it has historically not been observed at a frequency above 0.42 Hz. Throughout the course of a given day, as loading conditions change and different generators go on and off line, the frequency of this mode can naturally drift between approximately 0.34 Hz and 0.39 Hz. In this study, the generation unit with the largest amplitude of oscillation was observed to vary between Kemano, Coulee, and Sundance, with Kemano being the most common. This mode of oscillation was observed in all six WECC base cases, with all 23 monitored generators typically participating.

Geographically, the units which oscillate against one another in this mode are grouped into regions defined by sections of concentric annuli, or rings. Each ring can be visualized as the projection of a donut onto the WECC region. The generation units within each ring oscillate in phase with one another. The outer ring sweeps from Alberta down through western Wyoming, and wraps around to include Arizona and southern California. The inner ring sweeps from British Columbia down through Montana, and wraps around to include Utah and northern California. For particular loading conditions, the colors attributed to the rings flip; that is, the inner ring which is primarily red becomes blue. This occurs because the generation unit with the largest oscillation amplitude shifts from B.C. to Alberta, which results in the position of the angle reference moving from the inner ring to the outer ring.

In the 2012 heavy summer case, this mode is observed at a frequency of 0.35 Hz. A map of the participation of the monitored generator units is displayed in Figure 33. The distinguishing characterstic of the 0.35 Hz mode in the 2012 heavy summer case is that the generator with the largest amplitude of oscillation resides in Alberta. This was the only WECC base case for which a unit in Alberta had the largest amplitude of oscillation at this frequency. North Valmy, a coal-fueled plant in northern Nevada, had the largest amplitude of any monitored unit in the US. In both California and Nevada, generators in the northern half of the state oscillated against generators in the southern half of the state. A similar phenomenon occurs in Wyoming, in which the Jim Bridger plant in the western half of the state oscillates against the Laramie River plant in the eastern half of the state. Although the aforementioned intra-state modes involve generators within the same state oscillating against one another, none of the discussed pairs consist of two units which reside in the same WECC area.

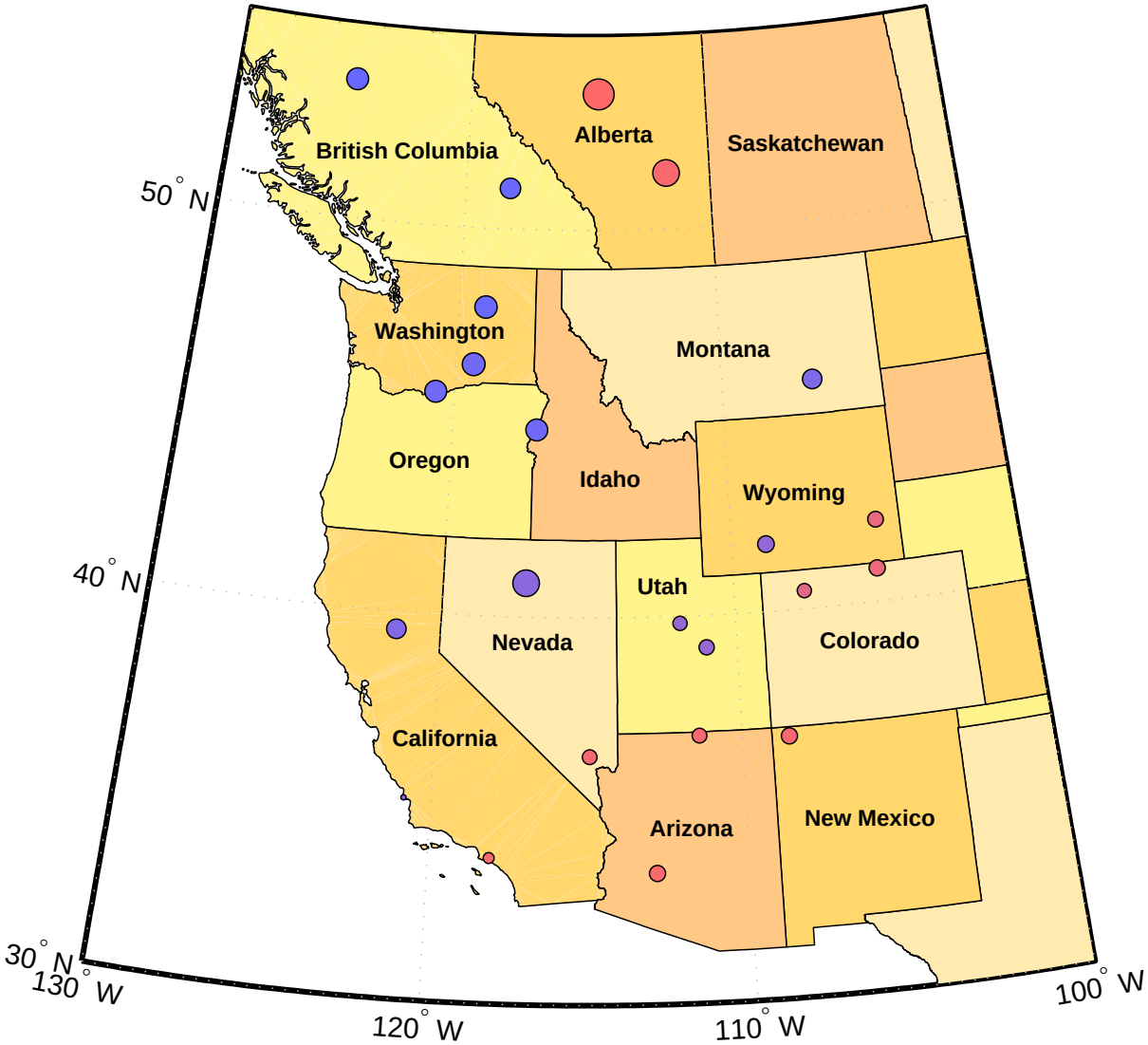

Figure 33: 2012 heavy summer, 0.35 Hz inter-area oscillation mode.

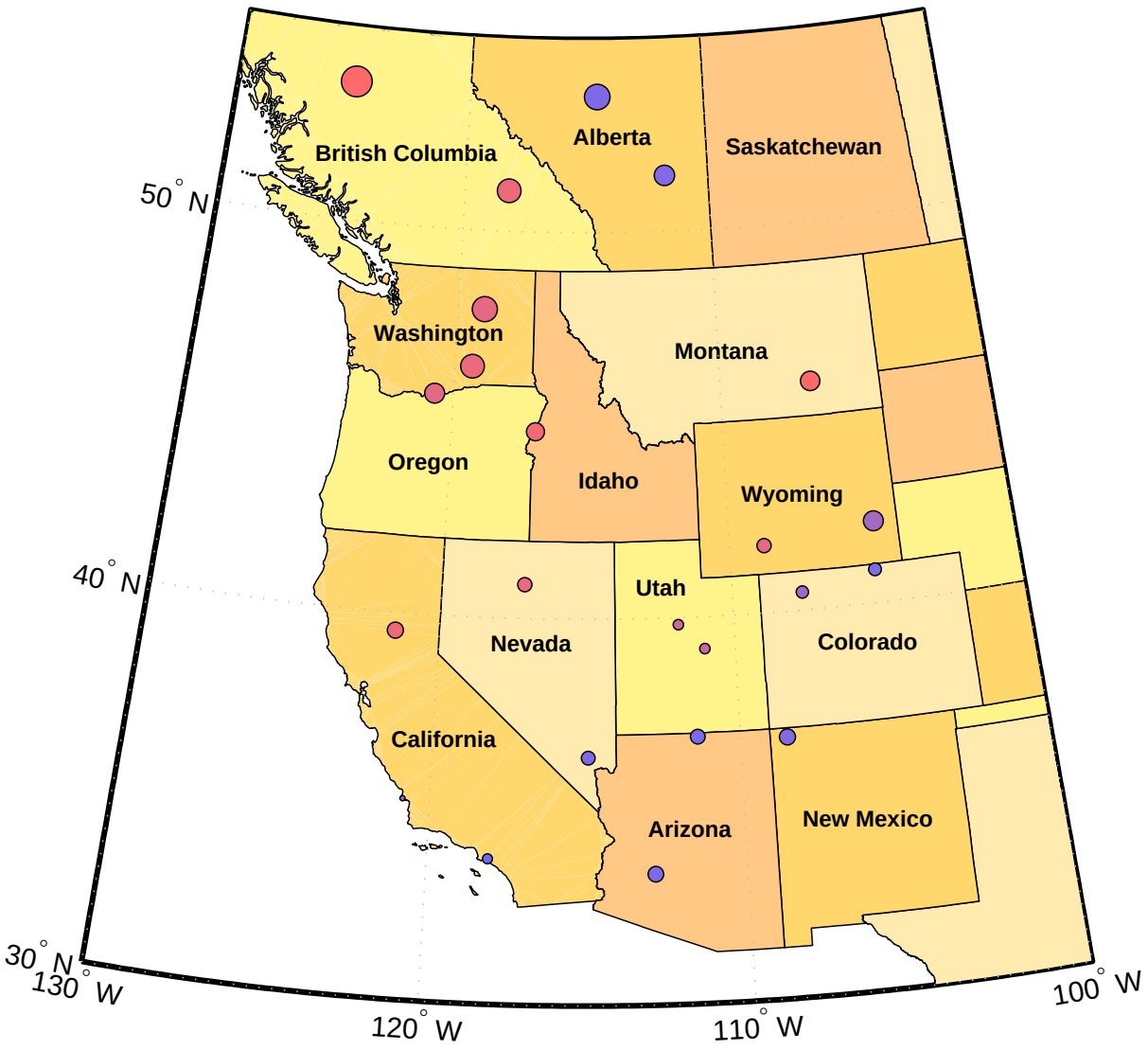

Figure 34: 2012 light summer, 0.40 Hz inter-area oscillation mode.

In the 2012 light summer case, the generator with the largest amplitude of oscillation is Kemano. The generator that is most out of phase with the reference is Haynes in southern California, and the units that are out of phase which exhibit the largest oscillation amplitude are Sundance and Sheerness in Alberta. In each of the 2012 cases, all 23 monitored generators participate in the mode. The generator that is least affected by the 0.34 to 0.47 Hz mode is Diablo Canyon in California. As shown in Figure 34, the marker for Diablo Canyon is barely visible (between Hyatt and Haynes), and its oscillation amplitude is merely three percent of the largest amplitude observed in the system.

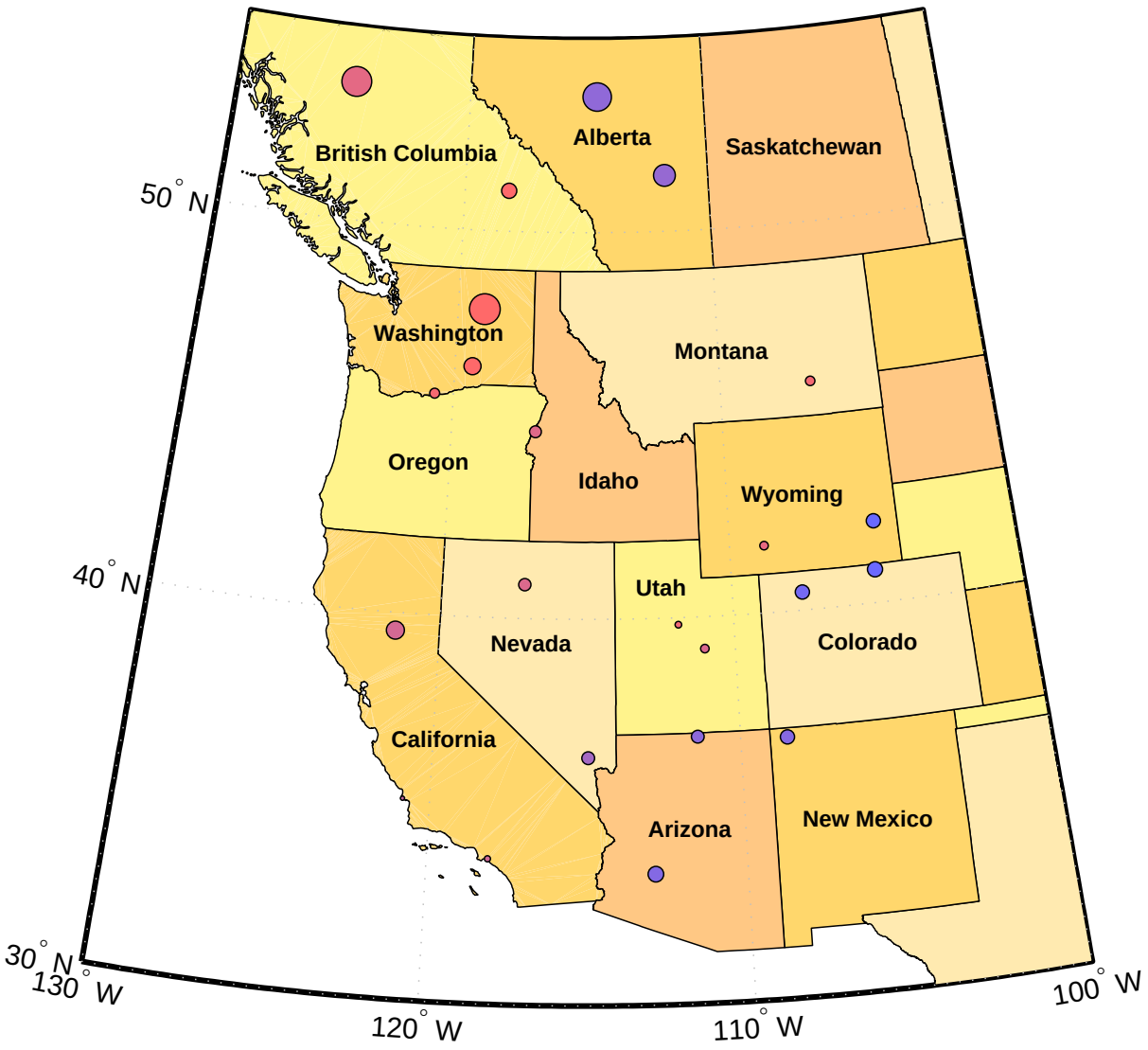

Figure 35: 2012 heavy winter, 0.35 Hz inter-area oscillation mode.

One of the distinguishing characteristics of the 2012 heavy winter case is the very high amount of generation in WECC Area 40, the American Pacific Northwest. In the 2012 heavy winter case the power generation in Area 40 is about 36 GW, as opposed to 29 GW in the 2012 heavy summer case and 18 GW in the 2012 light summer case. This very high level of generation in Washington could partially explain why the monitored unit with the largest amplitude of oscillation was Coulee. The 2012 heavy winter case was the only one in which a unit in the U.S. had the largest amplitude of oscillation. The pronounced asymmetry among the amplitudes of the monitored units in Washington was apparent only in this case.

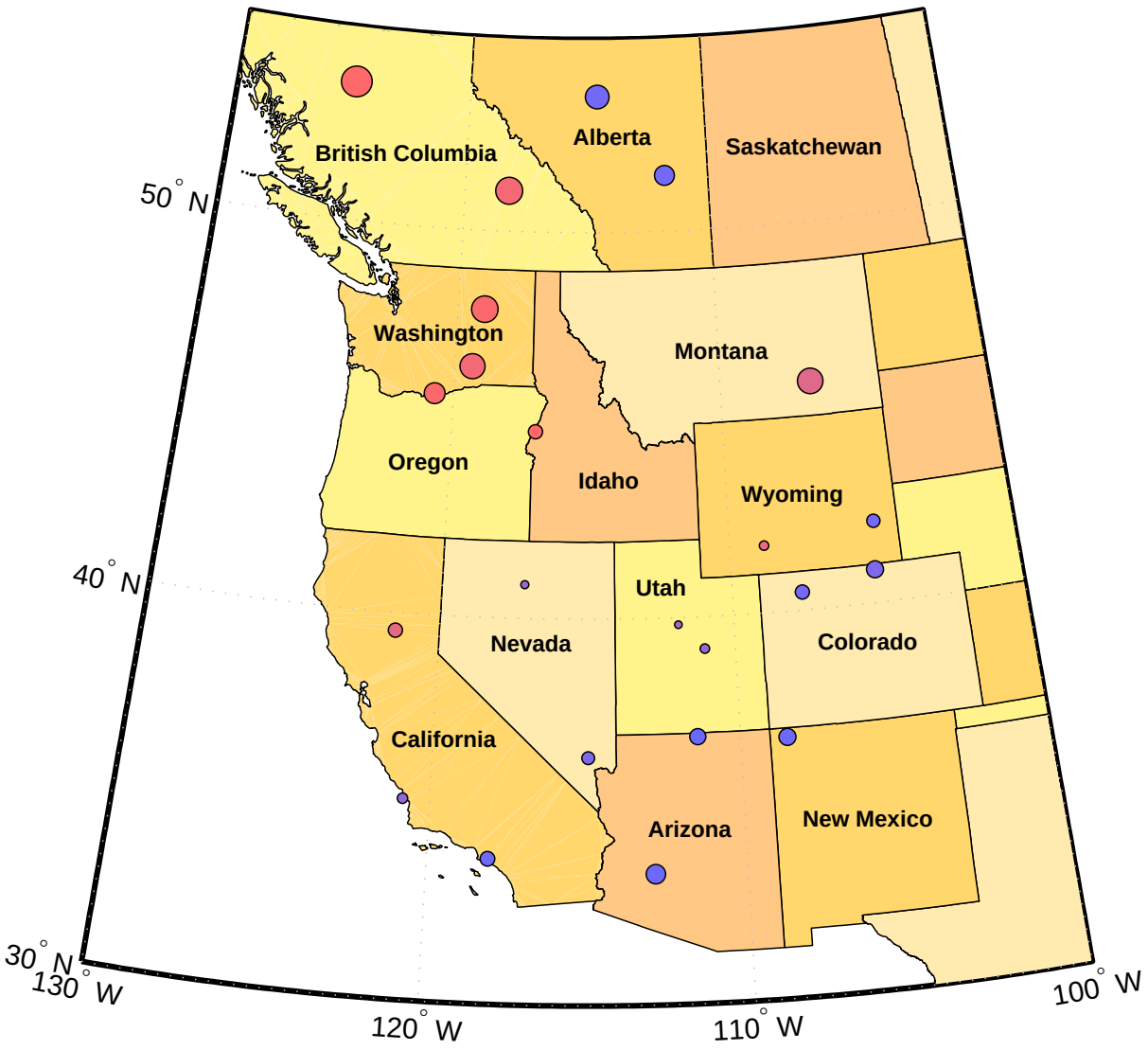

Figure 36: 2022 heavy winter, 0.39 Hz inter-area oscillation mode.

In the 2022 heavy winter case the mode shape displayed in Figure 36 was observed at a frequency of 0.39 Hz, very close to the 0.40 Hz frequency observed in the 2012 heavy winter case. The monitored generation unit with the largest amplitude of oscillation was Kemano. Of the units that oscillated against Kemano, Sundance and Sheerness in Alberta had the largest amplitude, and Navajo and Palo Verde were the most out of phase. The oscillations near 0.39 Hz for Revelstoke and Colstrip were stronger in the 2022 heavy winter case than the 2012 heavy winter case.

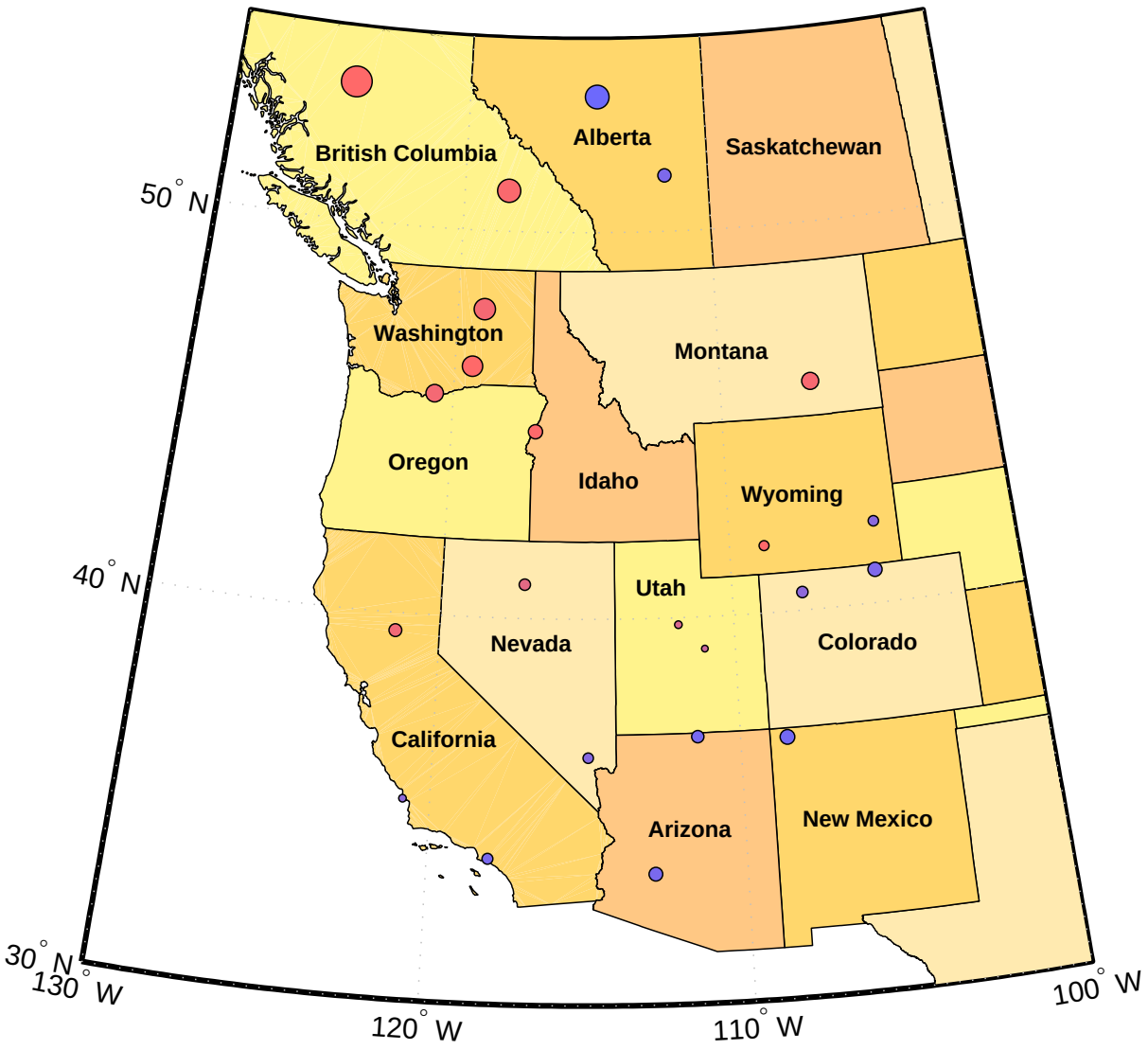

Figure 37: 2022 light summer, 0.47 Hz inter-area oscillation mode.

In the 2022 light summer case the mode shape displayed in Figure 37 was observed at a frequency of 0.47 Hz. In practice, the upper bound on the frequency at which this mode has been observed is roughly 0.42 Hz. This increase in frequency could be related to anticipated changes in transmission infrastructure which are reflected in the 2022 WECC base cases, but have not yet materialized in the physical system. The mode shape displayed in 37 is very similar to the one observed in the 2022 heavy winter case. The one appreciable difference between the two mode shapes is that the average amplitude of oscillation is slightly larger for the 2022 heavy winter case than the 2022 light summer case.

Figure 38: 2022 light spring, 0.46 Hz inter-area oscillation mode.

In the 2022 light spring case the mode shape displayed in Figure 38 was observed at a frequency of 0.46 Hz. The mode shape observed in this case bears a strong resemblance to that of the 2022 heavy winter and light summer cases. A minor difference is that the ringdown of Currant Creek in Utah did not have a 0.46 Hz frequency component in the 2022 light spring case. The average amplitude of oscillation experienced by the generation units located in the outer ring of the WECC region, discussed in Section 6.1.2, was slightly higher for the 2022 light spring case than the 2022 light summer case.

The 2022 light spring WECC base case is an important part of this study because it reflects projected load growth, changes in transmission infrastructure, and features a high level of renewable energy penetration. The 2022 light spring case was designed to meet renewable portfolio standards and features roughly 18 GW of wind power generation and nearly 29 GW of installed wind capacity. Yet, Figure 38 indicates that the mode shape of this inter-area oscillation is not adversely affected by the large increase in renewable energy generation and capacity.

6.1.3 Sporadically Observed Modes

As mentioned in Section 6.1, in addition to the 0.23 to 0.29 Hz North-South mode and the 0.34 to 0.47 Hz Alberta-B.C. mode, several other inter-area oscillation modes were observed in the WECC. Unlike the two system-wide modes previously discussed, the modes discussed in this section are characterized by the participation of a reduced number of monitored generators, typically about 15. Not only did fewer generation units participate in the sporadically observed modes, but the combination of participating units was also inconsistent across cases. Another important difference between the sporadically observed modes and the more prevalent system-wide modes was that they were excited for only a subset of the studied WECC base cases. The 0.23 to 0.29 Hz North-South mode was excited in five of the six studied cases, and the 0.34 to 0.47 Hz Alberta-B.C. mode was excited in all six studied cases. In contrast, none of the sporadically observed modes were excited in more than three of the cases.

The sporadically observed modes typically involved generation units in a specific area oscillating against a subset of the remaining generation units in the WECC region. Of these modes, the most frequently observed category was characterized by Kemano in northern British Columbia oscillating against monitored units along the Pacific coast of the United States. This type of oscillation was observed at frequencies ranging from 0.56 to 0.72 Hz. Notably, in the 2012 heavy winter case, Kemano's oscillations were out of phase with the rest of the system at two distinct frequencies. In that case Kemano oscillated against Hyatt and Diablo Canyon in California at 0.56 Hz and against the Columbia Generating Station in Washington at 0.68 Hz. At the 0.56 Hz frequency, Palo Verde experienced a low amplitude oscillation that was in phase with Kemano. At the 0.68 Hz frequency, no generation unit experienced an oscillation that was less than 45 degrees out of phase with Kemano. The 0.56 Hz B.C. mode is displayed in Figure 39, and the 0.68 Hz B.C. mode is displayed in Figure 40.

The second-most frequently observed category of modes was characterized by the oscillation of generation units in the American Pacific Northwest against other units in the WECC region. In two of the three cases for which this behavior was observed the monitored unit at the Grand Coulee Dam experienced the largest amplitude of oscillation. In the third case the generation unit with the largest amplitude of oscillation was Brownlee on the Oregon-Idaho border. Depending on the season and loading condition, the generation units which were most out of phase with the reference were located in Utah, Colorado, or Wyoming. In the 2012 heavy summer case, the generators along the Columbia River were observed to oscillate at a frequency of 0.60 Hz. In the 2012 light summer case, Brownlee was observed to oscillate at a frequency of 0.88 Hz. The 0.60 Hz Northwest mode is displayed in Figure 41, and the 0.88 Hz Northwest mode is displayed in Figure 42.

The defining characteristic of the remaining sporadically observed mode was the oscillation of Colstrip in Montana against other units in the WECC region. This mode has a nominal frequency of 0.80 Hz and in the past it has been referred to as the Montana mode [8]. A Chief Joseph Brake insertion excited this mode in the 2022 heavy winter case at a frequency of 0.79 Hz. The generation unit with the largest amplitude of oscillation was Colstrip, and of the units which were out of phase with the reference Currant Creek, Hunter, and Hyatt had the largest amplitude. Figure 43 displays the 0.79 Hz Montana mode for the 2022 heavy winter case. In southern California, the 0.79 Hz oscillation of Haynes was in phase with that of Colstrip.

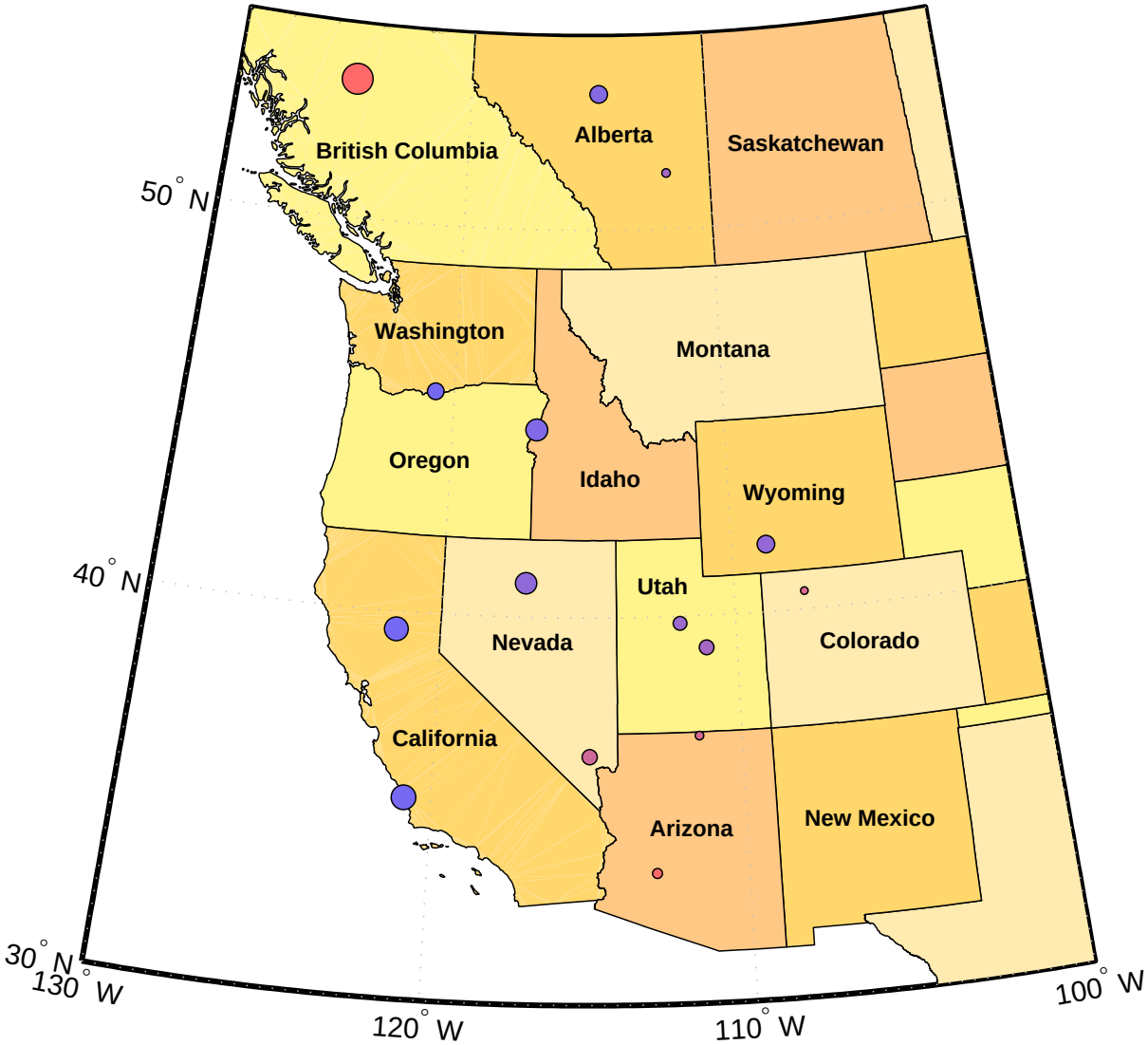

Figure 39: 2012 heavy winter, 0.56 Hz inter-area oscillation mode.

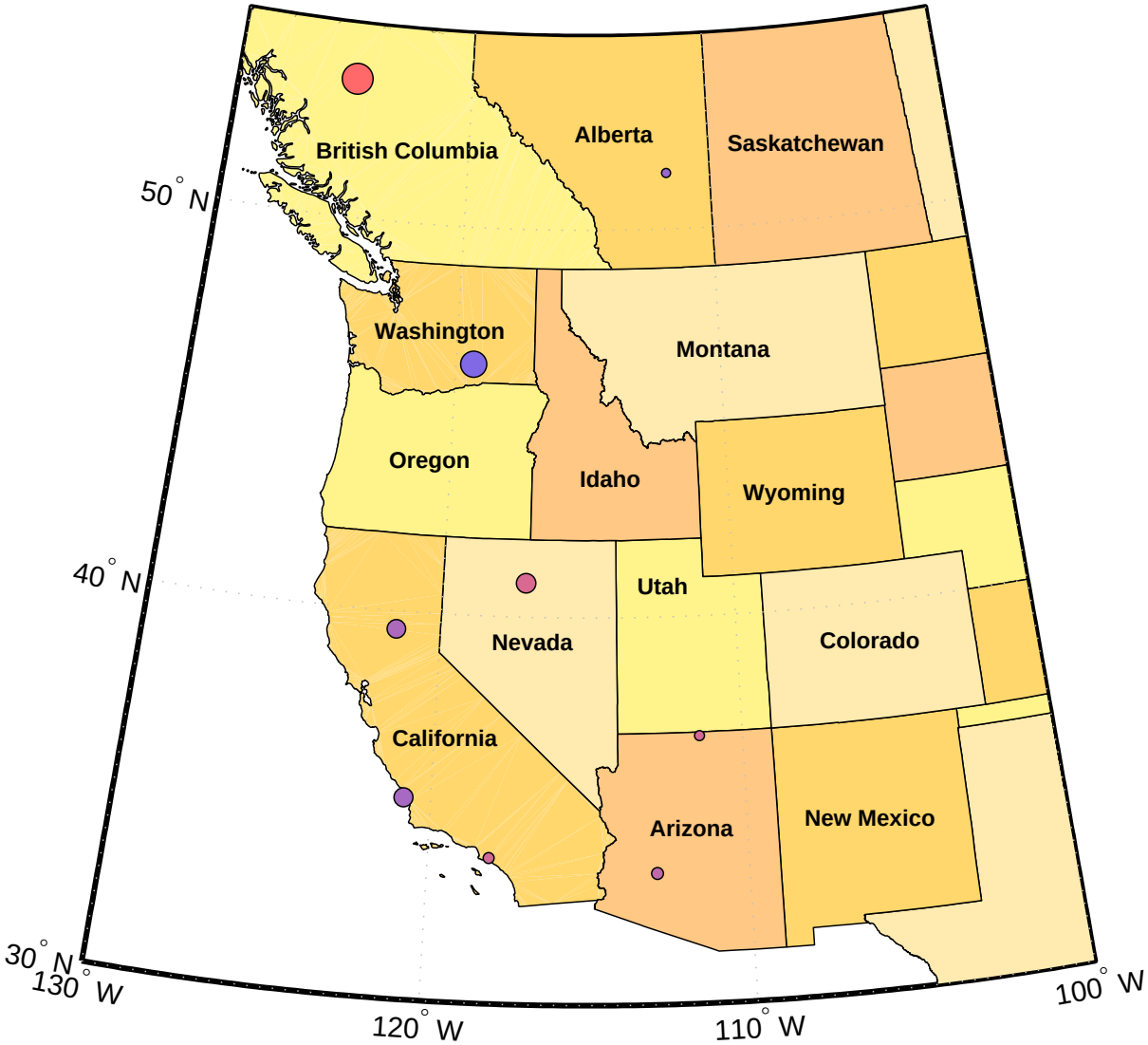

Figure 40: 2012 heavy winter, 0.68 Hz inter-area oscillation mode.

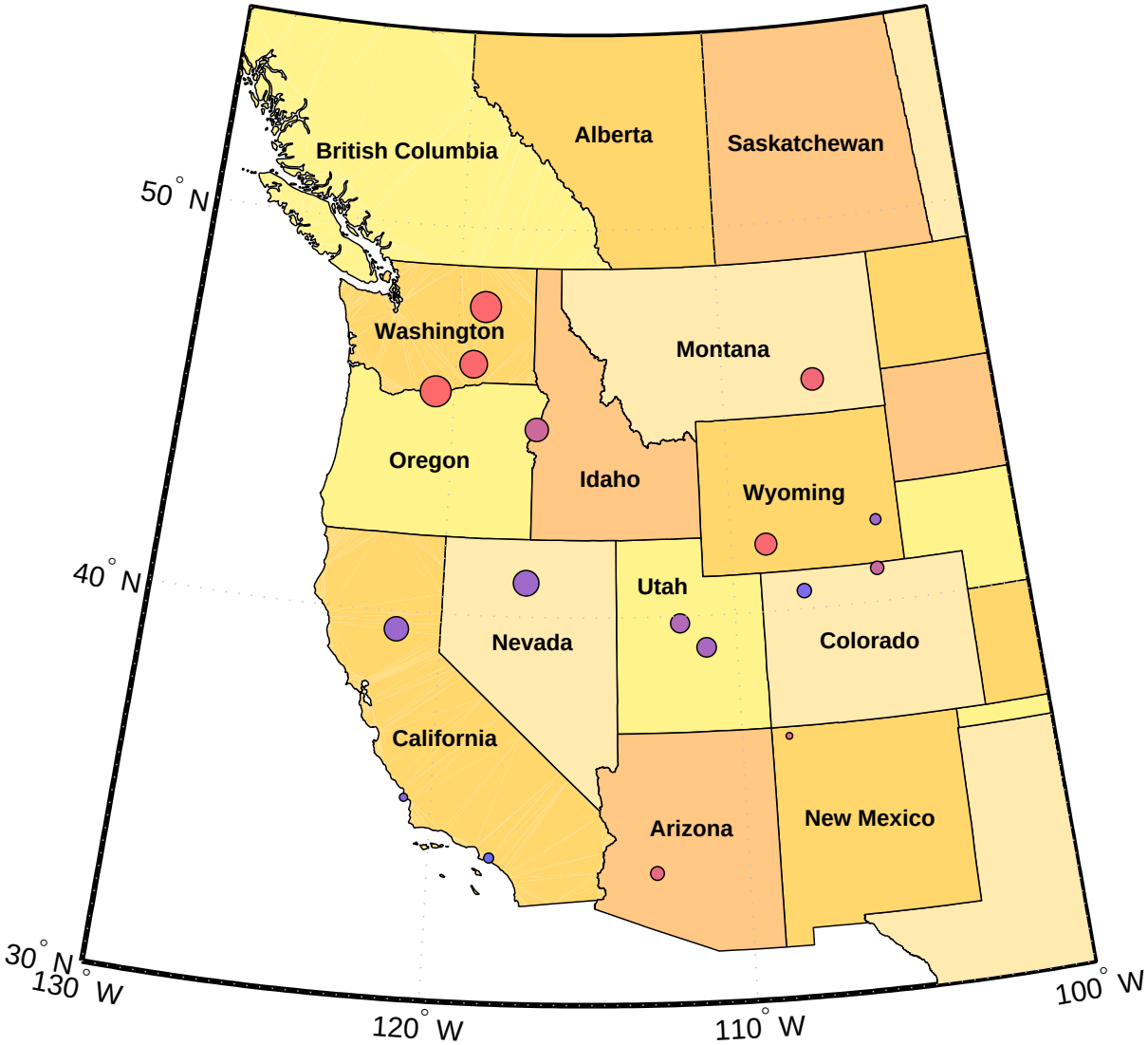

Figure 41: 2012 heavy summer, 0.60 Hz inter-area oscillation mode.

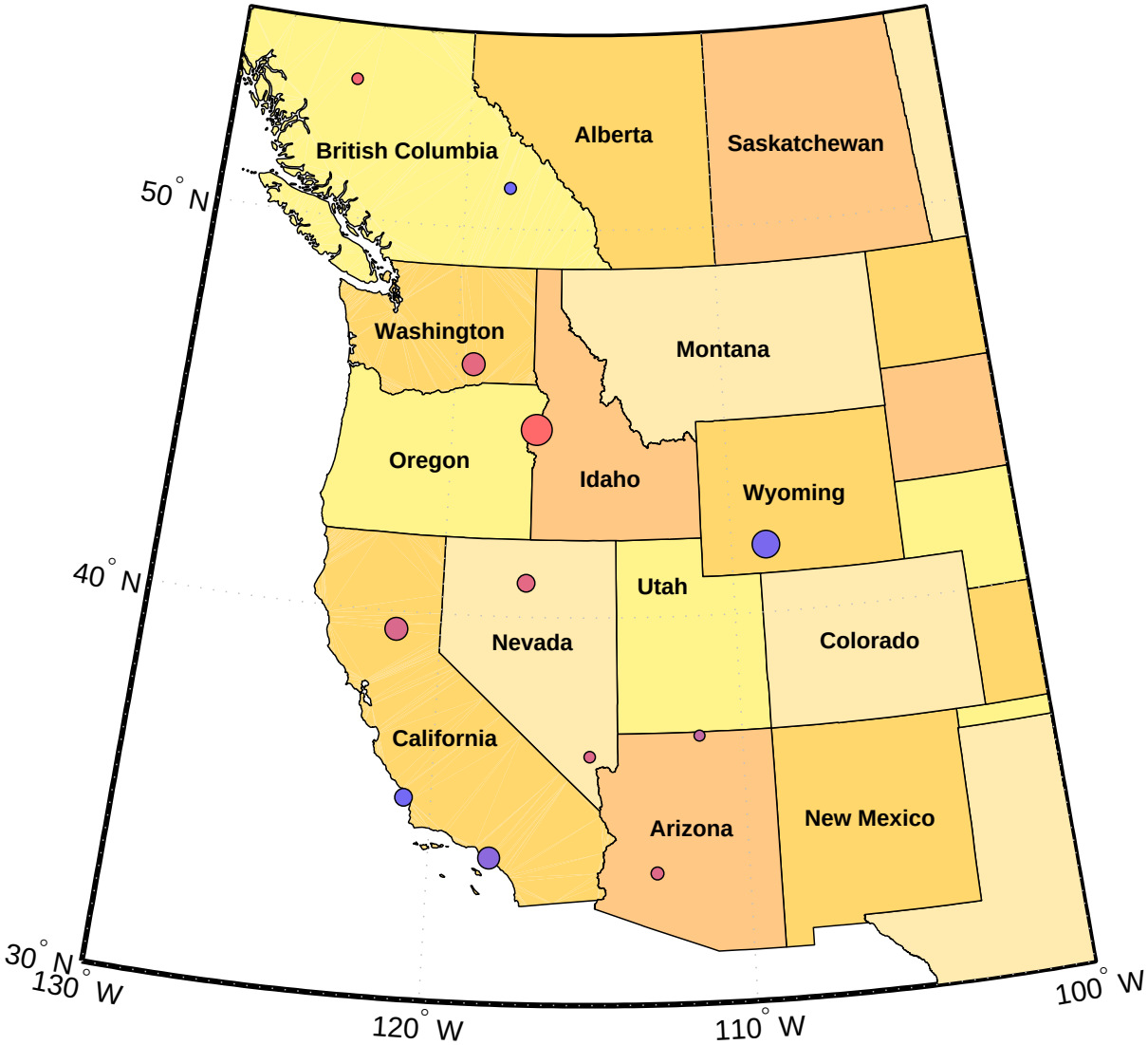

Figure 42: 2012 light summer, 0.88 Hz inter-area oscillation mode.

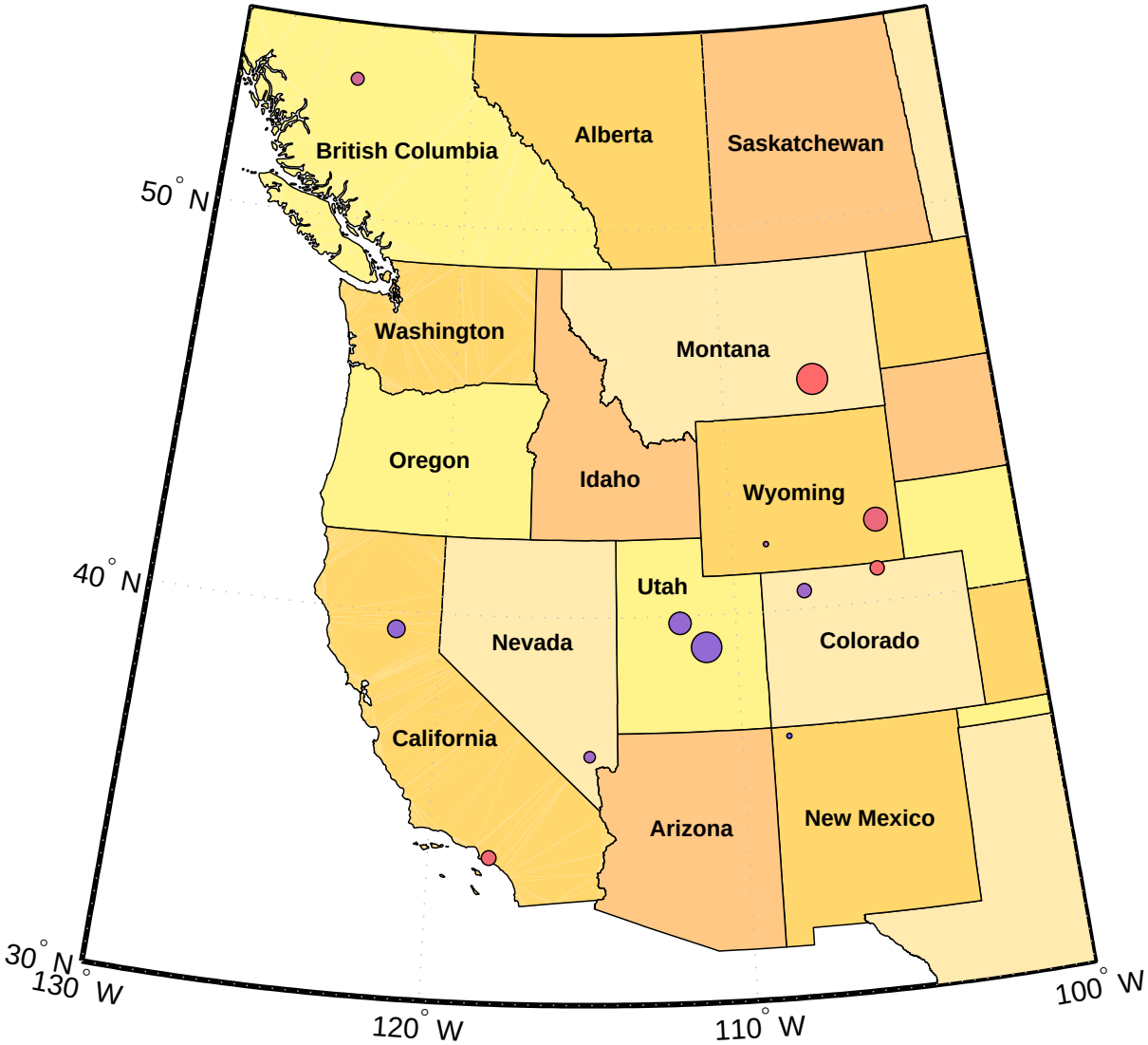

Figure 43: 2022 heavy winter, 0.79 Hz inter-area oscillation mode.

6.2 Small Signal Stability Conclusions

6.2.1 Mode Shape Considerations

For the two most prevalent inter-area oscillation modes in the WECC, the 0.23 to 0.29 Hz North-South mode and the 0.34 to 0.47 Hz Alberta-B.C. mode, the frequency of oscillation was observed to migrate upward between the 2012 and 2022 base cases. In the 2012 base cases the maximum frequency at which the North-South mode was observed was 0.24 Hz, while in the 2022 base cases the maximum frequency at which it was observed was 0.29 Hz. Likewise, in the 2012 base cases the maximum frequency at which the Alberta-B.C. mode was observed was 0.40 Hz, while in the 2022 base cases the maximum frequency at which it was observed was 0.47 Hz. Holding amplitudes fixed, as the frequency of a mode of oscillation increases, the first swing stability for that mode is improved because there is less time for the rotor angles of the participating machines to deviate. The change in rotor angle difference between two generators is proportional to the amplitude of the time-varying speed difference between the two generators. Therefore, if an increase in the frequency of a mode is accompanied by an increase in amplitudes, the benefit to first swing stability is diminished and potentially negated.

The mode shapes of the 0.23 to 0.29 Hz North-South mode and the 0.34 to 0.47 Hz Alberta-B.C. mode were fairly consistent across base cases. For the North-South mode, the monitored generation units in the Pacific Northwest and Montana did not participate in the 2012 and 2022 heavy winter cases. However, in the other cases their amplitude of oscillation was 85 percent smaller than the amplitude of the reference unit. The other minor difference in mode shape across the WECC base cases was the average amplitude of oscillation of the units south of the 45th parallel. In the 2012 heavy winter and 2022 light summer cases the residue magnitudes were greater for the units in the southern half of the mode than in the other cases. However, this behavior was observed in both 2012 and 2022, and was not apparent in the 2022 light spring case which features the highest penetration of renewable energy. If a mode shape were to get worse, one would expect the amplitude of oscillation of the participating units to increase, or the phase angles of those units to grow farther apart. None of the results produced in this study indicated that an increase in wind power generation would have an adverse effect on the mode shape of inter-area oscillation modes in the WECC. This outcome may have been a function of anticipated changes to the transmission infrastructure that were built-in to the 2022 WECC base cases.

6.2.2 Damping Ratio as a Function of Renewable Energy Penetration

As renewable energy penetration increases, power electronics based wind and solar resources supplant conventional generation, thereby reducing the amount of inertia that would otherwise be present in the system. Correspondingly, without energy storage, curtailment, or some other mechanism, wind and solar resources lack the ability to increase their power output on demand. Thus, renewable generation is unable to rapidly increase its power output to compensate for loss of generation in the event of a contingency. The inability of renewable generation to provide responsive headroom can be remedied by curtailing production, but this strategy results in an under-utilization of renewable resources. Likewise, adding energy storage increases the system cost, and under current rules, provides no additional revenue.

To study the effect of reduced inertia and reduced governor responsive headroom on small signal stability, several permutations of the 2022 light spring WECC base case were created. The 2022 light spring case was modified by altering the characteristics of the dynamic models of the wind generation in the system. The modified cases formed a two-by-two matrix with the first dimension corresponding to generator model, and the second dimension corresponding to whether the modified generator models were outfitted with a governor. In Table 7, the second and third columns correspond to cases in which type 3 and 4 wind turbines, which feature a power electronics interface to the grid, were replaced with round rotor generator models (**genrou**). Similarly, the fourth and fifth columns correspond to cases in which all wind generator models were replaced with conventional round rotor models.

Following a contingency, the frequency component of the post-disturbance oscillation with the greatest energy is referred to as the *dominant* mode. In the 2022 light spring case, the dominant mode excited

2022 Light Spring Modified Cases					
	Original case	**No 3 & 4, no governor**	**No 3 & 4, w/ governor**	**No wind, no governor**	**No wind, w/ governor**
Mean freq. (Hz)	0.456	0.443	0.446	0.441	0.443
Median freq. (Hz)	0.460	0.440	0.440	0.440	0.440
Mean damp. (%)	12.958	11.495	11.788	10.841	11.585
Median damp. (%)	11.920	11.150	11.840	11.005	11.800

Table 7: Frequency and damping of the dominant mode in the 2022 light spring case

by a Chief Joseph brake insertion was a 0.46 Hz oscillation. When type 3 and 4 wind turbine models were replaced with round rotor models, the median frequency of the mode migrated downward to 0.44 Hz. This may not seem significant, but the 20 mHz drift was equivalent a decrease of nearly five percent. As renewable energy penetration increases, the inertia present in the system is reduced which causes an upward drift in the frequency of observed inter-area oscillation modes.

The relationship between inertia and damping is less discernible from the quantities presented in Table 7, partly because the variation in frequency makes it difficult to compare damping across cases. However, one can draw a conclusion about the effect of governor control on the damping of inter-area oscillation modes. For the case in which type 3 and 4 wind turbines were replaced with round rotor models, the median damping ratio was approximately six percent higher when the replacement models contained governors than when they did not. For the case in which all wind turbines were replaced with round rotor models, the median damping ratio was approximately seven percent higher when the replacement models contained governors than when they did not. Hence, governor control modestly improved the damping of inter-area oscillations.

A summary of generator speeds with damping of less than 9% and a relative energy (for that mode) of greater than 0.1 appears in Table 81 of Appendix E. For the Chief Joseph brake insertions, the 2012 light summer case had the most lightly damped signals. Typically, only the first few modes with the largest energy are considered significant for Prony analysis. In general, none of the cases identified any significant signals with damping less than 5%. The columns of the table identify the generator ID, the mode frequency, the damping in percent, the relative energy (relative to that mode), and the absolute energy. The more lightly damped modes, e.g. less than 5%, are largely an artifact of the Prony fit. For this study, a 10th order fit was applied to the first 12 seconds of the brake insertions, and the first 25 seconds after a double Palo Verde contingency. An example of a lightly damped oscillations from Table 81 are shown in Figure 44. The signal in (a) is an example of a low-energy lightly damped 0.9 Hz mode observed in the Kemano speed. The oscillation is less than 1% of the energy in the dominant mode, and would typically be ignored.

The signal in (b) is a 0.44 Hz mode observed in the Rawhide generator speed. This is the largest mode observed at this node (relative energy is 1.0, relative to other modes observed at this generator). It is interesting to note the sensitivity of Prony results to the length of the data record. These results are for 20 seconds, and yield slightly higher damping than the number presented in the appendix. Also, the mode frequency is shifted slightly. Overall, there were no significant signals that exhibited worrisome low damping for any of the scenarios studied.

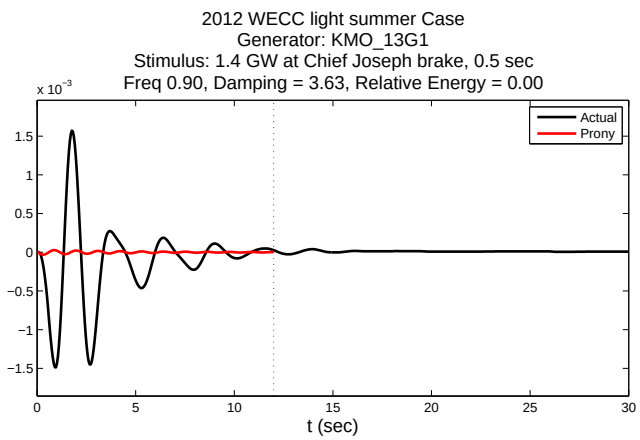

(a) 2012 light summer, 1.4 GW Chief Joseph brake, 0.5 seconds. Prony analysis of Kemano speed.

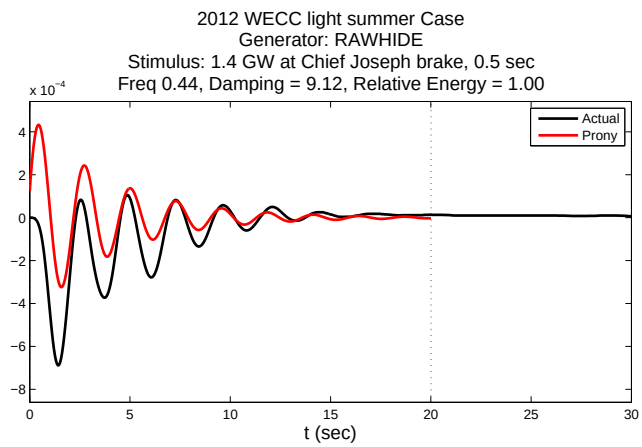

(b) 2012 light summer, 1.4 GW Chief Joseph brake, 0.5 seconds. Prony analysis of Rawhide speed.

Figure 44: 2012 light summer, 1.4 GW Chief Joseph brake, 0.5 seconds. Lightly damped modes from Prony analysis.

7 Summary and Conclusions

The goal of this study was to evaluate the transient and small signal stability of the WECC under high penetrations of renewable energy and then make recommendations for control algorithms that will improve system performance. Transient stability is the ability of the power system to maintain synchronism after a large disturbance while small signal stability is the ability of the power system to maintain synchronization in the face of small disturbances. For this study we employed generator speed relative to system speed as a measure of transient stability. Because small signal instability is often the result of insufficient damping of system oscillations, we analyzed the mode shape and damping of the WECC inter area oscillations to assess the small signal stability. In addition, we employed system frequency nadir to assess the adequacy of the primary frequency control reserves. The following WECC base cases were analyzed in this study:

- 2012 heavy summer
- 2012 light summer
- 2012 heavy winter
- 2022 light spring
- 2022 light summer
- 2022 heavy winter

The 2022 light spring case has the highest percentage of renewable generation and meets the renewable portfolio standards for the region.

There are many factors which influence the transient performance of a large power system like the WECC. In order to provide better insight into the cause and effect relationship of different factors, we also analyzed a simple 7-bus, 5-generator system under the following scenarios:

- Sensitivity to generation type: Generators configured to be all hydro, all coal, or all gas
- Sensitivity to system inertia: Generators configured to be all hydro, all coal, or all gas with inertia varied ($\pm$ 50%, $\pm$ 25%)
- Sensitivity to generation headroom: Generators configured to be all coal, and headroom is reduced by 60% and 80%
- Sensitivity to Wind generation: Generators are first configured to be all hydro, all coal, or all gas; then GEN3 is adjusted for loss of governor control and a change to wind generation with and without additional power compensation

These results highlight the sensitivity of the frequency nadir to generation type, system inertia, governor responsive headroom, and wind control algorithms. Similarly, the same system was utilized to show the effects of increased renewable penetration on inter-area modes and the mitigating nature of frequency droop and synthetic inertia controls.

Key results from this study are as follows:

- Even with a renewable penetration level that meets renewable portfolio standards, the WECC system frequency nadir for a double Palo Verde trip is well above the load shedding frequency of 59.5 Hz.
- While the 2022 light spring case has the highest renewable penetration of any WECC base case, and meets the renewable portfolio standards, the model still requires significant modifications to accurately characterize the future WECC system. First, solar models are absent from this base case. They are currently treated as negative loads or as wind plants. Second, the wind penetration appears to be incorrect. For instance, Alberta has over 1 GW of wind installed in 2012, yet the 2022 light spring case only reflects 50 MW. The simulation results are only as accurate as the model. More work needs to be put into updating the current WECC system models.

- Based on the simulation results from the WECC base cases, the mode shapes change with higher renewables penetration. These changes are subtle. Most modes increase slightly in frequency, which is consistent with reduced system inertia. Overall, the impact is negligible. There were no instances of lightly damped generator speeds with significant energy (e.g. damping less than 5 %), and the number of generators with damping bewteen 5 and 10% stayed roughly the same. It should be noted that these results are only as accurate as the system model.

- For each MW of wind added that displaces traditional generation, frequency droop has a stronger contribution to improving the system frequency nadir compared to replacing the lost inertia. Because frequency droop must be provided for a longer time period than synthetic inertia, several options for wind/solar providing this capability include:

  - Curtailment
  - Energy storage
  - Demand response with local frequency droop control

  Each option has its own economic impact. Curtailment results in lost revenue, energy storage adds additional costs, as does demand response. Ultimately, the final solution will depend on the economics of each approach. Therefore, some mechanism must be developed to compensate providers of frequency droop, whether it be a market product or pre-defined pricing scheme. The same argument applies for providing inertia.

- In the 7-bus, 5-generator system, the impacts of renewables penetration are more easily isolated. The effects include:

  - Reduced system inertia results in a faster initial drop in system frequency after the loss of generation. This results in a lower frequency nadir unless the speed and or quantity of governor response are modified.
  - Replacing conventional generation with a type 4 wind turbine results in a lower frequency nadir for the area with the wind. Areas without wind will have a higher frequency nadir. The system modes increase in frequency as a result of the decreased system inertia. The damping also improves.
  - By incorporating governor response (e.g. frequency droop) and synthetic inertia it is possible to equal or surpass the performance of the original synchronous generation system.
  - The energy storage, curtailment, or real-time demand response required to implement the frequency droop and synthetic inertia for a 7-bus, 5-generator system with 5 minutes of frequency droop, a 1.98 % loss of generation contingency, and 21% renewable penetration was calculated to be
    - 30.6 MW per GW of installed wind
    - 2.55 MW-hr per GW of installed wind
  - The area with increased renewables penetration has larger oscillations, while the rest of the system sees decreased oscillations.

- While this study has focused on the system-wide impacts of high renewables penetration on the WECC, many of the impacts of wind and solar generation occur at a local level. These include voltage support and oscillations caused by inverter control setting interacting with the rest of the system, not to mention the impact of variability and fast ramping. These items are beyond the scope of this study but need to be taken into account.

References

[1] P. Kundur, *Power System Stability and Control.* New York: McGraw-Hill, Inc., 1993.

[2] J. Eto, J. Undrill, P. Mackin, R. Daschmans, B. Williams, B. Haney, R. Hunt, J. Ellis, H. Illian, C. Martinez, M. O'Malley, K. Coughlin, and K. LaCommare, "Use of frequency response metrics to assess the planning and operating requirements for reliable integration of variable renewable generation," Tech. Rep. LBNL-4142E, Ernest Orlando Lawrence Berkeley National Laboratory, December 2010.

[3] GE Energy, "Western wind and solar integration study," Tech. Rep. NREL/SR-550-47434, National Renewable Energy Laboratory, 1617 Cole Boulevard, Golden, Colorado 80401, May 2010.

[4] P. Mackin, R. Daschmans, B. Williams, B. Haney, R. Hunt, and J. Ellis, "Dynamic simulation studies of the frequency response of the three U.S. interconnections with increased wind generation," Tech. Rep. LBNL-4146E, Ernest Orlando Lawrence Berkeley National Laboratory, December 2010.

[5] M. Wanik, I. Erlich, A. Mohamed, and A. Salam, "Influence of distributed generations and renewable energy resources power plant on power system transient stability," in *Power and Energy (PECon), 2010 IEEE International Conference on*, pp. 420 –425, November 29 - December 1, 2010 2010.

[6] Y. Chen, J. Fuller, R. Diao, N. Zhou, Z. Huang, and F. Tuffner, "The influence of topology changes on inter-area oscillation modes and mode shapes," in *2011 IEEE Power and Energy Society General Meeting*, pp. 1 –7, july 2011.

[7] D. J. Trudnowski, "Observability analysis of the minniWECC system model," tech. rep., Report to Bonneville Power Administration, Portland, OR, September 2010.

[8] D. J. Trudnowksi, "Baseline damping estimates," tech. rep., Report to Bonneville Power Administration, Portland, OR, 2008.

[9] D. Gautam, V. Vittal, and T. Harbour, "Impact of increased penetration of DFIG-based wind turbine generators on transient and small signal stability of power systems," *IEEE Transactions on Power Systems*, vol. 24, pp. 1426 –1434, August 2009.

[10] J. Morren, S. de Haan, W. Kling, and J. Ferreira, "Wind turbines emulating inertia and supporting primary frequency control," *IEEE Transactions on Power Systems*, vol. 21, pp. 433 – 434, February 2006.

[11] S. Seman and R. Sakki, "Inertial response – generators and the power electronics." National Renewable Energy Laboratory Workshop on Active Power Control from Wind Power, January 27 2011.

[12] R. Nelson, "Active power control in siemens wind turbines." National Renewable Energy Laboratory Workshop on Active Power Control from Wind Power, January 27 2011.

[13] N. Miller, K. Clark, and M. Shao, "Impact of frequency responsive wind plant controls on grid performance." National Renewable Energy Laboratory Workshop on Active Power Control from Wind Power, January 27 2011.

[14] R. Springer, "Active power control from wind power." National Renewable Energy Laboratory Workshop on Active Power Control from Wind Power, January 27 2011.

[15] C. L. DeMarco, C. A. Baone, Y. Han, and B. Lesieutre, "Primary and secondary control for high penetration renewables." PSERC Publication 12-06, March 2012.

[16] M. Molinas, J. A. Suul, and T. Undeland, "Extending the life of gear box in wind generators by smoothing transient torque with STATCOM," *IEEE Transactions on Industrial Electronics*, vol. 57, pp. 476 – 484, February 2010.

[17] V. Vittal, J. McCalley, V. Ajjarapu, and U. Shanbhag, "Impact of increased DFIG wind penetration on power systems and markets." PSERC publication 09-10, October 2009.

[18] R. Doherty, A. Mullane, G. Nolan, D. J. Burke, A. Bryson, and M. O'Malley, "An assessment of the impact of wind generation on system frequency control," *IEEE Transactions on Power Systems*, vol. 25, pp. 452–460, February 2010.

[19] C. A. Baone and C. L. DeMarco, "Observer-based distributed control design to coordinate wind generation and energy storage," in *Proceedings of the 2010 IEEE Conference on Innovative Smart Grid Technologies Europe*, (Gothenburg, Sweden), October 2010.

[20] A. Ellis and P. Pourbeyik, "WECC solar PV dynamic model specification." WECC report, September 2012.

[21] N. W. Miller, M. Shao, and S. Venkataraman, "California ISO (CAISO) frequency response study," tech. rep., GE Energy, 1 River Road, Building 53, Room 300Q, Schenectady, NY 12345, November 9 2011.

[22] J. Hauer, "Application of prony analysis to the determination of modal content and equivalent models for measured power system response," *IEEE Transactions on Power Systems*, vol. 6, pp. 1062–1068, August 1991.

[23] J. Hauer, C. Demeure, and L. Scharf, "Initial results in prony analysis of power system response signals," *IEEE Transactions on Power Systems*, vol. 5, pp. 80–89, Feb 1990.

[24] J. Hauer, "Identification of power system models for large scale damping control," in *Proceedings of the* 28th *IEEE Conference on Decision and Control*, vol. 2, pp. 1841–1846, Dec 1989.

[25] L. Scharf, *Statistical Signal Processing: Detection, Estimation, and Time Series Analysis.* New York: Addison-Wesley Publishing Company, 1991.

[26] D. Trudnowski, "Order reduction of large-scale linear oscillatory system models," *IEEE Transactions on Power Systems*, vol. 9, pp. 451–458, February 1994.

[27] D. Trudnowski, J. Johnson, and J. Hauer, "Making prony analysis more accurate using multiple signals," *IEEE Transactions on Power Systems*, vol. 14, pp. 226–231, February 1999.

[28] General Electric, "PSLF user's manual, release V18.0_01," tech. rep., General Electric, Schenectady, NY, October 24 2011.

[29] B. Pal and B. Chaudhuri, *Robust Control in Power Systems.* New York: Springer, 2005.

[30] C. Martini and T. Overbye, "Visualisation of oscillation mode shapes and participation factors," tech. rep., PSERC Publication, Department of Electrical and Computer Engineering, University of Illinois at Urbana-Champaign, Urbana, IL, 2010.

Appendix A - Statistics for the 2012 and 2022 WECC Base Cases

This section contains statistics for each of the WECC base cases employed in this study. A definition of each of the column headings appears below:

Area No - Name The WECC area number and name.

Power Generated The total power generated in MW in each area.

Online Capacity The total online capacity in MW in each area.

Installed Capacity The total installed capacity in MW in each area.

Head Room The difference in MW between the online capacity and the power generated in each area.

$$Headroom = Online\ capacity - Power\ generated$$

Capacity Factor The ratio of power generated to online capacity, expressed as a percentage.

$$Capacity\ factor = \frac{Power\ generated}{Online\ capacity}$$

2012 Heavy Summer, Power Generated by Conventional Units					
Area No - Name	**Power Generated**	**Online Capacity**	**Installed Capacity**	**Head room**	**Capacity Factor**
10 - NEW MEXICO	3093.1	3377.3	3674.3	284.2	91.6%
11 - EL PASO	966.3	1080.0	1917.0	113.7	89.5%
14 - ARIZONA	25577.2	28219.5	31884.9	2642.3	90.6%
18 - NEVADA	5571.4	6714.0	7342.0	1142.6	83.0%
20 - MEXICO-CFE	2135.0	2557.7	2973.7	422.7	83.5%
21 - IMPERIALCA	1252.3	1469.1	1469.1	216.8	85.2%
22 - SANDIEGO	3482.2	3662.3	4259.4	180.1	95.1%
24 - SOCALIF	21878.3	23715.4	30688.8	1837.1	92.3%
26 - LADWP	4875.5	6376.5	8498.5	1501.0	76.5%
30 - PG AND E	33288.6	38133.7	40573.1	4845.1	87.3%
40 - NORTHWEST	29178.3	34120.8	46042.1	4942.5	85.5%
50 - B.C. HYDRO	11099.1	12969.8	15322.9	1870.6	85.6%
52 - FORTISBC	862.7	1005.9	1258.8	143.2	85.8%
54 - ALBERTA	10064.4	12235.9	13966.5	2171.5	82.3%
60 - IDAHO	4350.6	5090.6	5511.5	740.0	85.5%
62 - MONTANA	3384.4	3835.3	3903.4	450.9	88.2%
63 - WAPA U.M.	46.8	108.0	108.0	61.2	43.3%
64 - SIERRA	1887.1	2165.8	2791.0	278.7	87.1%
65 - PACE	7927.9	8892.4	9191.1	964.5	89.2%
70 - PSCOLORADO	6870.1	7808.3	8927.3	938.2	88.0%
73 - WAPA R.M.	6096.7	6896.2	7251.1	799.5	88.4%

Table 8: 2012 heavy summer power generated by conventional units.

2012 Heavy Summer, Power Generated by Wind and Solar					
Area No - Name	**Power Generated**	**Online Capacity**	**Installed Capacity**	**Head room**	**Capacity Factor**
10 - NEW MEXICO	20.0	396.0	396.0	376.0	5.1%
11 - EL PASO	0.0	0.0	0.0	0.0	-
14 - ARIZONA	0.0	0.0	0.0	0.0	-
18 - NEVADA	0.0	0.0	0.0	0.0	-
20 - MEXICO-CFE	0.0	0.0	0.0	0.0	-
21 - IMPERIALCA	0.0	0.0	0.0	0.0	-
22 - SANDIEGO	0.0	0.0	0.0	0.0	-
24 - SOCALIF	0.0	0.0	720.0	0.0	-
26 - LADWP	80.0	278.5	278.5	198.5	28.7%
30 - PG AND E	682.2	687.5	687.5	5.3	99.2%
40 - NORTHWEST	0.0	0.0	5436.3	0.0	-
50 - B.C. HYDRO	0.0	0.0	0.0	0.0	-
52 - FORTISBC	0.0	0.0	0.0	0.0	-
54 - ALBERTA	69.7	81.6	81.6	11.9	85.4%
60 - IDAHO	5.0	10.5	46.2	5.5	47.6%
62 - MONTANA	0.0	0.0	0.0	0.0	-
63 - WAPA U.M.	0.0	0.0	0.0	0.0	-
64 - SIERRA	150.0	150.0	150.0	0.0	100.0%
65 - PACE	0.0	0.0	0.0	0.0	-
70 - PSCOLORADO	351.3	1672.5	1672.5	1321.2	21.0%
73 - WAPA R.M.	0.0	0.0	0.0	0.0	-

Table 9: 2012 heavy summer power generated by renewable units.

2012 Heavy Winter, Power Generated by Conventional Units					
Area No - Name	**Power Generated**	**Online Capacity**	**Installed Capacity**	**Head room**	**Capacity Factor**
10 - NEW MEXICO	2634.0	2807.3	3681.3	173.3	93.8%
11 - EL PASO	544.2	630.0	1917.0	85.8	86.4%
14 - ARIZONA	21244.1	23685.4	32578.8	2441.3	89.7%
18 - NEVADA	2363.8	3762.0	7317.0	1398.2	62.8%
20 - MEXICO-CFE	1490.7	1891.7	2897.7	401.0	78.8%
21 - IMPERIALCA	788.8	983.1	1168.1	194.3	80.2%
22 - SANDIEGO	1562.7	1821.6	4285.1	258.9	85.8%
24 - SOCALIF	10019.1	11418.4	30705.6	1399.3	87.7%
26 - LADWP	2620.0	4371.5	8698.5	1751.5	59.9%
30 - PG AND E	16912.7	21913.9	39833.2	5001.3	77.2%
40 - NORTHWEST	36517.8	42134.2	46918.4	5616.4	86.7%
50 - B.C. HYDRO	11972.7	14440.9	14987.1	2468.2	82.9%
52 - FORTISBC	944.1	1206.1	1258.8	262.0	78.3%
54 - ALBERTA	10126.6	12155.4	13821.2	2028.8	83.3%
60 - IDAHO	3331.0	3930.5	5199.5	599.5	84.7%
62 - MONTANA	3268.0	3776.5	4202.2	508.5	86.5%
63 - WAPA U.M.	35.0	61.8	61.8	26.8	56.7%
64 - SIERRA	1647.9	2027.1	2662.3	379.2	81.3%
65 - PACE	7242.6	8336.2	9222.1	1093.6	86.9%
70 - PSCOLORADO	5606.7	6891.7	9078.3	1285.0	81.4%
73 - WAPA R.M.	5599.4	6785.8	7330.9	1186.4	82.5%

Table 10: 2012 heavy winter power generated by conventional units.

2012 Heavy Winter, Power Generated by Wind and Solar					
Area No - Name	**Power Generated**	**Online Capacity**	**Installed Capacity**	**Head room**	**Capacity Factor**
10 - NEW MEXICO	20.0	396.0	396.0	376.0	5.1%
11 - EL PASO	0.0	0.0	0.0	0.0	-
14 - ARIZONA	0.0	0.0	0.0	0.0	-
18 - NEVADA	0.0	0.0	0.0	0.0	-
20 - MEXICO-CFE	0.0	0.0	0.0	0.0	-
21 - IMPERIALCA	0.0	0.0	0.0	0.0	-
22 - SANDIEGO	0.0	0.0	0.0	0.0	-
24 - SOCALIF	0.0	0.0	0.0	0.0	-
26 - LADWP	60.0	178.5	178.5	118.5	33.6%
30 - PG AND E	441.2	441.2	441.2	0.0	100.0%
40 - NORTHWEST	0.0	0.0	4417.2	0.0	-
50 - B.C. HYDRO	0.0	0.0	0.0	0.0	-
52 - FORTISBC	0.0	0.0	0.0	0.0	-
54 - ALBERTA	0.0	0.0	0.0	0.0	-
60 - IDAHO	0.0	0.0	0.0	0.0	-
62 - MONTANA	0.0	0.0	0.0	0.0	-
63 - WAPA U.M.	0.0	0.0	0.0	0.0	-
64 - SIERRA	0.0	0.0	0.0	0.0	-
65 - PACE	0.0	0.0	0.0	0.0	-
70 - PSCOLORADO	177.8	1422.5	1422.5	1244.7	12.5%
73 - WAPA R.M.	0.0	0.0	0.0	0.0	-

Table 11: 2012 heavy winter power generated by wind and solar.

2012 Light Summer, Power Generated by Conventional Units					
Area No - Name	**Power Generated**	**Online Capacity**	**Installed Capacity**	**Head room**	**Capacity Factor**
10 - NEW MEXICO	2343.4	2767.3	3661.3	423.9	84.7%
11 - EL PASO	711.9	841.0	1921.0	129.1	84.6%
14 - ARIZONA	20186.2	23689.5	31722.9	3503.3	85.2%
18 - NEVADA	3948.8	4977.0	6588.0	1028.2	79.3%
20 - MEXICO-CFE	1672.6	2242.7	2978.7	570.1	74.6%
21 - IMPERIALCA	1075.2	1241.4	1345.4	166.2	86.6%
22 - SANDIEGO	2138.1	2489.6	4259.4	351.5	85.9%
24 - SOCALIF	11787.3	13071.0	30855.7	1283.7	90.2%
26 - LADWP	2696.4	5291.0	7768.5	2594.6	51.0%
30 - PG AND E	14552.7	19687.4	40634.8	5134.7	73.9%
40 - NORTHWEST	18365.7	21892.6	45954.9	3526.9	83.9%
50 - B.C. HYDRO	6513.3	9599.4	15178.9	3086.1	67.9%
52 - FORTISBC	693.1	845.8	1258.7	152.7	81.9%
54 - ALBERTA	8594.5	10674.9	14047.3	2080.4	80.5%
60 - IDAHO	4151.9	4752.1	5511.5	600.2	87.4%
62 - MONTANA	3342.3	3835.3	3903.4	493.0	87.1%
63 - WAPA U.M.	40.8	61.8	61.8	21.0	66.0%
64 - SIERRA	1312.5	1613.9	2817.3	301.4	81.3%
65 - PACE	6276.3	8228.6	9254.3	1952.3	76.3%
70 - PSCOLORADO	4070.0	5200.7	8942.3	1130.7	78.3%
73 - WAPA R.M.	4651.0	6146.8	7325.5	1495.8	75.7%

Table 12: 2012 light summer power generated by conventional units.

2012 Light Summer, Power Generated by Wind and Solar					
Area No - Name	**Power Generated**	**Online Capacity**	**Installed Capacity**	**Head room**	**Capacity Factor**
10 - NEW MEXICO	20.0	396.0	396.0	376.0	5.1%
11 - EL PASO	0.0	0.0	0.0	0.0	-
14 - ARIZONA	0.0	0.0	0.0	0.0	-
18 - NEVADA	0.0	0.0	0.0	0.0	-
20 - MEXICO-CFE	0.0	0.0	0.0	0.0	-
21 - IMPERIALCA	0.0	0.0	0.0	0.0	-
22 - SANDIEGO	0.0	0.0	25.8	0.0	-
24 - SOCALIF	0.0	0.0	1020.0	0.0	-
26 - LADWP	90.0	278.5	278.5	188.5	32.3%
30 - PG AND E	287.2	288.5	736.5	1.3	99.5%
40 - NORTHWEST	0.0	0.0	5436.3	0.0	-
50 - B.C. HYDRO	0.0	0.0	0.0	0.0	-
52 - FORTISBC	0.0	0.0	0.0	0.0	-
54 - ALBERTA	69.7	81.6	81.6	11.9	85.4%
60 - IDAHO	5.0	10.5	46.2	5.5	47.6%
62 - MONTANA	0.0	0.0	0.0	0.0	-
63 - WAPA U.M.	0.0	0.0	0.0	0.0	-
64 - SIERRA	150.0	150.0	150.0	0.0	100.0%
65 - PACE	0.0	0.0	0.0	0.0	-
70 - PSCOLORADO	351.3	1672.5	1672.5	1321.2	21.0%
73 - WAPA R.M.	0.0	0.0	0.0	0.0	-

Table 13: 2012 light summer power generated by wind and solar.

2022 Heavy Winter, Power Generated by Conventional Units					
Area No - Name	**Power Generated**	**Online Capacity**	**Installed Capacity**	**Head room**	**Capacity Factor**
10 - NEW MEXICO	2962.8	3164.0	3705.5	201.2	93.6%
11 - EL PASO	768.5	900.0	1917.0	131.5	85.4%
14 - ARIZONA	23750.7	26861.2	33937.6	3110.5	88.4%
18 - NEVADA	2527.4	4098.2	9042.2	1570.8	61.7%
20 - MEXICO-CFE	2358.4	3242.0	4031.7	883.6	72.7%
21 - IMPERIALCA	832.0	1034.2	1164.2	202.2	80.4%
22 - SANDIEGO	2072.9	2337.6	4391.4	264.7	88.7%
24 - SOCALIF	21891.8	24206.7	32268.0	2314.9	90.4%
26 - LADWP	3967.3	6325.7	8439.3	2358.4	62.7%
30 - PG AND E	26035.8	31143.7	40787.3	5107.9	83.6%
40 - NORTHWEST	34596.9	40677.6	46284.2	6080.7	85.1%
50 - B.C. HYDRO	11153.6	14366.0	19337.2	3212.4	77.6%
52 - FORTISBC	916.9	1125.9	1258.7	209.0	81.4%
54 - ALBERTA	15807.7	19281.8	20998.7	3474.1	82.0%
60 - IDAHO	3393.2	4052.8	5513.7	659.6	83.7%
62 - MONTANA	3372.7	3857.9	4234.0	485.2	87.4%
63 - WAPA U.M.	52.0	61.8	61.8	9.8	84.2%
64 - SIERRA	2213.2	2594.0	3030.0	380.8	85.3%
65 - PACE	8114.8	9767.2	10418.9	1652.4	83.1%
70 - PSCOLORADO	7001.9	7823.3	9294.3	821.4	89.5%
73 - WAPA R.M.	6393.3	7583.6	8158.3	1190.3	84.3%

Table 14: 2022 heavy winter power generated by conventional units.

2022 Heavy Winter, Power Generated by Wind and Solar					
Area No - Name	**Power Generated**	**Online Capacity**	**Installed Capacity**	**Head room**	**Capacity Factor**
10 - NEW MEXICO	20.0	396.0	396.0	376.0	5.1%
11 - EL PASO	0.0	0.0	0.0	0.0	-
14 - ARIZONA	0.0	0.0	0.0	0.0	-
18 - NEVADA	100.0	586.0	586.0	486.0	17.1%
20 - MEXICO-CFE	0.0	0.0	0.0	0.0	-
21 - IMPERIALCA	0.0	0.0	0.0	0.0	-
22 - SANDIEGO	176.0	707.8	707.8	531.8	24.9%
24 - SOCALIF	720.0	720.0	1020.0	0.0	100.0%
26 - LADWP	120.0	178.5	178.5	58.5	67.2%
30 - PG AND E	297.2	317.5	587.5	20.3	93.6%
40 - NORTHWEST	0.0	0.0	6491.3	0.0	-
50 - B.C. HYDRO	0.0	0.0	0.0	0.0	-
52 - FORTISBC	0.0	0.0	0.0	0.0	-
54 - ALBERTA	17.2	81.6	81.6	64.4	21.1%
60 - IDAHO	128.0	430.2	476.4	302.2	29.8%
62 - MONTANA	0.0	0.0	0.0	0.0	-
63 - WAPA U.M.	0.0	0.0	0.0	0.0	-
64 - SIERRA	175.0	351.6	351.6	176.6	49.8%
65 - PACE	92.0	230.0	230.0	138.0	40.0%
70 - PSCOLORADO	430.4	2049.5	2049.5	1619.1	21.0%
73 - WAPA R.M.	0.0	0.0	0.0	0.0	-

Table 15: 2022 heavy winter power generated by wind and solar.

2022 Light Summer, Power Generated by Conventional Units					
Area No - Name	**Power Generated**	**Online Capacity**	**Installed Capacity**	**Head room**	**Capacity Factor**
10 - NEW MEXICO	2141.4	2700.3	3705.5	558.9	79.3%
11 - EL PASO	817.2	987.0	1917.0	169.8	82.8%
14 - ARIZONA	22319.1	25980.3	32405.7	3661.2	85.9%
18 - NEVADA	3498.2	5225.0	9040.8	1726.8	67.0%
20 - MEXICO-CFE	1460.5	2158.0	3861.2	697.5	67.7%
21 - IMPERIALCA	1097.5	1341.2	2024.2	243.7	81.8%
22 - SANDIEGO	1797.4	1985.2	4391.4	187.8	90.5%
24 - SOCALIF	25973.7	28162.4	32402.3	2188.7	92.2%
26 - LADWP	2771.4	4126.5	8499.3	1355.1	67.2%
30 - PG AND E	17589.4	23659.1	41564.5	6069.7	74.3%
40 - NORTHWEST	16205.3	21419.1	46376.2	5213.8	75.7%
50 - B.C. HYDRO	5008.3	9599.1	19673.4	4590.8	52.2%
52 - FORTISBC	862.6	1005.9	1258.8	143.3	85.8%
54 - ALBERTA	11345.0	14322.4	21835.6	2977.4	79.2%
60 - IDAHO	3646.5	4301.0	5513.7	654.5	84.8%
62 - MONTANA	2927.0	3424.0	4278.9	497.0	85.5%
63 - WAPA U.M.	43.4	61.8	61.8	18.4	70.2%
64 - SIERRA	1818.9	2129.1	2971.3	310.2	85.4%
65 - PACE	5958.3	8907.7	10316.6	2949.4	66.9%
70 - PSCOLORADO	4496.5	5277.7	9483.3	781.2	85.2%
73 - WAPA R.M.	4860.4	5963.6	8128.3	1103.2	81.5%

Table 16: 2022 light summer power generated by conventional units.

2022 Light Summer, Power Generated by Wind and Solar					
Area No - Name	**Power Generated**	**Online Capacity**	**Installed Capacity**	**Head room**	**Capacity Factor**
10 - NEW MEXICO	391.0	396.0	396.0	5.0	98.7%
11 - EL PASO	0.0	0.0	0.0	0.0	-
14 - ARIZONA	0.0	0.0	0.0	0.0	-
18 - NEVADA	100.0	586.0	586.0	486.0	17.1%
20 - MEXICO-CFE	0.0	0.0	0.0	0.0	-
21 - IMPERIALCA	0.0	0.0	0.0	0.0	-
22 - SANDIEGO	176.0	707.8	707.8	531.8	24.9%
24 - SOCALIF	720.0	720.0	1020.0	0.0	100.0%
26 - LADWP	74.0	178.5	178.5	104.5	41.5%
30 - PG AND E	237.2	317.5	1227.5	80.3	74.7%
40 - NORTHWEST	6093.0	6245.1	6245.1	152.1	97.6%
50 - B.C. HYDRO	0.0	0.0	0.0	0.0	-
52 - FORTISBC	0.0	0.0	0.0	0.0	-
54 - ALBERTA	68.0	81.6	81.6	13.6	83.4%
60 - IDAHO	249.0	476.4	476.4	227.4	52.3%
62 - MONTANA	0.0	0.0	0.0	0.0	-
63 - WAPA U.M.	0.0	0.0	0.0	0.0	-
64 - SIERRA	130.0	351.6	351.6	221.6	37.0%
65 - PACE	115.1	230.0	230.0	114.9	50.0%
70 - PSCOLORADO	1678.5	1873.5	1873.5	195.0	89.6%
73 - WAPA R.M.	0.0	0.0	0.0	0.0	-

Table 17: 2022 light summer power generated by wind and solar.

2022 Light Spring, Power Generated by Conventional Units					
Area No - Name	**Power Generated**	**Online Capacity**	**Installed Capacity**	**Head room**	**Capacity Factor**
10 - NEW MEXICO	1120.3	1676.2	3794.2	555.9	66.8%
11 - EL PASO	618.6	987.0	1917.0	368.4	62.7%
14 - ARIZONA	15056.0	18707.5	32486.0	3651.5	80.5%
18 - NEVADA	1816.5	2936.1	8441.8	1119.6	61.9%
20 - MEXICO-CFE	721.8	1109.0	3377.2	387.2	65.1%
21 - IMPERIALCA	1209.2	1427.2	2169.2	218.0	84.7%
22 - SANDIEGO	309.5	664.6	3142.1	355.1	46.6%
24 - SOCALIF	5110.1	7160.4	33477.7	2050.3	71.4%
26 - LADWP	2591.4	4126.5	8499.3	1535.1	62.8%
30 - PG AND E	13320.4	22833.1	44798.8	9512.7	58.3%
40 - NORTHWEST	14667.0	18420.7	44432.5	3753.7	79.6%
50 - B.C. HYDRO	9231.7	12291.0	18789.1	3059.4	75.1%
52 - FORTISBC	1084.4	1258.7	1258.7	174.3	86.2%
54 - ALBERTA	14111.1	17206.2	20580.8	3095.1	82.0%
60 - IDAHO	4094.7	4924.9	5583.7	830.2	83.1%
62 - MONTANA	2929.8	3602.0	4297.1	672.2	81.3%
63 - WAPA U.M.	69.8	69.8	69.8	0.0	100.0%
64 - SIERRA	1729.1	2062.7	2985.0	333.6	83.8%
65 - PACE	5562.3	9481.4	10458.6	3919.1	58.7%
70 - PSCOLORADO	3192.8	3652.9	8951.7	460.1	87.4%
73 - WAPA R.M.	3912.0	5116.8	8128.3	1204.7	76.5%

Table 18: 2022 light spring power generated by conventional units.

2022 Light Spring, Power Generated by Wind and Solar					
Area No - Name	**Power Generated**	**Online Capacity**	**Installed Capacity**	**Head room**	**Capacity Factor**
10 - NEW MEXICO	1035.2	1668.3	1668.3	633.2	62.0%
11 - EL PASO	0.0	0.0	0.0	0.0	-
14 - ARIZONA	50.4	50.4	50.4	0.0	100.0%
18 - NEVADA	0.0	0.0	586.0	0.0	-
20 - MEXICO-CFE	0.0	0.0	0.0	0.0	-
21 - IMPERIALCA	0.0	0.0	0.0	0.0	-
22 - SANDIEGO	794.4	1242.0	1242.0	447.6	64.0%
24 - SOCALIF	3791.1	5609.6	7720.1	1818.6	67.6%
26 - LADWP	150.0	430.5	430.5	280.5	34.8%
30 - PG AND E	693.3	1027.6	1360.8	334.3	67.5%
40 - NORTHWEST	8357.9	8714.8	11272.4	356.9	95.9%
50 - B.C. HYDRO	0.0	0.0	0.0	0.0	-
52 - FORTISBC	0.0	0.0	0.0	0.0	-
54 - ALBERTA	50.0	81.6	81.6	31.6	61.3%
60 - IDAHO	458.0	542.7	849.9	84.7	84.4%
62 - MONTANA	0.0	0.0	0.0	0.0	-
63 - WAPA U.M.	0.0	0.0	0.0	0.0	-
64 - SIERRA	130.0	351.6	351.6	221.6	37.0%
65 - PACE	40.0	99.0	99.0	59.0	40.4%
70 - PSCOLORADO	1907.0	2275.5	2275.5	368.5	83.8%
73 - WAPA R.M.	667.0	667.2	667.2	0.2	100.0%

Table 19: 2022 light spring power generated by wind and solar.

Quantity	Heavy Summer	Heavy Winter	Light Summer
Kt Ratio:	42.6%	49.2%	42.9%
GR Pgen / CU Pgen:	38.9%	44.8%	35.9%
GR Pgen / Total Pgen:	38.6%	44.5%	35.7%
GR Headroom / CU Pgen:	7.0%	9.2%	12.7%
GR Headroom / Total Pgen:	6.9%	9.2%	12.6%
MW Capability (MW):	198033.6	160649.3	135238.5
GR Pgen (MW):	71544.6	65560.8	42817.8
GR Online Capacity (MW):	84332.1	79039.2	57959.3
GR Installed Capacity (MW):	102536.5	104654.1	107532.7
GR Headroom (MW):	12787.5	13478.4	15141.5
GR Capacity Factor:	84.8%	82.9%	73.9%
BL Pgen (MW):	72261.8	60057.6	55342.6
BL Online Capacity (MW):	78667.6	66838.6	62363.3
BL Installed Capacity (MW):	86293.5	84184.3	81013.3
BL Headroom (MW):	6405.9	6781.1	7020.8
BL Capacity Factor:	91.9%	89.9%	88.7%
NG Pgen (MW):	40081.6	20853.5	20963.4
NG Online Capacity (MW):	47434.7	29153.4	28827.2
NG Installed Capacity (MW):	58724.5	58986.4	57445.5
NG Headroom (MW):	7353.1	8299.8	7863.8
NG Capacity Factor:	84.5%	71.5%	72.7%
CU Pgen (MW):	183888.0	146471.8	119123.8
CU Online Capacity (MW):	210434.6	175030.9	149149.8
CU Installed Capacity (MW):	247554.6	247824.7	245991.5
CU Headroom (MW):	26546.6	28559.0	30026.0
CU Capacity Factor:	87.4%	83.7%	79.9%
Wind/solar Pgen (MW):	1358.2	699.0	973.2
Wind/solar Online Capacity (MW):	3276.6	2438.2	2877.6
Wind/solar Installed Capacity (MW):	9468.6	6855.4	9843.4
Wind/solar Headroom (MW):	1918.4	1739.2	1904.4
Wind/solar Capacity Factor:	41.5%	28.7%	33.8%
Wind/solar Pgen / Total Pgen:	0.7%	0.5%	0.8%
Total Pgen (MW):	185246.2	147170.8	120097.0
Total Online Capacity (MW):	213711.2	177469.1	152027.4
Total Installed Capacity (MW):	257023.2	254680.1	255834.9
Total Headroom (MW):	28465.0	30298.3	31930.4
Total Capacity Factor:	86.7%	82.9%	79.0%

Table 20: Metrics for 2012 WECC Base Cases

Quantity	Heavy Winter	Light Summer	Light Spring
Kt Ratio:	44.9%	44.5%	45.8%
GR Pgen / CU Pgen:	39.7%	40.5%	44.4%
GR Pgen / Total Pgen:	39.2%	37.7%	37.8%
GR Headroom / CU Pgen:	10.3%	13.1%	17.5%
GR Headroom / Total Pgen:	10.2%	12.2%	14.9%
MW Capability (MW):	201099.3	164504.7	138559.2
GR Pgen (MW):	71612.6	55317.6	45536.0
GR Online Capacity (MW):	90252.5	73152.5	63512.3
GR Installed Capacity (MW):	114584.7	125629.3	118226.4
GR Headroom (MW):	18639.9	17834.8	17976.2
GR Capacity Factor:	79.3%	75.6%	71.7%
BL Pgen (MW):	65163.3	49805.4	44040.5
BL Online Capacity (MW):	72558.3	57081.1	53232.0
BL Installed Capacity (MW):	87697.0	76718.5	85883.6
BL Headroom (MW):	7395.0	7275.7	9191.5
BL Capacity Factor:	89.8%	87.3%	82.7%
NG Pgen (MW):	43407.6	31515.0	12882.2
NG Online Capacity (MW):	51694.3	42503.0	22970.7
NG Installed Capacity (MW):	65992.2	67361.9	63528.6
NG Headroom (MW):	8286.6	10987.9	10088.5
NG Capacity Factor:	84.0%	74.1%	56.1%
CU Pgen (MW):	180183.7	136638.1	102458.7
CU Online Capacity (MW):	214505.2	172736.3	139714.8
CU Installed Capacity (MW):	268273.8	269709.4	267638.5
CU Headroom (MW):	34321.5	36098.2	37256.1
CU Capacity Factor:	84.0%	79.1%	73.3%
Wind/solar Pgen (MW):	2275.8	10031.8	18124.2
Wind/solar Online Capacity (MW):	6048.7	12164.0	22760.8
Wind/solar Installed Capacity (MW):	13156.2	13374.0	28655.3
Wind/solar Headroom (MW):	3772.9	2132.2	4636.6
Wind/solar Capacity Factor:	37.6%	82.5%	79.6%
Wind/solar Pgen / Total Pgen:	1.2%	6.8%	15.0%
Total Pgen (MW):	182459.5	146670.0	120583.0
Total Online Capacity (MW):	220554.0	184900.3	162475.6
Total Installed Capacity (MW):	281429.8	283083.3	296293.9
Total Headroom (MW):	38094.5	38230.3	41892.6
Total Capacity Factor:	82.7%	79.3%	74.2%

Table 21: Metrics for 2022 WECC Base Cases

Model	PGEN (MW)	Percent (%)
genrou	72,272.34	49.11
gencc	1,588.38	1.08
gencls	0.00	0.00
genind	0.00	0.00
gensal	39,169.09	26.61
gensdo	0.00	0.00
gentpf	28,161.27	19.14
gentpj	4,404.77	2.99
motor1	476.04	0.32
shaft5	0.00	0.00
wt4g	0.00	0.00
wt3g	0.00	0.00
wt2g	0.00	0.00
wt1g	5.00	0.00
genwri	337.98	0.23
gewtg	356.00	0.24

Table 22: 2012 heavy winter, total generation: 147,171 MW, renewable generation: 699 MW.

Model	PGEN (MW)	Percent (%)
genrou	97,142.27	52.44
gencc	15,332.17	8.28
gencls	0.00	0.00
genind	0.00	0.00
gensal	384.89	0.21
gensdo	0.00	0.00
gentpf	26,530.97	14.32
gentpj	43,478.97	23.47
motor1	616.69	0.33
shaft5	0.00	0.00
wt4g	150.00	0.08
wt3g	69.71	0.04
wt2g	5.00	0.00
wt1g	5.00	0.00
genwri	337.98	0.18
gewtg	790.50	0.43

Table 23: 2012 heavy summer, total generation: 185,246 MW, renewable generation: 1,358 MW.

Model	PGEN (MW)	Percent (%)
genrou	71,874.59	59.85
gencc	3,484.72	2.90
gencls	0.00	0.00
genind	0.00	0.00
gensal	87.78	0.07
gensdo	0.00	0.00
gentpf	17,448.52	14.53
gentpj	25,514.10	21.24
motor1	312.05	0.26
shaft5	0.00	0.00
wt4g	150.00	0.12
wt3g	69.71	0.06
wt2g	5.00	0.00
wt1g	5.00	0.00
genwri	150.00	0.12
gewtg	593.49	0.49

Table 24: 2012 light summer, total generation: 120,097 MW, renewable generation: 973 MW.

Model	PGEN (MW)	Percent (%)
genrou	94,691.77	51.90
gencc	15,893.75	8.71
gencls	0.00	0.00
genind	0.00	0.00
gensal	560.00	0.31
gensdo	0.00	0.00
gentpf	24,912.80	13.65
gentpj	43,038.84	23.59
motor1	684.53	0.38
shaft5	0.00	0.00
wt4g	287.00	0.16
wt3g	871.24	0.48
wt2g	0.00	0.00
wt1g	5.00	0.00
genwri	267.97	0.15
gewtg	844.60	0.46

Table 25: 2022 heavy winter, total generation: 182,460 MW, renewable generation: 2,276 MW.

Model	PGEN (MW)	Percent (%)
genrou	55,675.21	46.17
gencc	50.01	0.04
gencls	0.00	0.00
genind	0.00	0.00
gensal	21.00	0.02
gensdo	0.00	0.00
gentpf	14,746.18	12.23
gentpj	30,668.61	25.43
motor1	895.80	0.74
shaft5	0.00	0.00
wt4g	8,631.66	7.16
wt3g	4,145.64	3.44
wt2g	1,479.59	1.23
wt1g	425.73	0.35
genwri	203.06	0.17
gewtg	3,238.53	2.69

Table 26: 2022 light spring, total generation: 120,583 MW, renewable generation: 18,124 MW.

Model	PGEN (MW)	Percent (%)
genrou	75,007.73	51.14
gencc	12,030.26	8.20
gencls	0.00	0.00
genind	0.00	0.00
gensal	349.30	0.24
gensdo	0.00	0.00
gentpf	18,103.13	12.34
gentpj	29,394.79	20.04
motor1	1,350.94	0.92
shaft5	0.00	0.00
wt4g	2,888.69	1.97
wt3g	2,813.13	1.92
wt2g	1,227.15	0.84
wt1g	522.17	0.36
genwri	232.98	0.16
gewtg	2,347.69	1.60

Table 27: 2022 light summer, total generation: 146,670 MW, renewable generation: 10,032 MW.

Appendix B - Monitored Generators

Area	Bus	Code	Name	Unit	Location	Fuel Type
50	50437	KMO_13G1	Kemano Power Station	1	Kemano, BC	Hydro
50	50644	REV_13G1	Revelstoke Dam	1	Revelstoke, BC	Hydro
54	54345	SUND#5GN	Sundance Power Plant	5	Wabamun Lake, AB	Coal
54	55482	SHEER_1	Sheerness Generating Station	1	Hanna, AB	Coal
40	40296	COULEE22	Grand Coulee Dam	22	Mason City, WA	Hydro
40	40063	CGS	Columbia Generating Station	1	Richland, WA	Nuclear
40	44072	JDA_0304	John Day Dam	3	Goldendale, OR	Hydro
60	60100	BRWNL_5	Brownlee Dam	5	Hells Canyon, ID	Hydro
62	62049	COLSTP_2	Colstrip Power Plant	2	Colstrip, MT	Coal
60	60086	BRIDGER1	Jim Bridger Power Plant	1	Point of Rocks, WY	Coal
73	73129	MBPP-1	Laramie River Generating Station	1	Wheatland, WY	Coal
30	38825	HYATT_1	Edward Hyatt Power Plant	1	Oroville, CA	Hydro
36	36411	DIABLO_1	Diablo Canyon Power Plant	1	Avila Beach, CA	Nuclear
26	26026	HAYNES1G	Haynes Generating Station	1	Seal Beach, CA	Gas
64	64132	VALMY_G2	North Valmy Generating Station	2	Valmy, NV	Coal
18	18401	SLHWKG1	Silverhawk Generating Station	1	Clark, NV	Gas
65	65391	CURRNTC1	Currant Creek Power Plant	1	Mona, UT	Gas
65	65490	EHUNTER1	Hunter Power Plant	1	Castle Dale, UT	Coal
73	79015	CRAIG_1	Craig Generating Station	1	Craig, CO	Coal
70	70350	RAWHIDE	Rawhide Energy Station	1	Wellington, CO	Coal
14	15981	NAVAJO_1	Navajo Generating Station	1	Page, AZ	Coal
14	14932	PALOVRD2	Palo Verde Nuclear Generating Station	2	Tonopah, AZ	Nuclear
10	10318	SJUAN_G1	San Juan Generating Station	1	Waterflow, NM	Coal

Table 28: Summary of monitored generators.

Appendix C - Generator Models and Circuit Parameters, 7-bus, 5-Generator System

```
#COULEE "HYDRO" SETTINGS
gentpj  41721 "COULEE01" 13.8 "1" : #9 mva=125 "Tpdo" 9.5 "Tppdo" 0.03 "Tpqo" 0 "Tppqo" 0.079\
                                    "H" 4.779 "D" 0 "Ld" 0.706 "Lq" 0.55 "Lpd" 0.302 \
                                    "Lpq" 0.55 "Lppd" 0.186 "Lppq" 0.186 "L1" 0.10 "S1" 0.132\
                                    "S12" 0.5203 "Ra" 0.0074 "Rcomp" 0 "Xcomp" 0 "accel" 0.5\
                                    "Kis" 0.05
exdc1   41721 "COULEE01" 13.8 "1" : #9 0 20 0.1 0 0 3 -1 1 0.3 0.01 0.4 0 1.65 0.12 2.2 0.2
psssb   41721 "COULEE01" 13.8 "1" : #9 2 0 0 0 30 0 1 0 0 0 0 0 0 0 0.01 1 2 4.7 0.5 0.02 0.5\
                                    0.02 0.05 -0.05 0 0 0 0 0 0.06
hyg3    41721 "COULEE01" 13.8 "1" : #9 mwcap=121.0 1.0 0 -1 0.05 0 0.03 0.1 0.15 0.125 -0.125\
                                    3.0 1.7 1.2 3 0 0 0 0 0.66 1 \
                                    1 0 1 0.1 0 0.4 0.32 0.6 0.6 0.7 0.72 0.8 0.83 0.9 0.92
#
#COLSTRIP "STEAM/COAL" SETTINGS
genrou   62047 "COLSTP 4"  26.00 "1 " : #9 mva=867.0 "tpdo" 6.0 "tppdo" 0.079 "tpqo" 0.53 \
                                        "tppqo" 0.072 "h" 3.70 "d" 0.0 "ld" 1.24  "lq" 1.22\
                                        "lpd" 0.26 "lpq" 0.36 "lppd" 0.21 "ll" 0.14 "s1" 0.173\
                                        "s12" 0.447 "ra" 0.003 "rcomp" 0.0 "xcomp" 0.0 \
                                        "accel" 1.0
rexs     62047 "COLSTP 4"  26.00 "1 " : #9 "tr" 0.0 "kvp" 550.0 "kvi" 0.0 "vimax"  999\
                                        "ta" 0.06 "tb1" 1.0 "tc1" 1.00 "tb2" 1.0\
                                        "tc2" 1.00 "vrmax"  8.05 "vrmin" -8.05 "kf" 0.05\
                                        "tf" 0.9 "tf1" 1.0 "tf2" 1.0 "fbf" 1.0 \
                                        "kip" 12.00 "kii" 0.0 "tp" 0.0 "vfmax"  105.0\
                                        "vfmin" -85.0 "kh" 1.0 "ke" 1.00 "te" 3.0
                                        "kc" 0.6 "kd" 0.368 "e1" 3.00 "se1" 0.01 \
                                        "e2" 4.00 "se2" 0.076  "rcomp" 0.0 "xcomp" 0.0\
                                        "nvphz" 0.0 "kvphz" 0.0 "flimf" 0.0 "xc" 0.0 \
                                        "vcmax" 0.0 "kefd" 0.0 "s0" 0.00
ieeest   62047 "COLSTP 4"  26.00 "1 " : #9 "j" 2.0 "k" 0.0 "a1" 0.03 "a2" 0.0 "a3" 0.0\
                                        "a4" 0.0 "a5" 0.0  "a6" 0.0 "t1" 0.11 "t2" 0.025\
                                        "t3" 0.11 "t4" 0.025 "t5" 22.0 "t6"  22.0 \
                                        "ks" 6.0 "lsmax" 0.05 "lsmin" -0.05\
                                        "vcu" 0.0  "vcl" 0.0 "tdelay" 0.0
oel1     62047 "COLSTP 4"  26.00 "1 " : #9 "ifdset" 2.33 "ifdmax"   2.66 "tpickup" -15.0\
                                        "runback" 0.0 "tmax" 999.0 "tset" 999.0\
                                        "ifcont" 2.22 "vfdflag" 0.0
ieeeg1   62047 "COLSTP 4"  26.00 "1 " : #9 mwcap=810.0 "k"  20.0 "t1" 0.0 "t2" 0.0 \
                                        "t3" 0.1 "uo" 0.4 "uc" -0.4 \
                                        "pmax" 1.0 "pmin" -0.011 "t4" 0.25 "k1" 0.274 "k2" 0.0\
                                        "t5"  10.0 "k3" 0.243 "k4" 0.0 "t6" 0.50 \
                                        "k5" 0.483 "k6" 0.0 "t7" 0.0 "k7" 0.0 "k8" 0.0\
                                        "db1" 0.0 "eps" 0.0 "db2" 0.0 "gv1" 0.0 "pgv1" 0.0\
                                        "gv2" 0.0 "pgv2" 0.0 "gv3" 0.0 "pgv3" 0.0 "gv4" 0.0\
                                        "pgv4" 0.0 "gv5" 0.0 "pgv5" 0.0 "gv6" 0.0 "pgv6" 0.0
lcfb1    62047 "COLSTP 4"  26.00 "1 " : #9 "type" 1.0 "db" 0.0 "emax" 0.1 "fb" 0.0 \
                                        "kp" 0.0 "ki" 0.05 "fbf" 0.0 "pbf" 1.0 \
                                        "tpelec" 1.0 "lrmax" 0.025  "pmwset" 0.0
```

```
#
#HAYNES "GAS" SETTINGS
gentpf   26026 "HAYNES1G"  18.00 "1 " : #9 mva=270.0 "Tpdo" 4.8 "Tppdo" 0.037 "Tpqo" 0.5\
                                        "Tppqo" 0.075 "H" 4.05 "D" 0.0 "Ld" 1.77 "Lq" 1.6\
                                        "Lpd" 0.25 "Lpq" 0.41  "Lppd" 0.2 "Lppq" 0.20\
                                        "L1" 0.155 "S1" 0.135 "S12" 0.568 "Ra" 0.0018\
                                        "Rcomp" 0.0 "Xcomp" 0.0 "accel" 1.0
exdc1    26026 "HAYNES1G"  18.00 "1 " : #9  0.020 50.0 0.02 0.0 0.0 3.2  -3.2 0.0 0.50\
                                        0.08 1.0 0.0 1.975 0.133 2.633 0.356
ieeeg1   26026 "HAYNES1G"  18.00 "1 " : #9 mwcap=230.0  18.2 0.1 0.0 0.26 0.10 -1.0 \
                                        1.0 0.0 0.1 0.272 0.00 5.00 0.428 0.0 0.40 0.30\
                                        0.0 0.0 0.0 0.0
pss2b    26026 "HAYNES1G"  18.00 "1 " : #9  1.00 0.0 3.0 0.0 999.0 -999.0 5.0 5.0 999.0\
                                        -999.0 5.0.0 0.0 5.0 0.617 1.0 0.5 0.1 1.0\
                                        5.0 4.0 0.2 0.04 0.3 0.03 0.3 0.03 0.05  -0.05\
                                        1.0 0.0 0.0 1.0
```

Bus number	Bus name	Voltage (kV)
1	GEN1	22.0
2	GEN2	22.0
3	GEN3	22.0
4	GEN4	22.0
5	BUS5	230.0
6	BUS6	230.0
7	GEN5	13.8

Table 29: 7-bus, 5-generator system line voltages.

Bus number from	Bus number to	CK	R (p.u.)	X (p.u.)
1	2	1	0.0025	0.0250
2	5	1	0.0	0.0100
3	4	1	0.0025	0.0250
4	5	1	0.0	0.0100
4	6	1	0.0	0.0100
5	6	1	0.0200	0.2200
5	6	2	0.0200	0.2200
5	6	3	0.0200	0.2200

Table 30: 7-bus, 5-generator system line parameters.

Appendix D - Prony Analysis

Note 1: For this case, type 3/4 wind turbines were replaced with **genrou** models with governors

Note 2: For this case, type 3/4 wind turbines were replaced with **genrou** models without governors

Note 3: For this case, all wind turbines were replaced with **genrou** models with governors

Note 4: For this case, all wind turbines were replaced with **genrou** models without governors

Table 31: 2012 heavy summer, 1.4 GW at Chief Joseph brake, 0.5 sec

Gen ID	**Freq**	**Damping**	**Residue**	**Angle**
HAYNES1G	0.87	4.84	1.00	0.00
CURRNTC1	0.85	5.21	0.83	-104.96
SHEER_1	0.85	3.48	0.50	79.32
CURRNTC1	0.72	12.36	1.00	0.00
EHUNTER1	0.73	11.99	0.95	-12.46
KMO_13G1	0.72	7.36	0.62	-155.44
REV_13G1	0.71	9.01	0.47	-3.91
HAYNES1G	0.70	14.67	0.20	-85.75
SJUAN_G1	0.71	6.26	0.05	23.99
SUND#5GN	0.70	5.06	0.03	-51.27
REV_13G1	0.53	14.36	1.00	0.00
SLHWKG1	0.56	17.27	0.84	44.61
SHEER_1	0.56	19.90	0.77	-106.42
PALOVRD2	0.55	10.07	0.64	-2.86
NAVAJO_1	0.55	8.64	0.23	-7.64
VALMY_G2	0.78	16.93	1.00	0.00
COLSTP_2	0.76	11.48	0.82	99.92
VALMY_G2	0.78	11.54	0.57	-138.03
MBPP-1	0.78	10.69	0.26	83.14
BRWNL_5	0.78	8.38	0.11	-81.75
CRAIG_1	0.77	10.46	0.09	-85.84
SLHWKG1	0.75	18.08	0.08	-142.74
PALOVRD2	0.79	16.17	0.08	113.00
RAWHIDE	0.79	10.01	0.06	96.72
CGS	0.74	5.92	0.05	66.68
NAVAJO_1	0.76	15.89	0.05	-167.66
JDA_0304	0.78	5.06	0.03	-53.55
HYATT_1	0.96	23.65	1.00	0.00
CRAIG_1	0.99	15.56	0.27	145.53
MBPP-1	0.97	7.57	0.07	146.76
RAWHIDE	0.99	9.62	0.07	64.88
SUND#5GN	0.97	10.31	0.03	99.66
JDA_0304	0.91	26.88	1.00	0.00
CGS	0.88	20.58	0.52	-5.68
COLSTP_2	0.92	10.88	0.26	67.73
EHUNTER1	0.90	5.27	0.01	-96.70
NAVAJO_1	0.89	7.49	0.00	-135.82
SUND#5GN	0.35	13.39	1.00	0.00
SHEER_1	0.34	13.30	0.74	6.71
VALMY_G2	0.34	19.55	0.73	138.69
CGS	0.35	13.10	0.55	169.27
COULEE22	0.35	13.01	0.52	178.21
KMO_13G1	0.34	10.27	0.51	-179.90
BRWNL_5	0.34	15.60	0.51	171.86
JDA_0304	0.35	15.07	0.50	170.70
REV_13G1	0.35	12.33	0.44	178.79
COLSTP_2	0.35	12.86	0.39	152.65

Table 31: 2012 heavy summer, 1.4 GW at Chief Joseph brake, 0.5 sec

Gen ID	**Freq**	**Damping**	**Residue**	**Angle**
HYATT_1	0.34	16.52	0.39	-150.59
BRIDGER1	0.35	14.41	0.29	128.93
PALOVRD2	0.35	13.21	0.28	-5.79
SJUAN_G1	0.36	13.09	0.27	-11.26
RAWHIDE	0.36	8.57	0.27	20.77
MBPP-1	0.36	10.25	0.26	27.26
EHUNTER1	0.34	16.28	0.24	123.62
NAVAJO_1	0.35	13.30	0.23	-7.65
SLHWKG1	0.35	13.65	0.23	9.78
CURRNTC1	0.34	15.63	0.22	125.55
CRAIG_1	0.36	10.16	0.21	34.55
HAYNES1G	0.34	11.57	0.13	6.15
DIABLO_1	0.37	6.16	0.03	-136.30
BRIDGER1	0.82	12.01	1.00	0.00
DIABLO_1	0.83	10.32	0.41	-13.29
HYATT_1	0.81	8.12	0.28	150.14
SJUAN_G1	0.80	1.15	0.02	-57.15
KMO_13G1	0.64	11.44	1.00	0.00
REV_13G1	0.68	19.36	0.32	108.78
BRIDGER1	0.65	14.62	0.28	108.25
DIABLO_1	0.66	11.59	0.07	33.70
SHEER_1	0.67	6.95	0.04	90.25
JDA_0304	0.60	24.68	1.00	0.00
COULEE22	0.61	17.97	0.98	3.27
CGS	0.60	17.27	0.80	-3.49
VALMY_G2	0.63	15.83	0.69	-116.43
HYATT_1	0.59	18.48	0.61	-119.39
BRWNL_5	0.61	14.89	0.56	-59.50
COLSTP_2	0.59	16.74	0.53	17.10
BRIDGER1	0.59	18.54	0.49	7.41
EHUNTER1	0.62	11.48	0.40	-102.89
CURRNTC1	0.62	11.74	0.38	-92.02
CRAIG_1	0.62	17.78	0.22	-156.59
PALOVRD2	0.61	25.38	0.20	-30.38
RAWHIDE	0.62	11.38	0.19	63.54
MBPP-1	0.61	11.85	0.13	112.23
HAYNES1G	0.59	10.11	0.11	176.16
DIABLO_1	0.57	7.99	0.07	-141.75
SJUAN_G1	0.59	5.56	0.05	-19.80
SUND#5GN	0.22	19.94	1.00	0.00
SHEER_1	0.22	17.66	0.74	-8.31
REV_13G1	0.21	21.93	0.44	19.80
EHUNTER1	0.25	26.85	0.26	-169.03
BRWNL_5	0.24	24.88	0.25	-70.13
CURRNTC1	0.25	25.10	0.20	-162.01
DIABLO_1	0.20	23.92	0.18	-105.25
HAYNES1G	0.21	18.68	0.17	-123.40
PALOVRD2	0.21	13.39	0.13	-128.73
SLHWKG1	0.22	14.95	0.12	-135.05
NAVAJO_1	0.21	12.92	0.12	-131.21

Table 31: 2012 heavy summer, 1.4 GW at Chief Joseph brake, 0.5 sec

Gen ID	**Freq**	**Damping**	**Residue**	**Angle**
CGS	0.21	12.67	0.11	41.71
JDA_0304	0.24	15.31	0.10	-64.60
CRAIG_1	0.23	14.11	0.10	178.39
MBPP-1	0.25	12.32	0.09	142.85
BRIDGER1	0.27	15.03	0.09	162.09
SJUAN_G1	0.21	7.40	0.07	-124.81
COLSTP_2	0.21	5.77	0.05	13.96
RAWHIDE	0.23	2.93	0.03	-173.24

Table 32: 2012 heavy summer, 1.4 GW at El Dorado bus, 0.5 sec

Gen ID	**Freq**	**Damping**	**Residue**	**Angle**
CURRNTC1	0.93	16.56	1.00	0.00
BRWNL_5	0.95	13.35	0.55	-40.88
EHUNTER1	0.93	13.72	0.46	3.73
JDA_0304	0.94	10.02	0.25	89.04
MBPP-1	0.93	7.74	0.06	85.61
PALOVRD2	0.53	11.08	1.00	0.00
SHEER_1	0.53	13.74	0.96	119.26
SJUAN_G1	0.55	8.12	0.62	-48.71
MBPP-1	0.54	2.88	0.01	-114.26
HAYNES1G	0.75	11.18	1.00	0.00
PALOVRD2	0.76	9.29	0.26	94.54
CURRNTC1	0.76	11.10	0.26	12.61
EHUNTER1	0.76	9.54	0.17	3.64
BRIDGER1	0.77	8.29	0.16	-44.43
MBPP-1	0.77	8.11	0.08	-83.58
SUND#5GN	0.75	6.55	0.02	108.00
JDA_0304	0.76	3.41	0.01	150.07
RAWHIDE	0.75	5.66	0.01	71.44
MBPP-1	0.30	20.37	1.00	0.00
RAWHIDE	0.29	18.07	0.83	2.68
CRAIG_1	0.29	20.48	0.70	17.67
EHUNTER1	0.29	14.95	0.22	26.14
CURRNTC1	0.29	14.08	0.20	27.27
VALMY_G2	0.27	15.67	0.16	101.01
BRIDGER1	0.30	10.11	0.11	27.93
HYATT_1	0.29	16.20	0.11	39.14
SUND#5GN	0.22	19.62	1.00	0.00
SHEER_1	0.22	20.20	0.91	2.57
KMO_13G1	0.21	26.88	0.79	32.75
REV_13G1	0.22	17.77	0.33	17.88
DIABLO_1	0.22	22.24	0.21	-157.55
CGS	0.21	13.07	0.12	35.15
COLSTP_2	0.22	15.80	0.12	-4.61
COULEE22	0.21	14.09	0.11	28.87
PALOVRD2	0.22	12.25	0.11	-145.68

Table 32: 2012 heavy summer, 1.4 GW at El Dorado bus, 0.5 sec

Gen ID	**Freq**	**Damping**	**Residue**	**Angle**
SJUAN_G1	0.22	11.71	0.10	-135.94
HAYNES1G	0.22	11.66	0.09	-159.59
BRWNL_5	0.22	7.63	0.03	2.91
JDA_0304	0.23	1.36	0.02	-20.27
DIABLO_1	0.99	8.40	1.00	0.00
COULEE22	0.97	11.68	0.22	145.12
HYATT_1	0.99	11.68	0.21	-142.66
COLSTP_2	0.96	4.88	0.06	44.72
VALMY_G2	0.97	3.87	0.02	110.49
RAWHIDE	0.96	5.26	0.01	-2.88
PALOVRD2	0.90	15.14	1.00	0.00
HAYNES1G	0.89	10.16	0.43	105.89
SJUAN_G1	0.89	9.70	0.18	15.83
CRAIG_1	0.88	10.94	0.06	-18.64
DIABLO_1	0.88	5.77	0.05	72.84
REV_13G1	0.89	9.81	0.03	112.88
BRIDGER1	0.91	6.22	0.01	-89.18
SHEER_1	0.90	5.61	0.01	-41.80
KMO_13G1	0.66	9.47	1.00	0.00
COLSTP_2	0.68	16.11	0.78	-131.20
HYATT_1	0.68	16.15	0.51	94.85
COULEE22	0.66	13.88	0.40	-118.72
CGS	0.68	12.10	0.27	-165.84
REV_13G1	0.68	9.87	0.21	102.78
KMO_13G1	0.50	16.34	1.00	0.00
VALMY_G2	0.47	21.91	0.53	-117.27
JDA_0304	0.51	15.73	0.23	-152.18
CGS	0.52	19.45	0.20	-152.73
REV_13G1	0.49	13.24	0.19	25.22
COLSTP_2	0.50	21.20	0.19	-119.18
BRWNL_5	0.50	15.12	0.19	-131.87
HYATT_1	0.50	12.15	0.17	-126.31
COULEE22	0.50	18.07	0.14	-115.52
BRIDGER1	0.49	14.32	0.13	-144.24
DIABLO_1	0.50	11.48	0.12	-138.51
SUND#5GN	0.50	13.96	0.11	159.83
CRAIG_1	0.51	20.04	0.04	17.93
RAWHIDE	0.50	4.53	0.00	2.11
HYATT_1	0.80	10.48	1.00	0.00
COLSTP_2	0.79	7.00	0.89	125.06
CGS	0.81	10.66	0.59	-126.97
VALMY_G2	0.59	12.89	1.00	0.00
CURRNTC1	0.58	8.39	0.25	69.66
EHUNTER1	0.58	7.51	0.19	57.88
SUND#5GN	0.35	13.58	1.00	0.00
SHEER_1	0.35	14.75	0.87	-1.96
VALMY_G2	0.35	23.65	0.82	140.53

Table 32: 2012 heavy summer, 1.4 GW at El Dorado bus, 0.5 sec

Gen ID	**Freq**	**Damping**	**Residue**	**Angle**
CGS	0.35	13.72	0.55	167.60
COLSTP_2	0.34	14.83	0.53	174.64
NAVAJO_1	0.36	19.26	0.49	-45.41
COULEE22	0.35	13.24	0.49	178.85
BRWNL_5	0.35	14.11	0.40	171.01
KMO_13G1	0.34	9.14	0.39	-160.11
HAYNES1G	0.36	18.58	0.39	-5.21
REV_13G1	0.35	12.11	0.38	171.45
JDA_0304	0.36	12.96	0.34	149.43
PALOVRD2	0.36	13.50	0.32	-21.18
SLHWKG1	0.36	14.44	0.29	-8.00
SJUAN_G1	0.37	13.11	0.28	-54.84
BRIDGER1	0.36	15.19	0.19	149.19
DIABLO_1	0.33	17.94	0.19	48.84
HYATT_1	0.37	9.19	0.09	127.28

Table 33: 2012 heavy summer, 1.4 GW at Hemingway Bus, 0.5 sec

Gen ID	**Freq**	**Damping**	**Residue**	**Angle**
DIABLO_1	0.55	17.42	1.00	0.00
HYATT_1	0.54	17.55	0.58	12.43
SJUAN_G1	0.53	10.78	0.20	-97.41
PALOVRD2	0.51	12.00	0.20	-56.47
NAVAJO_1	0.51	12.47	0.14	-58.07
CURRNTC1	0.53	10.53	0.05	28.53
KMO_13G1	0.64	9.32	1.00	0.00
COULEE22	0.63	16.01	0.59	-98.68
CGS	0.63	16.15	0.53	-105.58
SJUAN_G1	0.65	12.57	0.10	-112.02
NAVAJO_1	0.65	19.68	0.10	-116.28
PALOVRD2	0.63	13.43	0.09	-97.09
CRAIG_1	0.64	16.46	0.08	77.11
HAYNES1G	0.66	12.82	0.02	89.16
JDA_0304	0.90	19.63	1.00	0.00
SJUAN_G1	0.87	26.76	0.19	-14.23
CURRNTC1	0.90	7.13	0.03	9.88
EHUNTER1	0.89	6.66	0.03	33.21
SUND#5GN	0.91	20.97	0.01	-79.68
PALOVRD2	0.91	8.42	0.01	123.49
COULEE22	0.39	10.77	1.00	0.00
CGS	0.40	11.43	0.90	-30.16
COLSTP_2	0.42	12.12	0.47	-68.08
RAWHIDE	0.40	9.82	0.31	136.97
SUND#5GN	0.24	22.33	1.00	0.00
SHEER_1	0.24	18.82	0.63	-8.14
NAVAJO_1	0.25	-4.17	0.01	136.49
PALOVRD2	0.23	-34.70	0.00	-156.01

Table 33: 2012 heavy summer, 1.4 GW at Hemingway Bus, 0.5 sec

Gen ID	**Freq**	**Damping**	**Residue**	**Angle**
RAWHIDE	0.58	19.03	1.00	0.00
COLSTP_2	0.61	16.39	0.90	136.67
MBPP-1	0.58	18.12	0.44	22.07
HAYNES1G	0.57	11.61	0.23	58.99
CRAIG_1	0.98	19.15	1.00	0.00
COLSTP_2	0.95	9.13	0.45	-140.77
CGS	0.95	15.61	0.34	135.89
MBPP-1	0.98	5.38	0.04	7.60
DIABLO_1	0.98	4.88	0.02	177.54
SLHWKG1	0.99	6.95	0.01	96.68
COLSTP_2	0.78	11.71	1.00	0.00
KMO_13G1	0.74	7.87	0.61	37.00
COULEE22	0.79	9.77	0.46	-130.30
CGS	0.78	9.48	0.37	-114.95
MBPP-1	0.77	11.01	0.32	47.08
SLHWKG1	0.75	23.38	0.25	83.73
REV_13G1	0.79	9.64	0.21	62.14
RAWHIDE	0.76	11.19	0.17	148.59
HAYNES1G	0.77	5.07	0.04	3.83
SLHWKG1	0.77	0.20	0.00	16.59
KMO_13G1	0.48	15.06	1.00	0.00
DIABLO_1	0.49	18.55	0.58	-106.16
HYATT_1	0.48	16.17	0.42	-104.31
SUND#5GN	0.48	14.79	0.17	178.01
JDA_0304	0.47	12.63	0.17	-103.43
BRWNL_5	0.45	12.51	0.12	-50.23
SHEER_1	0.50	16.53	0.11	160.08
REV_13G1	0.49	8.00	0.10	14.91
SLHWKG1	0.50	11.75	0.06	34.86
EHUNTER1	0.50	3.10	0.00	159.10
EHUNTER1	0.68	26.37	1.00	0.00
CURRNTC1	0.70	25.32	0.83	-16.81
VALMY_G2	0.70	26.74	0.76	2.82
JDA_0304	0.71	20.05	0.52	-146.68
REV_13G1	0.68	11.77	0.13	125.80
DIABLO_1	0.69	15.77	0.06	21.32
SHEER_1	0.67	4.68	0.01	123.02
SUND#5GN	0.72	5.32	0.00	-83.86
BRIDGER1	0.81	20.36	1.00	0.00
JDA_0304	0.84	14.59	0.60	69.77
SHEER_1	0.85	7.95	0.01	-167.65
SUND#5GN	0.34	11.52	1.00	0.00
REV_13G1	0.38	16.79	0.99	106.99
SHEER_1	0.34	12.00	0.81	6.20
KMO_13G1	0.35	9.80	0.66	153.18
MBPP-1	0.31	16.62	0.46	-164.96
RAWHIDE	0.32	12.08	0.39	153.96

Table 33: 2012 heavy summer, 1.4 GW at Hemingway Bus, 0.5 sec

Gen ID	**Freq**	**Damping**	**Residue**	**Angle**
COLSTP_2	0.34	10.18	0.36	165.32
JDA_0304	0.34	11.30	0.35	-171.56
BRIDGER1	0.34	12.42	0.33	165.17
PALOVRD2	0.35	10.96	0.32	-5.64
BRWNL_5	0.34	10.57	0.31	176.12
NAVAJO_1	0.35	12.10	0.30	-8.98
EHUNTER1	0.33	14.85	0.30	153.10
CGS	0.33	8.41	0.29	-171.44
HAYNES1G	0.34	13.35	0.26	13.48
CRAIG_1	0.31	14.90	0.26	-164.01
CURRNTC1	0.33	14.30	0.26	173.62
SLHWKG1	0.34	11.44	0.25	18.44
HYATT_1	0.34	12.35	0.24	-165.08
COULEE22	0.33	6.19	0.18	-164.62
MBPP-1	0.36	10.40	0.18	17.15
SJUAN_G1	0.36	4.99	0.16	-13.22
CRAIG_1	0.37	8.53	0.08	-8.68
REV_13G1	0.30	3.81	0.08	-89.97
DIABLO_1	0.34	7.92	0.06	-29.51
SJUAN_G1	0.33	-6.12	0.01	-56.72

Table 34: 2012 heavy summer, 1.4 GW at Midway bus, 0.5 sec

Gen ID	**Freq**	**Damping**	**Residue**	**Angle**
BRWNL_5	0.53	16.62	1.00	0.00
CURRNTC1	0.55	13.79	0.46	-66.28
COULEE22	0.54	15.40	0.43	-21.34
CGS	0.54	14.26	0.38	-39.72
BRIDGER1	0.54	8.72	0.17	-91.38
BRIDGER1	0.39	26.20	1.00	0.00
SLHWKG1	0.39	18.04	0.35	166.27
REV_13G1	0.39	16.02	0.18	-50.19
COULEE22	0.64	17.30	1.00	0.00
CGS	0.65	15.89	0.73	-15.16
DIABLO_1	0.63	15.53	0.59	-164.41
CURRNTC1	0.66	9.06	0.17	-60.08
PALOVRD2	0.87	21.11	1.00	0.00
COLSTP_2	0.88	11.19	0.79	-32.96
SHEER_1	0.86	6.58	0.01	83.91
CGS	0.27	20.47	1.00	0.00
RAWHIDE	0.26	22.40	0.63	-39.79
CURRNTC1	0.29	20.44	0.43	-79.12
EHUNTER1	0.29	19.22	0.37	-84.72
BRIDGER1	0.29	17.14	0.26	-41.17
COLSTP_2	0.29	10.61	0.18	-35.62
VALMY_G2	0.28	15.53	0.16	-46.04
COULEE22	0.28	7.09	0.10	29.88

Table 34: 2012 heavy summer, 1.4 GW at Midway bus, 0.5 sec

Gen ID	**Freq**	**Damping**	**Residue**	**Angle**
BRWNL_5	0.29	8.79	0.08	-39.91
PALOVRD2	0.45	21.71	1.00	0.00
NAVAJO_1	0.44	18.56	0.58	1.82
NAVAJO_1	0.45	-0.54	0.01	148.07
COLSTP_2	0.76	16.31	1.00	0.00
BRWNL_5	0.73	16.77	0.32	-91.15
EHUNTER1	0.73	9.71	0.09	-116.05
HAYNES1G	0.75	8.40	0.08	-43.44
REV_13G1	0.76	10.20	0.07	111.18
CRAIG_1	0.73	13.63	0.07	-101.07
MBPP-1	0.76	9.48	0.06	40.29
SLHWKG1	0.77	6.93	0.03	-67.29
SUND#5GN	0.78	14.71	0.03	111.69
SUND#5GN	0.75	1.72	0.00	85.67
BRWNL_5	0.60	22.46	1.00	0.00
EHUNTER1	0.59	14.75	0.44	41.00
KMO_13G1	0.59	7.43	0.40	-133.90
COLSTP_2	0.57	15.15	0.35	115.52
SJUAN_G1	0.59	13.09	0.17	30.49
RAWHIDE	0.59	12.01	0.16	-141.80
MBPP-1	0.60	11.78	0.08	-149.71
BRIDGER1	0.60	8.18	0.08	80.82
HAYNES1G	0.59	9.10	0.05	-114.53
CRAIG_1	0.58	12.85	0.03	-24.70
HAYNES1G	0.94	14.37	1.00	0.00
CURRNTC1	0.93	15.10	0.49	149.59
MBPP-1	0.93	11.01	0.14	-76.33
EHUNTER1	0.95	6.53	0.06	123.98
SJUAN_G1	0.93	9.08	0.06	-163.16
VALMY_G2	0.96	5.29	0.03	3.85
KMO_13G1	0.94	1.63	0.00	-20.24
RAWHIDE	0.95	0.44	0.00	-164.90
VALMY_G2	0.52	15.86	1.00	0.00
KMO_13G1	0.50	9.09	0.82	-176.01
JDA_0304	0.52	14.85	0.81	29.07
EHUNTER1	0.49	21.87	0.77	70.93
REV_13G1	0.50	14.42	0.72	-144.42
SUND#5GN	0.51	11.32	0.19	9.71
SJUAN_G1	0.51	8.74	0.13	-135.59
SLHWKG1	0.49	9.09	0.07	-65.34
SHEER_1	0.51	9.75	0.06	14.76
PALOVRD2	0.48	-4.16	0.00	-36.74
RAWHIDE	0.35	18.83	1.00	0.00
MBPP-1	0.35	19.29	0.88	12.99
CRAIG_1	0.35	18.94	0.62	27.37
SHEER_1	0.34	13.60	0.13	-123.50
SUND#5GN	0.34	10.61	0.12	-115.21
HAYNES1G	0.36	10.85	0.06	-155.60

Table 34: 2012 heavy summer, 1.4 GW at Midway bus, 0.5 sec

Gen ID	**Freq**	**Damping**	**Residue**	**Angle**
REV_13G1	0.69	13.34	1.00	0.00
KMO_13G1	0.68	6.64	0.86	-120.93
VALMY_G2	0.70	11.01	0.40	-12.14
JDA_0304	0.69	14.96	0.39	78.92
PALOVRD2	0.71	13.08	0.16	28.65
RAWHIDE	0.70	11.46	0.14	-139.01
NAVAJO_1	0.71	9.54	0.06	33.07
SHEER_1	0.68	4.81	0.03	-16.07
BRIDGER1	0.82	7.68	1.00	0.00
COULEE22	0.80	6.24	0.94	-117.36
CGS	0.80	5.24	0.60	-112.68
CURRNTC1	0.84	3.43	0.19	38.85
JDA_0304	0.81	0.33	0.05	-140.39
CGS	0.24	29.21	1.00	0.00
SUND#5GN	0.22	17.13	0.76	-36.23
SHEER_1	0.22	17.51	0.68	-34.01
MBPP-1	0.25	22.43	0.22	128.66
REV_13G1	0.22	13.28	0.21	-24.19
CRAIG_1	0.24	20.97	0.15	153.07
KMO_13G1	0.22	5.48	0.12	-32.04
SJUAN_G1	0.22	11.94	0.10	177.64
SLHWKG1	0.22	10.52	0.08	169.64
HAYNES1G	0.21	10.49	0.07	-170.13
NAVAJO_1	0.22	7.55	0.06	172.17
PALOVRD2	0.22	4.67	0.05	172.33
JDA_0304	0.24	1.69	0.02	-85.62

Table 35: 2012 heavy summer, double Palo Verde trip

Gen ID	**Freq**	**Damping**	**Residue**	**Angle**
SUND#5GN	0.41	17.81	1.00	0.00
COLSTP_2	0.43	13.70	0.83	34.99
SHEER_1	0.43	14.17	0.36	-42.74
KMO_13G1	0.49	11.69	1.00	0.00
COLSTP_2	0.46	24.63	0.96	-147.76
HYATT_1	0.49	12.39	0.45	-130.16
BRWNL_5	0.48	12.86	0.30	-117.40
SJUAN_G1	0.49	11.96	0.27	31.46
VALMY_G2	0.48	12.05	0.27	-154.04
JDA_0304	0.48	11.87	0.26	-108.68
EHUNTER1	0.48	14.21	0.22	-118.71
SUND#5GN	0.50	12.05	0.19	140.70
CGS	0.49	13.26	0.19	-138.75
DIABLO_1	0.49	10.57	0.18	-126.00
REV_13G1	0.47	11.00	0.17	60.59
SLHWKG1	0.48	13.74	0.16	114.34
CURRNTC1	0.47	12.59	0.15	-95.01

Table 35: 2012 heavy summer, double Palo Verde trip

Gen ID	**Freq**	**Damping**	**Residue**	**Angle**
BRIDGER1	0.49	11.02	0.14	-149.81
NAVAJO_1	0.48	11.97	0.12	95.40
COULEE22	0.46	11.99	0.12	-40.78
SUND#5GN	0.34	12.33	1.00	0.00
CGS	0.34	13.53	0.82	-174.22
RAWHIDE	0.31	15.56	0.76	-147.34
KMO_13G1	0.34	11.87	0.75	155.93
SHEER_1	0.34	12.30	0.72	-1.89
COULEE22	0.34	13.06	0.71	-179.96
COLSTP_2	0.34	13.37	0.61	160.28
NAVAJO_1	0.33	15.87	0.60	44.05
MBPP-1	0.31	15.45	0.56	-131.41
BRWNL_5	0.34	14.13	0.55	-177.17
SLHWKG1	0.34	15.56	0.55	37.97
REV_13G1	0.34	11.82	0.47	168.67
JDA_0304	0.34	12.90	0.45	-177.15
BRIDGER1	0.33	14.20	0.39	-154.86
CRAIG_1	0.30	15.02	0.35	-110.61
HAYNES1G	0.33	14.82	0.33	45.87
SJUAN_G1	0.34	13.24	0.33	22.92
VALMY_G2	0.33	13.98	0.30	-174.13
RAWHIDE	0.35	9.84	0.24	-16.26
CURRNTC1	0.33	12.77	0.21	164.55
HYATT_1	0.34	12.23	0.20	-160.62
EHUNTER1	0.33	12.63	0.19	157.32
DIABLO_1	0.33	13.22	0.18	-1.41
MBPP-1	0.35	8.98	0.14	4.67
CRAIG_1	0.35	8.50	0.10	15.11
COLSTP_2	0.75	21.41	1.00	0.00
COULEE22	0.75	25.26	0.92	51.15
CURRNTC1	0.75	9.34	0.11	-27.04
KMO_13G1	0.73	9.00	0.09	-108.14
EHUNTER1	0.75	8.31	0.08	-30.99
HYATT_1	0.77	8.90	0.05	173.39
HAYNES1G	0.91	12.72	1.00	0.00
BRIDGER1	0.89	19.87	0.77	-49.18
CURRNTC1	0.90	19.53	0.38	-49.73
KMO_13G1	0.89	11.36	0.19	-29.18
BRWNL_5	0.93	8.58	0.15	-94.97
EHUNTER1	0.92	7.65	0.13	-7.45
MBPP-1	0.92	9.01	0.09	-114.93
KMO_13G1	0.60	9.43	1.00	0.00
COULEE22	0.60	13.49	0.64	-156.08
EHUNTER1	0.59	11.95	0.53	179.14
DIABLO_1	0.59	12.27	0.46	39.02
CURRNTC1	0.58	11.62	0.43	-166.96
COLSTP_2	0.62	9.89	0.38	137.40
BRWNL_5	0.58	13.46	0.36	-150.31
RAWHIDE	0.60	13.04	0.30	-28.24
REV_13G1	0.57	12.40	0.25	123.85

Table 35: 2012 heavy summer, double Palo Verde trip

Gen ID	**Freq**	**Damping**	**Residue**	**Angle**
CGS	0.60	9.59	0.24	-156.97
VALMY_G2	0.60	8.49	0.16	140.07
JDA_0304	0.60	10.27	0.16	-136.97
BRIDGER1	0.57	9.64	0.16	-131.28
BRWNL_5	0.62	6.69	0.05	120.07
SLHWKG1	0.83	14.44	1.00	0.00
DIABLO_1	0.82	25.84	0.95	152.01
NAVAJO_1	0.83	13.65	0.56	-38.53
SUND#5GN	0.81	6.88	0.02	36.02
SHEER_1	0.85	7.08	0.02	61.92
DIABLO_1	0.99	10.29	1.00	0.00
REV_13G1	0.98	14.47	0.17	34.28
SUND#5GN	1.01	9.99	0.04	37.51
COULEE22	0.39	23.49	1.00	0.00
DIABLO_1	0.37	29.40	0.61	132.29
CGS	0.38	16.29	0.43	25.34
SLHWKG1	0.37	18.03	0.42	-116.53
NAVAJO_1	0.36	16.21	0.40	-77.81
CURRNTC1	0.39	22.84	0.37	-41.53
JDA_0304	0.40	16.64	0.28	-10.12
BRWNL_5	0.39	15.70	0.27	7.12
BRIDGER1	0.37	14.80	0.23	67.56
EHUNTER1	0.40	19.34	0.22	-60.24
VALMY_G2	0.38	12.11	0.10	33.85
HYATT_1	0.38	12.83	0.10	70.98
HAYNES1G	0.39	11.16	0.04	-129.46
SJUAN_G1	0.56	17.10	1.00	0.00
HYATT_1	0.55	14.63	0.46	-123.37
SHEER_1	0.52	11.61	0.19	-0.88
MBPP-1	0.55	11.95	0.16	-170.10
REV_13G1	0.51	8.23	0.14	-109.49
RAWHIDE	0.51	11.60	0.14	-80.80
CRAIG_1	0.52	14.04	0.11	-70.21
HAYNES1G	0.54	9.81	0.09	-94.73
JDA_0304	0.52	7.26	0.02	90.11
SUND#5GN	0.20	16.04	1.00	0.00
SHEER_1	0.20	16.07	0.90	-1.89
KMO_13G1	0.20	15.98	0.54	4.53
REV_13G1	0.20	16.02	0.45	5.89
SJUAN_G1	0.20	16.59	0.30	-149.18
NAVAJO_1	0.20	16.32	0.29	-149.74
HAYNES1G	0.20	16.39	0.27	-146.53
DIABLO_1	0.20	16.78	0.26	-145.90
SLHWKG1	0.20	16.36	0.24	-135.09
CGS	0.20	15.82	0.23	17.38
COULEE22	0.20	15.95	0.21	6.89
COLSTP_2	0.20	15.83	0.19	-7.78
CRAIG_1	0.20	17.18	0.19	-128.22
RAWHIDE	0.21	16.20	0.17	-142.24

Table 35: 2012 heavy summer, double Palo Verde trip

Gen ID	**Freq**	**Damping**	**Residue**	**Angle**
MBPP-1	0.20	16.43	0.15	-130.65
EHUNTER1	0.20	16.09	0.12	-117.48
CURRNTC1	0.20	16.25	0.11	-108.91
JDA_0304	0.20	15.56	0.11	-18.18
VALMY_G2	0.20	16.04	0.10	-121.35
BRWNL_5	0.20	15.70	0.10	-27.41
BRIDGER1	0.20	16.01	0.09	-89.77
HYATT_1	0.20	16.49	0.07	-125.43
HYATT_1	0.65	24.44	1.00	0.00
NAVAJO_1	0.68	15.61	0.54	-145.28
REV_13G1	0.70	10.93	0.31	-31.54
HAYNES1G	0.67	9.12	0.25	-53.54
SHEER_1	0.66	14.58	0.24	59.91
SHEER_1	0.70	8.70	0.12	-28.88
SUND#5GN	0.66	8.65	0.05	85.26
KMO_13G1	0.68	3.65	0.05	-112.57
RAWHIDE	0.70	2.98	0.02	-176.41

Table 36: 2012 heavy winter, 1.4 GW at Chief Joseph brake, 0.5 sec

Gen ID	**Freq**	**Damping**	**Residue**	**Angle**
REV_13G1	0.72	16.20	1.00	0.00
COLSTP_2	0.70	9.01	0.45	135.32
CURRNTC1	0.71	11.60	0.41	15.49
EHUNTER1	0.72	10.85	0.39	-1.41
CRAIG_1	0.72	8.68	0.12	-29.44
SUND#5GN	0.70	9.22	0.12	-47.66
RAWHIDE	0.73	6.39	0.05	-153.95
BRWNL_5	0.73	5.04	0.02	-34.16
KMO_13G1	0.68	9.44	1.00	0.00
CGS	0.69	20.40	0.71	-150.35
VALMY_G2	0.69	12.14	0.40	46.93
DIABLO_1	0.65	13.00	0.38	105.83
HYATT_1	0.68	13.61	0.37	97.87
PALOVRD2	0.67	11.92	0.15	-77.90
HAYNES1G	0.68	12.87	0.13	54.19
NAVAJO_1	0.66	13.75	0.11	-55.48
SHEER_1	0.68	8.52	0.09	120.72
REV_13G1	0.60	11.67	1.00	0.00
SLHWKG1	0.61	24.82	0.90	-17.79
SJUAN_G1	0.63	12.07	0.76	-39.80
COLSTP_2	0.87	7.93	1.00	0.00
SHEER_1	0.90	7.25	0.14	-144.97
SUND#5GN	0.87	6.82	0.09	137.67
DIABLO_1	0.89	3.40	0.03	-25.40
RAWHIDE	0.86	1.11	0.00	-132.30
BRIDGER1	0.76	11.77	1.00	0.00
MBPP-1	0.74	7.57	0.25	94.10
HYATT_1	0.76	6.68	0.18	159.95
COULEE22	0.37	27.88	1.00	0.00
KMO_13G1	0.34	20.37	0.93	32.09
SUND#5GN	0.35	15.53	0.85	-133.39
SHEER_1	0.35	15.50	0.49	-125.68
HYATT_1	0.35	19.56	0.34	51.77
CGS	0.36	14.19	0.30	1.29
PALOVRD2	0.35	18.65	0.26	-147.87
REV_13G1	0.37	14.11	0.24	-1.81
RAWHIDE	0.36	14.38	0.24	-178.09
MBPP-1	0.37	16.11	0.22	179.84
SJUAN_G1	0.36	13.86	0.21	-145.16
CRAIG_1	0.37	15.76	0.21	-165.55
SLHWKG1	0.34	18.48	0.18	-108.31
NAVAJO_1	0.35	16.54	0.17	-138.35
VALMY_G2	0.34	16.47	0.16	43.38
BRWNL_5	0.35	13.49	0.15	39.07
JDA_0304	0.36	9.55	0.11	-10.18
COLSTP_2	0.36	10.66	0.10	12.88
BRIDGER1	0.34	13.64	0.08	29.02
EHUNTER1	0.34	21.39	0.08	-44.07

Table 36: 2012 heavy winter, 1.4 GW at Chief Joseph brake, 0.5 sec

Gen ID	**Freq**	**Damping**	**Residue**	**Angle**
CURRNTC1	0.34	16.64	0.05	-17.32
HAYNES1G	0.32	12.19	0.04	-55.85
DIABLO_1	0.37	9.63	0.02	68.90
COLSTP_2	0.48	16.80	1.00	0.00
SJUAN_G1	0.51	10.03	0.35	131.29
RAWHIDE	0.50	7.36	0.08	123.88
JDA_0304	0.96	10.23	1.00	0.00
CRAIG_1	0.96	18.02	0.36	-156.19
BRWNL_5	0.95	9.94	0.34	46.89
BRIDGER1	0.94	12.38	0.21	-48.50
HAYNES1G	0.96	14.91	0.14	102.23
VALMY_G2	0.94	9.14	0.13	40.21
VALMY_G2	0.98	9.34	0.11	-178.74
HYATT_1	0.97	5.63	0.06	-47.81
SUND#5GN	0.25	20.80	1.00	0.00
SHEER_1	0.25	20.49	0.72	1.71
SJUAN_G1	0.24	26.70	0.45	-114.14
DIABLO_1	0.23	28.33	0.43	-113.63
NAVAJO_1	0.23	25.35	0.42	-125.91
RAWHIDE	0.23	27.84	0.39	-110.67
EHUNTER1	0.25	26.56	0.32	-138.58
PALOVRD2	0.23	22.37	0.31	-114.53
SLHWKG1	0.24	22.12	0.30	-133.64
CRAIG_1	0.23	25.75	0.30	-101.89
MBPP-1	0.23	24.84	0.25	-119.57
KMO_13G1	0.27	12.44	0.24	-66.20
KMO_13G1	0.54	11.92	1.00	0.00
DIABLO_1	0.57	21.55	0.64	-162.83
HYATT_1	0.57	14.86	0.60	166.16
BRWNL_5	0.54	15.52	0.50	-150.42
VALMY_G2	0.56	12.64	0.48	132.52
BRIDGER1	0.57	13.47	0.33	130.40
SUND#5GN	0.57	18.20	0.33	146.25
JDA_0304	0.56	11.91	0.29	165.65
SLHWKG1	0.54	14.70	0.24	58.31
EHUNTER1	0.57	12.55	0.23	108.43
CURRNTC1	0.57	12.06	0.20	119.15
PALOVRD2	0.55	8.74	0.11	1.27
NAVAJO_1	0.53	9.79	0.08	50.49
SHEER_1	0.58	13.46	0.08	-109.68
CRAIG_1	0.54	18.57	0.06	45.48
KMO_13G1	0.82	12.79	1.00	0.00
CRAIG_1	0.82	14.37	0.27	54.04
MBPP-1	0.82	10.99	0.24	-156.84
SJUAN_G1	0.79	12.26	0.21	16.68
EHUNTER1	0.83	9.71	0.13	48.96
CURRNTC1	0.80	7.33	0.10	129.88
JDA_0304	0.78	6.08	0.09	54.24
HAYNES1G	0.79	4.84	0.05	-144.27

Table 36: 2012 heavy winter, 1.4 GW at Chief Joseph brake, 0.5 sec

Gen ID	Freq	Damping	Residue	Angle
NAVAJO_1	0.83	16.36	0.04	-76.37
PALOVRD2	0.80	5.30	0.02	17.08
SLHWKG1	0.79	3.27	0.01	-123.73

Table 37: 2012 heavy winter, 1.4 GW at El Dorado bus, 0.5 sec

Gen ID	Freq	Damping	Residue	Angle
SLHWKG1	0.41	22.87	1.00	0.00
NAVAJO_1	0.40	21.10	0.67	-3.95
PALOVRD2	0.40	19.44	0.59	1.46
DIABLO_1	0.40	19.22	0.59	36.77
HAYNES1G	0.40	16.54	0.39	32.86
HYATT_1	0.39	14.41	0.17	96.10
HYATT_1	0.70	16.10	1.00	0.00
KMO_13G1	0.69	8.90	0.91	-98.96
COLSTP_2	0.72	10.41	0.66	103.92
EHUNTER1	0.69	16.72	0.33	-50.38
SUND#5GN	0.69	15.93	0.31	-29.44
SHEER_1	0.70	10.84	0.19	19.74
REV_13G1	0.71	9.63	0.17	3.36
BRIDGER1	0.70	7.80	0.08	-155.40
SUND#5GN	0.58	19.59	1.00	0.00
SHEER_1	0.58	21.10	0.49	7.12
DIABLO_1	0.60	4.99	0.09	-50.12
NAVAJO_1	0.92	28.64	1.00	0.00
DIABLO_1	0.92	12.56	0.26	46.51
COLSTP_2	0.92	7.55	0.02	130.17
BRWNL_5	0.93	6.75	0.02	-175.45
CRAIG_1	0.93	4.69	0.00	158.57
CURRNTC1	0.83	11.27	1.00	0.00
EHUNTER1	0.83	9.62	0.54	9.63
RAWHIDE	0.82	22.59	0.15	139.02
SHEER_1	0.81	2.54	0.03	107.16
HYATT_1	0.81	1.53	0.02	-138.32
COULEE22	0.83	1.10	0.01	-63.31
JDA_0304	0.19	21.16	1.00	0.00
VALMY_G2	0.17	6.29	0.52	-60.53
BRWNL_5	0.18	-7.17	0.05	19.53
SUND#5GN	0.35	23.05	1.00	0.00
RAWHIDE	0.38	16.46	0.70	178.46
MBPP-1	0.38	17.39	0.64	175.18
KMO_13G1	0.36	26.93	0.60	152.97
SHEER_1	0.34	22.26	0.54	8.95
CRAIG_1	0.38	16.52	0.46	-162.49
REV_13G1	0.38	26.74	0.39	132.41

Table 37: 2012 heavy winter, 1.4 GW at El Dorado bus, 0.5 sec

Gen ID	**Freq**	**Damping**	**Residue**	**Angle**
SJUAN_G1	0.38	18.88	0.33	-36.24
COLSTP_2	0.37	22.15	0.31	165.01
BRIDGER1	0.36	21.81	0.21	-142.57
COULEE22	0.35	19.01	0.21	-179.24
CGS	0.35	18.65	0.20	173.85
BRWNL_5	0.36	17.34	0.15	170.72
EHUNTER1	0.35	21.35	0.13	-147.91
JDA_0304	0.36	15.70	0.13	146.97
CURRNTC1	0.35	14.36	0.07	-108.40
SUND#5GN	0.25	23.92	1.00	0.00
SHEER_1	0.25	23.30	0.69	1.73
KMO_13G1	0.23	20.16	0.22	32.78
MBPP-1	0.24	23.48	0.20	-151.34
REV_13G1	0.23	20.73	0.20	40.96
DIABLO_1	0.26	20.25	0.18	178.72
RAWHIDE	0.25	19.57	0.18	-175.27
SJUAN_G1	0.24	18.67	0.17	-145.97
PALOVRD2	0.24	18.37	0.16	-148.46
CGS	0.23	26.22	0.16	48.10
NAVAJO_1	0.24	18.05	0.15	-158.55
CRAIG_1	0.25	19.03	0.15	-165.07
HAYNES1G	0.24	18.96	0.15	-148.78
COULEE22	0.23	24.35	0.14	40.05
COLSTP_2	0.23	21.61	0.10	35.17
EHUNTER1	0.25	18.69	0.09	-153.29
BRIDGER1	0.25	16.45	0.04	-142.51
CURRNTC1	0.26	10.85	0.04	170.78
COULEE22	0.67	17.65	1.00	0.00
CGS	0.67	15.79	0.60	-11.88
VALMY_G2	0.63	6.79	0.11	-100.05
KMO_13G1	0.56	12.37	1.00	0.00
RAWHIDE	0.54	28.76	0.46	1.94
VALMY_G2	0.52	15.40	0.31	-101.25
REV_13G1	0.55	11.51	0.23	24.96
EHUNTER1	0.51	17.13	0.21	-90.64
HYATT_1	0.56	11.47	0.20	-158.82
JDA_0304	0.55	10.75	0.17	-150.09
BRWNL_5	0.55	11.45	0.16	-136.93
COLSTP_2	0.55	11.96	0.14	-134.15
BRIDGER1	0.53	12.18	0.14	-121.96
COULEE22	0.53	11.74	0.12	-87.65
CGS	0.54	10.25	0.11	-125.68
CURRNTC1	0.51	12.43	0.09	-74.97
SJUAN_G1	0.55	8.78	0.08	27.38
PALOVRD2	0.55	8.96	0.07	20.38
PALOVRD2	0.89	8.73	1.00	0.00
BRIDGER1	0.87	8.11	0.53	-39.85
MBPP-1	0.86	12.54	0.37	49.07
REV_13G1	0.89	0.88	0.01	69.58

Table 37: 2012 heavy winter, 1.4 GW at El Dorado bus, 0.5 sec

Gen ID	Freq	Damping	Residue	Angle
SJUAN_G1	0.77	27.09	1.00	0.00
CURRNTC1	0.75	23.56	0.53	-42.03
VALMY_G2	0.76	9.89	0.18	-108.77
HAYNES1G	0.76	9.62	0.18	-179.24
JDA_0304	0.74	10.72	0.09	-18.90
MBPP-1	0.75	7.93	0.07	92.24
CRAIG_1	0.77	6.83	0.04	-98.54
RAWHIDE	0.75	3.50	0.01	-138.05
BRWNL_5	0.77	1.98	0.01	-77.15
CGS	0.79	1.49	0.00	-178.40
SUND#5GN	1.00	22.88	1.00	0.00
SJUAN_G1	0.96	6.80	0.58	44.81
KMO_13G1	0.99	6.87	0.06	66.21

Table 38: 2012 heavy winter, 1.4 GW at Hemingway Bus, 0.5 sec

Gen ID	Freq	Damping	Residue	Angle
KMO_13G1	0.91	9.68	1.00	0.00
SLHWKG1	0.89	8.39	0.70	-131.56
RAWHIDE	0.91	8.40	0.52	-21.72
NAVAJO_1	0.90	11.69	0.46	-145.90
CGS	0.89	5.46	0.29	-7.88
SHEER_1	0.91	6.24	0.23	-9.62
KMO_13G1	0.35	16.84	1.00	0.00
SUND#5GN	0.35	13.20	0.83	-160.46
COULEE22	0.34	16.63	0.68	26.18
REV_13G1	0.35	16.84	0.65	-5.96
CGS	0.34	16.00	0.61	29.57
COLSTP_2	0.34	17.44	0.51	34.55
SHEER_1	0.35	12.34	0.42	-147.30
HAYNES1G	0.34	17.86	0.36	-131.12
PALOVRD2	0.35	14.60	0.36	-146.15
JDA_0304	0.35	14.21	0.30	28.54
NAVAJO_1	0.36	13.67	0.25	-173.15
SLHWKG1	0.38	11.14	0.12	176.63
HYATT_1	0.36	11.06	0.09	-11.21
VALMY_G2	0.71	18.31	1.00	0.00
COULEE22	0.69	12.81	0.18	-115.04
HYATT_1	0.68	12.77	0.17	133.44
KMO_13G1	0.72	6.15	0.12	-41.64
BRIDGER1	0.68	10.34	0.12	51.66
CGS	0.70	10.67	0.10	-152.60
REV_13G1	0.71	7.70	0.06	104.65
NAVAJO_1	0.69	16.18	0.06	-77.16
SHEER_1	0.70	17.84	0.05	132.62
RAWHIDE	0.68	8.93	0.04	150.67
DIABLO_1	0.69	6.87	0.03	93.01

Table 38: 2012 heavy winter, 1.4 GW at Hemingway Bus, 0.5 sec

Gen ID	**Freq**	**Damping**	**Residue**	**Angle**
SJUAN_G1	0.30	14.69	1.00	0.00
DIABLO_1	0.31	16.33	0.78	-45.16
SLHWKG1	0.30	11.93	0.48	-4.43
CRAIG_1	0.28	13.43	0.37	47.44
MBPP-1	0.31	8.31	0.28	-66.19
RAWHIDE	0.27	9.97	0.26	43.72
NAVAJO_1	0.27	8.02	0.20	48.04
CURRNTC1	0.78	20.89	1.00	0.00
EHUNTER1	0.76	20.55	0.96	30.33
COLSTP_2	0.74	11.70	0.60	-136.26
MBPP-1	0.77	10.46	0.12	-169.51
CRAIG_1	0.76	11.13	0.12	58.55
SLHWKG1	0.75	13.89	0.10	-89.47
HAYNES1G	0.75	6.32	0.04	-74.01
SJUAN_G1	0.73	3.81	0.01	142.29
KMO_13G1	0.55	11.48	1.00	0.00
BRWNL_5	0.54	21.13	0.64	-107.99
CURRNTC1	0.55	16.27	0.42	-145.53
JDA_0304	0.55	12.93	0.35	-162.88
REV_13G1	0.55	11.99	0.34	18.85
COLSTP_2	0.55	15.13	0.31	-162.05
EHUNTER1	0.54	14.95	0.29	-155.59
CGS	0.56	13.09	0.28	179.16
HYATT_1	0.55	11.35	0.25	-159.86
VALMY_G2	0.57	10.30	0.25	126.04
PALOVRD2	0.55	12.81	0.20	31.75
COULEE22	0.55	12.84	0.20	-157.22
SUND#5GN	0.56	14.23	0.19	177.48
SJUAN_G1	0.57	9.60	0.13	-20.06
NAVAJO_1	0.56	10.59	0.10	15.02
DIABLO_1	0.56	8.93	0.09	158.83
SLHWKG1	0.55	10.12	0.07	44.85
CRAIG_1	0.57	12.34	0.05	-22.26
COULEE22	0.96	11.85	1.00	0.00
SUND#5GN	0.94	9.32	0.08	-11.40
REV_13G1	0.94	5.72	0.03	-119.97
SUND#5GN	0.23	23.91	1.00	0.00
SHEER_1	0.23	26.50	0.98	-2.17
REV_13G1	0.25	28.95	0.82	-12.54
PALOVRD2	0.24	3.93	0.03	175.81
HYATT_1	0.85	21.78	1.00	0.00
PALOVRD2	0.87	29.61	0.45	-125.60
COLSTP_2	0.85	8.39	0.31	26.62
BRIDGER1	0.42	20.28	1.00	0.00
SJUAN_G1	0.39	12.11	0.24	-69.31
CRAIG_1	0.39	8.02	0.06	-158.11
RAWHIDE	0.40	2.60	0.03	140.67

Table 38: 2012 heavy winter, 1.4 GW at Hemingway Bus, 0.5 sec

Gen ID	**Freq**	**Damping**	**Residue**	**Angle**
KMO_13G1	0.65	9.80	1.00	0.00
JDA_0304	0.66	27.80	1.00	127.09
CURRNTC1	0.62	13.18	0.67	81.21
EHUNTER1	0.63	13.25	0.64	49.97
PALOVRD2	0.65	12.02	0.16	-77.59
SUND#5GN	0.64	12.83	0.13	90.17

Table 39: 2012 heavy winter, 1.4 GW at Midway bus, 0.5 sec

Gen ID	**Freq**	**Damping**	**Residue**	**Angle**
HAYNES1G	0.40	16.21	1.00	0.00
SLHWKG1	0.40	16.80	0.93	-1.41
NAVAJO_1	0.40	16.99	0.93	-26.07
SJUAN_G1	0.40	16.54	0.82	-61.58
CGS	0.39	25.42	0.64	160.97
REV_13G1	0.42	13.78	0.31	130.92
KMO_13G1	0.42	10.11	0.29	110.85
PALOVRD2	0.39	9.82	0.28	-11.34
SJUAN_G1	0.53	21.19	1.00	0.00
REV_13G1	0.54	12.81	0.74	-57.65
SLHWKG1	0.54	18.91	0.35	-24.09
NAVAJO_1	0.53	17.80	0.29	6.63
HYATT_1	0.54	9.37	0.28	153.77
SHEER_1	0.52	13.20	0.20	-134.46
VALMY_G2	0.88	13.78	1.00	0.00
SUND#5GN	0.86	18.10	0.64	67.15
SJUAN_G1	0.83	10.70	0.48	-90.19
COLSTP_2	0.87	5.92	0.42	-109.41
JDA_0304	0.84	7.13	0.26	140.99
BRWNL_5	0.84	5.46	0.09	-87.17
REV_13G1	0.86	2.79	0.02	42.02
PALOVRD2	0.93	14.45	1.00	0.00
KMO_13G1	0.93	16.60	0.47	-169.26
SUND#5GN	0.91	9.00	0.21	151.92
RAWHIDE	0.90	7.32	0.05	-120.48
SHEER_1	0.91	3.29	0.03	0.25
COLSTP_2	0.70	9.51	1.00	0.00
BRIDGER1	0.69	11.42	0.59	19.93
REV_13G1	0.70	9.86	0.46	-86.10
JDA_0304	0.72	12.38	0.29	145.22
NAVAJO_1	0.68	9.33	0.17	101.46
SHEER_1	0.68	6.77	0.11	-57.73
SUND#5GN	0.71	5.06	0.04	-178.45
RAWHIDE	0.71	3.55	0.04	166.33
RAWHIDE	0.38	15.92	1.00	0.00
MBPP-1	0.38	16.53	0.87	8.91

Table 39: 2012 heavy winter, 1.4 GW at Midway bus, 0.5 sec

Gen ID	**Freq**	**Damping**	**Residue**	**Angle**
SUND#5GN	0.36	28.25	0.82	-158.63
CRAIG_1	0.38	16.66	0.73	25.13
BRIDGER1	0.37	21.50	0.38	52.01
COLSTP_2	0.38	19.37	0.30	31.23
BRWNL_5	0.34	23.97	0.22	49.85
HYATT_1	0.37	21.36	0.21	-106.46
EHUNTER1	0.35	18.39	0.16	58.37
CURRNTC1	0.35	13.30	0.12	71.38
KMO_13G1	0.57	11.53	1.00	0.00
COULEE22	0.57	26.22	0.89	-109.24
COLSTP_2	0.60	15.60	0.55	159.21
BRIDGER1	0.58	14.62	0.39	164.86
CGS	0.56	14.90	0.29	-160.21
EHUNTER1	0.59	12.41	0.27	133.83
BRWNL_5	0.57	11.87	0.23	173.49
VALMY_G2	0.57	10.43	0.22	166.25
JDA_0304	0.55	11.16	0.17	-140.20
CURRNTC1	0.56	12.48	0.16	-175.76
KMO_13G1	0.67	7.65	1.00	0.00
COULEE22	0.66	13.65	0.83	-105.61
HYATT_1	0.67	10.24	0.53	86.78
DIABLO_1	0.67	9.26	0.43	69.58
SJUAN_G1	0.66	11.08	0.43	-91.71
HAYNES1G	0.65	12.27	0.41	103.26
CURRNTC1	0.65	10.81	0.37	-105.61
CGS	0.67	11.59	0.37	-126.09
CRAIG_1	0.64	16.72	0.25	163.29
EHUNTER1	0.66	9.43	0.24	-121.58
PALOVRD2	0.67	10.49	0.24	-94.39
BRWNL_5	0.66	8.66	0.11	-141.71
DIABLO_1	0.80	13.98	1.00	0.00
KMO_13G1	0.78	11.17	0.64	-161.42
MBPP-1	0.78	9.25	0.39	68.53
CRAIG_1	0.76	7.12	0.19	-31.58
EHUNTER1	0.81	7.18	0.19	-115.56
BRIDGER1	0.79	8.88	0.13	-10.49
CURRNTC1	0.81	5.71	0.12	-114.66
CGS	0.82	3.10	0.02	123.91
COULEE22	0.82	0.37	0.01	147.98
SUND#5GN	0.24	22.46	1.00	0.00
SHEER_1	0.25	23.53	0.92	-13.50
KMO_13G1	0.23	23.02	0.36	30.54
REV_13G1	0.23	23.06	0.32	27.46
RAWHIDE	0.27	18.13	0.23	152.56
COLSTP_2	0.23	28.00	0.22	29.72
CGS	0.22	28.95	0.22	55.90
COULEE22	0.23	25.65	0.19	37.10
SJUAN_G1	0.25	17.32	0.18	-154.61
NAVAJO_1	0.25	16.87	0.17	-167.92
SLHWKG1	0.25	17.85	0.16	-161.25

Table 39: 2012 heavy winter, 1.4 GW at Midway bus, 0.5 sec

Gen ID	**Freq**	**Damping**	**Residue**	**Angle**
MBPP-1	0.26	17.06	0.15	161.64
HAYNES1G	0.25	16.93	0.15	-167.91
PALOVRD2	0.24	15.82	0.15	-148.63
CRAIG_1	0.26	16.05	0.14	177.88
EHUNTER1	0.25	13.95	0.06	-155.71
BRIDGER1	0.24	15.96	0.04	-115.39
CURRNTC1	0.27	6.25	0.03	148.71

Table 40: 2012 heavy winter, double Palo Verde trip

Gen ID	**Freq**	**Damping**	**Residue**	**Angle**
KMO_13G1	0.65	10.05	1.00	0.00
EHUNTER1	0.63	15.16	0.82	133.50
HYATT_1	0.66	12.02	0.45	65.02
COULEE22	0.65	13.49	0.37	-145.48
SLHWKG1	0.65	16.23	0.37	-80.00
CGS	0.64	13.01	0.30	-141.26
CURRNTC1	0.66	9.72	0.25	88.60
DIABLO_1	0.66	11.57	0.22	39.63
SUND#5GN	0.34	12.91	1.00	0.00
SJUAN_G1	0.34	14.13	0.52	20.34
KMO_13G1	0.33	12.82	0.52	167.10
SHEER_1	0.34	12.38	0.51	3.17
COLSTP_2	0.33	14.61	0.38	-168.50
CGS	0.33	12.68	0.37	-177.79
COULEE22	0.33	12.78	0.37	-174.75
REV_13G1	0.33	12.89	0.36	173.36
NAVAJO_1	0.33	14.45	0.30	45.09
BRWNL_5	0.34	13.68	0.29	175.72
VALMY_G2	0.34	16.41	0.28	172.44
HAYNES1G	0.33	16.08	0.27	74.91
SLHWKG1	0.33	15.08	0.27	68.64
JDA_0304	0.34	11.27	0.21	168.83
HYATT_1	0.35	11.51	0.15	144.16
RAWHIDE	0.96	9.19	1.00	0.00
COULEE22	0.96	8.38	0.28	-111.76
REV_13G1	0.96	10.54	0.17	119.66
COLSTP_2	0.68	10.06	1.00	0.00
BRIDGER1	0.71	14.11	0.84	-177.71
BRWNL_5	0.67	10.56	0.44	-66.70
KMO_13G1	0.71	8.44	0.44	99.38
VALMY_G2	0.69	8.48	0.37	152.70
HAYNES1G	0.70	7.92	0.17	36.20
REV_13G1	0.70	7.10	0.14	-125.38
JDA_0304	0.68	5.81	0.07	-143.25
SHEER_1	0.70	6.49	0.07	-148.55
MBPP-1	0.48	25.64	1.00	0.00

Table 40: 2012 heavy winter, double Palo Verde trip

Gen ID	**Freq**	**Damping**	**Residue**	**Angle**
CRAIG_1	0.48	20.04	0.52	13.43
RAWHIDE	0.45	14.91	0.36	60.06
BRWNL_5	0.47	18.02	0.26	56.51
HAYNES1G	0.48	13.54	0.10	-11.64
BRIDGER1	0.82	21.24	1.00	0.00
SLHWKG1	0.84	10.74	0.47	-73.75
RAWHIDE	0.83	10.03	0.43	-167.93
NAVAJO_1	0.83	11.59	0.34	-60.29
COLSTP_2	0.84	8.69	0.21	-157.11
JDA_0304	0.80	8.53	0.13	168.34
SHEER_1	0.81	8.44	0.02	37.15
SUND#5GN	0.23	19.56	1.00	0.00
SHEER_1	0.23	19.70	0.77	1.17
KMO_13G1	0.23	19.76	0.42	9.32
SJUAN_G1	0.23	19.72	0.40	-145.17
NAVAJO_1	0.23	19.79	0.38	-147.30
REV_13G1	0.23	19.65	0.35	12.93
HAYNES1G	0.23	19.85	0.35	-141.49
RAWHIDE	0.23	19.98	0.35	-150.85
SLHWKG1	0.23	19.94	0.32	-133.22
CRAIG_1	0.23	20.32	0.32	-144.24
DIABLO_1	0.23	19.27	0.32	-149.17
MBPP-1	0.23	20.04	0.30	-147.98
EHUNTER1	0.23	19.63	0.22	-142.52
CURRNTC1	0.23	20.46	0.22	-139.25
BRIDGER1	0.23	25.92	0.22	-135.95
COLSTP_2	0.23	19.44	0.15	3.78
VALMY_G2	0.23	19.75	0.15	-148.07
COULEE22	0.23	19.09	0.14	11.92
HYATT_1	0.23	20.22	0.14	-145.72
CGS	0.23	18.71	0.13	23.18
BRWNL_5	0.24	19.16	0.06	-110.45
JDA_0304	0.24	16.79	0.04	-69.65
BRIDGER1	0.23	14.67	0.03	-88.76
VALMY_G2	0.62	19.55	1.00	0.00
SJUAN_G1	0.61	9.89	0.26	-122.57
HAYNES1G	0.59	10.72	0.17	52.98
CRAIG_1	0.63	16.29	0.14	100.80
RAWHIDE	0.36	11.30	1.00	0.00
MBPP-1	0.36	10.98	0.75	0.05
DIABLO_1	0.39	28.78	0.62	148.63
CRAIG_1	0.36	10.41	0.52	21.07
BRIDGER1	0.38	14.01	0.28	-34.61
CURRNTC1	0.37	10.64	0.13	-20.02
EHUNTER1	0.39	10.74	0.09	-45.97
KMO_13G1	0.38	8.10	0.09	128.13
CRAIG_1	0.38	7.35	0.07	-8.50
REV_13G1	0.38	8.57	0.07	131.38
COULEE22	0.38	7.00	0.04	-175.82
CGS	0.38	6.83	0.03	-178.26

Table 40: 2012 heavy winter, double Palo Verde trip

Gen ID	**Freq**	**Damping**	**Residue**	**Angle**
SUND#5GN	0.39	6.31	0.03	-82.70
JDA_0304	0.37	4.22	0.01	-96.45
EHUNTER1	0.36	4.43	0.01	10.13
SJUAN_G1	0.93	17.43	1.00	0.00
HAYNES1G	0.93	17.32	0.28	175.21
MBPP-1	0.92	11.84	0.25	167.76
VALMY_G2	0.91	16.12	0.09	-132.54
KMO_13G1	0.90	10.28	0.05	118.17
SUND#5GN	0.93	11.34	0.03	-37.92
CRAIG_1	0.92	4.98	0.03	143.12
NAVAJO_1	0.74	23.13	1.00	0.00
COLSTP_2	0.75	8.44	0.56	-19.56
CURRNTC1	0.75	8.69	0.40	-71.92
EHUNTER1	0.73	7.95	0.38	-2.80
JDA_0304	0.77	11.29	0.38	-156.88
MBPP-1	0.72	6.68	0.28	-162.03
BRWNL_5	0.72	8.63	0.27	-32.50
COULEE22	0.76	5.87	0.11	-156.61
CGS	0.75	5.41	0.07	-126.03
SUND#5GN	0.74	6.02	0.05	6.49
KMO_13G1	0.54	12.06	1.00	0.00
EHUNTER1	0.55	16.71	0.48	-173.66
SJUAN_G1	0.54	13.55	0.43	55.77
HYATT_1	0.50	27.20	0.36	-67.78
COLSTP_2	0.54	13.66	0.29	-151.24
VALMY_G2	0.56	10.91	0.27	124.93
BRIDGER1	0.56	12.55	0.27	142.07
REV_13G1	0.54	11.49	0.24	20.31
CURRNTC1	0.53	13.89	0.22	-162.97
JDA_0304	0.54	11.17	0.22	-149.84
COULEE22	0.54	12.92	0.20	-140.54
CGS	0.54	11.35	0.18	-154.35
BRWNL_5	0.55	10.55	0.16	-178.09
NAVAJO_1	0.54	11.94	0.13	63.22
HYATT_1	0.54	10.15	0.12	-161.69
DIABLO_1	0.52	12.50	0.09	-47.94
SUND#5GN	0.57	10.68	0.03	85.14
SHEER_1	0.55	7.73	0.03	25.30
SHEER_1	0.51	7.42	0.02	14.56

Table 41: 2012 light summer, 1.4 GW at Chief Joseph brake, 0.5 sec

Gen ID	Freq	Damping	Residue	Angle
REV_13G1	0.61	16.01	1.00	0.00
SUND#5GN	0.63	18.39	0.71	164.23
HYATT_1	0.60	14.30	0.61	-116.68
CURRNTC1	0.62	17.02	0.51	156.67
EHUNTER1	0.62	16.36	0.44	152.08
VALMY_G2	0.61	14.83	0.39	-174.96
SLHWKG1	0.60	23.60	0.30	41.11
JDA_0304	0.58	9.63	0.17	-144.20
KMO_13G1	0.55	15.31	1.00	0.00
BRWNL_5	0.56	20.90	0.52	-156.33
BRIDGER1	0.54	3.85	0.01	-154.99
KMO_13G1	0.41	11.71	1.00	0.00
SUND#5GN	0.40	11.86	0.68	-153.52
COULEE22	0.40	12.46	0.67	29.52
REV_13G1	0.40	11.66	0.59	22.62
CGS	0.40	12.03	0.59	23.07
SHEER_1	0.40	11.86	0.44	-148.31
JDA_0304	0.40	11.36	0.42	32.41
MBPP-1	0.41	9.52	0.41	-106.72
COLSTP_2	0.40	10.72	0.40	2.13
BRWNL_5	0.40	11.33	0.35	12.77
HYATT_1	0.41	13.03	0.27	19.24
SJUAN_G1	0.40	11.49	0.27	-145.70
PALOVRD2	0.40	10.48	0.26	-155.06
NAVAJO_1	0.40	10.91	0.23	-156.23
VALMY_G2	0.40	11.02	0.22	-21.66
BRIDGER1	0.41	8.95	0.22	-33.17
SLHWKG1	0.40	10.11	0.20	-153.84
RAWHIDE	0.41	4.28	0.17	-152.52
CRAIG_1	0.41	6.65	0.16	-118.26
CURRNTC1	0.41	8.84	0.12	-55.44
EHUNTER1	0.41	9.08	0.12	-61.35
HAYNES1G	0.40	7.51	0.11	-172.09
DIABLO_1	0.41	4.36	0.03	122.14
BRIDGER1	0.29	26.43	1.00	0.00
KMO_13G1	0.29	11.73	0.78	100.30
BRWNL_5	0.28	21.24	0.17	49.83
COLSTP_2	0.95	9.78	1.00	0.00
MBPP-1	0.92	8.52	0.48	-137.92
RAWHIDE	0.92	11.51	0.38	-169.59
CURRNTC1	0.92	2.62	0.02	171.16
EHUNTER1	0.92	2.34	0.02	179.36
KMO_13G1	0.70	10.25	1.00	0.00
REV_13G1	0.71	13.45	0.76	142.01
JDA_0304	0.71	23.74	0.76	-40.38
COLSTP_2	0.73	20.90	0.16	-120.78
COLSTP_2	0.81	9.67	1.00	0.00

Table 41: 2012 light summer, 1.4 GW at Chief Joseph brake, 0.5 sec

Gen ID	**Freq**	**Damping**	**Residue**	**Angle**
VALMY_G2	0.78	17.75	0.81	-65.65
CURRNTC1	0.78	11.56	0.60	-81.53
EHUNTER1	0.78	11.53	0.59	-80.72
RAWHIDE	0.82	14.11	0.52	86.22
MBPP-1	0.78	9.47	0.22	87.50
CRAIG_1	0.79	9.95	0.17	-114.25
SJUAN_G1	0.82	11.03	0.11	131.54
SLHWKG1	0.79	6.87	0.04	-19.19
SUND#5GN	0.81	1.14	0.03	134.26
SHEER_1	0.81	-0.08	0.02	-79.78
BRWNL_5	0.64	26.20	1.00	0.00
HYATT_1	0.67	15.88	0.41	-32.38
BRIDGER1	0.64	16.24	0.24	35.07
SUND#5GN	0.69	14.01	0.23	-141.40
DIABLO_1	0.65	9.10	0.15	15.33
PALOVRD2	0.65	11.77	0.10	-159.60
NAVAJO_1	0.65	13.33	0.07	-152.08
SJUAN_G1	0.65	8.16	0.07	-178.44
HAYNES1G	0.65	7.76	0.04	13.77
SHEER_1	0.64	11.13	0.02	47.67
CGS	0.49	25.74	1.00	0.00
DIABLO_1	0.51	28.69	0.35	85.31
PALOVRD2	0.50	18.54	0.20	177.84
SJUAN_G1	0.52	5.10	0.03	-173.01
MBPP-1	0.44	17.57	1.00	0.00
RAWHIDE	0.45	3.12	0.23	125.63
CRAIG_1	0.47	5.25	0.10	74.41
SUND#5GN	0.25	18.69	1.00	0.00
SHEER_1	0.25	18.76	0.83	-1.77
MBPP-1	0.24	28.85	0.36	-145.11
NAVAJO_1	0.23	22.02	0.26	-132.47
CURRNTC1	0.24	27.45	0.23	-136.00
REV_13G1	0.25	17.75	0.23	2.88
PALOVRD2	0.23	19.93	0.22	-120.27
EHUNTER1	0.24	24.90	0.20	-139.82
CRAIG_1	0.24	21.65	0.20	-146.96
SJUAN_G1	0.23	18.03	0.18	-118.03
RAWHIDE	0.24	18.26	0.17	-147.17
SLHWKG1	0.23	16.14	0.14	-126.49
DIABLO_1	0.22	20.82	0.13	-91.72
CGS	0.25	23.01	0.13	11.39
COLSTP_2	0.25	23.03	0.11	-26.25
HAYNES1G	0.25	-10.15	0.01	-150.39
BRWNL_5	0.86	10.01	1.00	0.00
BRIDGER1	0.90	9.75	0.78	160.09
CGS	0.90	6.84	0.55	-30.76
HYATT_1	0.85	9.27	0.55	-45.02
HAYNES1G	0.86	8.76	0.50	138.30
DIABLO_1	0.88	7.25	0.32	166.35

Table 41: 2012 light summer, 1.4 GW at Chief Joseph brake, 0.5 sec

Gen ID	**Freq**	**Damping**	**Residue**	**Angle**
VALMY_G2	0.85	6.95	0.32	-33.94
PALOVRD2	0.89	7.98	0.17	-38.54
REV_13G1	0.88	3.06	0.15	169.50
KMO_13G1	0.90	3.61	0.14	15.23
SLHWKG1	0.89	7.33	0.14	39.39
NAVAJO_1	0.86	8.06	0.13	72.09

Table 42: 2012 light summer, 1.4 GW at El Dorado bus, 0.5 sec

Gen ID	**Freq**	**Damping**	**Residue**	**Angle**
REV_13G1	0.73	13.29	1.00	0.00
KMO_13G1	0.72	8.58	0.76	-135.06
MBPP-1	0.71	8.33	0.11	-146.42
CURRNTC1	0.72	6.90	0.10	84.40
SHEER_1	0.72	8.87	0.09	-45.43
EHUNTER1	0.72	5.57	0.07	75.59
EHUNTER1	0.55	19.83	1.00	0.00
BRWNL_5	0.56	17.78	0.96	-28.05
BRIDGER1	0.55	19.28	0.92	-3.44
CURRNTC1	0.54	19.31	0.90	24.16
COLSTP_2	0.54	20.94	0.89	-16.45
VALMY_G2	0.55	20.44	0.84	-25.29
COULEE22	0.53	17.49	0.69	9.76
CGS	0.54	16.56	0.59	-12.54
JDA_0304	0.56	12.47	0.38	-39.86
JDA_0304	0.78	19.91	1.00	0.00
SLHWKG1	0.79	13.37	0.95	-146.32
HAYNES1G	0.81	10.79	0.87	141.35
COLSTP_2	0.79	7.89	0.86	140.16
HYATT_1	0.79	12.05	0.79	4.00
COLSTP_2	0.81	13.45	0.70	-74.15
JDA_0304	0.83	12.49	0.68	-170.22
COULEE22	0.78	16.41	0.53	-108.97
REV_13G1	0.81	22.04	0.48	-70.59
SJUAN_G1	0.81	9.46	0.32	-52.20
VALMY_G2	0.80	4.83	0.05	-3.49
SUND#5GN	0.82	18.06	0.05	175.11
RAWHIDE	0.81	3.17	0.01	-160.17
COULEE22	0.88	10.80	1.00	0.00
BRIDGER1	0.89	11.11	0.54	-98.56
MBPP-1	0.86	6.46	0.46	-100.02
VALMY_G2	0.90	11.62	0.40	126.94
KMO_13G1	0.86	10.82	0.38	103.57
CRAIG_1	0.88	7.39	0.26	29.07
CGS	0.87	6.33	0.21	63.74
EHUNTER1	0.89	4.91	0.20	4.89
BRWNL_5	0.85	4.69	0.17	81.17
CURRNTC1	0.89	3.38	0.11	6.27

Table 42: 2012 light summer, 1.4 GW at El Dorado bus, 0.5 sec

Gen ID	**Freq**	**Damping**	**Residue**	**Angle**
SHEER_1	0.88	-5.65	0.00	136.46
REV_13G1	0.85	-5.78	0.00	-4.61
SUND#5GN	0.84	-8.01	0.00	146.07
MBPP-1	0.75	26.64	1.00	0.00
BRIDGER1	0.76	11.46	0.38	54.94
CGS	0.76	13.13	0.22	64.40
CRAIG_1	0.76	9.82	0.16	-99.79
SHEER_1	0.74	25.99	0.15	96.68
BRWNL_5	0.76	2.96	0.01	-46.13
SUND#5GN	0.25	19.12	1.00	0.00
SHEER_1	0.24	19.09	0.83	-1.16
KMO_13G1	0.24	16.76	0.25	17.58
REV_13G1	0.24	17.79	0.22	21.47
NAVAJO_1	0.25	16.53	0.14	-177.52
PALOVRD2	0.25	15.55	0.14	175.89
SJUAN_G1	0.25	15.67	0.13	-178.83
SLHWKG1	0.25	16.60	0.13	-177.00
HAYNES1G	0.25	15.52	0.12	179.82
CGS	0.23	22.09	0.11	57.77
CRAIG_1	0.25	18.25	0.11	174.00
COULEE22	0.23	20.76	0.09	60.17
MBPP-1	0.25	17.63	0.09	177.86
DIABLO_1	0.26	14.72	0.09	179.43
COLSTP_2	0.24	18.94	0.07	1.42
HYATT_1	0.28	15.84	0.03	121.91
EHUNTER1	0.25	10.83	0.03	178.50
CURRNTC1	0.27	3.72	0.01	133.83
BRIDGER1	0.25	5.56	0.01	-147.26
VALMY_G2	0.23	-1.76	0.01	-85.86
KMO_13G1	0.59	12.58	1.00	0.00
SJUAN_G1	0.62	12.92	0.14	-79.06
HYATT_1	0.59	9.79	0.09	-166.68
DIABLO_1	0.64	8.35	0.07	73.86
REV_13G1	0.61	4.56	0.02	-44.99
RAWHIDE	0.40	16.45	1.00	0.00
MBPP-1	0.39	15.50	0.76	19.11
KMO_13G1	0.40	10.00	0.64	-5.68
SUND#5GN	0.40	10.49	0.50	-172.27
CRAIG_1	0.39	15.01	0.49	24.68
COLSTP_2	0.40	11.74	0.44	9.62
REV_13G1	0.40	10.09	0.40	7.49
COULEE22	0.40	10.56	0.39	21.28
CGS	0.40	10.49	0.39	11.45
BRIDGER1	0.39	13.43	0.36	34.97
SHEER_1	0.40	10.72	0.34	-168.30
BRWNL_5	0.40	11.23	0.33	6.84
PALOVRD2	0.40	11.20	0.30	-167.08
NAVAJO_1	0.40	11.78	0.28	-161.91
SLHWKG1	0.40	11.52	0.27	-154.26
CURRNTC1	0.38	14.41	0.26	42.40

Table 42: 2012 light summer, 1.4 GW at El Dorado bus, 0.5 sec

Gen ID	**Freq**	**Damping**	**Residue**	**Angle**
HAYNES1G	0.40	11.71	0.24	-151.79
EHUNTER1	0.38	14.60	0.23	29.52
VALMY_G2	0.39	12.76	0.23	3.21
JDA_0304	0.40	9.73	0.22	28.78
SJUAN_G1	0.41	10.28	0.21	170.56
DIABLO_1	0.40	12.49	0.15	-144.23
HYATT_1	0.40	9.74	0.12	-0.95

Table 43: 2012 light summer, 1.4 GW at Hemingway Bus, 0.5 sec

Gen ID	**Freq**	**Damping**	**Residue**	**Angle**
CURRNTC1	0.53	25.89	1.00	0.00
RAWHIDE	0.55	23.93	0.61	106.30
SLHWKG1	0.54	7.27	0.02	-165.02
VALMY_G2	0.89	18.46	1.00	0.00
KMO_13G1	0.88	6.59	0.10	-4.98
RAWHIDE	0.89	1.63	0.00	-155.71
BRIDGER1	0.84	18.98	1.00	0.00
KMO_13G1	0.85	15.13	0.60	-40.11
SJUAN_G1	0.82	13.50	0.11	-148.88
CGS	0.83	10.79	0.05	50.01
HAYNES1G	0.84	7.86	0.05	14.85
CGS	0.84	6.07	0.04	-94.67
MBPP-1	0.84	5.13	0.03	33.49
COULEE22	0.85	4.12	0.02	-102.01
DIABLO_1	0.83	4.89	0.01	109.13
SLHWKG1	0.82	3.39	0.00	18.51
SHEER_1	0.83	-0.61	0.00	-109.76
SUND#5GN	0.84	0.86	0.00	60.91
NAVAJO_1	0.83	3.74	0.00	-23.06
PALOVRD2	0.84	2.71	0.00	-90.90
KMO_13G1	0.40	11.42	1.00	0.00
SUND#5GN	0.40	10.92	0.62	-160.12
COULEE22	0.40	11.64	0.61	15.73
CGS	0.40	11.65	0.59	8.85
REV_13G1	0.40	11.18	0.59	4.14
COLSTP_2	0.40	11.12	0.48	-2.58
JDA_0304	0.40	11.50	0.43	31.81
SHEER_1	0.40	10.96	0.40	-155.11
BRWNL_5	0.40	11.38	0.40	4.00
PALOVRD2	0.40	11.68	0.39	-175.70
NAVAJO_1	0.39	11.95	0.33	-164.62
SJUAN_G1	0.39	12.10	0.32	-147.26
BRIDGER1	0.39	10.21	0.27	-0.13
SLHWKG1	0.40	10.08	0.24	-177.18
HAYNES1G	0.38	23.18	0.22	-89.92
DIABLO_1	0.39	14.99	0.21	-161.94
MBPP-1	0.39	7.57	0.20	-47.87

Table 43: 2012 light summer, 1.4 GW at Hemingway Bus, 0.5 sec

Gen ID	**Freq**	**Damping**	**Residue**	**Angle**
HAYNES1G	0.40	10.29	0.19	175.98
RAWHIDE	0.40	6.58	0.19	-67.32
HYATT_1	0.40	10.54	0.17	19.51
CURRNTC1	0.39	9.84	0.14	-12.51
CRAIG_1	0.40	6.70	0.12	-61.83
EHUNTER1	0.39	8.55	0.10	-15.53
KMO_13G1	0.59	13.72	1.00	0.00
REV_13G1	0.57	17.40	0.19	57.50
COULEE22	0.61	14.21	0.15	151.11
JDA_0304	0.59	13.16	0.13	171.88
BRWNL_5	0.57	14.58	0.12	-127.29
SUND#5GN	0.58	21.13	0.11	-160.41
HYATT_1	0.57	12.47	0.11	-124.16
DIABLO_1	0.61	12.83	0.10	143.33
SJUAN_G1	0.57	14.01	0.09	53.43
CGS	0.59	13.02	0.09	171.56
COLSTP_2	0.59	12.35	0.07	170.49
PALOVRD2	0.57	9.36	0.03	71.57
MBPP-1	0.57	9.85	0.02	19.15
SHEER_1	0.58	16.87	0.02	-154.19
NAVAJO_1	0.60	9.72	0.02	0.83
CRAIG_1	0.58	10.02	0.01	23.89
SLHWKG1	0.95	19.21	1.00	0.00
MBPP-1	0.92	-0.64	0.05	-18.53
COLSTP_2	0.92	-0.51	0.03	145.66
EHUNTER1	0.50	19.63	1.00	0.00
DIABLO_1	0.48	13.57	0.35	89.45
RAWHIDE	0.51	-3.52	0.01	-150.02
CURRNTC1	0.80	24.37	1.00	0.00
COLSTP_2	0.78	7.69	0.21	-74.47
CRAIG_1	0.78	10.39	0.06	146.87
REV_13G1	0.77	3.04	0.02	-164.27
SLHWKG1	0.78	16.26	0.02	-49.95
KMO_13G1	0.73	14.16	1.00	0.00
EHUNTER1	0.73	22.98	0.85	17.65
RAWHIDE	0.73	10.43	0.10	107.31
REV_13G1	0.72	6.60	0.08	151.34
CURRNTC1	0.70	7.31	0.07	35.38
SJUAN_G1	0.69	11.33	0.06	-5.57
EHUNTER1	0.70	5.95	0.04	12.56
SHEER_1	0.74	4.33	0.01	30.17
SUND#5GN	0.70	2.21	0.00	24.39
SUND#5GN	0.23	19.38	1.00	0.00
SHEER_1	0.23	19.28	0.84	-5.66
NAVAJO_1	0.22	-9.49	0.00	-123.98

Table 44: 2012 light summer, 1.4 GW at Midway bus, 0.5 sec

Gen ID	Freq	Damping	Residue	Angle
SUND#5GN	0.24	18.95	1.00	0.00
SHEER_1	0.24	19.05	0.84	-1.93
REV_13G1	0.24	17.39	0.21	15.80
KMO_13G1	0.24	14.55	0.20	13.28
RAWHIDE	0.26	19.96	0.18	145.01
SLHWKG1	0.26	17.04	0.15	164.86
MBPP-1	0.26	19.64	0.14	155.60
SJUAN_G1	0.25	14.83	0.13	175.40
HAYNES1G	0.26	15.34	0.13	159.52
PALOVRD2	0.25	14.28	0.13	176.50
NAVAJO_1	0.25	14.05	0.12	-179.86
EHUNTER1	0.25	12.79	0.05	-179.82
CURRNTC1	0.26	5.60	0.02	149.17
KMO_13G1	0.74	19.14	1.00	0.00
HYATT_1	0.72	15.60	0.53	-120.74
BRIDGER1	0.74	15.47	0.27	36.09
REV_13G1	0.71	9.65	0.26	-17.49
COLSTP_2	0.74	9.14	0.13	49.02
EHUNTER1	0.73	7.44	0.06	19.99
SUND#5GN	0.71	8.42	0.04	160.53
PALOVRD2	0.71	8.52	0.03	49.54
SHEER_1	0.73	3.16	0.01	-154.09
CURRNTC1	0.64	14.86	1.00	0.00
EHUNTER1	0.63	12.73	0.59	-3.36
COLSTP_2	0.63	11.29	0.38	6.44
HAYNES1G	0.87	15.36	1.00	0.00
EHUNTER1	0.89	11.61	0.25	103.53
MBPP-1	0.86	6.77	0.17	17.23
COULEE22	0.90	7.49	0.17	111.98
PALOVRD2	0.89	11.11	0.17	178.80
SLHWKG1	0.87	9.23	0.16	-101.40
BRIDGER1	0.85	8.94	0.10	29.17
BRWNL_5	0.85	6.06	0.09	-174.12
CGS	0.87	4.08	0.04	172.30
KMO_13G1	0.86	1.76	0.02	-98.43
SHEER_1	0.84	-2.29	0.01	-66.96
REV_13G1	0.86	-2.37	0.00	41.95
RAWHIDE	0.41	13.35	1.00	0.00
MBPP-1	0.41	13.64	0.86	7.80
CRAIG_1	0.42	14.18	0.73	2.48
BRIDGER1	0.41	16.11	0.39	46.87
CURRNTC1	0.40	17.06	0.33	40.61
EHUNTER1	0.41	16.65	0.28	27.66
COLSTP_2	0.39	14.86	0.26	49.00
VALMY_G2	0.40	18.69	0.19	21.87
HAYNES1G	0.41	12.24	0.17	-154.09
SLHWKG1	0.41	12.74	0.14	-145.73
BRWNL_5	0.39	13.09	0.13	42.71
PALOVRD2	0.40	10.87	0.11	-133.24

Table 44: 2012 light summer, 1.4 GW at Midway bus, 0.5 sec

Gen ID	**Freq**	**Damping**	**Residue**	**Angle**
NAVAJO_1	0.40	10.40	0.09	-135.94
SUND#5GN	0.40	8.59	0.09	-177.02
CGS	0.38	8.79	0.06	63.14
SHEER_1	0.41	8.42	0.06	-176.57
REV_13G1	0.39	5.80	0.04	19.75
KMO_13G1	0.40	2.97	0.04	-4.56
SJUAN_G1	0.43	6.74	0.04	89.40
COULEE22	0.38	4.87	0.03	55.80
JDA_0304	0.39	-3.76	0.00	50.36
CGS	0.22	27.63	1.00	0.00
CRAIG_1	0.22	18.58	0.67	-169.70
COULEE22	0.22	18.93	0.42	9.64
VALMY_G2	0.19	6.73	0.12	-51.68
BRIDGER1	0.22	10.93	0.11	-146.48
JDA_0304	0.21	12.88	0.11	119.84
CURRNTC1	0.79	23.33	1.00	0.00
COLSTP_2	0.80	6.35	0.26	-30.95
CRAIG_1	0.81	10.56	0.16	151.28
VALMY_G2	0.81	7.36	0.09	171.22
NAVAJO_1	0.83	9.24	0.06	-160.51
RAWHIDE	0.80	5.39	0.04	81.24
SUND#5GN	0.83	-1.92	0.00	88.79
KMO_13G1	0.69	12.04	1.00	0.00
JDA_0304	0.68	22.71	0.45	-62.31
DIABLO_1	0.70	14.19	0.34	13.10
COULEE22	0.68	16.13	0.20	-111.42
RAWHIDE	0.67	11.74	0.15	33.46
HAYNES1G	0.68	12.23	0.14	65.08
CGS	0.67	13.30	0.13	-104.88
VALMY_G2	0.66	13.65	0.09	-78.46
BRWNL_5	0.68	11.18	0.07	-114.72
MBPP-1	0.68	10.11	0.07	33.02
SJUAN_G1	0.70	8.61	0.07	170.79
KMO_13G1	0.59	14.34	1.00	0.00
SJUAN_G1	0.60	21.56	0.29	70.09
REV_13G1	0.57	21.90	0.27	68.47
PALOVRD2	0.58	27.24	0.27	75.93
NAVAJO_1	0.60	27.32	0.18	60.86
BRIDGER1	0.62	14.19	0.17	123.80
JDA_0304	0.56	15.06	0.13	-107.05
CRAIG_1	0.61	17.20	0.12	-14.28
SUND#5GN	0.55	25.22	0.12	-132.10
COULEE22	0.60	11.12	0.07	179.93
BRWNL_5	0.59	9.00	0.04	167.36
VALMY_G2	0.57	10.29	0.03	-146.71
CGS	0.59	7.63	0.02	178.97
SLHWKG1	0.61	10.71	0.02	3.55
MBPP-1	0.57	5.89	0.01	-3.37

Table 45: 2012 light summer, double Palo Verde trip

Gen ID	**Freq**	**Damping**	**Residue**	**Angle**
KMO_13G1	0.38	9.60	1.00	0.00
SUND#5GN	0.38	12.47	0.97	-131.53
CRAIG_1	0.39	20.16	0.65	97.77
CGS	0.38	10.10	0.62	16.54
REV_13G1	0.38	9.74	0.60	17.54
COULEE22	0.38	9.92	0.58	23.10
COLSTP_2	0.37	10.00	0.44	20.06
BRWNL_5	0.38	9.37	0.37	-6.59
SHEER_1	0.35	22.62	0.36	-64.83
BRIDGER1	0.38	10.60	0.35	11.38
MBPP-1	0.37	10.01	0.32	-24.35
RAWHIDE	0.38	9.60	0.31	-41.83
SLHWKG1	0.37	10.22	0.28	-126.09
JDA_0304	0.37	9.48	0.26	59.23
HAYNES1G	0.38	9.45	0.25	-132.97
SHEER_1	0.39	8.60	0.24	168.03
SJUAN_G1	0.37	10.80	0.23	-111.61
HYATT_1	0.38	9.81	0.21	-3.67
SJUAN_G1	0.40	10.05	0.21	136.86
CRAIG_1	0.38	9.27	0.20	-51.56
VALMY_G2	0.38	8.93	0.16	-16.38
DIABLO_1	0.37	10.09	0.15	-136.29
NAVAJO_1	0.37	9.78	0.15	-125.26
EHUNTER1	0.38	9.62	0.15	-50.02
CURRNTC1	0.38	9.74	0.15	-15.18
NAVAJO_1	0.39	7.87	0.12	-169.83
JDA_0304	0.53	13.23	1.00	0.00
COLSTP_2	0.52	14.33	0.68	-59.59
NAVAJO_1	0.51	13.49	0.35	154.29
KMO_13G1	0.83	18.60	1.00	0.00
SHEER_1	0.82	10.22	0.39	-65.74
HYATT_1	0.81	11.29	0.29	169.43
SUND#5GN	0.81	-0.04	0.02	-26.22
CGS	0.82	3.52	0.02	135.74
SUND#5GN	0.22	18.53	1.00	0.00
SHEER_1	0.22	18.46	0.83	-3.77
KMO_13G1	0.22	18.67	0.26	11.12
REV_13G1	0.22	17.76	0.17	10.87
SJUAN_G1	0.22	18.49	0.17	-156.46
NAVAJO_1	0.22	18.44	0.17	-165.84
HAYNES1G	0.22	18.96	0.16	-163.62
DIABLO_1	0.22	19.49	0.16	-160.16
SLHWKG1	0.22	19.08	0.16	-144.37
CURRNTC1	0.23	22.24	0.13	146.53
RAWHIDE	0.22	17.91	0.12	-167.78
CRAIG_1	0.22	18.50	0.12	-160.22
JDA_0304	0.22	22.95	0.12	151.43
MBPP-1	0.22	17.17	0.09	-162.64
EHUNTER1	0.22	18.42	0.09	-161.41
HYATT_1	0.23	19.33	0.07	-165.90

Table 45: 2012 light summer, double Palo Verde trip

Gen ID	**Freq**	**Damping**	**Residue**	**Angle**
BRIDGER1	0.22	18.75	0.06	-148.54
VALMY_G2	0.24	17.04	0.05	130.69
CGS	0.22	17.67	0.04	41.90
COLSTP_2	0.23	18.20	0.04	-43.41
COULEE22	0.22	15.39	0.02	16.51
BRWNL_5	0.23	15.98	0.01	-136.80
EHUNTER1	0.47	16.59	1.00	0.00
DIABLO_1	0.47	10.84	0.37	-80.72
HAYNES1G	0.48	12.06	0.33	-79.69
HAYNES1G	0.88	13.11	1.00	0.00
SUND#5GN	0.89	15.77	0.98	43.89
SLHWKG1	0.89	11.80	0.45	168.13
DIABLO_1	0.90	8.94	0.22	-60.20
JDA_0304	0.89	21.96	0.12	122.03
MBPP-1	0.89	9.11	0.12	-153.05
CRAIG_1	0.88	11.24	0.11	72.25
BRIDGER1	0.91	9.57	0.10	10.71
BRWNL_5	0.85	6.26	0.09	108.52
KMO_13G1	0.68	10.95	1.00	0.00
DIABLO_1	0.64	11.13	0.42	113.10
SHEER_1	0.68	16.50	0.40	18.41
CGS	0.66	15.02	0.39	-150.95
REV_13G1	0.69	11.03	0.37	131.47
COULEE22	0.66	13.56	0.32	-122.08
SJUAN_G1	0.66	10.35	0.27	-160.13
SUND#5GN	0.66	11.53	0.20	8.57
EHUNTER1	0.65	9.63	0.14	162.74
HYATT_1	0.66	8.73	0.13	95.95
HAYNES1G	0.66	9.56	0.11	51.22
BRWNL_5	0.67	9.48	0.11	107.28
RAWHIDE	0.65	9.52	0.08	-0.95
BRIDGER1	0.66	9.28	0.08	118.66
CRAIG_1	0.63	12.65	0.08	117.82
VALMY_G2	0.66	8.74	0.07	112.79
MBPP-1	0.64	9.38	0.07	39.97
COLSTP_2	0.69	7.11	0.04	107.09
JDA_0304	0.65	6.94	0.03	-5.85
HAYNES1G	0.16	26.24	1.00	0.00
KMO_13G1	0.15	25.59	0.76	54.23
NAVAJO_1	0.16	22.28	0.76	-16.04
DIABLO_1	0.14	24.91	0.73	56.52
BRWNL_5	0.15	24.70	0.62	41.47
BRIDGER1	0.15	21.77	0.40	40.61
SJUAN_G1	0.15	17.11	0.31	13.01
RAWHIDE	0.16	9.98	0.13	-12.68
CRAIG_1	0.16	8.82	0.11	-14.47
RAWHIDE	0.42	12.21	1.00	0.00
MBPP-1	0.42	12.47	0.89	18.25
SUND#5GN	0.40	11.26	0.77	69.54

Table 45: 2012 light summer, double Palo Verde trip

Gen ID	**Freq**	**Damping**	**Residue**	**Angle**
EHUNTER1	0.40	19.73	0.60	77.24
CRAIG_1	0.43	12.58	0.52	-20.12
BRWNL_5	0.43	24.59	0.46	93.72
HYATT_1	0.44	19.22	0.33	130.29
BRIDGER1	0.41	12.18	0.30	128.89
CGS	0.42	11.84	0.26	171.14
COULEE22	0.43	12.64	0.24	163.80
CURRNTC1	0.43	11.04	0.10	41.26
REV_13G1	0.41	6.28	0.10	-87.24
JDA_0304	0.41	6.99	0.09	-89.07
COLSTP_2	0.41	6.15	0.06	-106.71
KMO_13G1	0.42	4.02	0.05	-149.88
COLSTP_2	0.57	26.75	1.00	0.00
KMO_13G1	0.57	10.89	0.94	-159.38
JDA_0304	0.55	15.48	0.60	37.85
DIABLO_1	0.58	14.26	0.41	69.15
SJUAN_G1	0.58	13.37	0.21	-153.49
CGS	0.55	14.21	0.19	70.92
BRWNL_5	0.57	11.78	0.18	49.10
HYATT_1	0.56	10.94	0.14	96.44
COULEE22	0.55	12.07	0.13	76.57
BRIDGER1	0.56	11.03	0.13	54.19
HAYNES1G	0.55	17.28	0.10	-169.38
VALMY_G2	0.57	10.49	0.10	34.09
SLHWKG1	0.60	13.69	0.09	-171.32
CURRNTC1	0.57	9.43	0.06	24.40
EHUNTER1	0.57	7.89	0.03	46.47
RAWHIDE	0.56	6.45	0.01	-111.11
COLSTP_2	0.77	9.03	1.00	0.00
MBPP-1	0.76	12.09	0.38	74.88
HAYNES1G	0.78	7.42	0.30	94.66
SLHWKG1	0.79	7.60	0.26	68.38
DIABLO_1	0.78	7.46	0.19	57.17
VALMY_G2	0.77	7.04	0.18	-130.56
EHUNTER1	0.78	6.10	0.17	176.98
BRWNL_5	0.75	6.34	0.12	-21.36

Table 46: 2022 heavy winter, 1.4 GW at Chief Joseph brake, 0.5 sec

Gen ID	Freq	Damping	Residue	Angle
HAYNES1G	0.90	26.33	1.00	0.00
DIABLO_1	0.90	7.38	0.07	137.88
SUND#5GN	0.89	6.24	0.06	-65.07
CRAIG_1	0.88	6.20	0.03	-120.86
REV_13G1	0.74	14.48	1.00	0.00
BRWNL_5	0.73	13.71	0.76	88.21
BRIDGER1	0.73	10.00	0.50	64.97
VALMY_G2	0.74	12.02	0.43	60.81
SHEER_1	0.75	25.43	0.32	116.60
JDA_0304	0.75	13.16	0.31	79.22
NAVAJO_1	0.75	5.27	0.01	-19.04
MBPP-1	0.98	17.06	1.00	0.00
SHEER_1	0.99	9.71	0.64	115.10
CURRNTC1	1.00	10.80	0.60	-19.15
VALMY_G2	0.98	13.16	0.59	53.66
PALOVRD2	0.96	16.06	0.43	-169.28
REV_13G1	0.87	26.61	1.00	0.00
BRWNL_5	0.86	14.18	0.32	102.45
SHEER_1	0.85	10.03	0.13	-157.26
VALMY_G2	0.84	9.91	0.11	124.85
PALOVRD2	0.84	8.55	0.02	-21.56
KMO_13G1	0.55	20.10	1.00	0.00
JDA_0304	0.52	18.17	0.11	-124.23
BRWNL_5	0.50	19.69	0.08	-79.69
BRIDGER1	0.51	20.97	0.06	-112.64
SUND#5GN	0.53	14.86	0.02	168.40
SLHWKG1	0.53	5.95	0.00	42.64
KMO_13G1	0.69	11.89	1.00	0.00
CGS	0.68	24.06	1.00	-131.59
COULEE22	0.67	21.25	0.80	-81.10
COLSTP_2	0.70	16.89	0.54	-138.70
EHUNTER1	0.69	12.02	0.31	179.59
CURRNTC1	0.71	10.10	0.25	146.17
HAYNES1G	0.67	12.86	0.22	60.42
DIABLO_1	0.71	16.98	0.20	1.80
RAWHIDE	0.67	13.17	0.16	-7.60
SJUAN_G1	0.65	6.51	0.05	-92.37
MBPP-1	0.66	12.30	0.05	35.28
SLHWKG1	0.65	19.12	0.04	-118.59
SUND#5GN	0.68	8.25	0.02	55.65
SHEER_1	0.65	6.69	0.02	125.30
SUND#5GN	0.25	17.85	1.00	0.00
SHEER_1	0.25	17.13	0.79	-1.76
REV_13G1	0.25	23.45	0.55	-0.26
PALOVRD2	0.25	20.18	0.34	-158.68
KMO_13G1	0.25	14.87	0.24	-0.98
NAVAJO_1	0.24	17.97	0.23	-150.55

Table 46: 2022 heavy winter, 1.4 GW at Chief Joseph brake, 0.5 sec

Gen ID	Freq	Damping	Residue	Angle
VALMY_G2	0.23	22.85	0.23	-131.46
HAYNES1G	0.24	15.88	0.18	-145.96
DIABLO_1	0.23	17.75	0.17	-105.09
EHUNTER1	0.23	17.91	0.14	-114.75
CURRNTC1	0.22	18.23	0.12	-83.72
SJUAN_G1	0.23	11.66	0.12	-112.94
SLHWKG1	0.23	13.23	0.10	-99.66
CRAIG_1	0.24	10.43	0.09	-158.85
RAWHIDE	0.22	6.71	0.07	-110.06
BRWNL_5	0.24	17.84	0.06	-104.22
MBPP-1	0.22	6.51	0.05	-103.56
BRIDGER1	0.22	9.20	0.04	-71.58
JDA_0304	0.94	14.21	1.00	0.00
COLSTP_2	0.93	11.95	0.53	-173.56
EHUNTER1	0.93	6.41	0.02	-134.80
COLSTP_2	0.80	11.00	1.00	0.00
EHUNTER1	0.78	9.86	0.97	-129.51
MBPP-1	0.78	22.73	0.59	-23.28
CURRNTC1	0.79	8.18	0.53	-125.79
HYATT_1	0.78	13.25	0.33	-126.31
HAYNES1G	0.81	10.93	0.23	16.20
CRAIG_1	0.77	11.62	0.22	-114.21
RAWHIDE	0.77	12.16	0.22	3.61
KMO_13G1	0.79	6.83	0.18	55.18
SLHWKG1	0.77	10.93	0.14	-110.49
SJUAN_G1	0.79	5.32	0.03	174.63
BRIDGER1	0.79	2.79	0.03	-97.53
KMO_13G1	0.39	13.10	1.00	0.00
REV_13G1	0.39	14.55	0.76	13.00
COULEE22	0.39	14.90	0.73	4.31
COLSTP_2	0.40	17.76	0.68	-40.20
CGS	0.39	15.09	0.67	-15.12
SUND#5GN	0.39	13.88	0.59	168.54
JDA_0304	0.39	14.20	0.45	5.28
SHEER_1	0.39	14.36	0.42	168.80
PALOVRD2	0.39	15.12	0.40	174.61
SJUAN_G1	0.39	12.63	0.30	-172.92
RAWHIDE	0.38	11.12	0.30	154.23
NAVAJO_1	0.39	14.34	0.27	-179.08
HAYNES1G	0.39	14.91	0.23	-172.56
HYATT_1	0.40	14.32	0.22	-30.31
BRWNL_5	0.39	13.34	0.21	0.76
CRAIG_1	0.39	11.64	0.21	164.89
MBPP-1	0.38	10.71	0.19	164.78
SLHWKG1	0.39	13.40	0.17	-155.37
DIABLO_1	0.38	17.23	0.12	-133.45
BRIDGER1	0.37	16.14	0.10	-28.08
EHUNTER1	0.37	16.43	0.10	-121.29
VALMY_G2	0.40	17.69	0.07	-119.54
CURRNTC1	0.37	14.42	0.06	-107.84

Table 46: 2022 heavy winter, 1.4 GW at Chief Joseph brake, 0.5 sec

Gen ID	Freq	Damping	Residue	Angle
DIABLO_1	0.62	12.25	1.00	0.00
HYATT_1	0.61	12.78	1.00	42.48
PALOVRD2	0.60	13.20	0.58	-154.06
CURRNTC1	0.57	20.67	0.25	175.90
REV_13G1	0.57	8.62	0.24	-77.38
NAVAJO_1	0.59	10.82	0.17	-132.71
VALMY_G2	0.57	15.23	0.08	123.65
SJUAN_G1	0.57	1.02	0.02	-139.42

Table 47: 2022 heavy winter, 1.4 GW at El Dorado bus, 0.5 sec

Gen ID	Freq	Damping	Residue	Angle
COLSTP_2	0.97	15.48	1.00	0.00
CRAIG_1	0.96	8.62	0.29	102.50
EHUNTER1	0.96	2.34	0.11	55.24
RAWHIDE	0.51	19.49	1.00	0.00
CGS	0.53	14.46	0.72	-90.01
EHUNTER1	0.52	19.65	0.66	-101.37
BRWNL_5	0.53	13.82	0.52	-77.14
COULEE22	0.52	12.38	0.37	-39.96
MBPP-1	0.51	12.46	0.17	10.13
VALMY_G2	0.92	13.90	1.00	0.00
HAYNES1G	0.91	14.09	0.87	41.08
CURRNTC1	0.93	6.34	0.05	-98.16
BRIDGER1	0.94	6.11	0.03	-99.48
SJUAN_G1	0.76	25.42	1.00	0.00
CURRNTC1	0.77	11.51	0.53	117.91
EHUNTER1	0.77	11.66	0.52	121.17
HYATT_1	0.74	14.32	0.36	52.89
KMO_13G1	0.74	14.02	0.33	-15.23
BRIDGER1	0.76	11.21	0.29	137.03
BRWNL_5	0.73	16.62	0.28	-167.26
COULEE22	0.72	21.76	0.21	-119.92
REV_13G1	0.75	14.18	0.14	126.27
COLSTP_2	0.76	9.06	0.12	151.67
CRAIG_1	0.77	14.28	0.11	132.64
COULEE22	0.76	11.15	0.07	-62.12
MBPP-1	0.73	11.64	0.06	154.40
CGS	0.79	10.22	0.04	-117.70
JDA_0304	0.75	7.31	0.02	-41.36
RAWHIDE	0.40	16.39	1.00	0.00
KMO_13G1	0.39	14.43	0.93	7.24
MBPP-1	0.40	16.12	0.69	7.54
REV_13G1	0.39	15.80	0.67	18.91
SUND#5GN	0.40	15.91	0.59	167.75
CRAIG_1	0.41	16.73	0.58	9.45
PALOVRD2	0.40	16.87	0.51	-179.25

Table 47: 2022 heavy winter, 1.4 GW at El Dorado bus, 0.5 sec

Gen ID	**Freq**	**Damping**	**Residue**	**Angle**
CGS	0.38	16.17	0.50	20.16
COULEE22	0.39	15.14	0.50	30.03
NAVAJO_1	0.41	17.48	0.44	163.62
COLSTP_2	0.39	16.22	0.43	10.66
HAYNES1G	0.40	16.42	0.40	-167.25
SHEER_1	0.40	16.13	0.40	163.28
SJUAN_G1	0.40	17.02	0.37	176.49
BRWNL_5	0.38	17.99	0.34	30.34
JDA_0304	0.38	14.74	0.32	21.93
DIABLO_1	0.41	15.96	0.30	171.83
BRIDGER1	0.39	18.92	0.28	31.67
EHUNTER1	0.40	21.82	0.24	14.92
CURRNTC1	0.39	17.55	0.19	41.53
HYATT_1	0.37	7.27	0.03	25.82
PALOVRD2	1.00	19.37	1.00	0.00
DIABLO_1	1.01	17.75	0.56	51.10
COULEE22	0.99	7.57	0.02	109.08
SHEER_1	1.00	14.32	0.01	-91.77
COLSTP_2	0.99	1.81	0.00	-151.53
SHEER_1	1.01	1.94	0.00	138.93
SUND#5GN	1.00	-0.79	0.00	-105.33
SLHWKG1	0.84	21.28	1.00	0.00
PALOVRD2	0.83	13.27	0.41	-18.97
SJUAN_G1	0.85	9.71	0.11	-176.71
HYATT_1	0.84	10.45	0.05	-83.30
RAWHIDE	0.83	9.77	0.03	-107.32
KMO_13G1	0.56	13.70	1.00	0.00
VALMY_G2	0.58	22.81	0.30	167.25
SJUAN_G1	0.58	15.79	0.27	18.35
HYATT_1	0.55	13.81	0.25	-132.48
PALOVRD2	0.58	15.38	0.21	18.23
REV_13G1	0.57	11.81	0.17	18.26
DIABLO_1	0.56	13.54	0.17	-155.08
CRAIG_1	0.57	23.60	0.17	-70.84
JDA_0304	0.54	11.94	0.13	-124.33
CURRNTC1	0.56	17.66	0.13	-152.72
BRIDGER1	0.55	14.98	0.11	-138.81
COLSTP_2	0.54	13.32	0.10	-121.40
SUND#5GN	0.25	18.83	1.00	0.00
SHEER_1	0.25	18.78	0.86	-2.54
REV_13G1	0.25	18.04	0.31	0.78
KMO_13G1	0.24	14.91	0.25	2.53
SJUAN_G1	0.26	16.08	0.19	156.01
PALOVRD2	0.26	15.82	0.19	149.80
RAWHIDE	0.26	16.22	0.19	145.43
HAYNES1G	0.26	15.62	0.16	157.73
MBPP-1	0.26	16.24	0.15	150.85
CRAIG_1	0.26	16.14	0.15	160.96
DIABLO_1	0.27	15.07	0.13	151.47
COULEE22	0.23	15.93	0.10	23.11

Table 47: 2022 heavy winter, 1.4 GW at El Dorado bus, 0.5 sec

Gen ID	Freq	Damping	Residue	Angle
COLSTP_2	0.24	16.18	0.09	-14.77
EHUNTER1	0.26	15.25	0.09	169.09
CGS	0.23	17.72	0.09	17.20
CURRNTC1	0.27	12.73	0.07	140.37
HYATT_1	0.29	12.58	0.05	120.76
BRIDGER1	0.26	13.90	0.05	-171.50
JDA_0304	0.22	10.88	0.03	29.08

Table 48: 2022 heavy winter, 1.4 GW at Hemingway Bus, 0.5 sec

Gen ID	Freq	Damping	Residue	Angle
HYATT_1	0.43	18.01	1.00	0.00
RAWHIDE	0.43	10.55	0.36	85.13
CRAIG_1	0.42	10.77	0.25	155.62
MBPP-1	0.43	8.58	0.16	102.39
KMO_13G1	0.56	14.72	1.00	0.00
JDA_0304	0.55	16.26	0.20	-146.54
REV_13G1	0.56	12.30	0.15	19.00
SJUAN_G1	0.56	13.12	0.14	-9.99
PALOVRD2	0.57	12.58	0.12	-19.08
NAVAJO_1	0.57	13.59	0.08	-13.15
SUND#5GN	0.56	18.11	0.07	174.81
RAWHIDE	0.66	17.56	1.00	0.00
SJUAN_G1	0.69	13.18	0.62	153.37
CRAIG_1	0.68	21.31	0.38	-81.24
SUND#5GN	0.66	7.49	0.06	-40.33
HYATT_1	0.59	14.44	1.00	0.00
DIABLO_1	0.60	12.32	0.58	-46.87
HAYNES1G	0.62	16.19	0.46	-114.50
MBPP-1	0.63	11.03	0.07	-128.21
SHEER_1	0.61	6.62	0.04	-95.22
COULEE22	0.89	18.21	1.00	0.00
VALMY_G2	0.89	16.00	0.52	46.50
CGS	0.86	17.73	0.46	2.15
COLSTP_2	0.85	11.79	0.25	155.94
DIABLO_1	0.87	10.71	0.06	-104.41
SUND#5GN	0.87	4.95	0.01	-36.24
SUND#5GN	0.24	17.35	1.00	0.00
SHEER_1	0.24	16.80	0.82	-2.69
RAWHIDE	0.29	23.90	0.76	92.85
CRAIG_1	0.28	26.81	0.66	117.24
MBPP-1	0.28	23.00	0.46	113.64
EHUNTER1	0.28	27.68	0.40	132.51
SLHWKG1	0.28	25.03	0.35	132.80
SJUAN_G1	0.27	21.58	0.34	134.30
KMO_13G1	0.24	16.16	0.32	9.40

Table 48: 2022 heavy winter, 1.4 GW at Hemingway Bus, 0.5 sec

Gen ID	**Freq**	**Damping**	**Residue**	**Angle**
PALOVRD2	0.27	19.95	0.29	124.40
REV_13G1	0.23	14.92	0.23	38.10
HAYNES1G	0.27	17.91	0.20	119.52
CGS	0.26	20.75	0.19	-48.57
NAVAJO_1	0.26	18.14	0.19	141.21
CURRNTC1	0.28	20.82	0.16	144.26
COLSTP_2	0.28	15.60	0.16	-92.00
COULEE22	0.24	14.45	0.11	-9.60
DIABLO_1	0.26	15.68	0.09	156.32
KMO_13G1	0.39	13.76	1.00	0.00
REV_13G1	0.39	15.49	0.77	12.35
DIABLO_1	0.37	25.66	0.54	-115.89
COULEE22	0.39	13.00	0.42	18.98
SUND#5GN	0.39	12.83	0.41	176.60
JDA_0304	0.40	14.08	0.36	0.29
SJUAN_G1	0.39	14.81	0.34	-163.51
NAVAJO_1	0.39	15.89	0.33	-166.62
PALOVRD2	0.39	14.34	0.33	-170.76
SHEER_1	0.40	13.13	0.29	164.24
HAYNES1G	0.39	15.45	0.28	-151.64
CGS	0.39	10.72	0.25	-0.81
SLHWKG1	0.40	15.67	0.24	-175.54
COLSTP_2	0.39	8.61	0.12	13.05
BRWNL_5	0.49	17.41	1.00	0.00
COULEE22	0.52	15.84	0.53	-50.08
CGS	0.54	11.76	0.36	-95.43
COLSTP_2	0.51	11.54	0.22	-35.79
KMO_13G1	0.71	10.95	1.00	0.00
BRIDGER1	0.73	22.12	0.99	-10.60
COLSTP_2	0.74	14.88	0.72	-98.85
COULEE22	0.75	13.20	0.68	-146.25
CGS	0.74	13.74	0.53	-162.01
REV_13G1	0.72	12.24	0.50	112.92
PALOVRD2	0.72	14.35	0.16	-125.78
JDA_0304	0.76	9.82	0.16	146.27
NAVAJO_1	0.71	18.79	0.10	-86.46
DIABLO_1	0.72	9.36	0.08	76.36
CRAIG_1	0.75	9.01	0.03	37.79
MBPP-1	0.73	9.41	0.02	26.66
HAYNES1G	0.72	4.77	0.02	51.36
EHUNTER1	0.79	26.20	1.00	0.00
CURRNTC1	0.82	25.76	0.78	-10.23
VALMY_G2	0.81	13.29	0.08	-13.43
HYATT_1	0.77	14.50	0.07	98.78
REV_13G1	0.82	13.88	0.06	-49.39
KMO_13G1	0.80	9.68	0.05	-122.57
CURRNTC1	0.81	8.05	0.04	-35.95
EHUNTER1	0.82	6.73	0.02	-53.30
RAWHIDE	0.79	7.62	0.00	118.33
SHEER_1	0.79	2.62	0.00	-123.49

Table 48: 2022 heavy winter, 1.4 GW at Hemingway Bus, 0.5 sec

Gen ID	Freq	Damping	Residue	Angle
SJUAN_G1	0.83	3.54	0.00	176.36

Table 49: 2022 heavy winter, 1.4 GW at Midway bus, 0.5 sec

Gen ID	Freq	Damping	Residue	Angle
JDA_0304	0.85	10.36	1.00	0.00
CGS	0.85	7.77	0.32	-6.26
SUND#5GN	0.85	4.43	0.06	-32.86
SHEER_1	0.86	1.53	0.03	21.22
HYATT_1	0.67	19.76	1.00	0.00
MBPP-1	0.67	22.53	0.68	35.44
DIABLO_1	0.67	14.21	0.67	0.75
RAWHIDE	0.67	21.79	0.57	58.48
RAWHIDE	0.68	13.75	0.39	-70.23
REV_13G1	0.68	11.43	0.38	77.95
CGS	0.69	13.73	0.36	157.44
KMO_13G1	0.66	5.50	0.36	12.71
HAYNES1G	0.67	12.42	0.34	25.07
SJUAN_G1	0.67	11.86	0.33	-173.83
HAYNES1G	0.68	18.54	0.27	80.12
JDA_0304	0.68	11.00	0.15	-170.41
BRIDGER1	0.70	7.33	0.06	169.22
COLSTP_2	0.64	17.12	1.00	0.00
EHUNTER1	0.64	13.39	0.35	4.68
COULEE22	0.62	13.08	0.34	70.01
CURRNTC1	0.63	12.92	0.31	14.01
CGS	0.60	13.73	0.29	86.80
BRWNL_5	0.61	12.99	0.22	71.52
VALMY_G2	0.61	16.33	0.20	57.04
BRIDGER1	0.61	12.19	0.17	47.33
PALOVRD2	0.63	7.95	0.05	101.19
SHEER_1	0.64	2.30	0.01	-102.18
SUND#5GN	0.25	17.82	1.00	0.00
SHEER_1	0.25	17.91	0.87	-3.19
RAWHIDE	0.26	23.96	0.46	151.38
DIABLO_1	0.27	21.62	0.36	139.21
SJUAN_G1	0.26	18.83	0.28	148.97
REV_13G1	0.25	15.93	0.27	3.27
CRAIG_1	0.26	21.81	0.27	167.27
PALOVRD2	0.26	18.70	0.27	156.41
MBPP-1	0.26	21.35	0.27	157.18
KMO_13G1	0.24	14.46	0.25	11.71
SLHWKG1	0.26	19.56	0.22	157.04
NAVAJO_1	0.25	17.58	0.20	163.32
HAYNES1G	0.26	17.15	0.19	162.27
EHUNTER1	0.26	21.43	0.18	168.88
BRIDGER1	0.26	22.91	0.12	-156.65
CURRNTC1	0.27	17.40	0.12	148.99

Table 49: 2022 heavy winter, 1.4 GW at Midway bus, 0.5 sec

Gen ID	**Freq**	**Damping**	**Residue**	**Angle**
CGS	0.24	18.36	0.11	-8.34
COULEE22	0.24	14.95	0.11	3.14
VALMY_G2	0.26	15.16	0.09	161.53
JDA_0304	0.25	17.49	0.07	-26.18
COLSTP_2	0.25	12.29	0.07	-33.64
BRWNL_5	0.27	17.64	0.03	-128.87
HAYNES1G	0.89	14.91	1.00	0.00
HYATT_1	0.88	16.91	0.53	-110.50
PALOVRD2	0.90	10.79	0.19	-159.91
NAVAJO_1	0.90	13.21	0.07	-108.53
COULEE22	0.88	8.43	0.07	88.43
BRWNL_5	0.90	8.46	0.04	105.80
SJUAN_G1	0.88	8.12	0.04	130.80
COULEE22	0.72	15.46	1.00	0.00
MBPP-1	0.74	16.28	0.59	41.72
KMO_13G1	0.73	5.60	0.28	125.13
BRWNL_5	0.71	10.03	0.25	-8.52
VALMY_G2	0.73	10.64	0.14	-75.79
CURRNTC1	0.75	7.25	0.13	-104.41
CRAIG_1	0.75	13.84	0.12	-170.79
EHUNTER1	0.74	6.80	0.12	-98.36
SUND#5GN	0.71	9.94	0.05	142.44
COLSTP_2	0.58	21.42	1.00	0.00
PALOVRD2	0.59	18.11	0.96	146.90
KMO_13G1	0.58	8.26	0.78	68.88
NAVAJO_1	0.56	20.36	0.51	170.15
REV_13G1	0.56	12.76	0.41	156.43
JDA_0304	0.59	13.00	0.36	-90.93
SJUAN_G1	0.56	12.65	0.28	178.08
SLHWKG1	0.58	17.00	0.19	154.04
SUND#5GN	0.53	11.75	0.06	9.99
CRAIG_1	0.55	15.28	0.04	-173.02
VALMY_G2	0.93	12.82	1.00	0.00
CURRNTC1	0.94	13.28	0.93	-162.92
EHUNTER1	0.94	11.25	0.63	-161.36
BRIDGER1	0.96	9.80	0.29	-163.62
SLHWKG1	0.92	8.05	0.17	151.79
RAWHIDE	0.94	9.95	0.08	-87.91
RAWHIDE	0.40	15.97	1.00	0.00
MBPP-1	0.40	16.27	0.73	16.95
CRAIG_1	0.40	16.57	0.61	18.18
CGS	0.38	20.24	0.25	60.11
BRIDGER1	0.40	18.63	0.25	47.24
BRWNL_5	0.39	23.30	0.24	49.50
SUND#5GN	0.40	17.97	0.24	-154.06
PALOVRD2	0.40	16.72	0.24	-137.73
KMO_13G1	0.39	13.48	0.24	68.26
COULEE22	0.39	18.00	0.23	64.94
HAYNES1G	0.40	15.16	0.21	-147.02

Table 49: 2022 heavy winter, 1.4 GW at Midway bus, 0.5 sec

Gen ID	**Freq**	**Damping**	**Residue**	**Angle**
JDA_0304	0.38	22.42	0.21	63.86
REV_13G1	0.39	15.72	0.21	62.41
CURRNTC1	0.40	17.14	0.19	38.06
COLSTP_2	0.40	15.94	0.18	37.68
SJUAN_G1	0.43	19.38	0.18	159.62
SLHWKG1	0.40	17.15	0.17	-141.58
EHUNTER1	0.40	18.03	0.16	23.70
SHEER_1	0.40	16.72	0.13	-164.24
NAVAJO_1	0.39	14.53	0.13	-136.01

Table 50: 2022 heavy winter, double Palo Verde trip

Gen ID	**Freq**	**Damping**	**Residue**	**Angle**
VALMY_G2	0.60	15.94	1.00	0.00
SLHWKG1	0.60	9.15	0.15	-148.98
EHUNTER1	0.61	7.25	0.12	-142.60
VALMY_G2	0.62	7.16	0.08	137.85
CURRNTC1	0.61	6.23	0.06	177.26
SHEER_1	0.36	27.19	1.00	0.00
JDA_0304	0.35	29.11	0.59	-67.87
MBPP-1	0.33	15.69	0.15	-125.78
VALMY_G2	0.34	18.24	0.11	-173.91
DIABLO_1	0.35	14.23	0.08	-117.71
CRAIG_1	0.36	11.13	0.05	131.35
COULEE22	0.35	7.82	0.02	152.65
KMO_13G1	0.32	1.61	0.00	-75.35
KMO_13G1	0.66	10.32	1.00	0.00
CURRNTC1	0.68	11.63	0.70	170.66
DIABLO_1	0.65	13.24	0.68	38.35
COLSTP_2	0.68	13.41	0.63	-178.04
HYATT_1	0.67	13.31	0.51	19.14
EHUNTER1	0.67	9.97	0.42	-162.96
VALMY_G2	0.68	12.48	0.35	145.98
RAWHIDE	0.65	12.51	0.30	-45.88
COULEE22	0.65	10.53	0.27	-111.09
BRWNL_5	0.68	11.79	0.26	152.29
JDA_0304	0.66	12.41	0.24	-114.70
BRIDGER1	0.69	9.47	0.22	159.05
CGS	0.64	9.12	0.16	-76.35
HAYNES1G	0.65	8.70	0.11	56.45
REV_13G1	0.65	7.25	0.08	148.49
SHEER_1	0.64	9.01	0.06	171.72
RAWHIDE	0.64	2.51	0.01	65.77
NAVAJO_1	0.85	16.85	1.00	0.00
COULEE22	0.87	10.13	0.08	-114.25
VALMY_G2	0.87	7.11	0.07	-35.16
SUND#5GN	0.24	16.96	1.00	0.00

Table 50: 2022 heavy winter, double Palo Verde trip

Gen ID	**Freq**	**Damping**	**Residue**	**Angle**
SHEER_1	0.24	17.13	0.87	-2.20
KMO_13G1	0.24	17.03	0.36	-2.10
REV_13G1	0.24	17.56	0.34	-0.11
SJUAN_G1	0.24	16.32	0.23	-165.37
RAWHIDE	0.24	16.06	0.21	-166.89
NAVAJO_1	0.24	16.29	0.21	-174.98
HAYNES1G	0.24	16.15	0.20	-167.55
CRAIG_1	0.24	16.01	0.18	-170.09
DIABLO_1	0.25	16.05	0.18	-172.41
SLHWKG1	0.25	15.85	0.15	-179.68
COULEE22	0.24	17.29	0.14	-6.45
EHUNTER1	0.24	16.05	0.14	-159.30
MBPP-1	0.24	14.11	0.13	-164.58
VALMY_G2	0.24	15.58	0.13	-173.97
CURRNTC1	0.24	16.74	0.12	-143.56
COLSTP_2	0.24	16.65	0.10	-18.33
CGS	0.24	17.11	0.10	-37.13
BRIDGER1	0.24	15.57	0.09	-148.97
HYATT_1	0.25	15.85	0.08	-153.86
BRWNL_5	0.24	15.29	0.06	-115.10
JDA_0304	0.24	15.82	0.06	-51.55
SUND#5GN	0.25	2.19	0.00	139.01
SHEER_1	0.25	0.56	0.00	135.72
MBPP-1	0.47	21.85	1.00	0.00
CURRNTC1	0.50	19.91	0.88	45.54
EHUNTER1	0.48	18.23	0.40	64.35
JDA_0304	0.50	11.40	0.17	-61.92
HAYNES1G	0.79	13.04	1.00	0.00
BRIDGER1	0.81	12.12	0.34	19.06
COLSTP_2	0.80	10.16	0.26	-44.51
SHEER_1	0.80	8.47	0.02	-72.59
KMO_13G1	0.56	12.22	1.00	0.00
SJUAN_G1	0.57	19.24	0.65	57.07
REV_13G1	0.56	12.89	0.32	23.59
NAVAJO_1	0.56	20.36	0.30	70.83
HYATT_1	0.55	14.01	0.20	-143.53
COLSTP_2	0.56	14.93	0.20	-149.88
BRWNL_5	0.57	11.72	0.13	-170.58
JDA_0304	0.55	9.76	0.10	-121.92
DIABLO_1	0.55	10.32	0.10	-135.93
CGS	0.56	9.37	0.08	171.17
BRIDGER1	0.54	11.89	0.06	-139.57
SUND#5GN	0.55	13.08	0.03	-155.97
HYATT_1	0.57	7.49	0.03	-146.62
COULEE22	0.55	5.41	0.01	-93.14
BRIDGER1	0.58	5.25	0.01	165.90
HAYNES1G	0.58	3.45	0.01	-140.51
KMO_13G1	0.39	14.92	1.00	0.00
SUND#5GN	0.38	20.07	0.96	96.60
SLHWKG1	0.40	21.97	0.71	118.22

Table 50: 2022 heavy winter, double Palo Verde trip

Gen ID	Freq	Damping	Residue	Angle
SUND#5GN	0.37	16.03	0.67	-109.72
MBPP-1	0.40	16.05	0.66	0.75
RAWHIDE	0.42	15.51	0.65	-57.75
SLHWKG1	0.37	20.59	0.60	-62.08
COULEE22	0.38	15.62	0.55	6.00
HAYNES1G	0.38	17.33	0.43	-132.44
REV_13G1	0.39	12.36	0.42	-12.65
COLSTP_2	0.39	15.59	0.38	-3.94
SHEER_1	0.38	15.20	0.38	-165.46
CRAIG_1	0.41	14.84	0.37	-7.94
SJUAN_G1	0.39	15.13	0.37	-170.59
NAVAJO_1	0.40	16.23	0.32	-178.31
DIABLO_1	0.41	16.30	0.29	164.43
CGS	0.39	11.34	0.20	-29.30
BRIDGER1	0.40	19.70	0.19	5.86
JDA_0304	0.38	12.48	0.18	16.73
RAWHIDE	0.38	12.59	0.14	94.11
CGS	0.41	12.32	0.13	-2.92
HYATT_1	0.41	14.64	0.13	-57.49
BRWNL_5	0.39	12.33	0.13	-17.46
REV_13G1	0.41	8.96	0.05	69.59
NAVAJO_1	0.38	11.09	0.04	-166.54
HYATT_1	0.41	9.04	0.03	176.53
CURRNTC1	0.39	11.48	0.03	24.53
NAVAJO_1	0.70	20.12	1.00	0.00
EHUNTER1	0.73	14.21	0.90	-48.46
JDA_0304	0.74	6.75	0.14	-166.16
KMO_13G1	0.71	2.28	0.02	36.50
SLHWKG1	0.92	15.22	1.00	0.00
HAYNES1G	0.93	15.75	0.93	-99.48
CURRNTC1	0.92	16.34	0.37	160.36
EHUNTER1	0.92	14.42	0.29	169.74
DIABLO_1	0.94	8.66	0.28	-156.53
VALMY_G2	0.95	9.87	0.19	-112.51
SJUAN_G1	0.90	8.33	0.16	-132.99
BRIDGER1	0.92	12.05	0.15	-145.21
COLSTP_2	0.95	13.11	0.13	75.50
MBPP-1	0.96	8.91	0.08	16.01
CRAIG_1	0.93	6.66	0.02	-169.29
SLHWKG1	0.19	24.83	1.00	0.00
KMO_13G1	0.17	6.42	0.03	100.64
RAWHIDE	0.15	3.63	0.02	-160.10
CRAIG_1	0.18	3.81	0.02	52.84
COLSTP_2	0.14	-5.60	0.01	-53.39

Table 51: 2022 light summer, 1.4 GW at Chief Joseph brake, 0.5 sec

Gen ID	Freq	Damping	Residue	Angle
KMO_13G1	0.96	22.60	1.00	0.00
SHEER_1	0.97	13.15	0.77	59.45
MBPP-1	0.97	11.27	0.50	111.07
NAVAJO_1	0.96	19.92	0.09	-102.37
RAWHIDE	0.97	6.77	0.04	102.33
SJUAN_G1	0.97	9.93	0.03	-49.82
PALOVRD2	0.96	6.15	0.01	-113.50
KMO_13G1	0.70	11.56	1.00	0.00
CURRNTC1	0.74	12.00	0.51	35.91
EHUNTER1	0.73	11.42	0.35	46.60
COLSTP_2	0.73	12.04	0.28	112.23
BRWNL_5	0.73	13.00	0.25	44.18
COULEE22	0.71	13.03	0.25	162.93
VALMY_G2	0.72	13.35	0.22	51.15
RAWHIDE	0.71	10.97	0.16	-139.47
CGS	0.71	11.63	0.15	130.43
HAYNES1G	0.70	10.70	0.15	-43.65
CRAIG_1	0.71	15.43	0.11	-24.52
KMO_13G1	0.47	13.04	1.00	0.00
SUND#5GN	0.47	13.36	0.58	-175.57
REV_13G1	0.47	13.17	0.57	5.87
COULEE22	0.47	12.70	0.48	12.16
CGS	0.47	12.48	0.44	0.44
JDA_0304	0.47	12.41	0.32	13.36
COLSTP_2	0.47	12.91	0.31	-9.21
SJUAN_G1	0.48	12.85	0.23	-166.38
BRWNL_5	0.47	12.34	0.21	2.61
RAWHIDE	0.47	10.52	0.21	-154.20
PALOVRD2	0.47	13.95	0.20	-159.92
SHEER_1	0.47	12.54	0.19	-156.17
HYATT_1	0.47	11.95	0.17	17.22
NAVAJO_1	0.47	13.65	0.16	-162.80
VALMY_G2	0.47	12.67	0.14	32.09
CRAIG_1	0.47	10.76	0.14	-135.12
HAYNES1G	0.47	14.14	0.13	-159.06
MBPP-1	0.47	10.09	0.12	-138.80
SLHWKG1	0.47	13.54	0.12	-144.05
BRIDGER1	0.47	13.05	0.11	-1.85
DIABLO_1	0.46	12.16	0.06	132.72
CURRNTC1	0.47	12.06	0.06	-46.92
EHUNTER1	0.47	11.43	0.05	-64.77
COLSTP_2	0.88	13.60	1.00	0.00
CGS	0.89	13.94	0.52	92.98
KMO_13G1	0.84	11.29	0.37	103.08
SUND#5GN	0.84	15.52	0.28	109.51
CGS	0.87	9.25	0.23	-44.17
REV_13G1	0.85	8.21	0.13	-121.83
BRIDGER1	0.87	10.81	0.11	16.92
MBPP-1	0.78	23.24	1.00	0.00

Table 51: 2022 light summer, 1.4 GW at Chief Joseph brake, 0.5 sec

Gen ID	Freq	Damping	Residue	Angle
EHUNTER1	0.80	12.04	0.41	151.64
JDA_0304	0.80	12.90	0.34	63.81
SJUAN_G1	0.77	7.36	0.03	102.42
HAYNES1G	0.80	4.77	0.01	-36.90
CURRNTC1	0.91	12.94	1.00	0.00
EHUNTER1	0.93	9.40	0.40	-0.93
CRAIG_1	0.91	9.26	0.11	20.96
SUND#5GN	0.93	6.54	0.09	-68.41
HYATT_1	0.91	5.23	0.05	-42.37
CURRNTC1	0.92	4.72	0.04	101.59
SLHWKG1	0.93	7.06	0.04	-32.07
REV_13G1	0.69	15.34	1.00	0.00
HYATT_1	0.67	13.62	0.53	-127.71
DIABLO_1	0.68	12.45	0.36	-167.16
SUND#5GN	0.68	16.40	0.29	-155.45
MBPP-1	0.66	14.20	0.14	-154.66
SJUAN_G1	0.66	9.63	0.12	24.11
PALOVRD2	0.64	8.75	0.06	98.15
NAVAJO_1	0.65	7.55	0.03	72.43
SLHWKG1	0.68	4.07	0.01	1.13
SUND#5GN	0.29	18.52	1.00	0.00
SHEER_1	0.28	18.74	0.71	11.63
KMO_13G1	0.29	18.00	0.35	-2.01
REV_13G1	0.29	18.54	0.32	6.42
SJUAN_G1	0.29	22.12	0.29	-147.23
RAWHIDE	0.28	24.81	0.28	-135.62
PALOVRD2	0.29	20.99	0.24	-157.09
MBPP-1	0.28	25.03	0.24	-144.96
HAYNES1G	0.29	20.59	0.21	-157.98
DIABLO_1	0.28	21.61	0.21	-148.32
NAVAJO_1	0.29	20.37	0.21	-163.81
CRAIG_1	0.28	23.87	0.21	-134.73
CURRNTC1	0.28	27.74	0.20	-122.79
SLHWKG1	0.28	21.04	0.18	-135.43
VALMY_G2	0.32	17.41	0.18	31.45
EHUNTER1	0.28	23.77	0.16	-129.56
COLSTP_2	0.30	18.95	0.15	-32.70
BRIDGER1	0.27	25.55	0.11	-112.80
CGS	0.30	14.82	0.09	-28.96
RAWHIDE	0.55	20.32	1.00	0.00
CRAIG_1	0.54	24.95	0.60	38.99
BRIDGER1	0.53	26.38	0.45	124.51

Table 52: 2022 light summer, 1.4 GW at El Dorado bus, 0.5 sec

Gen ID	Freq	Damping	Residue	Angle
RAWHIDE	0.73	18.61	1.00	0.00

Table 52: 2022 light summer, 1.4 GW at El Dorado bus, 0.5 sec

Gen ID	Freq	Damping	Residue	Angle
CURRNTC1	0.73	15.22	0.98	-90.52
EHUNTER1	0.73	12.62	0.53	-109.88
BRWNL_5	0.72	11.13	0.20	-97.35
BRIDGER1	0.72	9.45	0.15	-83.74
KMO_13G1	0.63	12.76	1.00	0.00
REV_13G1	0.64	10.77	0.10	30.20
JDA_0304	0.63	8.88	0.05	-152.10
CGS	0.63	7.34	0.04	178.94
COLSTP_2	0.63	7.59	0.04	167.91
COULEE22	0.63	6.95	0.03	175.97
VALMY_G2	0.97	24.74	1.00	0.00
CGS	1.00	15.44	0.13	65.06
HYATT_1	0.98	9.71	0.03	-132.05
MBPP-1	1.00	2.11	0.01	-121.93
REV_13G1	0.98	1.51	0.00	-116.40
HYATT_1	0.58	21.73	1.00	0.00
MBPP-1	0.56	22.88	0.63	28.36
BRWNL_5	0.58	12.50	0.15	16.42
SJUAN_G1	0.56	1.26	0.02	-51.89
KMO_13G1	0.84	20.16	1.00	0.00
MBPP-1	0.81	16.33	0.75	-42.44
CRAIG_1	0.86	16.11	0.27	-143.59
SHEER_1	0.83	9.36	0.17	162.10
COLSTP_2	0.84	8.99	0.16	-99.30
JDA_0304	0.82	7.89	0.08	-37.19
KMO_13G1	0.82	3.28	0.03	43.92
HYATT_1	0.82	3.54	0.02	20.53
SUND#5GN	0.29	19.79	1.00	0.00
SHEER_1	0.29	17.09	0.63	15.14
KMO_13G1	0.29	20.33	0.39	3.19
REV_13G1	0.29	20.93	0.36	8.34
HAYNES1G	0.27	22.34	0.18	-107.05
COULEE22	0.28	21.91	0.18	15.14
CGS	0.28	22.33	0.16	11.43
COLSTP_2	0.28	22.12	0.15	11.53
VALMY_G2	0.28	15.34	0.15	160.04
PALOVRD2	0.28	18.44	0.14	-141.65
SJUAN_G1	0.29	14.58	0.10	-150.14
DIABLO_1	0.28	16.47	0.09	-137.94
CRAIG_1	0.29	17.37	0.09	-155.71
RAWHIDE	0.28	14.94	0.07	-132.66
MBPP-1	0.30	14.43	0.06	-172.84
SHEER_1	0.25	11.18	0.06	-52.93
CURRNTC1	0.28	17.75	0.05	-108.05
EHUNTER1	0.27	14.99	0.04	-99.95
BRIDGER1	0.28	12.20	0.02	-141.98
HYATT_1	0.29	10.00	0.01	-138.53
SJUAN_G1	0.75	19.63	1.00	0.00

Table 52: 2022 light summer, 1.4 GW at El Dorado bus, 0.5 sec

Gen ID	Freq	Damping	Residue	Angle
REV_13G1	0.79	13.72	0.17	30.06
SUND#5GN	0.76	7.00	0.01	-76.17
SUND#5GN	0.67	23.25	1.00	0.00
DIABLO_1	0.67	11.66	0.74	39.16
SHEER_1	0.69	26.06	0.62	-95.53
RAWHIDE	0.45	16.76	1.00	0.00
KMO_13G1	0.47	13.93	0.90	23.16
MBPP-1	0.44	15.75	0.56	31.08
BRIDGER1	0.46	21.63	0.52	91.08
REV_13G1	0.47	14.10	0.51	26.28
HAYNES1G	0.47	19.27	0.47	-155.48
SUND#5GN	0.47	13.47	0.47	-146.15
COULEE22	0.47	13.80	0.43	45.77
CGS	0.47	13.99	0.42	36.97
CRAIG_1	0.45	15.20	0.41	26.58
COLSTP_2	0.46	15.05	0.38	34.10
BRWNL_5	0.46	16.18	0.32	48.98
JDA_0304	0.47	14.20	0.28	56.94
SHEER_1	0.47	14.52	0.22	-147.39
PALOVRD2	0.45	15.13	0.22	-92.95
CURRNTC1	0.46	15.74	0.21	14.89
BRIDGER1	0.49	14.75	0.18	-73.00
DIABLO_1	0.43	15.24	0.18	-75.45
VALMY_G2	0.47	13.05	0.17	71.11
HYATT_1	0.49	13.66	0.16	12.34
NAVAJO_1	0.44	15.40	0.16	-68.19
EHUNTER1	0.47	9.59	0.04	-1.57
SJUAN_G1	0.43	4.29	0.02	-47.99
SLHWKG1	0.92	18.36	1.00	0.00
NAVAJO_1	0.93	15.82	0.57	-54.51
BRWNL_5	0.90	15.34	0.22	-56.62
COULEE22	0.92	10.76	0.15	-28.14
EHUNTER1	0.94	9.39	0.11	162.77
DIABLO_1	0.90	8.58	0.07	-169.84
CURRNTC1	0.92	7.40	0.06	-158.57
COLSTP_2	0.90	7.20	0.05	57.61
COULEE22	0.89	7.66	0.04	-178.11
BRIDGER1	0.94	7.31	0.04	-168.91
JDA_0304	0.93	0.92	0.00	17.49
RAWHIDE	0.89	-2.54	0.00	-37.70

Table 53: 2022 light summer, 1.4 GW at Hemingway Bus, 0.5 sec

Gen ID	Freq	Damping	Residue	Angle
DIABLO_1	0.19	13.53	1.00	0.00
MBPP-1	0.21	10.20	0.73	-39.39
RAWHIDE	0.21	5.77	0.48	-27.55

Table 53: 2022 light summer, 1.4 GW at Hemingway Bus, 0.5 sec

Gen ID	Freq	Damping	Residue	Angle
COLSTP_2	0.90	10.47	1.00	0.00
SUND#5GN	0.89	21.53	0.52	56.59
REV_13G1	0.89	9.76	0.41	148.17
KMO_13G1	0.92	10.22	0.22	-49.17
CGS	0.91	6.38	0.11	-96.46
MBPP-1	0.91	7.62	0.04	41.94
COULEE22	0.89	3.18	0.04	-35.86
SUND#5GN	0.88	-0.49	0.00	-71.95
SUND#5GN	0.29	21.69	1.00	0.00
SHEER_1	0.30	21.90	0.86	-38.32
REV_13G1	0.28	28.54	0.60	13.24
COLSTP_2	0.29	26.55	0.19	-1.71
SJUAN_G1	0.29	13.43	0.08	-163.38
RAWHIDE	0.66	24.62	1.00	0.00
COULEE22	0.70	19.30	0.64	86.65
HYATT_1	0.65	18.13	0.39	41.65
MBPP-1	0.68	17.46	0.28	-10.52
DIABLO_1	0.66	11.39	0.22	60.37
HAYNES1G	0.70	13.12	0.19	-17.33
CRAIG_1	0.67	21.65	0.15	1.10
NAVAJO_1	0.68	12.31	0.12	-153.38
NAVAJO_1	0.24	28.10	1.00	0.00
HAYNES1G	0.25	26.71	0.79	-10.74
PALOVRD2	0.24	26.58	0.73	0.90
CRAIG_1	0.22	5.25	0.07	60.06
CURRNTC1	0.75	18.26	1.00	0.00
EHUNTER1	0.75	18.55	0.99	0.26
KMO_13G1	0.75	11.50	0.68	34.27
CGS	0.72	21.28	0.38	-82.86
RAWHIDE	0.76	17.45	0.29	53.71
REV_13G1	0.76	9.60	0.22	-177.37
SJUAN_G1	0.73	11.64	0.14	-76.67
SHEER_1	0.75	12.61	0.08	179.85
PALOVRD2	0.75	10.67	0.06	-124.71
SUND#5GN	0.74	5.14	0.01	61.30
DIABLO_1	0.83	12.70	1.00	0.00
CURRNTC1	0.85	6.30	0.88	141.20
EHUNTER1	0.85	5.70	0.69	137.47
HAYNES1G	0.85	9.00	0.40	-26.38
KMO_13G1	0.61	15.29	1.00	0.00
REV_13G1	0.59	21.86	0.36	42.61
PALOVRD2	0.63	16.84	0.11	-38.93
SJUAN_G1	0.63	13.54	0.08	-35.40
HYATT_1	0.61	10.77	0.07	-154.23
JDA_0304	0.60	12.67	0.06	-163.37
KMO_13G1	0.47	12.92	1.00	0.00
SUND#5GN	0.47	14.18	0.69	-164.45

Table 53: 2022 light summer, 1.4 GW at Hemingway Bus, 0.5 sec

Gen ID	Freq	Damping	Residue	Angle
REV_13G1	0.47	12.67	0.50	14.87
COULEE22	0.47	12.07	0.44	15.12
CGS	0.46	12.96	0.43	22.27
JDA_0304	0.47	13.43	0.37	26.85
COLSTP_2	0.46	13.56	0.34	16.80
BRIDGER1	0.47	16.97	0.34	-34.63
PALOVRD2	0.48	15.00	0.29	-172.11
SHEER_1	0.47	13.81	0.24	-157.29
SJUAN_G1	0.48	13.51	0.24	-159.66
HAYNES1G	0.47	14.90	0.20	-167.92
RAWHIDE	0.45	9.62	0.20	-69.72
NAVAJO_1	0.48	13.58	0.18	-178.64
SLHWKG1	0.48	14.34	0.17	-159.70
MBPP-1	0.45	10.02	0.15	-41.72
HYATT_1	0.46	11.96	0.15	49.61
VALMY_G2	0.50	12.91	0.15	-41.34
CURRNTC1	0.45	13.31	0.13	2.87
CRAIG_1	0.45	9.20	0.12	-52.72
EHUNTER1	0.47	12.73	0.10	-45.54
DIABLO_1	0.50	9.43	0.03	36.32

Table 54: 2022 light summer, 1.4 GW at Midway bus, 0.5 sec

Gen ID	Freq	Damping	Residue	Angle
SJUAN_G1	0.84	18.09	1.00	0.00
EHUNTER1	0.85	9.42	0.48	41.23
COULEE22	0.84	7.76	0.27	-67.18
CURRNTC1	0.85	7.76	0.26	59.61
MBPP-1	0.84	8.88	0.12	-145.38
COLSTP_2	0.44	19.67	1.00	0.00
SLHWKG1	0.42	20.95	0.95	-102.09
BRWNL_5	0.43	22.28	0.90	3.16
DIABLO_1	0.43	16.31	0.89	-161.44
HAYNES1G	0.42	14.87	0.60	-118.53
SHEER_1	0.43	7.49	0.05	-111.74
DIABLO_1	0.72	16.72	1.00	0.00
REV_13G1	0.74	13.84	0.68	119.60
HAYNES1G	0.74	14.34	0.52	-11.38
BRWNL_5	0.74	18.53	0.23	126.10
SHEER_1	0.73	15.27	0.21	134.11
HYATT_1	0.92	12.58	1.00	0.00
SUND#5GN	0.93	14.02	0.26	-126.85
SHEER_1	0.96	7.00	0.09	-13.81
KMO_13G1	0.94	8.05	0.04	127.98
BRWNL_5	0.95	5.63	0.03	-71.86
RAWHIDE	0.37	29.16	1.00	0.00
REV_13G1	0.39	24.89	0.39	-0.35

Table 54: 2022 light summer, 1.4 GW at Midway bus, 0.5 sec

Gen ID	**Freq**	**Damping**	**Residue**	**Angle**
KMO_13G1	0.37	20.72	0.38	48.08
NAVAJO_1	0.38	21.94	0.35	-94.54
PALOVRD2	0.37	16.86	0.17	-70.69
KMO_13G1	0.80	11.29	1.00	0.00
JDA_0304	0.80	14.24	0.47	37.73
BRIDGER1	0.76	8.07	0.10	-82.92
RAWHIDE	0.78	3.84	0.01	23.56
SUND#5GN	0.29	20.17	1.00	0.00
SHEER_1	0.29	21.50	0.87	-1.16
KMO_13G1	0.28	26.50	0.62	27.34
REV_13G1	0.28	24.15	0.49	12.63
COULEE22	0.28	27.71	0.35	11.99
CGS	0.30	22.60	0.20	-36.42
SJUAN_G1	0.28	20.19	0.19	-129.15
COLSTP_2	0.28	24.26	0.18	6.10
NAVAJO_1	0.25	20.53	0.12	-77.86
SLHWKG1	0.28	16.46	0.08	-133.04
VALMY_G2	0.30	8.79	0.06	116.04
MBPP-1	0.24	18.57	0.06	-42.18
PALOVRD2	0.25	15.09	0.06	-79.10
EHUNTER1	0.29	15.46	0.05	-149.14
CURRNTC1	0.26	17.02	0.05	-81.90
BRIDGER1	0.26	17.24	0.04	-102.99
CRAIG_1	0.25	12.64	0.04	-76.70
RAWHIDE	0.24	9.27	0.02	-41.77
VALMY_G2	0.26	-36.88	0.00	-178.69
RAWHIDE	0.46	15.40	1.00	0.00
MBPP-1	0.46	16.14	0.80	22.61
CRAIG_1	0.47	15.65	0.58	6.31
CGS	0.47	27.46	0.48	40.61
CURRNTC1	0.45	20.20	0.40	48.28
BRIDGER1	0.46	18.78	0.35	60.35
EHUNTER1	0.45	19.00	0.29	55.32
VALMY_G2	0.47	16.99	0.18	68.77
SUND#5GN	0.48	15.44	0.12	179.50
EHUNTER1	0.87	24.42	1.00	0.00
COLSTP_2	0.89	11.79	0.84	6.38
VALMY_G2	0.89	12.87	0.33	-120.56
REV_13G1	0.88	9.58	0.13	-135.08
PALOVRD2	0.91	7.87	0.05	-108.50
CGS	0.86	5.66	0.05	66.90
CRAIG_1	0.89	4.02	0.01	-171.26
COLSTP_2	0.68	16.65	1.00	0.00
COULEE22	0.68	14.17	0.58	17.45
SJUAN_G1	0.69	14.51	0.54	-59.42
JDA_0304	0.66	16.05	0.53	51.50
KMO_13G1	0.70	8.71	0.52	155.48
EHUNTER1	0.68	14.12	0.50	-12.82
CURRNTC1	0.69	13.80	0.49	-17.05

Table 54: 2022 light summer, 1.4 GW at Midway bus, 0.5 sec

Gen ID	Freq	Damping	Residue	Angle
HYATT_1	0.70	14.59	0.44	141.35
CGS	0.67	13.17	0.43	14.75
BRWNL_5	0.66	13.56	0.32	40.52
RAWHIDE	0.68	12.05	0.27	119.62
BRIDGER1	0.68	12.17	0.22	0.42
SUND#5GN	0.70	14.56	0.21	111.82
MBPP-1	0.68	12.96	0.19	153.17
PALOVRD2	0.69	12.88	0.15	-47.66
VALMY_G2	0.67	12.76	0.15	21.95
CRAIG_1	0.68	13.95	0.11	-149.36
SLHWKG1	0.69	13.23	0.10	-50.23
NAVAJO_1	0.69	11.79	0.09	-59.77
DIABLO_1	0.58	21.80	1.00	0.00
COLSTP_2	0.64	24.18	0.99	-99.95
HAYNES1G	0.59	22.60	0.82	41.86
KMO_13G1	0.62	9.37	0.74	9.85
REV_13G1	0.62	15.99	0.59	97.06
HYATT_1	0.60	10.27	0.10	-68.45

Table 55: 2022 light summer, double Palo Verde trip

Gen ID	Freq	Damping	Residue	Angle
COLSTP_2	0.94	12.17	1.00	0.00
HYATT_1	0.94	15.21	0.45	156.36
CURRNTC1	0.95	24.22	0.43	152.11
HAYNES1G	0.95	13.70	0.25	-83.59
REV_13G1	0.93	8.98	0.21	133.98
SHEER_1	0.96	6.65	0.11	-20.66
SUND#5GN	0.94	5.97	0.03	-138.97
REV_13G1	0.76	16.65	1.00	0.00
EHUNTER1	0.75	12.74	0.87	-28.47
BRIDGER1	0.76	11.22	0.23	-71.31
VALMY_G2	0.74	12.60	0.17	18.21
SUND#5GN	0.75	10.08	0.03	-129.13
JDA_0304	0.60	21.25	1.00	0.00
COLSTP_2	0.60	22.02	0.82	38.50
HYATT_1	0.59	14.15	0.31	22.50
SJUAN_G1	0.60	8.86	0.19	-167.52
SLHWKG1	0.59	8.72	0.11	-114.65
NAVAJO_1	0.60	6.42	0.04	-140.08
RAWHIDE	0.61	4.00	0.01	-72.35
COULEE22	0.50	19.06	1.00	0.00
MBPP-1	0.48	12.07	0.21	2.94
CRAIG_1	0.51	15.14	0.14	-121.20
CURRNTC1	0.49	14.06	0.13	-8.75
COLSTP_2	0.80	7.85	1.00	0.00

Table 55: 2022 light summer, double Palo Verde trip

Gen ID	Freq	Damping	Residue	Angle
REV_13G1	0.81	8.15	0.95	158.63
KMO_13G1	0.79	7.66	0.75	90.09
HYATT_1	0.80	9.96	0.43	150.37
VALMY_G2	0.82	11.68	0.41	168.85
CGS	0.80	6.58	0.20	-33.43
CURRNTC1	0.81	4.80	0.10	167.43
KMO_13G1	0.65	10.15	1.00	0.00
DIABLO_1	0.65	17.59	0.47	-71.74
JDA_0304	0.67	16.77	0.32	91.40
SHEER_1	0.66	25.28	0.24	43.08
COULEE22	0.68	14.96	0.22	104.60
BRIDGER1	0.65	15.40	0.20	175.59
KMO_13G1	0.67	7.24	0.12	117.21
HAYNES1G	0.68	10.85	0.09	-47.26
VALMY_G2	0.63	9.10	0.05	-120.50
SUND#5GN	0.27	18.21	1.00	0.00
SHEER_1	0.27	18.39	0.76	2.67
KMO_13G1	0.27	17.90	0.34	12.58
REV_13G1	0.27	17.59	0.26	15.49
NAVAJO_1	0.27	19.59	0.26	-162.27
SJUAN_G1	0.27	18.89	0.25	-155.55
HAYNES1G	0.26	22.34	0.24	-106.29
VALMY_G2	0.27	15.86	0.22	154.99
DIABLO_1	0.28	17.62	0.19	165.66
COLSTP_2	0.28	18.79	0.17	-13.51
RAWHIDE	0.28	17.65	0.16	-174.67
SLHWKG1	0.27	17.73	0.15	-155.51
HYATT_1	0.28	20.66	0.14	-163.48
MBPP-1	0.27	18.31	0.13	-154.04
EHUNTER1	0.28	18.20	0.13	173.04
COULEE22	0.27	17.69	0.12	7.29
CGS	0.27	17.63	0.12	9.79
CRAIG_1	0.27	16.79	0.11	-143.81
JDA_0304	0.28	21.42	0.07	-67.08
CURRNTC1	0.29	19.72	0.06	176.78
BRIDGER1	0.25	23.27	0.06	-101.32
HAYNES1G	0.30	13.34	0.04	93.23
BRWNL_5	0.28	15.78	0.03	-80.82
BRIDGER1	0.27	13.98	0.03	-147.15
CURRNTC1	0.26	13.29	0.02	-105.71
EHUNTER1	0.92	26.92	1.00	0.00
SLHWKG1	0.88	14.43	0.32	-11.71
NAVAJO_1	0.91	15.86	0.18	-56.27
CGS	0.91	8.52	0.18	-67.15
COULEE22	0.89	7.67	0.12	-14.34
KMO_13G1	0.90	7.93	0.10	34.62
VALMY_G2	0.92	10.72	0.09	-141.50
JDA_0304	0.91	6.10	0.04	-71.75
CGS	0.70	13.70	1.00	0.00
SJUAN_G1	0.70	11.53	1.00	9.70

Table 55: 2022 light summer, double Palo Verde trip

Gen ID	**Freq**	**Damping**	**Residue**	**Angle**
BRWNL_5	0.71	12.09	0.82	9.42
CURRNTC1	0.73	8.71	0.74	-34.81
RAWHIDE	0.73	10.05	0.43	91.92
MBPP-1	0.71	11.65	0.41	149.38
SLHWKG1	0.72	9.39	0.15	-39.27
EHUNTER1	0.56	27.68	1.00	0.00
CGS	0.54	17.97	0.54	43.60
SUND#5GN	0.57	28.92	0.39	-113.51
BRWNL_5	0.56	14.35	0.19	27.74
NAVAJO_1	0.56	14.29	0.14	-118.64
REV_13G1	0.57	10.93	0.14	-69.47
DIABLO_1	0.35	18.33	1.00	0.00
SHEER_1	0.32	22.39	0.65	92.31
RAWHIDE	0.35	13.84	0.39	51.62
KMO_13G1	0.46	14.20	1.00	0.00
COULEE22	0.45	15.30	0.73	28.13
SUND#5GN	0.45	14.08	0.60	-176.17
CGS	0.45	14.31	0.55	13.08
REV_13G1	0.46	13.85	0.53	0.39
COLSTP_2	0.45	14.87	0.51	6.84
MBPP-1	0.44	13.53	0.48	5.10
RAWHIDE	0.42	14.22	0.40	40.40
CRAIG_1	0.44	12.65	0.36	-14.26
HAYNES1G	0.45	15.57	0.35	-156.89
JDA_0304	0.46	13.97	0.32	14.12
RAWHIDE	0.46	11.58	0.28	-103.96
BRWNL_5	0.45	14.05	0.27	16.21
SJUAN_G1	0.46	15.94	0.23	-151.54
SHEER_1	0.46	13.59	0.23	177.59
VALMY_G2	0.45	12.64	0.23	70.85
DIABLO_1	0.45	14.06	0.23	166.05
NAVAJO_1	0.45	14.80	0.22	-147.07
CURRNTC1	0.44	14.38	0.21	19.71
SLHWKG1	0.45	14.33	0.17	-127.37
BRIDGER1	0.45	12.81	0.17	11.91
HYATT_1	0.46	13.13	0.13	14.18
EHUNTER1	0.87	11.08	1.00	0.00
DIABLO_1	0.85	11.38	0.39	-12.40
SJUAN_G1	0.86	10.77	0.28	-73.05
BRWNL_5	0.83	9.06	0.26	165.04

Table 56: 2022 light spring, 1.4 GW at Chief Joseph brake, 0.5 sec

Gen ID	Freq	Damping	Residue	Angle
COLSTP_2	0.54	21.44	1.00	0.00
MBPP-1	0.55	16.40	0.47	-62.10
SLHWKG1	0.54	15.64	0.33	-161.83
RAWHIDE	0.54	11.98	0.28	-50.12
CURRNTC1	0.52	13.21	0.23	42.65
COULEE22	0.86	11.32	1.00	0.00
JDA_0304	0.84	14.31	0.74	15.80
BRWNL_5	0.85	15.12	0.69	-61.34
COLSTP_2	0.85	11.71	0.64	1.26
CGS	0.85	11.67	0.63	-9.56
KMO_13G1	0.84	11.48	0.55	67.67
CURRNTC1	0.84	10.97	0.50	177.58
EHUNTER1	0.84	10.01	0.39	-140.49
SUND#5GN	0.82	15.08	0.16	147.38
PALOVRD2	0.84	9.86	0.04	26.30
SLHWKG1	0.85	5.55	0.02	131.68
SJUAN_G1	0.85	3.87	0.01	-70.33
KMO_13G1	0.63	15.25	1.00	0.00
REV_13G1	0.64	10.62	0.10	-38.65
JDA_0304	0.63	9.27	0.05	140.48
HYATT_1	0.63	7.75	0.04	156.31
CGS	0.65	8.88	0.04	78.51
DIABLO_1	0.63	9.23	0.03	169.32
SUND#5GN	0.62	12.45	0.03	-169.11
REV_13G1	0.78	19.91	1.00	0.00
SHEER_1	0.79	11.81	0.33	-51.70
BRIDGER1	0.80	11.11	0.31	9.57
VALMY_G2	0.78	10.78	0.11	54.42
HAYNES1G	0.80	11.54	0.10	-99.15
MBPP-1	0.97	7.77	1.00	0.00
SLHWKG1	0.94	7.10	0.21	-33.35
NAVAJO_1	0.98	8.14	0.06	-124.51
KMO_13G1	0.45	11.40	1.00	0.00
REV_13G1	0.45	11.50	0.59	8.67
PALOVRD2	0.47	25.79	0.47	-50.74
COULEE22	0.46	11.61	0.43	4.00
SUND#5GN	0.46	11.43	0.43	-171.71
PALOVRD2	0.46	12.62	0.43	159.93
HAYNES1G	0.46	13.44	0.40	-174.39
NAVAJO_1	0.46	25.47	0.38	-58.91
CGS	0.46	11.57	0.37	-6.65
SJUAN_G1	0.46	12.23	0.35	-179.64
COLSTP_2	0.46	12.34	0.35	-8.83
NAVAJO_1	0.46	12.34	0.34	152.66
MBPP-1	0.47	19.28	0.28	-134.38
RAWHIDE	0.45	16.90	0.27	-154.38
SLHWKG1	0.45	12.24	0.27	-161.61
JDA_0304	0.46	11.51	0.24	2.38

Table 56: 2022 light spring, 1.4 GW at Chief Joseph brake, 0.5 sec

Gen ID	Freq	Damping	Residue	Angle
CRAIG_1	0.46	15.20	0.21	-160.07
BRWNL_5	0.46	11.54	0.21	-6.92
DIABLO_1	0.45	11.04	0.13	-179.24
EHUNTER1	0.44	23.87	0.13	-139.06
VALMY_G2	0.45	12.50	0.10	89.14
SHEER_1	0.46	11.23	0.10	-169.22
BRIDGER1	0.45	9.41	0.05	-13.33
HYATT_1	0.46	9.87	0.05	-10.75
SJUAN_G1	0.59	26.31	1.00	0.00
BRWNL_5	0.58	19.14	0.51	159.85
EHUNTER1	0.60	11.60	0.08	103.26
BRIDGER1	0.57	8.26	0.06	-174.04
VALMY_G2	0.57	8.31	0.03	-169.12
CRAIG_1	0.57	5.16	0.01	124.37
REV_13G1	0.89	11.60	1.00	0.00
VALMY_G2	0.90	13.98	0.50	103.47
DIABLO_1	0.89	7.39	0.50	-49.78
RAWHIDE	0.91	10.42	0.26	150.11
HAYNES1G	0.88	5.35	0.15	-77.91
NAVAJO_1	0.87	5.40	0.03	-92.31
KMO_13G1	0.70	9.57	1.00	0.00
SJUAN_G1	0.68	13.82	0.89	-158.51
PALOVRD2	0.66	11.98	0.42	-120.76
HYATT_1	0.69	11.27	0.27	32.83
NAVAJO_1	0.66	11.47	0.26	-123.13
SLHWKG1	0.68	9.54	0.11	-138.37
BRWNL_5	0.69	7.57	0.09	-99.56
SHEER_1	0.69	8.71	0.07	161.55
CURRNTC1	0.69	3.64	0.02	-122.82
CURRNTC1	0.76	14.94	1.00	0.00
DIABLO_1	0.72	16.29	0.62	-67.79
EHUNTER1	0.75	11.04	0.48	27.02
CRAIG_1	0.76	15.84	0.19	-84.66
RAWHIDE	0.74	9.56	0.19	-168.37
MBPP-1	0.74	9.18	0.10	-118.58
COLSTP_2	0.72	5.85	0.05	156.31

Table 57: 2022 light spring, 1.4 GW at El Dorado bus, 0.5 sec

Gen ID	Freq	Damping	Residue	Angle
BRWNL_5	0.70	21.27	1.00	0.00
SHEER_1	0.68	16.18	0.61	9.79
CURRNTC1	0.69	9.26	0.29	69.94
CRAIG_1	0.71	9.47	0.08	-129.68
CRAIG_1	0.97	14.26	1.00	0.00
HYATT_1	0.95	5.73	0.92	129.93

Table 57: 2022 light spring, 1.4 GW at El Dorado bus, 0.5 sec

Gen ID	Freq	Damping	Residue	Angle
COLSTP_2	0.96	6.69	0.87	-108.94
COULEE22	0.95	8.06	0.69	-62.36
RAWHIDE	0.96	11.26	0.48	130.30
JDA_0304	0.95	7.32	0.32	27.38
MBPP-1	0.96	8.35	0.24	160.75
SHEER_1	0.94	5.06	0.15	-164.67
SJUAN_G1	0.92	11.94	1.00	0.00
EHUNTER1	0.91	15.78	0.53	60.85
VALMY_G2	0.93	9.03	0.31	-171.49
REV_13G1	0.89	27.72	0.19	2.12
DIABLO_1	0.91	3.80	0.10	-117.69
CGS	0.91	-0.56	0.00	94.84
SUND#5GN	0.90	0.02	0.00	159.17
KMO_13G1	0.64	10.86	1.00	0.00
HYATT_1	0.63	17.00	0.66	-140.12
REV_13G1	0.65	13.50	0.36	42.94
BRWNL_5	0.63	11.85	0.27	-143.59
CGS	0.64	11.90	0.25	-175.06
JDA_0304	0.65	12.37	0.24	164.25
COULEE22	0.66	11.42	0.20	172.49
COLSTP_2	0.66	9.39	0.13	156.06
EHUNTER1	0.67	10.36	0.12	154.93
SUND#5GN	0.64	16.75	0.08	-127.68
VALMY_G2	0.67	10.18	0.06	178.97
RAWHIDE	0.51	13.65	1.00	0.00
RAWHIDE	0.53	9.52	0.95	-153.39
BRIDGER1	0.50	24.30	0.75	-21.25
MBPP-1	0.51	9.51	0.61	-65.22
DIABLO_1	0.52	13.77	0.39	77.45
CRAIG_1	0.51	6.56	0.33	-63.32
CURRNTC1	0.52	20.25	0.33	-3.40
HYATT_1	0.49	11.22	0.20	-158.24
VALMY_G2	0.49	14.57	0.17	1.48
EHUNTER1	0.51	9.73	0.17	-40.53
CURRNTC1	0.53	7.49	0.10	-103.31
CRAIG_1	0.53	0.13	0.02	4.68
COLSTP_2	0.53	3.98	0.01	-126.82
PALOVRD2	0.81	19.27	1.00	0.00
MBPP-1	0.80	5.10	0.04	-118.96
BRIDGER1	0.79	2.42	0.02	-51.83
SUND#5GN	0.27	19.99	1.00	0.00
SHEER_1	0.27	20.05	0.73	2.78
SJUAN_G1	0.28	19.55	0.27	174.23
REV_13G1	0.26	23.60	0.26	31.03
PALOVRD2	0.27	20.06	0.26	173.96
NAVAJO_1	0.27	19.98	0.24	177.43
VALMY_G2	0.26	16.74	0.24	163.65
RAWHIDE	0.28	19.36	0.23	145.43
HAYNES1G	0.27	18.82	0.21	176.97

Table 57: 2022 light spring, 1.4 GW at El Dorado bus, 0.5 sec

Gen ID	**Freq**	**Damping**	**Residue**	**Angle**
CRAIG_1	0.28	19.11	0.19	160.33
DIABLO_1	0.28	17.70	0.19	158.76
MBPP-1	0.28	19.41	0.19	157.29
KMO_13G1	0.26	18.22	0.18	15.61
EHUNTER1	0.28	19.38	0.16	165.79
CURRNTC1	0.28	19.52	0.13	152.57
BRIDGER1	0.27	18.55	0.09	-178.18
HYATT_1	0.27	16.63	0.09	175.86
BRWNL_5	0.30	11.06	0.03	120.19
JDA_0304	0.29	11.68	0.02	134.43
SHEER_1	0.31	-36.10	0.00	-25.24
KMO_13G1	0.73	16.41	1.00	0.00
DIABLO_1	0.73	18.52	0.62	-24.57
BRIDGER1	0.72	14.98	0.61	-87.58
RAWHIDE	0.76	8.29	0.09	-27.42
SLHWKG1	0.88	19.55	1.00	0.00
HYATT_1	0.86	7.29	0.08	83.98
SHEER_1	0.84	15.61	0.07	83.34
COLSTP_2	0.87	6.32	0.06	-140.34
CGS	0.86	23.81	0.05	-143.01
COULEE22	0.87	4.93	0.04	-110.44
CURRNTC1	0.86	8.48	0.03	146.60
JDA_0304	0.87	6.14	0.02	-50.60
BRWNL_5	0.85	5.92	0.01	-93.19
CGS	0.83	1.19	0.00	-55.98
REV_13G1	0.88	0.88	0.00	92.43
KMO_13G1	0.84	-1.26	0.00	66.92
SJUAN_G1	0.61	11.83	1.00	0.00
MBPP-1	0.58	10.14	0.40	-80.47
PALOVRD2	0.60	7.58	0.40	55.20
BRIDGER1	0.56	6.60	0.26	-14.60
KMO_13G1	0.45	11.31	1.00	0.00
PALOVRD2	0.46	15.90	0.53	-148.91
COULEE22	0.46	11.86	0.47	-1.72
NAVAJO_1	0.45	15.94	0.45	-145.55
SLHWKG1	0.45	16.67	0.43	-121.30
COULEE22	0.47	26.40	0.42	125.01
SUND#5GN	0.46	11.13	0.41	-165.51
COLSTP_2	0.45	14.91	0.41	25.48
BRWNL_5	0.45	16.55	0.41	30.38
SJUAN_G1	0.46	12.14	0.41	167.78
REV_13G1	0.45	8.10	0.36	34.23
HAYNES1G	0.46	14.99	0.36	-139.15
CGS	0.45	11.58	0.34	5.13
JDA_0304	0.47	9.34	0.18	-37.48
REV_13G1	0.42	8.60	0.16	-4.67
SHEER_1	0.47	10.96	0.10	175.63
DIABLO_1	0.44	13.25	0.05	-82.50

Table 58: 2022 light spring, 1.4 GW at Hemingway Bus, 0.5 sec

Gen ID	**Freq**	**Damping**	**Residue**	**Angle**
CGS	0.83	17.81	1.00	0.00
KMO_13G1	0.82	11.42	0.34	112.87
PALOVRD2	0.83	15.84	0.07	71.61
KMO_13G1	0.62	10.73	1.00	0.00
DIABLO_1	0.63	15.92	0.64	161.79
CGS	0.63	12.01	0.32	160.69
PALOVRD2	0.63	9.79	0.19	1.68
REV_13G1	0.63	9.52	0.19	24.31
JDA_0304	0.63	10.13	0.18	147.63
COULEE22	0.63	10.43	0.16	165.00
NAVAJO_1	0.63	8.84	0.09	10.16
COLSTP_2	0.65	8.40	0.09	114.54
SLHWKG1	0.64	6.66	0.05	-7.59
SUND#5GN	0.63	8.95	0.03	-168.62
DIABLO_1	0.46	28.34	1.00	0.00
KMO_13G1	0.46	10.88	0.69	119.75
HAYNES1G	0.45	18.92	0.41	-0.36
REV_13G1	0.46	11.02	0.40	131.87
PALOVRD2	0.45	15.92	0.39	-19.73
SJUAN_G1	0.45	13.61	0.35	-40.88
SLHWKG1	0.44	16.62	0.33	6.77
SUND#5GN	0.45	11.56	0.31	-37.24
NAVAJO_1	0.45	15.51	0.31	-20.44
CGS	0.45	11.90	0.27	133.10
COULEE22	0.46	10.84	0.27	134.01
COLSTP_2	0.45	12.82	0.22	143.09
SHEER_1	0.45	14.62	0.11	-9.02
CURRNTC1	0.99	13.71	1.00	0.00
SLHWKG1	0.97	9.12	0.23	2.17
SUND#5GN	1.00	8.06	0.16	-6.16
HAYNES1G	0.99	7.14	0.14	-38.83
NAVAJO_1	0.99	12.85	0.13	-45.55
SJUAN_G1	0.95	5.27	0.06	169.73
EHUNTER1	0.89	24.74	1.00	0.00
MBPP-1	0.91	23.31	0.23	-59.44
REV_13G1	0.90	19.28	0.14	24.34
SUND#5GN	0.26	19.36	1.00	0.00
SHEER_1	0.26	19.60	0.75	1.36
KMO_13G1	0.25	21.66	0.26	29.08
REV_13G1	0.26	20.86	0.23	23.32
SJUAN_G1	0.28	16.32	0.22	139.69
NAVAJO_1	0.27	15.55	0.17	156.46
RAWHIDE	0.28	16.21	0.17	140.02
CRAIG_1	0.27	17.24	0.16	158.04
PALOVRD2	0.28	14.51	0.16	147.54
SLHWKG1	0.29	15.34	0.16	133.64
MBPP-1	0.27	16.56	0.14	159.92
EHUNTER1	0.27	17.72	0.13	170.69

Table 58: 2022 light spring, 1.4 GW at Hemingway Bus, 0.5 sec

Gen ID	Freq	Damping	Residue	Angle
HAYNES1G	0.28	13.29	0.13	142.82
DIABLO_1	0.28	11.70	0.09	147.47
COULEE22	0.79	16.22	1.00	0.00
JDA_0304	0.79	12.97	0.20	-14.87
SHEER_1	0.78	8.19	0.05	-165.12
SUND#5GN	0.80	13.24	0.03	74.08
COULEE22	0.74	28.23	1.00	0.00
COLSTP_2	0.76	14.60	0.50	165.10
CGS	0.71	17.33	0.50	-91.15
CURRNTC1	0.72	11.26	0.29	-156.50
REV_13G1	0.76	12.86	0.24	30.22
DIABLO_1	0.76	13.83	0.23	-30.71
EHUNTER1	0.75	9.66	0.17	162.58
RAWHIDE	0.73	11.02	0.17	-13.76
MBPP-1	0.72	12.54	0.15	32.89
SJUAN_G1	0.72	11.04	0.13	-134.33
KMO_13G1	0.74	7.80	0.12	-60.71
BRIDGER1	0.75	9.48	0.09	-177.46
CRAIG_1	0.74	11.76	0.07	29.99
HAYNES1G	0.76	11.26	0.05	5.58
NAVAJO_1	0.72	7.96	0.02	-111.37
PALOVRD2	0.75	6.51	0.02	-166.07
SLHWKG1	0.74	1.59	0.00	-114.24
SHEER_1	0.73	-5.11	0.00	49.41
MBPP-1	0.51	9.78	1.00	0.00
RAWHIDE	0.48	9.99	0.63	61.27
CRAIG_1	0.49	8.59	0.55	43.86
EHUNTER1	0.51	8.29	0.25	-18.56
SJUAN_G1	0.61	12.65	1.00	0.00
HYATT_1	0.60	9.93	0.56	-153.84
CRAIG_1	0.56	10.58	0.35	44.33
SHEER_1	0.59	15.42	0.24	59.11
MBPP-1	0.57	11.67	0.23	-14.01
HAYNES1G	0.59	4.40	0.03	123.91

Table 59: 2022 light spring, 1.4 GW at Midway bus, 0.5 sec

Gen ID	Freq	Damping	Residue	Angle
KMO_13G1	0.62	13.33	1.00	0.00
REV_13G1	0.61	18.44	0.56	62.45
CGS	0.62	13.88	0.21	-167.49
JDA_0304	0.61	9.78	0.10	-148.79
COULEE22	0.61	10.63	0.08	-117.85
COLSTP_2	0.56	18.45	1.00	0.00
MBPP-1	0.57	19.77	0.53	-138.09
VALMY_G2	0.57	14.54	0.36	20.20

Table 59: 2022 light spring, 1.4 GW at Midway bus, 0.5 sec

Gen ID	**Freq**	**Damping**	**Residue**	**Angle**
DIABLO_1	0.55	7.45	0.23	148.54
KMO_13G1	0.71	12.93	1.00	0.00
COULEE22	0.71	17.69	0.55	-85.70
BRIDGER1	0.71	14.94	0.47	-111.13
CGS	0.72	17.22	0.45	-135.55
PALOVRD2	0.70	19.05	0.21	-146.50
EHUNTER1	0.70	10.37	0.19	-128.38
HAYNES1G	0.71	18.30	0.18	106.83
DIABLO_1	0.71	14.65	0.17	54.33
CURRNTC1	0.69	10.23	0.16	-129.32
MBPP-1	0.70	11.83	0.15	41.17
SHEER_1	0.68	15.07	0.13	-154.37
RAWHIDE	0.70	9.51	0.13	11.34
NAVAJO_1	0.72	12.75	0.06	-165.41
SJUAN_G1	0.69	-1.12	0.00	-35.89
COULEE22	0.92	15.38	1.00	0.00
DIABLO_1	0.93	9.32	0.79	-17.37
COLSTP_2	0.91	6.50	0.23	156.55
VALMY_G2	0.92	4.22	0.04	-75.03
NAVAJO_1	0.40	19.35	1.00	0.00
COLSTP_2	0.41	18.22	0.96	142.76
PALOVRD2	0.41	15.80	0.77	-21.51
SJUAN_G1	0.81	23.36	1.00	0.00
BRIDGER1	0.78	15.24	0.76	-65.58
SHEER_1	0.79	12.25	0.34	-123.12
EHUNTER1	0.80	8.16	0.21	-56.06
CURRNTC1	0.79	7.85	0.21	-58.98
RAWHIDE	0.79	8.46	0.07	135.31
BRWNL_5	0.64	17.62	1.00	0.00
SUND#5GN	0.65	13.42	0.09	40.71
CRAIG_1	0.66	7.01	0.04	128.95
RAWHIDE	0.51	9.42	1.00	0.00
MBPP-1	0.51	10.29	0.94	19.17
CRAIG_1	0.51	9.37	0.63	28.57
NAVAJO_1	0.54	15.39	0.44	127.29
PALOVRD2	0.54	14.35	0.42	130.57
BRIDGER1	0.52	12.57	0.39	18.88
SLHWKG1	0.52	12.20	0.31	-179.04
CURRNTC1	0.51	10.87	0.28	36.45
EHUNTER1	0.51	10.92	0.27	43.46
HAYNES1G	0.53	10.05	0.22	162.94
COULEE22	0.89	9.94	1.00	0.00
CGS	0.87	8.68	0.23	25.12
REV_13G1	0.87	9.97	0.14	-125.45
SJUAN_G1	0.89	5.75	0.05	-93.34
HYATT_1	0.76	21.50	1.00	0.00

Table 59: 2022 light spring, 1.4 GW at Midway bus, 0.5 sec

Gen ID	Freq	Damping	Residue	Angle
BRWNL_5	0.74	16.32	0.96	-162.29
COLSTP_2	0.73	15.31	0.94	-110.30
JDA_0304	0.76	18.35	0.86	-118.33
REV_13G1	0.73	16.35	0.77	111.95
SLHWKG1	0.77	14.50	0.22	145.53
VALMY_G2	0.73	11.71	0.20	-127.33
CRAIG_1	0.77	14.75	0.14	13.29
COLSTP_2	1.00	8.98	1.00	0.00
HYATT_1	0.94	5.21	0.57	42.99
PALOVRD2	0.98	10.87	0.47	-95.48
BRWNL_5	0.95	10.64	0.40	-121.10
JDA_0304	0.95	8.18	0.40	-79.03
SHEER_1	0.95	28.88	0.38	67.22
CRAIG_1	0.99	9.82	0.15	77.01
EHUNTER1	0.99	6.19	0.08	107.44
CURRNTC1	0.98	6.66	0.07	98.63
SHEER_1	0.96	3.54	0.03	1.44
SUND#5GN	0.96	8.37	0.03	175.28
BRIDGER1	0.96	4.67	0.02	-167.96
KMO_13G1	0.46	12.56	1.00	0.00
DIABLO_1	0.49	20.43	0.89	-116.14
BRWNL_5	0.45	23.56	0.74	54.54
REV_13G1	0.45	12.87	0.59	12.84
SUND#5GN	0.46	11.30	0.33	-168.35
HAYNES1G	0.44	19.20	0.33	-94.30
VALMY_G2	0.47	20.20	0.32	146.20
SJUAN_G1	0.46	11.57	0.30	-177.11
COULEE22	0.45	11.34	0.29	19.84
CGS	0.45	11.19	0.23	13.35
HYATT_1	0.49	10.42	0.23	-95.58
JDA_0304	0.46	8.31	0.12	-34.07
SHEER_1	0.46	8.79	0.05	-163.04
SUND#5GN	0.27	19.55	1.00	0.00
SHEER_1	0.27	19.69	0.75	-3.96
KMO_13G1	0.26	22.64	0.30	12.09
REV_13G1	0.26	22.12	0.26	14.56
SJUAN_G1	0.27	18.04	0.23	174.49
VALMY_G2	0.28	15.24	0.22	130.98
RAWHIDE	0.28	18.45	0.21	151.04
HAYNES1G	0.27	18.30	0.21	173.64
DIABLO_1	0.28	18.09	0.19	171.72
PALOVRD2	0.27	17.45	0.19	-177.75
MBPP-1	0.28	18.99	0.19	150.08
CRAIG_1	0.28	17.99	0.18	152.75
SLHWKG1	0.28	17.28	0.18	162.51
NAVAJO_1	0.26	17.70	0.18	-170.93
EHUNTER1	0.28	19.11	0.17	159.30
CURRNTC1	0.28	19.74	0.13	152.56
BRIDGER1	0.27	20.00	0.12	177.04
HYATT_1	0.28	16.40	0.09	162.61
JDA_0304	0.28	16.59	0.03	149.80

Table 59: 2022 light spring, 1.4 GW at Midway bus, 0.5 sec

Gen ID	Freq	Damping	Residue	Angle
BRWNL_5	0.29	8.80	0.02	118.99

Table 60: 2022 light spring, double Palo Verde trip

Gen ID	Freq	Damping	Residue	Angle
COULEE22	0.55	26.04	1.00	0.00
MBPP-1	0.56	21.76	0.54	13.86
EHUNTER1	0.53	10.52	0.45	115.87
SHEER_1	0.76	10.43	1.00	0.00
BRIDGER1	0.75	11.13	0.77	120.82
SUND#5GN	0.76	11.51	0.16	-79.62
VALMY_G2	0.15	10.14	1.00	0.00
NAVAJO_1	0.16	7.02	0.43	-13.78
RAWHIDE	0.16	5.18	0.18	1.38
JDA_0304	0.14	-9.58	0.04	106.75
COLSTP_2	0.21	27.78	1.00	0.00
CURRNTC1	0.23	18.17	0.95	86.25
COULEE22	0.23	20.73	0.35	-89.74
HYATT_1	0.22	19.91	0.35	-84.44
KMO_13G1	0.69	13.63	1.00	0.00
COULEE22	0.67	11.22	0.25	-97.49
SHEER_1	0.68	16.12	0.22	153.33
DIABLO_1	0.65	12.21	0.14	-49.22
VALMY_G2	0.66	10.26	0.09	-63.53
EHUNTER1	0.66	9.10	0.08	-112.70
CRAIG_1	0.69	11.33	0.08	35.11
KMO_13G1	0.45	11.83	1.00	0.00
REV_13G1	0.45	11.08	0.44	15.86
CGS	0.45	11.93	0.39	16.26
COULEE22	0.46	11.47	0.36	10.55
SUND#5GN	0.46	10.76	0.30	-176.77
COLSTP_2	0.45	11.59	0.23	23.55
CGS	0.45	18.82	0.21	-143.68
BRWNL_5	0.45	11.88	0.18	25.90
SLHWKG1	0.45	11.59	0.17	-132.83
NAVAJO_1	0.45	11.21	0.17	-146.43
VALMY_G2	0.44	11.97	0.14	116.59
HAYNES1G	0.45	10.74	0.14	-145.80
JDA_0304	0.45	11.35	0.14	42.18
SJUAN_G1	0.45	9.45	0.13	-179.05
DIABLO_1	0.45	10.28	0.09	-163.10
BRIDGER1	0.44	13.60	0.08	73.68
HYATT_1	0.44	14.75	0.07	69.35
SHEER_1	0.46	11.42	0.07	178.69
MBPP-1	0.51	8.68	1.00	0.00

Table 60: 2022 light spring, double Palo Verde trip

Gen ID	Freq	Damping	Residue	Angle
EHUNTER1	0.50	13.49	0.84	66.46
RAWHIDE	0.50	7.66	0.80	-9.34
CURRNTC1	0.51	9.67	0.41	-4.35
HYATT_1	0.50	10.82	0.36	-138.87
CRAIG_1	0.49	7.08	0.32	43.09
DIABLO_1	0.51	9.11	0.31	179.71
CRAIG_1	0.52	6.28	0.29	-5.07
SJUAN_G1	0.48	9.43	0.27	150.71
HAYNES1G	0.51	9.00	0.25	168.05
BRIDGER1	0.52	7.87	0.20	-25.53
RAWHIDE	0.53	4.81	0.15	-32.35
JDA_0304	0.49	8.62	0.11	-108.38
REV_13G1	0.52	8.75	0.11	168.59
NAVAJO_1	0.53	7.01	0.06	102.50
VALMY_G2	0.52	5.73	0.04	-8.62
COLSTP_2	0.52	5.33	0.03	-66.34
BRWNL_5	0.52	5.44	0.03	-86.25
KMO_13G1	0.61	10.57	1.00	0.00
HYATT_1	0.63	13.00	0.54	136.66
JDA_0304	0.62	13.16	0.52	123.81
CGS	0.63	12.40	0.51	108.62
SJUAN_G1	0.63	11.25	0.44	-52.34
BRIDGER1	0.64	12.81	0.42	106.88
BRWNL_5	0.63	11.24	0.39	133.07
REV_13G1	0.63	12.05	0.34	-15.94
COLSTP_2	0.62	10.06	0.22	142.83
HAYNES1G	0.64	11.75	0.14	-52.82
SLHWKG1	0.62	9.14	0.10	8.80
NAVAJO_1	0.62	8.15	0.09	-8.05
SUND#5GN	0.61	8.61	0.02	-87.67
SJUAN_G1	0.73	16.02	1.00	0.00
RAWHIDE	0.71	10.66	0.37	137.49
CURRNTC1	0.72	11.74	0.33	-35.21
COLSTP_2	0.70	9.89	0.30	19.16
DIABLO_1	0.70	9.40	0.27	-152.61
BRWNL_5	0.71	10.12	0.24	-6.77
JDA_0304	0.72	11.61	0.19	5.62
MBPP-1	0.73	10.47	0.18	141.10
CGS	0.72	9.10	0.14	-35.13
HYATT_1	0.71	8.42	0.12	-164.45
REV_13G1	0.73	8.83	0.12	-120.32
EHUNTER1	0.71	7.78	0.11	44.00
SUND#5GN	0.26	18.04	1.00	0.00
SHEER_1	0.26	20.04	0.66	17.55
VALMY_G2	0.26	16.52	0.27	175.18
SJUAN_G1	0.27	17.86	0.25	-178.66
KMO_13G1	0.27	19.56	0.24	-2.61
SLHWKG1	0.27	18.59	0.22	-164.85
DIABLO_1	0.27	17.33	0.21	179.76
HAYNES1G	0.27	17.41	0.21	-176.43
NAVAJO_1	0.27	17.15	0.21	-178.38

Table 60: 2022 light spring, double Palo Verde trip

Gen ID	**Freq**	**Damping**	**Residue**	**Angle**
REV_13G1	0.26	19.53	0.20	12.55
RAWHIDE	0.27	17.23	0.19	171.73
CRAIG_1	0.27	17.52	0.18	174.92
MBPP-1	0.27	17.30	0.16	178.64
HYATT_1	0.27	18.99	0.16	-177.04
EHUNTER1	0.27	17.42	0.15	175.89
SHEER_1	0.28	15.85	0.12	-71.52
SUND#5GN	0.27	12.93	0.12	116.79
BRIDGER1	0.27	17.89	0.12	-176.35
JDA_0304	0.27	19.32	0.08	162.74
CURRNTC1	0.26	15.33	0.08	-138.30
BRWNL_5	0.29	20.57	0.07	153.63
BRWNL_5	0.27	10.82	0.01	170.94
EHUNTER1	0.80	11.74	1.00	0.00
NAVAJO_1	0.80	15.49	0.70	50.34
CURRNTC1	0.81	8.97	0.46	-47.58
KMO_13G1	0.84	6.60	0.35	119.84
CGS	0.82	6.23	0.19	113.20
COLSTP_2	0.82	4.90	0.19	133.82
COULEE22	0.82	4.97	0.13	133.08
JDA_0304	0.83	5.44	0.09	118.12
DIABLO_1	0.83	4.82	0.06	-78.46
HYATT_1	0.91	4.98	1.00	0.00
COLSTP_2	0.92	3.66	0.72	135.07
HAYNES1G	0.94	6.57	0.68	105.33
KMO_13G1	0.38	17.62	1.00	0.00
COULEE22	0.39	9.97	0.07	-76.68
SHEER_1	0.40	8.90	0.06	110.47
SUND#5GN	0.40	4.01	0.02	42.12

Table 61: 2022 light spring (Note 1), 1.4 GW at Chief Joseph brake, 0.5 sec

Gen ID	Freq	Damping	Residue	Angle
COULEE22	0.84	12.61	1.00	0.00
JDA_0304	0.83	15.61	0.97	-9.73
CGS	0.84	13.99	0.90	-28.99
CURRNTC1	0.84	11.14	0.41	145.46
SUND#5GN	0.85	13.30	0.11	77.45
HAYNES1G	0.87	5.53	0.05	38.18
PALOVRD2	0.84	7.23	0.03	21.51
CRAIG_1	0.85	7.45	0.02	175.10
SJUAN_G1	0.85	3.02	0.01	-105.58
KMO_13G1	0.70	9.06	1.00	0.00
DIABLO_1	0.70	13.47	0.88	15.62
SJUAN_G1	0.69	11.64	0.61	-147.08
CRAIG_1	0.69	19.54	0.21	44.01
RAWHIDE	0.71	9.00	0.20	-53.89
HYATT_1	0.69	10.01	0.20	68.86
MBPP-1	0.70	7.24	0.06	-5.65
EHUNTER1	0.71	2.44	0.01	-172.85
PALOVRD2	0.65	12.68	1.00	0.00
NAVAJO_1	0.65	12.15	0.59	9.90
SLHWKG1	0.63	13.63	0.52	56.17
HYATT_1	0.64	8.49	0.44	-152.98
REV_13G1	0.64	8.31	0.42	25.26
JDA_0304	0.64	7.61	0.28	179.82
SUND#5GN	0.64	11.70	0.23	-160.22
BRWNL_5	0.56	18.77	1.00	0.00
BRIDGER1	0.56	10.76	0.16	-23.30
CURRNTC1	0.56	7.59	0.05	-23.61
CRAIG_1	0.55	4.70	0.04	-96.05
SLHWKG1	0.22	28.74	1.00	0.00
CRAIG_1	0.22	29.04	1.00	-20.82
EHUNTER1	0.22	29.92	0.94	-16.86
CURRNTC1	0.21	25.81	0.63	8.55
KMO_13G1	0.45	11.30	1.00	0.00
REV_13G1	0.44	11.75	0.64	14.33
COULEE22	0.44	12.50	0.59	14.48
SUND#5GN	0.44	11.95	0.54	-158.57
CGS	0.45	12.30	0.51	3.05
COLSTP_2	0.44	13.88	0.46	25.40
SJUAN_G1	0.44	12.41	0.39	-157.22
PALOVRD2	0.44	12.11	0.35	-161.81
JDA_0304	0.45	11.75	0.32	13.27
RAWHIDE	0.46	12.17	0.32	-166.45
NAVAJO_1	0.44	11.89	0.29	-165.24
BRWNL_5	0.44	12.28	0.27	12.65
MBPP-1	0.47	11.67	0.27	-175.43
SLHWKG1	0.44	11.51	0.25	-150.77
CRAIG_1	0.46	11.78	0.24	-160.49
SHEER_1	0.44	13.87	0.22	-155.01

Table 61: 2022 light spring (Note 1), 1.4 GW at Chief Joseph brake, 0.5 sec

Gen ID	Freq	Damping	Residue	Angle
HAYNES1G	0.44	11.16	0.22	-156.87
DIABLO_1	0.43	10.56	0.12	-156.96
HYATT_1	0.45	11.84	0.11	0.18
VALMY_G2	0.43	11.14	0.10	91.34
EHUNTER1	0.47	13.48	0.08	-164.72
BRIDGER1	0.44	9.09	0.07	-17.35
CURRNTC1	0.46	8.74	0.04	-130.07
REV_13G1	0.92	14.15	1.00	0.00
DIABLO_1	0.89	7.28	0.23	10.29
HYATT_1	0.93	2.62	0.02	-82.42
MBPP-1	0.93	3.88	0.02	158.41
SLHWKG1	0.93	3.04	0.01	-140.17
REV_13G1	0.79	20.13	1.00	0.00
BRWNL_5	0.81	18.08	0.64	44.99
EHUNTER1	0.82	12.37	0.60	-58.67
COLSTP_2	0.81	14.45	0.54	108.03
KMO_13G1	0.82	11.10	0.31	164.86
BRIDGER1	0.77	9.98	0.24	36.45
SHEER_1	0.80	10.14	0.15	-41.33
RAWHIDE	0.81	13.30	0.08	99.79
SLHWKG1	0.80	8.06	0.03	-56.05
BRIDGER1	0.81	6.07	0.02	79.57
NAVAJO_1	0.82	5.00	0.01	-165.94
EHUNTER1	0.74	15.08	1.00	0.00
CURRNTC1	0.75	11.28	0.69	-58.69
VALMY_G2	0.76	12.26	0.32	-23.83
HAYNES1G	0.74	13.35	0.23	-143.78
SHEER_1	0.72	7.29	0.07	-42.34
COLSTP_2	0.73	2.74	0.02	31.24
KMO_13G1	0.61	14.08	1.00	0.00
SJUAN_G1	0.58	13.90	0.12	62.88
DIABLO_1	0.61	9.43	0.04	-164.03
VALMY_G2	0.59	10.65	0.02	-157.49
COLSTP_2	0.49	16.93	1.00	0.00
MBPP-1	0.50	26.35	0.80	128.07
RAWHIDE	0.53	8.98	0.21	-175.28
HAYNES1G	0.51	19.52	0.16	104.39

Table 62: 2022 light spring (Note 1), 1.4 GW at El Dorado bus, 0.5 sec

Gen ID	Freq	Damping	Residue	Angle
KMO_13G1	0.62	12.52	1.00	0.00
REV_13G1	0.64	14.56	0.35	10.47
JDA_0304	0.63	13.77	0.26	171.10
BRWNL_5	0.64	12.52	0.25	143.12
CGS	0.63	12.61	0.23	154.25

Table 62: 2022 light spring (Note 1), 1.4 GW at El Dorado bus, 0.5 sec

Gen ID	**Freq**	**Damping**	**Residue**	**Angle**
COULEE22	0.65	12.54	0.19	153.29
SJUAN_G1	0.63	12.32	0.18	3.49
COLSTP_2	0.65	11.43	0.16	126.73
COLSTP_2	0.54	26.18	1.00	0.00
CURRNTC1	0.55	12.04	0.83	24.45
REV_13G1	0.53	-0.06	0.01	-57.98
SLHWKG1	0.89	19.36	1.00	0.00
NAVAJO_1	0.90	20.02	0.33	-3.10
SJUAN_G1	0.89	10.19	0.25	121.50
HAYNES1G	0.91	17.15	0.22	149.62
VALMY_G2	0.91	10.25	0.12	-59.22
DIABLO_1	0.92	4.34	0.04	-47.21
CRAIG_1	0.88	9.75	0.01	163.26
SUND#5GN	0.89	4.03	0.00	-102.82
SHEER_1	0.90	-23.48	0.00	-103.59
KMO_13G1	0.70	13.74	1.00	0.00
EHUNTER1	0.68	14.88	0.64	-110.15
SHEER_1	0.67	16.27	0.27	-163.81
CURRNTC1	0.69	11.07	0.22	-126.58
BRIDGER1	0.68	10.42	0.16	-88.00
KMO_13G1	0.44	11.64	1.00	0.00
REV_13G1	0.44	12.13	0.63	13.67
DIABLO_1	0.44	17.46	0.63	-107.14
COLSTP_2	0.44	15.12	0.57	7.38
BRIDGER1	0.45	19.56	0.53	28.15
SUND#5GN	0.44	11.50	0.50	-173.72
PALOVRD2	0.45	14.09	0.50	-167.34
BRWNL_5	0.45	15.09	0.50	-7.03
HAYNES1G	0.45	14.83	0.49	-160.24
COULEE22	0.44	11.96	0.48	8.08
CGS	0.44	12.11	0.44	0.08
SLHWKG1	0.45	14.74	0.43	-148.64
NAVAJO_1	0.44	13.86	0.41	-164.11
SJUAN_G1	0.45	10.78	0.31	168.15
VALMY_G2	0.45	15.87	0.26	90.63
JDA_0304	0.44	9.84	0.19	2.69
SHEER_1	0.45	11.64	0.16	171.86
HYATT_1	0.45	7.92	0.09	-60.34
CRAIG_1	0.44	15.02	0.03	-65.52
SUND#5GN	0.27	20.97	1.00	0.00
SHEER_1	0.26	20.67	0.72	1.42
VALMY_G2	0.27	17.07	0.23	158.89
REV_13G1	0.25	22.13	0.23	31.11
KMO_13G1	0.25	20.41	0.21	29.84
PALOVRD2	0.28	18.09	0.19	167.47
SJUAN_G1	0.27	17.36	0.19	172.66
RAWHIDE	0.28	19.02	0.18	157.22
HAYNES1G	0.28	17.05	0.16	166.38
CRAIG_1	0.28	17.90	0.15	154.48

Table 62: 2022 light spring (Note 1), 1.4 GW at El Dorado bus, 0.5 sec

Gen ID	**Freq**	**Damping**	**Residue**	**Angle**
DIABLO_1	0.27	15.73	0.13	176.73
MBPP-1	0.27	17.47	0.12	174.46
EHUNTER1	0.28	17.87	0.11	162.52
HYATT_1	0.29	18.20	0.10	145.01
CURRNTC1	0.29	17.48	0.09	143.50
COLSTP_2	0.25	26.19	0.08	20.77
BRIDGER1	0.28	16.24	0.06	164.00
JDA_0304	0.30	20.24	0.05	144.83
BRWNL_5	0.29	1.67	0.00	142.35
PALOVRD2	0.97	13.29	1.00	0.00
BRWNL_5	0.98	10.58	0.24	-170.83
HYATT_1	0.95	5.03	0.24	-94.24
COULEE22	0.95	6.90	0.19	84.32
COLSTP_2	0.96	5.09	0.16	30.20
SUND#5GN	0.94	27.47	0.13	45.70
SHEER_1	0.95	4.61	0.04	-49.00
JDA_0304	0.95	3.72	0.03	-167.83
RAWHIDE	0.94	4.20	0.02	-110.72
MBPP-1	0.96	0.43	0.01	-98.75
RAWHIDE	0.76	11.81	1.00	0.00
MBPP-1	0.78	8.91	0.47	-23.44
DIABLO_1	0.76	4.83	0.18	-14.02
EHUNTER1	0.61	29.31	1.00	0.00
HYATT_1	0.59	15.05	0.39	-16.53
SUND#5GN	0.61	16.62	0.11	-21.97
BRIDGER1	0.57	8.34	0.06	46.38
DIABLO_1	0.51	24.88	1.00	0.00
RAWHIDE	0.49	10.31	0.62	-114.17
CURRNTC1	0.49	20.26	0.50	-49.17
MBPP-1	0.49	10.61	0.48	-98.49
CRAIG_1	0.49	9.98	0.37	-85.52
EHUNTER1	0.50	11.25	0.14	-109.45
HAYNES1G	0.82	11.71	1.00	0.00
HYATT_1	0.85	6.22	0.26	111.59
COLSTP_2	0.86	6.60	0.25	-102.90
SHEER_1	0.84	12.31	0.22	115.23
COULEE22	0.86	5.71	0.20	-74.36
BRIDGER1	0.87	11.34	0.17	-138.31
CURRNTC1	0.86	9.30	0.11	149.63
SJUAN_G1	0.83	3.34	0.10	77.11
CGS	0.86	3.36	0.05	-104.19
BRWNL_5	0.86	5.05	0.03	-106.62
JDA_0304	0.86	3.63	0.03	-25.21
KMO_13G1	0.84	3.75	0.03	41.12
REV_13G1	0.86	3.45	0.02	126.40
EHUNTER1	0.87	1.75	0.01	-177.81

Table 63: 2022 light spring (Note 1), 1.4 GW at Hemingway Bus, 0.5 sec

Gen ID	Freq	Damping	Residue	Angle
KMO_13G1	0.44	11.92	1.00	0.00
DIABLO_1	0.45	19.84	0.71	-152.74
HAYNES1G	0.45	17.93	0.70	-154.50
REV_13G1	0.44	11.82	0.57	13.49
SJUAN_G1	0.43	14.36	0.52	-156.59
PALOVRD2	0.44	14.66	0.50	-155.16
SUND#5GN	0.44	11.85	0.47	-155.95
NAVAJO_1	0.44	14.85	0.44	-153.48
SLHWKG1	0.43	15.02	0.41	-132.94
COULEE22	0.44	11.32	0.41	10.49
CGS	0.44	10.92	0.33	9.34
COLSTP_2	0.44	12.33	0.32	8.95
JDA_0304	0.43	9.48	0.17	25.79
SHEER_1	0.42	11.40	0.11	-121.20
BRIDGER1	0.57	19.44	1.00	0.00
HAYNES1G	0.56	28.50	0.61	-161.29
SHEER_1	0.58	10.21	0.05	164.91
BRWNL_5	0.92	22.44	1.00	0.00
MBPP-1	0.91	15.99	0.19	-172.27
RAWHIDE	0.93	7.35	0.01	164.38
SUND#5GN	0.91	-1.64	0.00	-81.08
COULEE22	0.76	14.81	1.00	0.00
REV_13G1	0.75	12.63	0.57	-155.39
CGS	0.77	13.80	0.57	-52.64
COLSTP_2	0.74	10.92	0.43	-7.13
KMO_13G1	0.74	7.65	0.31	98.01
DIABLO_1	0.77	12.47	0.28	98.60
JDA_0304	0.74	11.32	0.22	53.28
EHUNTER1	0.73	7.67	0.17	-10.95
PALOVRD2	0.73	11.64	0.16	11.27
SHEER_1	0.76	8.89	0.12	-169.63
HAYNES1G	0.74	9.42	0.09	-164.25
CRAIG_1	0.75	9.97	0.05	167.58
SLHWKG1	0.74	10.17	0.02	-20.36
KMO_13G1	0.61	12.00	1.00	0.00
SJUAN_G1	0.60	17.01	0.44	50.37
PALOVRD2	0.62	12.50	0.23	6.75
REV_13G1	0.63	10.32	0.20	-12.05
HYATT_1	0.61	10.51	0.18	-167.01
JDA_0304	0.61	10.12	0.14	175.31
NAVAJO_1	0.61	12.56	0.14	23.51
CGS	0.60	11.71	0.13	-135.14
SUND#5GN	0.65	13.35	0.12	137.02
SLHWKG1	0.62	10.00	0.07	15.07
COULEE22	0.63	7.06	0.05	131.15
COLSTP_2	0.60	8.14	0.05	-167.48
EHUNTER1	0.84	25.48	1.00	0.00
JDA_0304	0.84	16.39	0.23	-141.79

Table 63: 2022 light spring (Note 1), 1.4 GW at Hemingway Bus, 0.5 sec

Gen ID	**Freq**	**Damping**	**Residue**	**Angle**
KMO_13G1	0.81	11.18	0.21	0.33
BRIDGER1	0.46	29.08	1.00	0.00
RAWHIDE	0.49	9.06	0.18	-29.79
MBPP-1	0.49	9.10	0.13	-42.46
CRAIG_1	0.48	7.36	0.07	17.87
HYATT_1	0.47	7.07	0.03	-117.96
SJUAN_G1	0.98	10.26	1.00	0.00
HYATT_1	0.95	5.26	0.62	12.58
DIABLO_1	0.95	4.12	0.33	15.64
NAVAJO_1	0.96	13.03	0.26	-128.03
PALOVRD2	0.99	2.08	0.02	131.88
CURRNTC1	0.68	16.73	1.00	0.00
DIABLO_1	0.67	12.41	0.60	-101.67
SJUAN_G1	0.70	11.40	0.49	16.12
MBPP-1	0.68	20.92	0.33	164.43
SUND#5GN	0.72	15.72	0.22	58.30
HYATT_1	0.70	9.45	0.21	-154.23
RAWHIDE	0.71	9.42	0.21	120.33
NAVAJO_1	0.71	10.39	0.10	-9.91
BRIDGER1	0.72	6.50	0.09	-13.25
MBPP-1	0.69	9.31	0.09	-133.07
CGS	0.68	5.71	0.03	119.71
SUND#5GN	0.26	20.76	1.00	0.00
SHEER_1	0.25	20.62	0.72	5.42
KMO_13G1	0.24	20.75	0.23	42.76
REV_13G1	0.25	20.72	0.23	24.18
SJUAN_G1	0.29	9.94	0.09	115.11
CRAIG_1	0.28	13.88	0.09	131.15
PALOVRD2	0.28	11.29	0.09	147.47
SLHWKG1	0.29	11.69	0.08	118.11
NAVAJO_1	0.28	10.29	0.08	147.96
RAWHIDE	0.28	10.82	0.07	126.79
MBPP-1	0.28	11.07	0.06	131.70
DIABLO_1	0.28	7.59	0.05	155.41
HAYNES1G	0.28	5.46	0.04	151.68

Table 64: 2022 light spring (Note 1), 1.4 GW at Midway bus, 0.5 sec

Gen ID	**Freq**	**Damping**	**Residue**	**Angle**
PALOVRD2	0.45	17.24	1.00	0.00
COLSTP_2	0.44	18.09	0.97	168.02
KMO_13G1	0.43	11.68	0.96	156.88
NAVAJO_1	0.45	17.02	0.86	-0.53
BRWNL_5	0.44	17.71	0.79	166.43
REV_13G1	0.43	11.30	0.54	165.69
SUND#5GN	0.44	11.58	0.50	-25.26
CGS	0.44	12.88	0.47	156.42

Table 64: 2022 light spring (Note 1), 1.4 GW at Midway bus, 0.5 sec

Gen ID	**Freq**	**Damping**	**Residue**	**Angle**
COULEE22	0.43	11.30	0.39	169.08
SJUAN_G1	0.45	9.77	0.27	-50.98
SHEER_1	0.45	11.00	0.14	-35.89
JDA_0304	0.45	5.18	0.08	84.66
COLSTP_2	0.96	12.94	1.00	0.00
JDA_0304	0.95	8.40	0.15	-56.15
BRWNL_5	0.96	9.01	0.08	-95.49
VALMY_G2	0.97	3.99	0.04	-81.99
CRAIG_1	0.96	6.76	0.03	90.90
SHEER_1	0.97	4.45	0.01	6.77
EHUNTER1	0.96	3.52	0.01	-152.66
BRIDGER1	0.96	3.23	0.01	-154.36
KMO_13G1	0.66	12.82	1.00	0.00
JDA_0304	0.66	17.60	0.67	-114.92
SJUAN_G1	0.66	16.72	0.37	105.52
REV_13G1	0.64	17.31	0.25	130.64
CRAIG_1	0.67	13.53	0.08	-34.86
SJUAN_G1	0.67	4.80	0.02	-123.72
SHEER_1	0.79	13.92	1.00	0.00
BRWNL_5	0.76	12.14	0.83	160.00
RAWHIDE	0.78	17.39	0.64	171.57
EHUNTER1	0.80	9.04	0.59	62.59
CURRNTC1	0.79	8.41	0.54	66.31
BRIDGER1	0.77	8.86	0.46	146.29
KMO_13G1	0.60	24.89	1.00	0.00
COULEE22	0.61	13.13	0.15	113.94
CGS	0.58	12.62	0.08	143.47
MBPP-1	0.57	15.48	0.02	-28.92
RAWHIDE	0.49	10.21	1.00	0.00
MBPP-1	0.48	11.22	0.91	32.01
RAWHIDE	0.47	26.01	0.70	103.20
CRAIG_1	0.49	10.33	0.66	29.00
SLHWKG1	0.47	17.36	0.52	-122.35
HAYNES1G	0.48	13.64	0.40	-135.51
DIABLO_1	0.48	12.11	0.40	-147.47
BRIDGER1	0.49	14.14	0.39	30.96
CURRNTC1	0.48	11.92	0.24	41.67
EHUNTER1	0.48	11.74	0.23	45.84
VALMY_G2	0.48	12.96	0.17	95.92
HYATT_1	0.47	8.83	0.11	-69.33
DIABLO_1	0.91	7.95	1.00	0.00
COLSTP_2	0.94	6.43	0.64	49.57
PALOVRD2	0.94	13.24	0.51	164.00
HYATT_1	0.93	4.89	0.30	-66.19
SLHWKG1	0.92	4.30	0.07	-109.95
SJUAN_G1	0.90	3.67	0.04	90.25
COULEE22	0.88	8.66	1.00	0.00

Table 64: 2022 light spring (Note 1), 1.4 GW at Midway bus, 0.5 sec

Gen ID	**Freq**	**Damping**	**Residue**	**Angle**
CGS	0.87	9.36	0.63	-2.65
KMO_13G1	0.87	8.92	0.25	59.76
REV_13G1	0.87	8.47	0.19	-147.78
SUND#5GN	0.86	6.35	0.04	135.16
JDA_0304	0.71	24.00	1.00	0.00
KMO_13G1	0.73	12.57	0.58	99.63
COULEE22	0.71	14.06	0.32	69.40
COLSTP_2	0.69	12.83	0.31	76.65
HYATT_1	0.73	15.14	0.25	179.43
REV_13G1	0.72	13.23	0.24	-111.79
CGS	0.70	12.56	0.23	65.68
DIABLO_1	0.72	11.77	0.20	165.11
EHUNTER1	0.70	10.09	0.20	35.49
RAWHIDE	0.70	11.93	0.19	177.29
CURRNTC1	0.69	9.77	0.16	30.59
BRWNL_5	0.68	10.90	0.15	96.32
SLHWKG1	0.74	16.22	0.11	-57.13
SHEER_1	0.70	13.15	0.11	-22.87
BRIDGER1	0.68	9.54	0.10	73.09
HAYNES1G	0.69	11.90	0.08	-87.35
MBPP-1	0.70	10.91	0.07	-151.67
VALMY_G2	0.69	10.04	0.07	73.46
SUND#5GN	0.68	14.28	0.04	171.83
NAVAJO_1	0.73	9.86	0.03	-10.33
PALOVRD2	0.72	6.55	0.01	12.33
SUND#5GN	0.26	20.59	1.00	0.00
SHEER_1	0.26	20.55	0.74	-2.16
KMO_13G1	0.25	20.64	0.23	28.57
SLHWKG1	0.28	19.87	0.21	168.92
REV_13G1	0.25	20.33	0.20	27.00
SJUAN_G1	0.28	17.70	0.20	164.89
PALOVRD2	0.28	18.34	0.20	165.85
NAVAJO_1	0.27	18.17	0.19	166.91
HAYNES1G	0.28	16.98	0.17	149.86
MBPP-1	0.28	19.55	0.17	145.42
VALMY_G2	0.28	13.98	0.16	130.61
RAWHIDE	0.28	17.06	0.15	139.37
CRAIG_1	0.28	17.70	0.15	150.69
EHUNTER1	0.28	19.24	0.14	149.94
CURRNTC1	0.29	19.04	0.10	142.58
BRIDGER1	0.28	18.56	0.08	166.43
COLSTP_2	0.25	21.12	0.05	11.71
JDA_0304	0.27	22.69	0.04	-146.19
BRWNL_5	0.31	7.43	0.01	96.65

Table 65: 2022 light spring (Note 1), double Palo Verde trip

Gen ID	**Freq**	**Damping**	**Residue**	**Angle**
JDA_0304	0.41	21.26	1.00	0.00

Table 65: 2022 light spring (Note 1), double Palo Verde trip

Gen ID	Freq	Damping	Residue	Angle
BRIDGER1	0.39	27.41	0.99	15.26
COULEE22	0.40	12.58	0.41	29.32
SUND#5GN	0.26	19.25	1.00	0.00
SHEER_1	0.26	20.38	0.80	-0.55
VALMY_G2	0.24	19.58	0.33	-160.51
SJUAN_G1	0.25	19.25	0.25	-143.32
EHUNTER1	0.24	24.19	0.22	-142.11
HYATT_1	0.23	23.89	0.15	-112.33
COULEE22	0.24	25.92	0.12	32.23
HAYNES1G	0.26	14.13	0.12	-168.44
SLHWKG1	0.26	14.52	0.11	175.58
NAVAJO_1	0.25	11.83	0.07	-126.23
CURRNTC1	0.25	14.22	0.06	-155.14
DIABLO_1	0.25	6.76	0.02	-125.22
CRAIG_1	0.25	1.19	0.00	-151.79
MBPP-1	0.25	0.48	0.00	-172.31
RAWHIDE	0.25	-0.19	0.00	175.47
BRWNL_5	0.24	-1.90	0.00	-105.25
CGS	0.20	26.50	1.00	0.00
COULEE22	0.19	16.56	0.14	45.86
KMO_13G1	0.17	5.56	0.02	53.27
SJUAN_G1	0.72	13.98	1.00	0.00
SJUAN_G1	0.71	10.03	0.40	-143.18
VALMY_G2	0.71	22.90	0.38	-154.13
EHUNTER1	0.74	9.82	0.29	-85.59
CURRNTC1	0.73	7.84	0.17	-99.95
DIABLO_1	0.71	5.25	0.06	-172.49
RAWHIDE	0.71	11.58	0.05	18.53
SHEER_1	0.72	7.23	0.05	-87.03
BRIDGER1	0.75	6.83	0.05	-114.44
HAYNES1G	0.74	3.71	0.01	165.78
BRWNL_5	0.73	2.68	0.01	-41.55
HYATT_1	0.73	3.01	0.01	144.83
CURRNTC1	0.71	1.32	0.00	146.77
REV_13G1	0.44	21.38	1.00	0.00
COLSTP_2	0.45	15.39	0.31	-32.52
SUND#5GN	0.44	11.79	0.24	179.37
KMO_13G1	0.44	8.67	0.22	-19.49
HAYNES1G	0.46	13.16	0.19	-179.76
DIABLO_1	0.46	13.51	0.18	-171.24
RAWHIDE	0.47	6.42	0.15	-22.93
MBPP-1	0.48	7.11	0.14	-8.82
HYATT_1	0.44	13.21	0.12	-43.54
SLHWKG1	0.46	11.51	0.11	164.37
SJUAN_G1	0.45	8.73	0.10	151.59
CRAIG_1	0.47	6.08	0.09	6.15
NAVAJO_1	0.47	9.95	0.09	127.86
CGS	0.47	8.99	0.09	-90.82
VALMY_G2	0.46	9.67	0.07	61.93
SHEER_1	0.45	11.77	0.06	147.76

Table 65: 2022 light spring (Note 1), double Palo Verde trip

Gen ID	Freq	Damping	Residue	Angle
REV_13G1	0.46	6.47	0.05	-117.43
COULEE22	0.46	7.15	0.04	-43.25
BRWNL_5	0.46	9.21	0.04	-44.84
CURRNTC1	0.48	7.67	0.03	6.40
BRIDGER1	0.46	5.38	0.01	79.73
EHUNTER1	0.46	2.39	0.00	84.33
COULEE22	0.90	5.92	1.00	0.00
COLSTP_2	0.92	4.86	0.72	-69.90
HYATT_1	0.92	3.76	0.47	128.72
KMO_13G1	0.61	13.93	1.00	0.00
HYATT_1	0.60	20.62	0.55	-156.15
DIABLO_1	0.58	23.66	0.32	-134.76
HAYNES1G	0.62	24.84	0.17	-21.81
BRWNL_5	0.58	8.57	0.05	-159.18
SUND#5GN	0.60	11.10	0.03	-138.19
CGS	0.37	22.13	1.00	0.00
BRWNL_5	0.39	15.10	0.40	-9.47
NAVAJO_1	0.38	20.34	0.40	-134.93
SLHWKG1	0.35	18.70	0.27	-51.54
KMO_13G1	0.39	8.29	0.14	9.12
REV_13G1	0.36	11.26	0.13	157.40
CGS	0.36	9.47	0.12	174.63
BRWNL_5	0.36	10.08	0.12	-132.08
SJUAN_G1	0.37	11.81	0.09	-136.33
HAYNES1G	0.34	13.05	0.08	-32.41
VALMY_G2	0.37	7.20	0.04	135.42
COULEE22	0.34	8.59	0.04	-35.16
JDA_0304	0.37	6.38	0.03	171.55
BRIDGER1	0.36	6.32	0.03	171.81
COLSTP_2	0.37	5.50	0.02	90.65
HYATT_1	0.36	5.96	0.02	-146.32
RAWHIDE	0.38	1.94	0.01	82.76
EHUNTER1	0.36	3.44	0.01	-145.00
MBPP-1	0.38	2.12	0.01	80.55
CRAIG_1	0.37	2.41	0.01	113.91
CURRNTC1	0.38	3.35	0.01	59.88
SUND#5GN	0.39	0.40	0.00	-119.98
RAWHIDE	0.28	28.78	1.00	0.00
MBPP-1	0.29	25.89	0.59	5.74
CRAIG_1	0.29	25.36	0.51	-1.72
KMO_13G1	0.28	15.79	0.41	164.60
REV_13G1	0.27	16.51	0.38	-170.55
DIABLO_1	0.30	20.55	0.37	-16.63
CURRNTC1	0.30	13.95	0.07	31.36
COLSTP_2	0.29	11.17	0.05	123.33
SUND#5GN	0.29	-1.21	0.00	20.57
SHEER_1	0.28	-3.22	0.00	119.02
KMO_13G1	0.69	9.67	1.00	0.00
EHUNTER1	0.65	17.00	0.90	-43.65

Table 65: 2022 light spring (Note 1), double Palo Verde trip

Gen ID	**Freq**	**Damping**	**Residue**	**Angle**
REV_13G1	0.68	12.90	0.60	111.79
CGS	0.67	10.87	0.48	-102.96
JDA_0304	0.69	12.03	0.47	-104.74
COLSTP_2	0.68	10.00	0.43	-123.07
COULEE22	0.68	10.03	0.40	-86.78
VALMY_G2	0.69	11.51	0.39	-121.86
CURRNTC1	0.64	12.42	0.39	-49.72
BRIDGER1	0.67	8.70	0.20	-95.94
RAWHIDE	0.68	8.71	0.15	-1.83
MBPP-1	0.70	11.39	0.14	-17.36
BRWNL_5	0.66	6.10	0.11	-77.57
NAVAJO_1	0.64	8.66	0.11	-170.05
SLHWKG1	0.67	5.10	0.10	137.17
SHEER_1	0.66	8.00	0.08	117.15
CRAIG_1	0.68	10.04	0.07	58.45
KMO_13G1	0.68	-0.53	0.00	-71.77
COLSTP_2	0.52	28.82	1.00	0.00
JDA_0304	0.54	14.42	0.46	54.02
EHUNTER1	0.51	10.55	0.16	-153.39
REV_13G1	0.53	9.65	0.15	8.76
BRIDGER1	0.54	9.90	0.12	88.16
CGS	0.52	6.73	0.05	177.54
JDA_0304	0.50	4.21	0.04	2.68
CRAIG_1	0.50	2.54	0.03	-57.27
RAWHIDE	0.50	1.66	0.02	-80.91
MBPP-1	0.50	0.26	0.01	-11.15
VALMY_G2	0.83	8.04	1.00	0.00
SHEER_1	0.85	9.43	0.92	-85.85
COLSTP_2	0.82	3.11	0.21	-137.81

Table 66: 2022 light spring (Note 2), 1.4 GW at Chief Joseph brake, 0.5 sec

Gen ID	**Freq**	**Damping**	**Residue**	**Angle**
CURRNTC1	0.74	12.06	1.00	0.00
EHUNTER1	0.74	10.63	0.73	13.02
HAYNES1G	0.75	13.35	0.34	-109.44
RAWHIDE	0.73	7.34	0.11	178.20
COLSTP_2	0.74	6.58	0.10	39.76
NAVAJO_1	0.29	18.18	1.00	0.00
BRWNL_5	0.30	25.73	0.73	20.24
PALOVRD2	0.29	14.33	0.63	-2.03
BRIDGER1	0.29	13.31	0.30	8.30
DIABLO_1	0.70	18.47	1.00	0.00
BRWNL_5	0.69	17.17	0.83	-135.19
MBPP-1	0.71	7.81	0.06	0.10
COULEE22	0.85	14.19	1.00	0.00
BRWNL_5	0.83	22.12	0.68	-75.68
JDA_0304	0.84	16.32	0.67	-1.25
CGS	0.84	14.10	0.54	-14.20
REV_13G1	0.82	16.15	0.53	-141.84
KMO_13G1	0.82	13.21	0.42	66.53
COLSTP_2	0.81	12.68	0.33	22.16
CURRNTC1	0.84	11.76	0.30	165.89
EHUNTER1	0.84	10.32	0.23	-155.19
SLHWKG1	0.85	9.89	0.06	144.31
SUND#5GN	0.82	13.55	0.05	129.78
PALOVRD2	0.84	9.02	0.03	35.80
NAVAJO_1	0.85	8.98	0.02	63.08
SJUAN_G1	0.84	5.75	0.02	-73.22
BRIDGER1	0.81	5.02	0.01	2.22
RAWHIDE	0.84	6.54	0.01	3.92
KMO_13G1	0.44	11.58	1.00	0.00
REV_13G1	0.44	11.66	0.61	8.69
SUND#5GN	0.44	11.66	0.49	-168.46
COULEE22	0.44	11.57	0.47	7.17
CGS	0.44	11.56	0.42	-0.92
SJUAN_G1	0.45	12.48	0.40	176.93
RAWHIDE	0.46	9.72	0.30	158.29
JDA_0304	0.44	11.29	0.29	5.19
COLSTP_2	0.43	11.71	0.28	9.28
SLHWKG1	0.44	12.40	0.27	-173.53
PALOVRD2	0.44	10.93	0.25	-177.55
CRAIG_1	0.46	9.89	0.22	176.93
SLHWKG1	0.46	24.74	0.21	-46.63
NAVAJO_1	0.44	10.95	0.20	177.83
BRWNL_5	0.44	10.80	0.20	2.40
MBPP-1	0.46	8.83	0.17	178.78
HAYNES1G	0.43	11.01	0.17	-160.49
SHEER_1	0.44	11.61	0.13	-165.41
HYATT_1	0.45	10.19	0.10	-5.29
DIABLO_1	0.42	10.53	0.08	-153.08
VALMY_G2	0.42	10.77	0.07	107.04

Table 66: 2022 light spring (Note 2), 1.4 GW at Chief Joseph brake, 0.5 sec

Gen ID	Freq	Damping	Residue	Angle
EHUNTER1	0.47	13.60	0.07	174.97
BRIDGER1	0.43	8.07	0.05	3.43
CURRNTC1	0.46	8.32	0.03	-143.47
BRIDGER1	0.77	9.97	1.00	0.00
SHEER_1	0.78	10.76	0.86	-56.45
VALMY_G2	0.76	11.57	0.54	37.51
CRAIG_1	0.79	12.85	0.17	-43.97
SUND#5GN	0.27	20.93	1.00	0.00
SHEER_1	0.26	21.25	0.76	-0.19
SJUAN_G1	0.26	20.64	0.33	-150.05
SLHWKG1	0.25	22.26	0.28	-120.42
REV_13G1	0.25	23.60	0.24	20.29
RAWHIDE	0.26	18.70	0.23	-151.68
DIABLO_1	0.22	20.71	0.23	-74.70
HAYNES1G	0.24	19.88	0.22	-106.67
EHUNTER1	0.26	21.00	0.20	-154.61
MBPP-1	0.27	17.64	0.19	-170.10
KMO_13G1	0.25	21.08	0.19	19.62
CRAIG_1	0.26	16.54	0.16	-153.21
CURRNTC1	0.24	18.32	0.13	-98.17
REV_13G1	0.91	24.83	1.00	0.00
VALMY_G2	0.92	19.46	0.17	-126.06
DIABLO_1	0.90	7.14	0.11	56.88
HAYNES1G	0.88	5.01	0.04	67.10
SLHWKG1	0.90	6.09	0.03	-49.33
CRAIG_1	0.89	4.19	0.01	159.93
SJUAN_G1	0.91	-3.46	0.00	113.88
KMO_13G1	0.65	16.18	1.00	0.00
KMO_13G1	0.65	7.09	0.11	-174.03
SJUAN_G1	0.67	10.61	0.09	-112.45
DIABLO_1	0.64	11.76	0.08	139.10
HYATT_1	0.66	9.85	0.07	94.48
PALOVRD2	0.65	10.47	0.05	-68.96
NAVAJO_1	0.65	9.76	0.03	-73.21
JDA_0304	0.63	8.22	0.03	112.17
REV_13G1	0.64	6.53	0.02	-54.34
SUND#5GN	0.63	11.15	0.02	147.83
BRWNL_5	0.61	6.77	0.02	147.79
SLHWKG1	0.66	7.61	0.01	-79.54
SHEER_1	0.68	4.29	0.00	-171.87
CURRNTC1	0.62	-2.17	0.00	87.19
RAWHIDE	0.51	26.23	1.00	0.00
CRAIG_1	0.55	22.85	0.44	-17.24
COLSTP_2	0.52	13.88	0.36	-110.14
BRIDGER1	0.55	10.66	0.14	-167.39
VALMY_G2	0.55	4.65	0.02	-123.68
EHUNTER1	0.53	-1.42	0.00	7.43

Table 67: 2022 light spring (Note 2), 1.4 GW at El Dorado bus, 0.5 sec

Gen ID	Freq	Damping	Residue	Angle
SJUAN_G1	0.90	11.96	1.00	0.00
DIABLO_1	0.91	3.15	0.07	-132.18
SHEER_1	0.91	5.47	0.04	-144.69
CRAIG_1	0.88	6.42	0.01	74.05
SUND#5GN	0.89	1.01	0.00	177.75
KMO_13G1	0.62	12.42	1.00	0.00
DIABLO_1	0.60	25.49	0.52	-162.80
BRIDGER1	0.62	17.27	0.49	-169.59
CGS	0.63	13.85	0.35	167.98
REV_13G1	0.63	13.63	0.33	12.71
HYATT_1	0.61	14.02	0.26	-144.40
JDA_0304	0.63	13.27	0.26	166.89
BRWNL_5	0.64	12.21	0.25	138.42
CURRNTC1	0.63	12.73	0.18	154.08
COULEE22	0.64	11.37	0.16	154.84
SJUAN_G1	0.62	11.54	0.16	21.76
COLSTP_2	0.63	11.31	0.16	156.25
PALOVRD2	0.61	11.84	0.16	46.46
HAYNES1G	0.62	15.01	0.16	159.01
SUND#5GN	0.62	16.68	0.09	-154.81
CURRNTC1	0.79	15.73	1.00	0.00
KMO_13G1	0.79	5.11	0.13	-57.47
BRIDGER1	0.81	4.42	0.05	165.01
CURRNTC1	0.80	-0.80	0.01	152.14
SHEER_1	0.96	19.49	1.00	0.00
HYATT_1	0.96	5.37	0.64	131.68
COLSTP_2	0.96	5.95	0.54	-95.56
COULEE22	0.95	7.07	0.54	-27.96
RAWHIDE	0.97	12.46	0.41	72.86
BRWNL_5	0.95	7.90	0.32	122.36
CGS	0.95	7.23	0.24	-21.18
MBPP-1	0.94	6.68	0.14	135.08
REV_13G1	0.94	5.85	0.08	165.39
JDA_0304	0.95	1.81	0.05	87.48
KMO_13G1	0.96	2.95	0.01	86.49
SUND#5GN	0.26	19.59	1.00	0.00
SHEER_1	0.26	19.62	0.75	-1.77
RAWHIDE	0.26	22.41	0.26	171.27
VALMY_G2	0.26	18.37	0.26	175.23
SJUAN_G1	0.26	20.32	0.26	-173.48
PALOVRD2	0.26	20.65	0.26	-179.87
KMO_13G1	0.26	19.71	0.24	15.82
NAVAJO_1	0.26	20.61	0.24	-176.15
REV_13G1	0.26	20.04	0.24	13.50
DIABLO_1	0.27	20.12	0.22	173.75
CRAIG_1	0.26	22.37	0.22	-171.12
MBPP-1	0.26	21.54	0.19	-179.45
HAYNES1G	0.27	20.66	0.18	-173.32
EHUNTER1	0.26	21.71	0.17	179.53

Table 67: 2022 light spring (Note 2), 1.4 GW at El Dorado bus, 0.5 sec

Gen ID	Freq	Damping	Residue	Angle
CURRNTC1	0.27	23.14	0.15	160.77
HYATT_1	0.27	22.45	0.14	166.32
BRIDGER1	0.26	22.28	0.11	-164.98
COULEE22	0.26	23.09	0.09	21.25
COLSTP_2	0.28	15.51	0.04	-31.29
BRWNL_5	0.25	14.41	0.02	-168.18
SLHWKG1	0.84	20.79	1.00	0.00
NAVAJO_1	0.87	23.65	0.54	-22.75
HAYNES1G	0.84	10.96	0.10	-46.34
HYATT_1	0.86	6.00	0.08	60.20
COULEE22	0.86	6.14	0.07	-105.72
COLSTP_2	0.86	5.84	0.07	-149.32
CGS	0.86	7.13	0.05	-113.65
REV_13G1	0.87	7.74	0.03	81.42
SJUAN_G1	0.83	2.10	0.02	28.06
BRWNL_5	0.86	4.75	0.01	-161.71
JDA_0304	0.84	3.41	0.01	-29.74
SHEER_1	0.68	27.77	1.00	0.00
SHEER_1	0.66	23.34	0.90	176.16
CGS	0.66	20.83	0.29	108.78
EHUNTER1	0.66	13.22	0.24	-113.31
BRIDGER1	0.71	21.18	1.00	0.00
KMO_13G1	0.71	11.23	0.82	-164.23
RAWHIDE	0.74	11.86	0.15	132.76
MBPP-1	0.76	11.53	0.10	100.31
COLSTP_2	0.73	15.49	0.07	14.30
KMO_13G1	0.44	12.30	1.00	0.00
RAWHIDE	0.47	10.29	0.80	-32.85
MBPP-1	0.47	10.68	0.65	-16.95
REV_13G1	0.43	12.70	0.63	10.00
SUND#5GN	0.44	12.31	0.53	-170.99
PALOVRD2	0.44	13.84	0.53	-165.13
DIABLO_1	0.46	13.19	0.47	-168.00
CRAIG_1	0.47	10.00	0.47	-8.48
COLSTP_2	0.44	13.56	0.47	-4.51
HAYNES1G	0.45	13.90	0.47	-158.53
COULEE22	0.44	12.37	0.45	5.63
NAVAJO_1	0.44	13.69	0.44	-163.47
SLHWKG1	0.44	14.11	0.44	-145.80
CGS	0.43	12.62	0.44	4.93
BRWNL_5	0.45	13.57	0.40	-16.73
BRIDGER1	0.46	14.19	0.39	-9.98
SJUAN_G1	0.44	11.33	0.30	-176.02
VALMY_G2	0.44	11.80	0.17	89.31
CURRNTC1	0.47	11.39	0.17	-2.44
JDA_0304	0.43	10.29	0.16	14.15
SHEER_1	0.44	12.38	0.16	-177.21
EHUNTER1	0.47	9.55	0.12	-16.34
HYATT_1	0.46	7.23	0.07	-100.75

Table 68: 2022 light spring (Note 2), 1.4 GW at Hemingway Bus, 0.5 sec

Gen ID	Freq	Damping	Residue	Angle
RAWHIDE	0.48	11.08	1.00	0.00
MBPP-1	0.48	11.25	0.81	7.12
CRAIG_1	0.49	9.94	0.47	20.74
REV_13G1	0.65	25.42	1.00	0.00
SJUAN_G1	0.63	13.05	0.46	-99.55
SLHWKG1	0.66	27.50	0.36	16.32
DIABLO_1	0.65	9.48	0.20	4.37
SHEER_1	0.65	16.57	0.17	-56.99
SLHWKG1	0.64	10.98	0.13	-111.72
REV_13G1	0.64	7.69	0.12	-142.85
SUND#5GN	0.63	12.11	0.08	92.28
HYATT_1	0.70	9.44	1.00	0.00
NAVAJO_1	0.68	11.23	0.92	-167.55
MBPP-1	0.70	10.96	0.70	-19.74
SHEER_1	0.71	6.08	0.21	54.23
KMO_13G1	0.68	0.34	0.06	56.70
CURRNTC1	0.81	22.60	1.00	0.00
COULEE22	0.83	22.66	0.64	-104.31
CRAIG_1	0.82	16.29	0.16	68.40
JDA_0304	0.83	10.51	0.10	-96.51
SHEER_1	0.80	7.81	0.04	121.42
DIABLO_1	0.84	-7.31	0.00	44.34
KMO_13G1	0.44	11.73	1.00	0.00
REV_13G1	0.44	11.75	0.59	14.87
SUND#5GN	0.44	11.96	0.51	-166.06
NAVAJO_1	0.45	14.36	0.46	-176.55
PALOVRD2	0.44	13.36	0.45	-168.06
HAYNES1G	0.44	14.01	0.42	-161.95
COULEE22	0.44	11.09	0.40	16.76
DIABLO_1	0.45	14.83	0.39	-161.00
SJUAN_G1	0.44	12.57	0.38	-179.21
SLHWKG1	0.44	13.62	0.38	-158.27
CGS	0.45	10.56	0.35	-15.40
JDA_0304	0.43	11.96	0.26	28.53
COLSTP_2	0.44	9.95	0.24	-3.26
SHEER_1	0.44	11.90	0.14	-167.88
KMO_13G1	0.61	13.60	1.00	0.00
BRWNL_5	0.57	21.91	0.42	-94.06
BRIDGER1	0.59	17.30	0.26	-115.41
NAVAJO_1	0.60	18.44	0.22	43.91
PALOVRD2	0.62	12.70	0.18	-1.63
HYATT_1	0.61	11.17	0.15	-166.39
JDA_0304	0.59	11.70	0.12	-155.08
HAYNES1G	0.60	20.93	0.10	76.82
COULEE22	0.60	8.14	0.04	-157.01
COLSTP_2	0.59	5.78	0.02	-135.02

Table 68: 2022 light spring (Note 2), 1.4 GW at Hemingway Bus, 0.5 sec

Gen ID	Freq	Damping	Residue	Angle
EHUNTER1	0.76	24.45	1.00	0.00
KMO_13G1	0.76	11.21	0.45	-2.90
CGS	0.76	14.42	0.37	-89.27
REV_13G1	0.76	14.10	0.32	108.57
COULEE22	0.74	12.61	0.27	-22.64
COLSTP_2	0.75	11.01	0.23	-67.52
SJUAN_G1	0.73	11.27	0.14	-62.36
EHUNTER1	0.73	8.11	0.11	-76.86
CURRNTC1	0.72	8.18	0.11	-68.64
PALOVRD2	0.72	12.04	0.09	-38.05
RAWHIDE	0.72	9.64	0.09	115.98
SUND#5GN	0.74	14.99	0.05	38.27
HAYNES1G	0.73	9.11	0.05	159.90
DIABLO_1	0.75	6.29	0.04	113.91
MBPP-1	0.94	10.84	1.00	0.00
EHUNTER1	0.94	2.50	0.20	-154.78
SJUAN_G1	0.91	3.17	0.08	-88.19
SUND#5GN	0.91	1.53	0.01	139.59
SUND#5GN	0.26	18.33	1.00	0.00
SHEER_1	0.26	18.14	0.74	-4.13
SJUAN_G1	0.27	22.03	0.32	161.60
EHUNTER1	0.27	27.03	0.31	160.09
CRAIG_1	0.25	25.08	0.27	176.40
KMO_13G1	0.26	18.28	0.26	9.81
PALOVRD2	0.27	20.74	0.26	158.73
SLHWKG1	0.28	22.39	0.26	148.31
DIABLO_1	0.29	20.44	0.25	123.49
RAWHIDE	0.26	22.76	0.25	164.83
MBPP-1	0.28	24.09	0.24	117.55
REV_13G1	0.26	17.18	0.23	-3.58
HAYNES1G	0.27	19.38	0.21	147.13
NAVAJO_1	0.25	17.34	0.17	-168.61
COULEE22	0.27	22.65	0.14	2.90

Table 69: 2022 light spring (Note 2), 1.4 GW at Midway bus, 0.5 sec

Gen ID	Freq	Damping	Residue	Angle
KMO_13G1	0.42	13.13	1.00	0.00
BRWNL_5	0.44	15.49	0.66	-14.57
SUND#5GN	0.43	13.63	0.63	176.52
REV_13G1	0.42	13.26	0.62	6.29
CGS	0.42	14.56	0.51	21.92
COULEE22	0.42	13.02	0.41	16.07
SJUAN_G1	0.42	11.23	0.29	-178.18
SHEER_1	0.43	11.44	0.14	170.87
KMO_13G1	0.71	11.59	1.00	0.00
COULEE22	0.70	14.61	0.70	-85.34

Table 69: 2022 light spring (Note 2), 1.4 GW at Midway bus, 0.5 sec

Gen ID	Freq	Damping	Residue	Angle
COLSTP_2	0.72	14.34	0.65	-150.65
HYATT_1	0.72	16.18	0.59	15.64
DIABLO_1	0.71	11.01	0.32	15.58
RAWHIDE	0.69	11.62	0.30	19.50
CURRNTC1	0.69	9.03	0.29	-133.37
MBPP-1	0.69	13.57	0.28	48.50
MBPP-1	0.69	23.01	0.28	-123.77
EHUNTER1	0.68	9.21	0.26	-102.59
BRIDGER1	0.68	9.82	0.22	-84.19
SHEER_1	0.72	12.01	0.21	114.93
BRWNL_5	0.71	8.91	0.20	-124.85
CGS	0.75	10.17	0.16	-174.28
VALMY_G2	0.69	9.17	0.12	-91.37
HAYNES1G	0.70	4.74	0.04	104.14
SLHWKG1	0.72	7.17	0.02	-163.82
PALOVRD2	0.74	5.64	0.01	156.82
DIABLO_1	0.91	8.65	1.00	0.00
COLSTP_2	0.91	7.36	0.55	139.51
HYATT_1	0.93	4.75	0.23	-61.29
KMO_13G1	0.90	10.64	0.11	-164.61
MBPP-1	0.90	13.77	0.10	-174.60
SJUAN_G1	0.91	3.33	0.03	76.30
SUND#5GN	0.26	18.96	1.00	0.00
SHEER_1	0.26	19.16	0.77	-3.42
SJUAN_G1	0.26	21.92	0.31	-173.66
KMO_13G1	0.26	19.95	0.27	15.28
PALOVRD2	0.26	19.58	0.25	177.80
REV_13G1	0.26	19.71	0.24	12.53
NAVAJO_1	0.26	19.40	0.23	179.60
SLHWKG1	0.27	19.44	0.21	171.86
MBPP-1	0.27	21.09	0.21	167.21
VALMY_G2	0.27	15.11	0.20	139.78
CRAIG_1	0.26	20.38	0.19	-176.92
RAWHIDE	0.26	19.02	0.18	-179.13
EHUNTER1	0.26	21.09	0.17	173.87
CURRNTC1	0.28	22.96	0.16	151.40
BRIDGER1	0.27	22.90	0.14	173.32
HYATT_1	0.27	20.71	0.12	176.34
HAYNES1G	0.27	19.30	0.09	-174.03
COULEE22	0.25	22.86	0.08	44.58
COLSTP_2	0.28	14.18	0.04	-52.12
BRWNL_5	0.27	15.81	0.03	154.72
REV_13G1	0.76	10.24	1.00	0.00
EHUNTER1	0.77	9.05	0.98	55.55
BRIDGER1	0.77	10.14	0.73	67.71
CURRNTC1	0.78	7.44	0.46	17.78
RAWHIDE	0.79	12.46	0.29	122.56
RAWHIDE	0.47	9.71	1.00	0.00
MBPP-1	0.47	10.60	0.91	17.35
CRAIG_1	0.47	9.65	0.63	17.30

Table 69: 2022 light spring (Note 2), 1.4 GW at Midway bus, 0.5 sec

Gen ID	**Freq**	**Damping**	**Residue**	**Angle**
HYATT_1	0.49	24.04	0.53	2.77
DIABLO_1	0.47	11.35	0.41	-165.16
PALOVRD2	0.45	14.03	0.40	-132.40
COLSTP_2	0.45	14.80	0.35	22.32
NAVAJO_1	0.45	13.58	0.33	-135.96
BRIDGER1	0.46	12.36	0.31	35.19
SLHWKG1	0.46	12.69	0.30	-130.45
HAYNES1G	0.46	12.80	0.27	-135.46
HYATT_1	0.48	10.79	0.24	-154.27
CURRNTC1	0.46	11.07	0.21	35.94
EHUNTER1	0.47	10.01	0.16	24.59
VALMY_G2	0.46	11.32	0.16	99.17
JDA_0304	0.46	3.41	0.02	-80.43
COLSTP_2	0.98	8.90	1.00	0.00
COULEE22	0.98	13.45	0.77	78.65
VALMY_G2	0.98	8.76	0.69	-147.27
PALOVRD2	0.96	10.79	0.37	-114.79
JDA_0304	0.95	8.62	0.36	-99.24
NAVAJO_1	0.97	13.48	0.32	-149.38
BRWNL_5	0.99	8.85	0.13	162.82
CRAIG_1	0.95	9.80	0.09	75.42
CURRNTC1	0.99	8.33	0.08	35.04
REV_13G1	0.97	13.14	0.08	59.63
SHEER_1	0.99	5.46	0.03	-112.54
BRIDGER1	0.96	3.71	0.01	170.02
JDA_0304	0.68	24.77	1.00	0.00
JDA_0304	0.66	18.39	0.70	175.85
SJUAN_G1	0.67	17.30	0.25	48.34
PALOVRD2	0.66	24.38	0.25	55.19
KMO_13G1	0.64	10.58	0.24	-6.17
NAVAJO_1	0.67	19.20	0.12	33.06
REV_13G1	0.65	11.22	0.08	26.37
COLSTP_2	0.65	12.45	0.08	-172.36
SHEER_1	0.63	27.51	0.07	140.70
CGS	0.65	10.19	0.07	137.78
CRAIG_1	0.67	14.36	0.04	-88.21
SUND#5GN	0.67	12.60	0.02	-162.44
BRWNL_5	0.65	6.21	0.02	110.38
SJUAN_G1	0.67	4.72	0.01	174.97
COULEE22	0.88	8.86	1.00	0.00
BRWNL_5	0.85	15.28	0.49	-2.23
CGS	0.86	7.40	0.31	37.47
SHEER_1	0.86	10.51	0.27	-154.80
VALMY_G2	0.87	5.91	0.15	-158.10
SUND#5GN	0.83	8.92	0.07	176.61
REV_13G1	0.84	2.70	0.02	-32.78

Table 70: 2022 light spring (Note 2), double Palo Verde trip

Gen ID	Freq	Damping	Residue	Angle
COLSTP_2	0.67	13.52	1.00	0.00
JDA_0304	0.66	13.58	0.95	56.12
CGS	0.63	14.03	0.94	81.30
COULEE22	0.64	12.97	0.87	76.25
BRIDGER1	0.65	13.49	0.84	97.51
SHEER_1	0.66	16.56	0.70	-51.76
SLHWKG1	0.65	11.39	0.25	-38.61
BRWNL_5	0.67	7.54	0.22	25.35
SUND#5GN	0.65	12.48	0.13	114.11
CRAIG_1	0.65	9.68	0.10	-124.92
CURRNTC1	0.67	5.67	0.10	21.93
HAYNES1G	0.66	5.08	0.05	-112.19
VALMY_G2	0.90	15.08	1.00	0.00
HYATT_1	0.90	8.41	0.50	-36.69
DIABLO_1	0.88	5.37	0.40	24.29
COULEE22	0.89	5.46	0.20	-123.41
COLSTP_2	0.89	2.48	0.04	155.20
KMO_13G1	0.41	9.65	1.00	0.00
BRIDGER1	0.39	15.32	0.55	131.22
REV_13G1	0.41	10.19	0.43	49.84
CRAIG_1	0.41	10.51	0.21	62.77
COULEE22	0.39	6.87	0.10	109.96
CGS	0.39	7.69	0.10	132.35
COLSTP_2	0.38	6.49	0.06	149.62
CURRNTC1	0.40	9.86	0.05	135.41
SUND#5GN	0.38	-1.59	0.00	29.82
DIABLO_1	0.32	15.44	1.00	0.00
BRIDGER1	0.34	10.50	0.61	-66.04
KMO_13G1	0.30	7.74	0.50	52.82
REV_13G1	0.30	8.04	0.44	84.36
CRAIG_1	0.32	8.79	0.40	23.35
HAYNES1G	0.33	10.36	0.38	9.20
SJUAN_G1	0.34	8.55	0.34	-14.92
RAWHIDE	0.32	5.67	0.21	-4.26
EHUNTER1	0.34	7.20	0.18	-80.58
NAVAJO_1	0.35	7.30	0.14	-38.16
SHEER_1	0.36	5.78	0.14	-14.57
HYATT_1	0.34	5.71	0.12	-70.79
COLSTP_2	0.30	4.49	0.11	133.20
COULEE22	0.31	3.79	0.09	93.49
MBPP-1	0.32	3.14	0.08	-4.16
JDA_0304	0.35	3.38	0.08	-168.86
BRWNL_5	0.34	3.68	0.07	-128.39
CGS	0.30	2.65	0.07	108.00
SJUAN_G1	0.77	26.96	1.00	0.00
CGS	0.75	13.27	0.09	53.34
CURRNTC1	0.76	8.03	0.09	-47.94
BRIDGER1	0.76	8.21	0.04	-38.25

Table 70: 2022 light spring (Note 2), double Palo Verde trip

Gen ID	Freq	Damping	Residue	Angle
MBPP-1	0.49	14.84	1.00	0.00
BRWNL_5	0.51	14.79	0.62	-49.24
RAWHIDE	0.52	11.49	0.46	-20.66
DIABLO_1	0.50	14.23	0.18	-100.33
CRAIG_1	0.52	6.69	0.06	37.27
VALMY_G2	0.49	7.15	0.06	102.05
KMO_13G1	0.62	13.40	1.00	0.00
REV_13G1	0.62	22.19	0.55	93.34
COLSTP_2	0.58	24.16	0.42	-120.66
NAVAJO_1	0.60	16.08	0.20	61.22
CURRNTC1	0.58	23.31	0.11	158.44
RAWHIDE	0.62	8.73	0.05	-45.14
CURRNTC1	0.60	6.73	0.02	167.47
BRWNL_5	0.58	5.25	0.01	-118.52
HAYNES1G	0.58	3.62	0.01	53.69
BRIDGER1	0.61	4.96	0.01	102.45
MBPP-1	0.61	2.94	0.00	-15.50
VALMY_G2	0.14	19.96	1.00	0.00
SHEER_1	0.13	18.91	0.71	123.69
JDA_0304	0.13	15.10	0.37	108.44
SUND#5GN	0.14	-11.29	0.02	77.64
KMO_13G1	0.94	7.01	1.00	0.00
SHEER_1	0.92	5.05	0.28	34.93
SUND#5GN	0.93	3.63	0.12	-10.11
KMO_13G1	0.70	10.11	1.00	0.00
EHUNTER1	0.70	17.69	0.92	-45.80
REV_13G1	0.69	14.17	0.84	111.01
EHUNTER1	0.73	9.86	0.57	119.99
DIABLO_1	0.68	12.33	0.36	26.04
BRIDGER1	0.69	11.45	0.23	167.21
SHEER_1	0.72	10.66	0.22	18.75
RAWHIDE	0.72	10.08	0.10	-83.07
HYATT_1	0.70	8.55	0.09	-49.34
MBPP-1	0.69	9.29	0.06	7.40
BRWNL_5	0.73	5.61	0.03	-178.37
EHUNTER1	0.70	4.00	0.02	96.33
RAWHIDE	0.69	4.84	0.01	1.97
SUND#5GN	0.26	18.96	1.00	0.00
SHEER_1	0.26	19.86	0.72	6.40
KMO_13G1	0.26	27.61	0.44	26.11
REV_13G1	0.25	26.87	0.33	37.18
VALMY_G2	0.26	14.01	0.21	165.40
SJUAN_G1	0.27	14.49	0.17	174.20
NAVAJO_1	0.26	15.52	0.17	-179.02
SLHWKG1	0.27	15.50	0.16	166.18
HAYNES1G	0.27	14.32	0.15	169.67
CRAIG_1	0.27	13.91	0.13	161.41
RAWHIDE	0.26	13.55	0.12	166.54
CURRNTC1	0.25	18.73	0.12	-139.35

Table 70: 2022 light spring (Note 2), double Palo Verde trip

Gen ID	**Freq**	**Damping**	**Residue**	**Angle**
DIABLO_1	0.26	13.20	0.12	171.87
MBPP-1	0.26	13.64	0.10	-178.33
EHUNTER1	0.26	12.41	0.07	165.02
HYATT_1	0.26	10.76	0.05	178.11
BRIDGER1	0.27	10.48	0.04	160.68
JDA_0304	0.26	7.48	0.01	177.02
SHEER_1	0.27	2.53	0.01	-3.82
BRWNL_5	0.26	5.91	0.01	-165.30
SUND#5GN	0.28	-5.57	0.00	-63.92
MBPP-1	0.46	12.00	1.00	0.00
RAWHIDE	0.45	8.79	0.77	10.34
JDA_0304	0.46	29.13	0.70	94.08
BRWNL_5	0.44	14.08	0.58	1.28
HAYNES1G	0.45	11.85	0.47	-169.80
VALMY_G2	0.44	14.00	0.46	97.46
SUND#5GN	0.44	10.31	0.45	173.67
DIABLO_1	0.45	12.24	0.44	-173.73
COLSTP_2	0.45	11.67	0.44	-26.66
NAVAJO_1	0.44	11.88	0.42	-174.14
KMO_13G1	0.44	7.68	0.42	10.42
SLHWKG1	0.45	11.62	0.37	-169.17
CGS	0.44	10.17	0.36	-25.00
SJUAN_G1	0.45	9.89	0.34	149.88
COULEE22	0.44	9.62	0.33	-15.10
REV_13G1	0.44	8.42	0.29	-9.15
JDA_0304	0.44	10.98	0.27	-29.38
CRAIG_1	0.46	7.31	0.26	9.37
HYATT_1	0.44	11.00	0.21	-68.73
RAWHIDE	0.43	7.82	0.20	-87.71
BRIDGER1	0.47	9.40	0.15	-48.17
SHEER_1	0.44	11.60	0.15	165.13
CURRNTC1	0.47	8.31	0.09	-27.04
EHUNTER1	0.47	7.53	0.08	-49.53
MBPP-1	0.44	2.64	0.02	166.46
JDA_0304	0.83	12.31	1.00	0.00
NAVAJO_1	0.85	13.98	0.79	-78.52
COULEE22	0.82	5.19	0.53	-7.55
REV_13G1	0.84	5.58	0.39	57.73
KMO_13G1	0.83	4.96	0.38	-49.41
COLSTP_2	0.81	3.65	0.24	15.05
DIABLO_1	0.86	2.68	0.16	-23.76
BRWNL_5	0.82	3.81	0.10	-115.64
CGS	0.82	2.18	0.07	-30.84

Table 71: 2022 light spring (Note 3), 1.4 GW at Chief Joseph brake, 0.5 sec

Gen ID	Freq	Damping	Residue	Angle
JDA_0304	0.81	18.95	1.00	0.00
BRWNL_5	0.80	20.22	0.60	-82.34
REV_13G1	0.79	15.92	0.42	-145.14
COLSTP_2	0.79	14.13	0.38	-4.91
BRIDGER1	0.80	12.14	0.12	-131.49
SLHWKG1	0.80	9.49	0.04	178.82
BRWNL_5	0.58	21.81	1.00	0.00
PALOVRD2	0.59	24.53	0.96	-154.80
SJUAN_G1	0.59	14.66	0.41	160.28
HYATT_1	0.59	11.66	0.21	-6.41
CURRNTC1	0.75	10.19	1.00	0.00
EHUNTER1	0.75	9.57	0.76	26.27
SHEER_1	0.76	11.40	0.68	-29.70
BRIDGER1	0.76	10.76	0.50	34.89
SLHWKG1	0.75	24.05	0.46	122.78
VALMY_G2	0.77	10.94	0.39	29.89
COLSTP_2	0.74	3.31	0.03	51.22
PALOVRD2	0.66	14.27	1.00	0.00
KMO_13G1	0.62	8.62	0.98	46.54
NAVAJO_1	0.64	12.03	0.37	40.46
SLHWKG1	0.61	12.91	0.27	110.89
JDA_0304	0.63	8.01	0.19	-146.88
REV_13G1	0.63	6.94	0.17	51.53
SUND#5GN	0.63	11.87	0.15	-126.57
DIABLO_1	0.62	9.14	0.14	-95.78
SHEER_1	0.64	11.00	0.09	37.85
DIABLO_1	0.89	6.97	1.00	0.00
CURRNTC1	0.94	7.54	0.70	101.36
CRAIG_1	0.89	6.90	0.21	55.07
SLHWKG1	0.92	5.65	0.19	-151.67
HYATT_1	0.92	1.55	0.07	-63.76
NAVAJO_1	0.91	-0.06	0.01	-91.29
SUND#5GN	0.28	21.49	1.00	0.00
SHEER_1	0.28	21.30	0.72	-1.91
REV_13G1	0.26	28.75	0.31	13.75
HAYNES1G	0.26	20.35	0.27	-129.02
PALOVRD2	0.24	21.00	0.27	-91.39
SJUAN_G1	0.23	19.99	0.25	-72.65
NAVAJO_1	0.25	19.97	0.25	-119.30
HYATT_1	0.23	26.09	0.24	-77.77
RAWHIDE	0.24	19.29	0.22	-98.70
MBPP-1	0.25	19.98	0.21	-111.58
EHUNTER1	0.24	19.67	0.17	-92.04
CRAIG_1	0.24	17.49	0.17	-105.06
CURRNTC1	0.23	18.01	0.13	-54.70
BRIDGER1	0.25	18.68	0.11	-108.18
BRWNL_5	0.23	18.69	0.08	-65.83

Table 71: 2022 light spring (Note 3), 1.4 GW at Chief Joseph brake, 0.5 sec

Gen ID	**Freq**	**Damping**	**Residue**	**Angle**
COULEE22	0.84	13.07	1.00	0.00
CGS	0.83	13.97	0.77	-12.42
KMO_13G1	0.83	14.53	0.76	27.97
EHUNTER1	0.83	9.44	0.29	-141.88
CURRNTC1	0.86	8.91	0.23	125.58
SUND#5GN	0.83	15.11	0.13	106.59
RAWHIDE	0.83	12.08	0.07	-7.60
HAYNES1G	0.86	6.22	0.06	74.68
SHEER_1	0.87	6.58	0.02	83.07
PALOVRD2	0.83	6.56	0.02	50.36
SJUAN_G1	0.86	2.87	0.01	-107.81
NAVAJO_1	0.84	-1.82	0.00	21.36
MBPP-1	0.53	27.21	1.00	0.00
BRIDGER1	0.56	16.65	0.74	101.68
RAWHIDE	0.53	13.14	0.69	3.68
CURRNTC1	0.55	11.59	0.19	117.85
VALMY_G2	0.56	9.74	0.13	145.18
CRAIG_1	0.54	6.44	0.09	55.63
KMO_13G1	0.69	15.04	1.00	0.00
DIABLO_1	0.71	12.48	0.17	14.66
SJUAN_G1	0.69	11.71	0.14	-138.02
HYATT_1	0.68	11.71	0.13	81.85
CRAIG_1	0.71	25.80	0.09	50.62
RAWHIDE	0.72	8.05	0.04	-66.55
HAYNES1G	0.73	9.86	0.03	6.01
MBPP-1	0.71	8.50	0.02	-12.46
BRWNL_5	0.70	5.21	0.01	-114.72
KMO_13G1	0.44	12.06	1.00	0.00
REV_13G1	0.44	11.93	0.58	9.51
COULEE22	0.44	12.17	0.48	7.78
SUND#5GN	0.44	11.65	0.46	-166.36
CGS	0.44	12.19	0.43	-1.91
SJUAN_G1	0.44	12.23	0.34	-166.29
COLSTP_2	0.43	12.87	0.33	13.01
RAWHIDE	0.46	12.18	0.32	-177.17
PALOVRD2	0.44	11.70	0.29	-170.48
JDA_0304	0.44	11.85	0.28	6.47
BRWNL_5	0.44	12.05	0.24	0.10
NAVAJO_1	0.44	11.32	0.23	-174.17
MBPP-1	0.46	11.23	0.21	-170.61
SLHWKG1	0.44	11.18	0.21	-157.29
CRAIG_1	0.46	11.80	0.21	-166.95
HAYNES1G	0.44	10.50	0.18	-174.78
SHEER_1	0.44	11.64	0.13	-161.39
DIABLO_1	0.43	9.76	0.10	-164.78
HYATT_1	0.44	12.72	0.10	9.23
VALMY_G2	0.43	11.25	0.08	94.40
BRIDGER1	0.44	9.93	0.08	-25.59
EHUNTER1	0.47	12.98	0.06	-160.97
CURRNTC1	0.46	9.26	0.03	-123.67

Table 72: 2022 light spring (Note 3), 1.4 GW at El Dorado bus, 0.5 sec

Gen ID	Freq	Damping	Residue	Angle
HAYNES1G	0.84	10.51	1.00	0.00
CURRNTC1	0.82	11.81	0.27	-113.41
SJUAN_G1	0.83	4.74	0.25	130.85
SHEER_1	0.83	10.35	0.20	156.32
BRWNL_5	0.83	5.75	0.05	29.11
KMO_13G1	0.85	2.46	0.02	54.25
REV_13G1	0.67	17.64	1.00	0.00
COLSTP_2	0.66	11.81	0.77	164.97
RAWHIDE	0.65	18.60	0.74	-50.69
EHUNTER1	0.66	10.61	0.65	164.13
SHEER_1	0.67	14.92	0.58	67.40
KMO_13G1	0.44	11.68	1.00	0.00
DIABLO_1	0.46	18.07	0.84	-151.46
HAYNES1G	0.46	17.86	0.80	-166.60
REV_13G1	0.44	11.63	0.60	7.18
PALOVRD2	0.44	14.98	0.56	-159.34
SUND#5GN	0.44	11.77	0.53	-171.06
SLHWKG1	0.44	15.76	0.50	-147.75
NAVAJO_1	0.44	14.92	0.49	-162.73
COLSTP_2	0.44	14.20	0.47	6.81
COULEE22	0.44	11.83	0.47	8.93
BRIDGER1	0.46	18.29	0.46	10.46
CGS	0.44	12.25	0.46	2.93
BRWNL_5	0.44	13.81	0.38	11.28
SJUAN_G1	0.44	11.50	0.36	173.65
JDA_0304	0.44	10.72	0.24	-2.41
VALMY_G2	0.43	15.12	0.19	130.13
SHEER_1	0.45	11.28	0.15	-179.89
HYATT_1	0.46	7.24	0.08	-71.22
KMO_13G1	0.71	14.72	1.00	0.00
CURRNTC1	0.72	5.11	0.04	-161.27
BRIDGER1	0.70	3.83	0.02	-87.29
SJUAN_G1	0.89	9.22	1.00	0.00
BRIDGER1	0.86	17.71	0.44	94.57
COLSTP_2	0.86	6.85	0.27	109.72
HYATT_1	0.86	5.59	0.26	-45.63
MBPP-1	0.89	19.39	0.22	48.18
COULEE22	0.87	5.61	0.20	119.54
SUND#5GN	0.87	17.02	0.14	-132.35
JDA_0304	0.86	6.53	0.08	-158.05
CGS	0.86	3.68	0.05	114.42
REV_13G1	0.87	6.09	0.04	-41.82
RAWHIDE	0.49	9.88	1.00	0.00
MBPP-1	0.49	10.43	0.83	14.91
CRAIG_1	0.48	9.46	0.58	29.76
CURRNTC1	0.48	14.33	0.36	33.78

Table 72: 2022 light spring (Note 3), 1.4 GW at El Dorado bus, 0.5 sec

Gen ID	Freq	Damping	Residue	Angle
EHUNTER1	0.49	9.02	0.14	24.30
SHEER_1	0.48	-3.91	0.00	-19.73
SUND#5GN	0.26	20.55	1.00	0.00
SHEER_1	0.26	20.56	0.74	-0.44
HAYNES1G	0.28	23.00	0.33	157.04
VALMY_G2	0.26	19.75	0.30	165.93
PALOVRD2	0.28	21.07	0.27	168.16
SJUAN_G1	0.27	20.02	0.25	169.83
RAWHIDE	0.28	20.92	0.23	146.21
CRAIG_1	0.28	21.32	0.22	152.90
KMO_13G1	0.25	19.46	0.21	21.61
DIABLO_1	0.28	19.29	0.20	166.23
REV_13G1	0.26	19.42	0.20	18.60
MBPP-1	0.28	21.17	0.19	156.40
EHUNTER1	0.27	21.48	0.16	171.26
CURRNTC1	0.28	21.17	0.13	149.99
HYATT_1	0.29	20.55	0.12	153.48
BRIDGER1	0.27	22.59	0.11	-178.60
COLSTP_2	0.26	18.22	0.04	-9.07
KMO_13G1	0.62	12.13	1.00	0.00
JDA_0304	0.63	14.69	0.30	163.44
CGS	0.63	13.03	0.25	161.16
HYATT_1	0.59	13.81	0.23	-114.04
BRWNL_5	0.62	12.06	0.22	-171.16
REV_13G1	0.61	13.09	0.22	64.52
COULEE22	0.64	12.68	0.20	167.43
SJUAN_G1	0.62	12.79	0.17	16.79
CRAIG_1	0.58	23.88	0.15	-0.23
PALOVRD2	0.62	10.19	0.09	46.33
COLSTP_2	0.60	12.83	0.07	-96.34
CURRNTC1	0.60	8.78	0.06	-135.56
BRIDGER1	0.61	7.73	0.06	-153.80
SUND#5GN	0.62	14.89	0.06	-131.83
SLHWKG1	0.92	18.37	1.00	0.00
HYATT_1	0.96	5.76	0.05	-166.40
COULEE22	0.96	8.68	0.04	7.84
DIABLO_1	0.92	4.27	0.04	-14.75
COLSTP_2	0.97	5.38	0.03	-31.84
JDA_0304	0.95	6.70	0.02	118.12
CRAIG_1	0.93	10.31	0.01	122.84
SUND#5GN	0.93	5.62	0.01	172.51
SHEER_1	0.96	4.68	0.01	-133.97
MBPP-1	0.95	-0.33	0.00	-129.04
RAWHIDE	0.95	1.16	0.00	-176.73

Table 73: 2022 light spring (Note 3), 1.4 GW at Hemingway Bus, 0.5 sec

Gen ID	Freq	Damping	Residue	Angle

Table 73: 2022 light spring (Note 3), 1.4 GW at Hemingway Bus, 0.5 sec

Gen ID	Freq	Damping	Residue	Angle
COULEE22	0.75	13.49	1.00	0.00
CGS	0.76	12.45	0.63	-35.65
BRWNL_5	0.77	12.89	0.55	-78.59
REV_13G1	0.76	11.50	0.51	-167.72
COLSTP_2	0.75	9.88	0.43	-14.20
DIABLO_1	0.76	12.26	0.41	112.72
EHUNTER1	0.76	7.05	0.20	-113.52
SHEER_1	0.75	9.20	0.17	-154.57
CURRNTC1	0.74	6.22	0.12	-72.34
CRAIG_1	0.75	11.20	0.10	172.99
SJUAN_G1	0.29	17.59	1.00	0.00
CRAIG_1	0.28	22.81	0.96	20.83
NAVAJO_1	0.27	17.46	0.76	31.61
EHUNTER1	0.29	20.32	0.71	-5.06
PALOVRD2	0.28	15.76	0.70	11.25
RAWHIDE	0.28	18.02	0.68	2.29
SLHWKG1	0.30	13.19	0.56	-32.71
MBPP-1	0.28	17.74	0.54	18.25
HAYNES1G	0.28	11.92	0.38	11.93
DIABLO_1	0.29	10.24	0.32	-3.92
BRWNL_5	0.49	15.81	1.00	0.00
MBPP-1	0.50	9.86	0.42	77.86
RAWHIDE	0.48	6.18	0.19	99.44
CRAIG_1	0.51	3.20	0.14	28.48
BRWNL_5	0.97	9.85	1.00	0.00
MBPP-1	0.92	13.36	0.74	-175.20
NAVAJO_1	0.95	17.22	0.22	117.37
DIABLO_1	0.94	4.39	0.17	-71.18
RAWHIDE	0.93	2.71	0.01	166.51
CURRNTC1	0.73	23.29	1.00	0.00
EHUNTER1	0.73	18.90	0.72	12.99
KMO_13G1	0.73	8.99	0.25	77.73
SJUAN_G1	0.73	10.44	0.13	-32.39
SUND#5GN	0.70	21.91	0.10	42.79
JDA_0304	0.71	10.52	0.10	56.72
HYATT_1	0.71	9.99	0.09	-172.27
RAWHIDE	0.71	9.48	0.08	134.42
MBPP-1	0.70	11.52	0.07	-173.71
PALOVRD2	0.73	10.75	0.07	-41.01
HAYNES1G	0.73	8.13	0.03	149.37
NAVAJO_1	0.73	9.00	0.02	-26.88
SUND#5GN	0.26	19.77	1.00	0.00
SHEER_1	0.26	19.53	0.73	-2.44
KMO_13G1	0.25	18.66	0.22	24.65
REV_13G1	0.25	17.21	0.19	10.51
COULEE22	0.23	22.25	0.09	69.61
JDA_0304	0.82	14.12	1.00	0.00
SHEER_1	0.85	12.52	0.21	97.90

Table 73: 2022 light spring (Note 3), 1.4 GW at Hemingway Bus, 0.5 sec

Gen ID	Freq	Damping	Residue	Angle
SUND#5GN	0.83	5.93	0.02	55.16
KMO_13G1	0.44	11.65	1.00	0.00
REV_13G1	0.44	12.04	0.62	15.74
DIABLO_1	0.44	18.62	0.61	-137.59
HAYNES1G	0.44	16.74	0.57	-141.75
SUND#5GN	0.44	11.49	0.47	-158.06
PALOVRD2	0.44	13.77	0.45	-150.46
COULEE22	0.44	11.16	0.42	9.80
SLHWKG1	0.42	14.97	0.39	-109.72
NAVAJO_1	0.44	13.47	0.37	-157.05
SJUAN_G1	0.44	11.86	0.36	-161.51
COLSTP_2	0.43	12.65	0.35	15.15
CGS	0.45	9.77	0.29	-19.72
JDA_0304	0.44	10.04	0.20	16.06
SHEER_1	0.43	11.17	0.12	-145.89
KMO_13G1	0.61	11.30	1.00	0.00
SJUAN_G1	0.62	13.23	0.37	2.51
JDA_0304	0.62	11.92	0.25	175.93
HYATT_1	0.62	10.98	0.24	-176.12
PALOVRD2	0.62	11.81	0.22	7.62
HAYNES1G	0.58	21.14	0.17	116.54
NAVAJO_1	0.62	11.11	0.13	3.40
REV_13G1	0.62	8.22	0.12	19.02
COLSTP_2	0.59	10.29	0.08	-131.96
COULEE22	0.63	7.39	0.06	134.45
SUND#5GN	0.64	9.56	0.05	129.30
SHEER_1	0.60	10.73	0.04	48.90
BRIDGER1	0.56	17.95	1.00	0.00
RAWHIDE	0.53	16.21	0.50	112.95
CRAIG_1	0.54	5.15	0.11	-154.54
SLHWKG1	0.55	10.52	0.09	-162.76

Table 74: 2022 light spring (Note 3), 1.4 GW at Midway bus, 0.5 sec

Gen ID	Freq	Damping	Residue	Angle
NAVAJO_1	0.44	19.83	1.00	0.00
COLSTP_2	0.43	20.22	0.95	175.69
PALOVRD2	0.45	18.13	0.83	-4.79
KMO_13G1	0.43	11.57	0.71	150.58
BRWNL_5	0.44	16.44	0.47	161.38
REV_13G1	0.43	11.26	0.41	158.04
SUND#5GN	0.44	11.51	0.37	-25.31
CGS	0.43	11.62	0.29	156.18
COULEE22	0.43	10.74	0.27	162.48
SJUAN_G1	0.44	10.54	0.24	-43.69
SHEER_1	0.45	10.90	0.10	-39.61
JDA_0304	0.44	3.97	0.05	118.18

Table 74: 2022 light spring (Note 3), 1.4 GW at Midway bus, 0.5 sec

Gen ID	Freq	Damping	Residue	Angle
KMO_13G1	0.66	13.92	1.00	0.00
REV_13G1	0.64	16.31	0.17	109.59
CURRNTC1	0.65	27.04	0.13	-163.96
BRWNL_5	0.67	11.78	0.12	167.06
CRAIG_1	0.67	12.54	0.05	-23.68
SJUAN_G1	0.66	3.24	0.01	-90.19
VALMY_G2	0.97	5.94	1.00	0.00
CRAIG_1	0.98	11.63	0.74	151.74
BRWNL_5	0.97	8.59	0.69	-41.62
CURRNTC1	0.98	6.73	0.23	-166.50
SHEER_1	0.96	5.03	0.17	78.96
EHUNTER1	0.98	4.16	0.13	-135.29
SUND#5GN	0.98	4.88	0.07	-126.71
REV_13G1	1.00	3.28	0.01	-133.61
KMO_13G1	0.73	12.86	1.00	0.00
SHEER_1	0.71	21.05	0.57	-23.42
COULEE22	0.69	13.98	0.44	-11.56
CGS	0.69	13.64	0.42	-37.03
SHEER_1	0.74	14.14	0.41	133.97
SJUAN_G1	0.68	15.40	0.37	-56.75
HYATT_1	0.72	15.07	0.37	97.62
COLSTP_2	0.70	12.05	0.35	-37.84
JDA_0304	0.72	14.42	0.31	-47.59
REV_13G1	0.73	13.17	0.30	133.93
DIABLO_1	0.71	10.54	0.20	86.99
EHUNTER1	0.70	9.30	0.20	-63.59
BRIDGER1	0.70	10.30	0.19	-46.65
BRWNL_5	0.74	12.05	0.19	-154.68
RAWHIDE	0.71	10.74	0.17	38.74
CURRNTC1	0.71	8.04	0.16	-107.74
SLHWKG1	0.74	16.11	0.13	-155.16
VALMY_G2	0.69	9.74	0.08	-23.16
MBPP-1	0.70	9.50	0.08	116.52
HAYNES1G	0.69	9.99	0.07	159.78
SUND#5GN	0.68	13.52	0.05	77.44
NAVAJO_1	0.73	10.10	0.04	-108.77
PALOVRD2	0.70	7.21	0.02	-26.55
BRIDGER1	0.79	12.27	1.00	0.00
EHUNTER1	0.79	7.35	0.57	6.89
CURRNTC1	0.79	3.28	0.11	1.95
COULEE22	0.88	14.66	1.00	0.00
CGS	0.87	10.25	0.20	-69.13
KMO_13G1	0.86	10.00	0.09	2.86
REV_13G1	0.88	9.51	0.06	140.47
SUND#5GN	0.87	8.99	0.02	62.79
BRIDGER1	0.88	-2.82	0.00	30.69
SUND#5GN	0.26	20.27	1.00	0.00
SHEER_1	0.26	20.14	0.74	-1.07
SLHWKG1	0.28	21.92	0.28	157.55

Table 74: 2022 light spring (Note 3), 1.4 GW at Midway bus, 0.5 sec

Gen ID	Freq	Damping	Residue	Angle
NAVAJO_1	0.27	21.61	0.27	174.91
PALOVRD2	0.27	20.67	0.26	166.70
SJUAN_G1	0.27	19.78	0.25	169.67
DIABLO_1	0.28	20.37	0.24	167.02
HAYNES1G	0.28	19.60	0.23	150.73
KMO_13G1	0.25	20.00	0.23	19.21
RAWHIDE	0.28	20.21	0.21	148.64
REV_13G1	0.26	19.49	0.20	17.81
CRAIG_1	0.28	20.17	0.19	155.55
MBPP-1	0.28	21.01	0.19	155.61
VALMY_G2	0.27	15.12	0.18	134.85
EHUNTER1	0.28	21.13	0.17	159.98
CURRNTC1	0.29	21.01	0.13	143.17
BRIDGER1	0.27	23.14	0.12	175.84
HYATT_1	0.28	20.05	0.12	152.15
BRWNL_5	0.29	12.96	0.02	128.86
RAWHIDE	0.48	10.49	1.00	0.00
MBPP-1	0.48	10.83	0.79	18.79
CRAIG_1	0.48	10.02	0.58	21.89
SLHWKG1	0.47	18.18	0.55	-137.75
HAYNES1G	0.48	14.89	0.47	-153.41
DIABLO_1	0.49	12.03	0.36	-179.03
BRIDGER1	0.48	14.03	0.34	26.09
CURRNTC1	0.48	12.08	0.24	31.32
VALMY_G2	0.47	13.95	0.18	93.76
EHUNTER1	0.48	10.79	0.18	32.99
HYATT_1	0.47	7.00	0.08	-97.99
KMO_13G1	0.62	23.37	1.00	0.00
PALOVRD2	0.63	26.90	0.48	-111.88
CGS	0.60	18.07	0.18	126.81
COULEE22	0.60	16.92	0.13	155.60
RAWHIDE	0.61	15.09	0.10	-167.25
JDA_0304	0.62	12.75	0.10	72.99
COLSTP_2	0.92	15.43	1.00	0.00
COULEE22	0.93	10.01	0.42	-109.48
DIABLO_1	0.92	7.97	0.40	151.24
COLSTP_2	0.95	6.17	0.20	166.57
PALOVRD2	0.95	11.64	0.14	-52.60
HYATT_1	0.93	4.86	0.12	94.37
JDA_0304	0.95	7.19	0.07	-48.34
SLHWKG1	0.92	4.63	0.03	52.29
NAVAJO_1	0.95	5.66	0.02	-29.53
SJUAN_G1	0.91	3.93	0.02	-137.89

Table 75: 2022 light spring (Note 3), double Palo Verde trip

Gen ID	Freq	Damping	Residue	Angle
COLSTP_2	0.30	8.72	1.00	0.00

Table 75: 2022 light spring (Note 3), double Palo Verde trip

Gen ID	**Freq**	**Damping**	**Residue**	**Angle**
COULEE22	0.31	6.56	0.71	-43.85
BRWNL_5	0.30	6.46	0.55	20.79
HYATT_1	0.34	5.42	0.47	-178.54
SUND#5GN	0.33	1.83	0.39	60.09
CGS	0.30	4.12	0.35	18.73
SHEER_1	0.32	1.89	0.25	115.76
EHUNTER1	0.31	2.57	0.22	-62.64
CRAIG_1	0.30	0.79	0.16	2.05
CURRNTC1	0.32	2.89	0.14	-121.86
RAWHIDE	0.30	-0.53	0.12	11.97
MBPP-1	0.31	-3.20	0.05	-31.38
JDA_0304	0.41	28.55	1.00	0.00
DIABLO_1	0.45	18.69	0.64	140.63
KMO_13G1	0.44	8.95	0.42	-59.33
SUND#5GN	0.43	10.82	0.37	135.79
REV_13G1	0.44	9.94	0.31	-72.49
BRWNL_5	0.44	14.99	0.30	-70.00
HAYNES1G	0.45	13.92	0.30	132.48
CGS	0.44	10.84	0.27	-75.40
COLSTP_2	0.45	12.04	0.22	-87.97
VALMY_G2	0.44	14.75	0.21	33.82
SLHWKG1	0.46	13.10	0.21	115.43
COULEE22	0.44	9.08	0.19	-56.63
SJUAN_G1	0.45	7.90	0.11	113.36
SHEER_1	0.44	11.13	0.10	126.60
NAVAJO_1	0.44	8.76	0.07	144.69
HYATT_1	0.43	8.92	0.06	-67.48
SUND#5GN	0.42	-0.62	0.00	52.80
KMO_13G1	0.61	13.97	1.00	0.00
HYATT_1	0.61	15.00	0.32	-151.06
BRWNL_5	0.60	12.76	0.22	176.29
CURRNTC1	0.62	10.77	0.12	130.02
SHEER_1	0.62	15.55	0.11	12.72
SJUAN_G1	0.61	9.36	0.08	71.70
EHUNTER1	0.60	9.98	0.08	169.59
NAVAJO_1	0.62	9.56	0.06	52.20
BRIDGER1	0.75	10.30	1.00	0.00
EHUNTER1	0.75	7.63	0.59	4.13
CURRNTC1	0.75	7.76	0.58	-16.05
BRWNL_5	0.73	7.18	0.36	68.26
EHUNTER1	0.76	29.06	0.26	37.92
SHEER_1	0.73	7.58	0.25	-38.50
DIABLO_1	0.72	4.58	0.21	-88.90
HAYNES1G	0.72	5.62	0.16	-8.00
HYATT_1	0.72	3.49	0.06	-60.10
RAWHIDE	0.74	5.17	0.06	-156.66
NAVAJO_1	0.38	16.35	1.00	0.00
SLHWKG1	0.35	14.25	0.54	104.18
SJUAN_G1	0.37	11.04	0.40	25.30
KMO_13G1	0.40	5.86	0.26	96.85

Table 75: 2022 light spring (Note 3), double Palo Verde trip

Gen ID	**Freq**	**Damping**	**Residue**	**Angle**
HAYNES1G	0.35	10.18	0.17	92.40
REV_13G1	0.39	5.41	0.11	153.40
VALMY_G2	0.37	6.19	0.11	-41.42
JDA_0304	0.37	4.56	0.08	-77.02
COULEE22	0.40	3.91	0.08	123.05
COLSTP_2	0.38	4.82	0.08	-154.55
BRWNL_5	0.38	4.37	0.06	-132.13
CGS	0.38	2.23	0.03	-164.36
BRIDGER1	0.38	2.14	0.03	-133.89
RAWHIDE	0.38	-1.16	0.01	-127.86
CRAIG_1	0.38	-0.83	0.01	-103.73
SHEER_1	0.40	0.60	0.01	-35.83
MBPP-1	0.38	-2.72	0.00	-138.68
CGS	0.91	16.09	1.00	0.00
DIABLO_1	0.94	3.81	0.61	141.05
HAYNES1G	0.93	5.32	0.60	12.61
COULEE22	0.91	6.12	0.42	4.66
SUND#5GN	0.94	4.26	0.05	68.00
SUND#5GN	0.26	16.47	1.00	0.00
SHEER_1	0.26	16.64	0.76	-4.63
BRIDGER1	0.25	29.06	0.46	-140.35
SJUAN_G1	0.23	28.95	0.44	-90.63
RAWHIDE	0.26	21.36	0.42	179.77
MBPP-1	0.25	22.15	0.35	-162.38
CRAIG_1	0.26	20.14	0.34	174.00
DIABLO_1	0.25	18.97	0.33	-152.80
KMO_13G1	0.28	14.29	0.30	-89.80
REV_13G1	0.25	26.97	0.30	68.25
CURRNTC1	0.24	21.12	0.21	-127.23
EHUNTER1	0.26	17.19	0.19	-174.32
BRWNL_5	0.26	21.81	0.18	-174.56
HAYNES1G	0.26	13.49	0.15	-172.11
REV_13G1	0.28	12.73	0.14	-84.72
SLHWKG1	0.28	11.53	0.11	125.64
HYATT_1	0.25	13.36	0.08	-143.66
NAVAJO_1	0.27	8.95	0.06	118.61
VALMY_G2	0.27	7.23	0.06	114.81
SJUAN_G1	0.27	5.82	0.03	141.62
BRIDGER1	0.29	-1.14	0.00	-29.85
JDA_0304	0.28	-3.32	0.00	58.33
RAWHIDE	0.48	6.74	1.00	0.00
MBPP-1	0.48	7.68	0.94	14.00
CRAIG_1	0.47	6.48	0.60	32.21
BRIDGER1	0.50	10.70	0.48	-53.62
JDA_0304	0.48	8.50	0.40	-134.86
EHUNTER1	0.48	8.62	0.29	22.25
CURRNTC1	0.49	8.03	0.25	5.42
SJUAN_G1	0.52	8.38	0.18	7.68
NAVAJO_1	0.52	6.45	0.10	55.21
HYATT_1	0.49	4.74	0.08	-153.22
CRAIG_1	0.50	3.12	0.07	31.88

Table 75: 2022 light spring (Note 3), double Palo Verde trip

Gen ID	**Freq**	**Damping**	**Residue**	**Angle**
COLSTP_2	0.52	6.09	0.07	-112.92
RAWHIDE	0.50	1.57	0.04	20.93
MBPP-1	0.51	-1.29	0.00	-31.87
REV_13G1	0.56	16.46	1.00	0.00
JDA_0304	0.54	10.88	0.41	-126.05
REV_13G1	0.54	6.47	0.04	154.12
SUND#5GN	0.57	5.02	0.01	-170.53
KMO_13G1	0.69	8.91	1.00	0.00
BRIDGER1	0.65	15.19	0.73	-63.62
CGS	0.67	10.35	0.50	-106.26
COULEE22	0.67	10.50	0.48	-90.81
JDA_0304	0.70	11.31	0.44	-119.74
REV_13G1	0.68	10.75	0.42	100.46
COLSTP_2	0.67	8.56	0.35	-124.80
MBPP-1	0.70	10.89	0.13	-27.78
VALMY_G2	0.68	5.88	0.13	-125.93
SUND#5GN	0.67	16.28	0.11	-59.29
RAWHIDE	0.68	7.34	0.09	-20.52
SLHWKG1	0.70	5.35	0.08	165.65
CRAIG_1	0.68	9.87	0.07	43.25
EHUNTER1	0.66	4.68	0.05	-76.18
CURRNTC1	0.66	2.22	0.01	-78.94
HYATT_1	0.64	2.13	0.01	163.19
KMO_13G1	0.69	0.15	0.01	-163.92

Table 76: 2022 light spring (Note 4), 1.4 GW at Chief Joseph brake, 0.5 sec

Gen ID	**Freq**	**Damping**	**Residue**	**Angle**
SJUAN_G1	0.24	29.35	1.00	0.00
RAWHIDE	0.24	27.48	0.81	-13.33
DIABLO_1	0.21	29.69	0.76	36.41
CRAIG_1	0.24	26.76	0.68	-19.39
EHUNTER1	0.24	28.43	0.62	-13.59
SLHWKG1	0.23	26.70	0.59	13.68
CURRNTC1	0.23	21.07	0.29	24.12
COLSTP_2	0.76	13.32	1.00	0.00
BRIDGER1	0.75	10.49	0.42	-62.06
VALMY_G2	0.76	11.47	0.31	-57.31
COULEE22	0.97	20.16	1.00	0.00
REV_13G1	0.95	20.17	0.24	-89.39
MBPP-1	0.96	3.55	0.01	3.14
KMO_13G1	0.64	14.79	1.00	0.00
KMO_13G1	0.66	7.95	0.20	139.45
SJUAN_G1	0.67	10.49	0.10	-111.50
HYATT_1	0.66	9.95	0.08	102.79
PALOVRD2	0.65	10.84	0.06	-59.73
SHEER_1	0.62	19.21	0.06	41.32
NAVAJO_1	0.65	10.56	0.04	-55.50
JDA_0304	0.63	8.63	0.03	122.68
SLHWKG1	0.63	10.86	0.03	-19.38
REV_13G1	0.63	6.93	0.03	-40.04
SUND#5GN	0.64	11.72	0.02	139.73
CURRNTC1	0.63	10.40	0.02	114.33
EHUNTER1	0.66	-0.77	0.00	-22.70
KMO_13G1	0.44	11.48	1.00	0.00
REV_13G1	0.44	11.63	0.62	8.83
SUND#5GN	0.44	11.67	0.51	-165.03
COULEE22	0.44	11.62	0.49	11.83
CGS	0.44	11.43	0.43	-0.11
SJUAN_G1	0.44	12.65	0.42	-164.54
RAWHIDE	0.46	10.79	0.39	166.37
JDA_0304	0.44	11.34	0.30	6.83
COLSTP_2	0.43	10.85	0.27	0.57
PALOVRD2	0.44	11.01	0.27	-172.92
CRAIG_1	0.45	10.39	0.24	-178.94
NAVAJO_1	0.44	11.00	0.23	-171.67
BRWNL_5	0.44	10.96	0.22	5.97
SLHWKG1	0.43	11.16	0.21	-154.36
MBPP-1	0.46	9.24	0.19	-179.76
SHEER_1	0.44	12.38	0.16	-155.63
DIABLO_1	0.42	10.29	0.09	-151.80
HYATT_1	0.45	9.54	0.09	-12.07
VALMY_G2	0.42	10.18	0.07	96.65
EHUNTER1	0.45	12.02	0.06	-165.34
BRIDGER1	0.44	8.21	0.06	-23.42
CURRNTC1	0.45	8.66	0.03	-127.06

Table 76: 2022 light spring (Note 4), 1.4 GW at Chief Joseph brake, 0.5 sec

Gen ID	**Freq**	**Damping**	**Residue**	**Angle**
COULEE22	0.85	14.91	1.00	0.00
JDA_0304	0.83	18.54	0.91	11.51
CGS	0.83	15.08	0.55	-1.46
REV_13G1	0.79	17.33	0.53	-101.64
BRWNL_5	0.81	20.66	0.50	-51.98
KMO_13G1	0.81	13.08	0.38	81.84
EHUNTER1	0.82	11.38	0.30	-139.13
CURRNTC1	0.82	10.26	0.24	-153.07
SHEER_1	0.80	10.61	0.11	-143.97
BRIDGER1	0.82	9.56	0.06	-101.11
SUND#5GN	0.83	14.21	0.05	117.66
SLHWKG1	0.81	8.54	0.03	-160.93
PALOVRD2	0.84	8.24	0.02	31.39
SJUAN_G1	0.84	6.39	0.02	-67.12
COLSTP_2	0.80	3.54	0.01	150.43
RAWHIDE	0.85	5.33	0.01	-7.20
NAVAJO_1	0.83	4.49	0.00	74.83
DIABLO_1	0.61	12.26	1.00	0.00
BRWNL_5	0.60	10.06	0.76	-8.05
BRIDGER1	0.59	6.68	0.13	19.76
SUND#5GN	0.27	17.79	1.00	0.00
SHEER_1	0.27	16.56	0.67	-12.21
MBPP-1	0.25	27.12	0.57	-152.86
BRIDGER1	0.26	28.01	0.36	-153.22
PALOVRD2	0.27	17.89	0.28	173.22
NAVAJO_1	0.27	17.21	0.24	-178.99
REV_13G1	0.29	15.47	0.17	-29.92
KMO_13G1	0.29	11.41	0.12	-46.25
EHUNTER1	0.74	11.73	1.00	0.00
DIABLO_1	0.69	14.00	0.95	-94.90
CURRNTC1	0.73	9.80	0.61	-7.97
SHEER_1	0.71	11.94	0.41	0.21
BRWNL_5	0.70	11.38	0.40	97.90
RAWHIDE	0.73	7.31	0.13	147.98
MBPP-1	0.71	7.73	0.07	-127.12
CRAIG_1	0.71	10.30	0.03	22.49
VALMY_G2	0.92	22.65	1.00	0.00
DIABLO_1	0.90	8.01	0.76	-154.45
CRAIG_1	0.89	10.70	0.51	-52.43
SLHWKG1	0.92	4.78	0.07	74.52
HYATT_1	0.92	1.68	0.04	145.90
SJUAN_G1	0.92	-0.92	0.00	-134.73
RAWHIDE	0.49	20.57	1.00	0.00
SJUAN_G1	0.51	21.41	0.90	8.55
CRAIG_1	0.53	26.62	0.69	-21.75

Table 77: 2022 light spring (Note 4), 1.4 GW at El Dorado bus, 0.5 sec

Gen ID	Freq	Damping	Residue	Angle
CGS	0.79	26.96	1.00	0.00
CRAIG_1	0.78	14.53	0.27	93.88
REV_13G1	0.80	11.55	0.22	-149.76
BRIDGER1	0.79	4.57	0.03	116.02
HYATT_1	0.96	6.23	1.00	0.00
COLSTP_2	0.95	6.08	0.71	157.20
CURRNTC1	0.95	12.85	0.68	-76.72
COULEE22	0.96	7.83	0.52	174.55
BRWNL_5	0.96	8.14	0.36	-28.55
RAWHIDE	0.97	9.28	0.24	-45.76
MBPP-1	0.95	6.50	0.16	5.08
JDA_0304	0.97	4.80	0.12	-105.19
REV_13G1	0.96	-20.15	0.00	10.34
KMO_13G1	0.62	13.62	1.00	0.00
BRIDGER1	0.63	14.89	0.26	145.98
REV_13G1	0.62	13.25	0.23	18.05
CGS	0.62	13.89	0.22	172.25
COULEE22	0.63	13.20	0.18	170.89
JDA_0304	0.63	12.77	0.16	159.50
BRWNL_5	0.65	11.53	0.16	122.55
COULEE22	0.65	28.32	0.16	-2.52
EHUNTER1	0.67	11.56	0.12	84.23
SHEER_1	0.66	16.55	0.11	8.98
COLSTP_2	0.66	10.89	0.10	99.03
SJUAN_G1	0.62	10.58	0.09	14.25
PALOVRD2	0.61	10.89	0.09	31.91
SUND#5GN	0.61	15.49	0.06	-148.64
KMO_13G1	0.68	14.46	1.00	0.00
CURRNTC1	0.71	10.47	0.13	-177.39
CGS	0.70	13.93	0.11	134.85
SLHWKG1	0.84	21.42	1.00	0.00
SJUAN_G1	0.87	10.63	0.44	86.53
PALOVRD2	0.86	20.25	0.22	8.26
HAYNES1G	0.84	9.93	0.18	-87.96
CRAIG_1	0.83	20.81	0.18	130.65
HYATT_1	0.86	6.39	0.09	49.51
COLSTP_2	0.86	7.13	0.09	-155.95
SHEER_1	0.83	14.08	0.07	80.20
SJUAN_G1	0.86	4.43	0.06	-61.90
COULEE22	0.86	5.04	0.04	-127.66
SUND#5GN	0.87	21.65	0.02	-44.23
CGS	0.87	4.22	0.02	-176.27
JDA_0304	0.87	5.40	0.01	-88.25
BRWNL_5	0.86	5.43	0.01	-155.93
KMO_13G1	0.84	4.42	0.01	-34.79
KMO_13G1	0.43	11.73	1.00	0.00
RAWHIDE	0.47	10.28	0.84	-32.16
MBPP-1	0.47	10.64	0.68	-17.43

Table 77: 2022 light spring (Note 4), 1.4 GW at El Dorado bus, 0.5 sec

Gen ID	Freq	Damping	Residue	Angle
REV_13G1	0.43	11.72	0.60	8.22
SUND#5GN	0.44	12.00	0.55	-173.63
PALOVRD2	0.44	13.49	0.53	-170.93
COLSTP_2	0.44	13.98	0.53	1.49
HAYNES1G	0.46	13.33	0.52	-175.79
BRWNL_5	0.45	14.02	0.50	-27.79
CRAIG_1	0.47	9.93	0.49	-9.93
SLHWKG1	0.44	14.11	0.47	-149.68
COULEE22	0.43	12.07	0.47	14.14
CGS	0.43	12.34	0.46	3.58
NAVAJO_1	0.44	13.18	0.44	-168.33
DIABLO_1	0.45	12.67	0.44	-158.86
BRIDGER1	0.46	14.76	0.44	-8.83
SJUAN_G1	0.44	11.08	0.31	177.81
CURRNTC1	0.47	13.53	0.26	3.46
VALMY_G2	0.45	13.33	0.23	83.44
JDA_0304	0.43	9.90	0.17	5.04
SHEER_1	0.44	12.14	0.17	175.56
EHUNTER1	0.47	9.48	0.12	-21.41
HYATT_1	0.45	6.36	0.07	-88.75
HYATT_1	0.60	14.13	1.00	0.00
CURRNTC1	0.58	14.38	0.63	12.15
COLSTP_2	0.57	15.42	0.39	48.10
RAWHIDE	0.74	10.97	1.00	0.00
MBPP-1	0.76	10.31	0.58	-21.93
REV_13G1	0.76	-3.93	0.01	29.04
NAVAJO_1	0.90	18.35	1.00	0.00
VALMY_G2	0.91	9.33	0.36	-42.12
DIABLO_1	0.91	3.76	0.12	-22.26
SHEER_1	0.93	4.46	0.03	-86.65
SUND#5GN	0.93	2.65	0.01	-177.27
SUND#5GN	0.26	20.12	1.00	0.00
SHEER_1	0.26	20.00	0.74	0.06
KMO_13G1	0.25	20.66	0.25	27.25
REV_13G1	0.25	20.50	0.23	25.72
VALMY_G2	0.26	16.26	0.21	165.43
RAWHIDE	0.27	19.83	0.21	161.31
PALOVRD2	0.27	17.92	0.20	167.98
SJUAN_G1	0.27	17.57	0.20	176.51
CRAIG_1	0.27	19.13	0.17	160.44
DIABLO_1	0.27	15.62	0.14	168.65
MBPP-1	0.27	17.54	0.13	173.97
EHUNTER1	0.27	18.06	0.11	173.89
CURRNTC1	0.28	19.06	0.10	148.04
HYATT_1	0.29	18.79	0.10	145.40
COLSTP_2	0.25	22.75	0.07	9.51
BRIDGER1	0.27	17.01	0.06	179.50
JDA_0304	0.29	24.37	0.03	169.54
BRWNL_5	0.28	-1.89	0.00	145.29

Table 78: 2022 light spring (Note 4), 1.4 GW at Hemingway Bus, 0.5 sec

Gen ID	Freq	Damping	Residue	Angle
MBPP-1	0.92	10.37	1.00	0.00
EHUNTER1	0.93	4.65	0.70	-145.18
SUND#5GN	0.91	6.97	0.10	161.30
CURRNTC1	0.75	22.65	1.00	0.00
KMO_13G1	0.76	14.62	0.96	-29.78
CGS	0.76	13.22	0.27	-64.21
COULEE22	0.76	12.47	0.27	-39.58
COLSTP_2	0.75	11.40	0.23	-53.79
REV_13G1	0.76	11.35	0.17	156.91
SHEER_1	0.76	8.32	0.05	148.31
SJUAN_G1	0.75	8.16	0.04	-64.47
KMO_13G1	0.43	11.69	1.00	0.00
SUND#5GN	0.44	11.71	0.51	-169.20
SJUAN_G1	0.45	13.17	0.48	155.62
DIABLO_1	0.45	15.46	0.44	-167.54
PALOVRD2	0.44	13.04	0.44	-168.69
NAVAJO_1	0.44	13.80	0.43	-174.95
REV_13G1	0.43	9.85	0.41	6.97
COULEE22	0.44	10.73	0.40	0.09
HAYNES1G	0.45	14.94	0.39	-150.64
CGS	0.44	10.89	0.39	-14.85
COLSTP_2	0.44	10.70	0.29	-15.44
SLHWKG1	0.44	11.83	0.29	-169.83
BRIDGER1	0.44	15.50	0.27	14.88
EHUNTER1	0.42	24.25	0.25	114.79
JDA_0304	0.43	11.07	0.24	10.18
SHEER_1	0.42	13.62	0.17	-122.00
SUND#5GN	0.26	19.66	1.00	0.00
SHEER_1	0.25	22.36	0.91	10.23
KMO_13G1	0.27	25.44	0.52	-28.49
SLHWKG1	0.25	28.05	0.40	-147.67
VALMY_G2	0.29	21.20	0.38	82.48
PALOVRD2	0.28	15.84	0.17	144.78
HAYNES1G	0.25	7.62	0.13	143.74
NAVAJO_1	0.27	12.51	0.11	171.34
CRAIG_1	0.25	13.85	0.10	-150.15
SJUAN_G1	0.25	12.21	0.09	-151.30
MBPP-1	0.28	10.17	0.07	146.53
DIABLO_1	0.97	6.75	1.00	0.00
SHEER_1	0.94	11.97	0.81	-143.18
HYATT_1	0.95	5.00	0.66	47.54
SJUAN_G1	0.95	3.97	0.15	109.67
NAVAJO_1	0.97	6.22	0.08	-66.26
KMO_13G1	0.71	13.18	1.00	0.00
BRWNL_5	0.73	11.70	0.19	159.58
JDA_0304	0.72	11.79	0.15	-128.93

Table 78: 2022 light spring (Note 4), 1.4 GW at Hemingway Bus, 0.5 sec

Gen ID	Freq	Damping	Residue	Angle
NAVAJO_1	0.70	12.99	0.08	-152.80
HYATT_1	0.70	8.99	0.07	61.10
EHUNTER1	0.72	7.28	0.07	178.46
PALOVRD2	0.73	11.18	0.07	172.42
CURRNTC1	0.74	7.01	0.07	80.85
MBPP-1	0.70	10.74	0.05	43.53
HAYNES1G	0.73	9.05	0.05	41.44
SUND#5GN	0.73	13.33	0.04	-91.86
VALMY_G2	0.46	16.17	1.00	0.00
MBPP-1	0.48	10.59	0.55	-79.31
CRAIG_1	0.49	9.17	0.32	-59.89
KMO_13G1	0.62	10.29	1.00	0.00
BRIDGER1	0.60	17.61	0.48	-96.00
SJUAN_G1	0.65	11.26	0.40	-32.00
NAVAJO_1	0.62	14.55	0.30	47.32
JDA_0304	0.62	11.36	0.28	-173.03
PALOVRD2	0.62	11.89	0.27	31.95
HYATT_1	0.61	10.62	0.23	-142.04
SUND#5GN	0.63	12.94	0.11	-166.62
REV_13G1	0.62	6.16	0.07	33.26
SLHWKG1	0.63	8.36	0.07	12.81
CGS	0.61	5.56	0.04	-168.51
COULEE22	0.61	5.50	0.03	-143.49
COLSTP_2	0.60	4.82	0.02	-121.08
EHUNTER1	0.86	19.40	1.00	0.00
JDA_0304	0.85	18.19	0.53	173.76
COLSTP_2	0.88	16.27	0.23	14.60

Table 79: 2022 light spring (Note 4), 1.4 GW at Midway bus, 0.5 sec

Gen ID	Freq	Damping	Residue	Angle
COULEE22	0.97	11.05	1.00	0.00
PALOVRD2	0.97	11.46	0.68	116.00
COLSTP_2	0.98	6.16	0.51	-94.32
VALMY_G2	0.99	6.97	0.49	79.71
BRWNL_5	0.97	7.81	0.19	79.41
SHEER_1	0.98	5.88	0.08	164.16
CURRNTC1	1.00	6.56	0.07	-72.96
SUND#5GN	0.26	19.47	1.00	0.00
SHEER_1	0.26	20.02	0.79	-2.68
KMO_13G1	0.25	23.14	0.33	22.88
REV_13G1	0.25	23.06	0.29	28.52
SLHWKG1	0.26	21.52	0.25	-157.65
PALOVRD2	0.26	19.58	0.24	178.54
NAVAJO_1	0.26	18.61	0.21	179.67
SJUAN_G1	0.27	15.77	0.18	174.76
HAYNES1G	0.27	15.47	0.15	166.38

Table 79: 2022 light spring (Note 4), 1.4 GW at Midway bus, 0.5 sec

Gen ID	Freq	Damping	Residue	Angle
VALMY_G2	0.27	11.59	0.13	131.96
MBPP-1	0.27	16.07	0.12	172.73
CRAIG_1	0.26	15.72	0.12	-161.23
COLSTP_2	0.24	27.44	0.10	15.25
EHUNTER1	0.25	15.99	0.09	-152.60
CURRNTC1	0.28	15.97	0.08	151.32
RAWHIDE	0.27	8.49	0.06	144.07
HYATT_1	0.27	12.89	0.05	166.63
BRIDGER1	0.28	12.70	0.05	153.46
SJUAN_G1	0.60	22.31	1.00	0.00
JDA_0304	0.63	17.14	0.88	163.04
KMO_13G1	0.64	9.52	0.80	-96.11
REV_13G1	0.63	12.94	0.39	-14.44
COULEE22	0.61	16.76	0.39	-152.04
CGS	0.63	10.86	0.21	105.24
COULEE22	0.88	10.43	1.00	0.00
SHEER_1	0.87	17.71	0.70	138.08
CGS	0.86	8.84	0.33	-1.49
KMO_13G1	0.84	9.59	0.31	92.39
REV_13G1	0.86	8.54	0.11	-161.76
VALMY_G2	0.86	4.70	0.07	-162.68
SUND#5GN	0.86	5.15	0.01	105.49
MBPP-1	0.83	4.32	0.01	42.72
RAWHIDE	0.47	9.49	1.00	0.00
MBPP-1	0.47	10.51	0.92	14.88
CRAIG_1	0.47	9.55	0.64	14.96
PALOVRD2	0.45	14.67	0.47	-137.19
SLHWKG1	0.46	14.80	0.46	-131.02
KMO_13G1	0.42	12.51	0.46	43.74
NAVAJO_1	0.45	14.70	0.42	-136.20
COLSTP_2	0.44	15.71	0.42	36.30
HAYNES1G	0.46	12.06	0.40	-141.89
BRIDGER1	0.46	12.41	0.35	42.53
SUND#5GN	0.43	13.04	0.29	-139.19
REV_13G1	0.42	12.53	0.28	57.67
BRWNL_5	0.44	14.71	0.28	40.42
CURRNTC1	0.47	11.25	0.23	18.84
CGS	0.42	13.16	0.21	54.71
COULEE22	0.42	11.98	0.18	62.43
VALMY_G2	0.47	11.63	0.17	83.80
EHUNTER1	0.47	9.49	0.15	26.59
HYATT_1	0.44	11.66	0.13	-47.48
SJUAN_G1	0.43	7.94	0.08	-148.77
SHEER_1	0.44	11.48	0.07	-145.83
JDA_0304	0.44	1.07	0.01	-32.29
BRIDGER1	0.41	2.60	0.01	-25.36
DIABLO_1	0.91	8.47	1.00	0.00
SJUAN_G1	0.95	26.41	0.64	-99.71
HYATT_1	0.93	5.16	0.30	-58.18
JDA_0304	0.95	7.62	0.17	144.04

Table 79: 2022 light spring (Note 4), 1.4 GW at Midway bus, 0.5 sec

Gen ID	Freq	Damping	Residue	Angle
NAVAJO_1	0.93	8.09	0.10	-149.03
CRAIG_1	0.92	11.66	0.09	-24.80
SLHWKG1	0.93	3.57	0.04	-124.20
REV_13G1	0.96	11.40	0.03	-0.44
HAYNES1G	0.93	2.77	0.03	-129.84
SHEER_1	0.75	24.00	1.00	0.00
COLSTP_2	0.75	15.74	0.85	144.07
BRWNL_5	0.75	12.53	0.46	146.49
BRIDGER1	0.77	9.93	0.24	106.64
NAVAJO_1	0.74	12.62	0.21	164.88
EHUNTER1	0.78	7.49	0.20	93.30
CURRNTC1	0.78	6.76	0.15	76.23
JDA_0304	0.71	17.03	1.00	0.00
PALOVRD2	0.68	22.67	0.73	-10.94
COULEE22	0.70	13.46	0.72	30.59
KMO_13G1	0.72	8.94	0.67	114.66
COLSTP_2	0.68	12.09	0.54	52.47
HYATT_1	0.72	14.14	0.54	145.73
DIABLO_1	0.71	10.79	0.42	137.25
REV_13G1	0.73	11.87	0.39	-163.49
CGS	0.71	11.43	0.37	-14.80
SHEER_1	0.71	13.05	0.37	-100.54
BRWNL_5	0.67	10.59	0.34	60.49
RAWHIDE	0.69	10.89	0.32	134.51
EHUNTER1	0.69	8.73	0.31	2.01
BRIDGER1	0.68	10.00	0.29	30.53
CURRNTC1	0.69	8.20	0.27	-13.44
SLHWKG1	0.71	15.59	0.20	-64.89
MBPP-1	0.69	11.26	0.17	169.47
HAYNES1G	0.69	10.42	0.17	-139.93
SJUAN_G1	0.70	8.59	0.16	11.88
VALMY_G2	0.69	8.74	0.14	14.76
CRAIG_1	0.67	13.99	0.13	-138.93
SUND#5GN	0.66	13.14	0.08	159.08

Table 80: 2022 light spring (Note 4), double Palo Verde trip

Gen ID	Freq	Damping	Residue	Angle
KMO_13G1	0.44	9.97	1.00	0.00
BRWNL_5	0.44	14.34	0.80	17.65
CGS	0.44	11.88	0.72	3.46
SLHWKG1	0.45	13.28	0.70	-153.07
SUND#5GN	0.44	11.06	0.67	-169.78
COLSTP_2	0.45	12.62	0.65	-8.80
HAYNES1G	0.45	12.32	0.64	-148.23
DIABLO_1	0.44	13.15	0.63	-131.75
VALMY_G2	0.44	13.34	0.59	102.82
NAVAJO_1	0.44	12.16	0.58	-158.51
REV_13G1	0.44	9.13	0.40	-11.20

Table 80: 2022 light spring (Note 4), double Palo Verde trip

Gen ID	Freq	Damping	Residue	Angle
SJUAN_G1	0.44	9.25	0.39	167.56
COULEE22	0.44	7.45	0.36	57.48
JDA_0304	0.43	11.08	0.33	16.90
EHUNTER1	0.43	18.85	0.26	78.93
COULEE22	0.42	6.97	0.25	-25.50
HYATT_1	0.44	10.18	0.23	-53.02
SHEER_1	0.44	11.52	0.19	-174.82
BRWNL_5	0.52	19.59	1.00	0.00
DIABLO_1	0.51	15.40	0.51	-87.25
SJUAN_G1	0.51	8.08	0.08	-22.20
CURRNTC1	0.71	24.62	1.00	0.00
KMO_13G1	0.72	8.28	0.53	-1.75
COULEE22	0.70	7.90	0.21	-119.53
SUND#5GN	0.26	19.42	1.00	0.00
SHEER_1	0.26	19.18	0.70	-0.07
SLHWKG1	0.28	17.31	0.31	154.24
CURRNTC1	0.26	21.29	0.24	-174.22
VALMY_G2	0.26	13.36	0.19	161.83
NAVAJO_1	0.26	15.06	0.16	172.63
SJUAN_G1	0.27	13.71	0.15	167.38
DIABLO_1	0.26	14.75	0.14	-173.58
HAYNES1G	0.27	13.86	0.14	163.92
RAWHIDE	0.26	12.19	0.09	171.87
EHUNTER1	0.26	13.50	0.08	177.42
CRAIG_1	0.25	12.17	0.08	-155.41
MBPP-1	0.26	11.36	0.07	179.40
HYATT_1	0.26	12.01	0.05	-174.62
BRIDGER1	0.26	11.49	0.04	177.41
JDA_0304	0.26	8.07	0.02	-178.41
BRWNL_5	0.26	5.21	0.01	-169.74
SHEER_1	0.27	-0.36	0.00	17.14
SUND#5GN	0.27	-2.49	0.00	-22.49
RAWHIDE	0.41	24.59	1.00	0.00
MBPP-1	0.40	22.91	0.71	0.26
REV_13G1	0.39	12.09	0.36	28.09
BRIDGER1	0.40	15.03	0.28	1.07
KMO_13G1	0.39	8.18	0.10	7.59
COLSTP_2	0.38	8.78	0.07	68.31
HYATT_1	0.75	21.21	1.00	0.00
BRWNL_5	0.76	16.57	0.20	87.90
SHEER_1	0.75	8.11	0.12	18.16
HYATT_1	0.75	4.52	0.03	-94.38
KMO_13G1	0.60	13.35	1.00	0.00
COLSTP_2	0.59	19.88	0.57	-147.29
BRIDGER1	0.61	18.71	0.47	-176.35
NAVAJO_1	0.60	17.82	0.36	36.90
EHUNTER1	0.64	18.46	0.27	-175.09
COULEE22	0.61	6.91	0.13	117.43

Table 80: 2022 light spring (Note 4), double Palo Verde trip

Gen ID	Freq	Damping	Residue	Angle
COULEE22	0.63	5.87	0.08	-165.98
RAWHIDE	0.60	5.76	0.02	-23.67
RAWHIDE	0.48	7.46	1.00	0.00
CRAIG_1	0.47	9.33	0.99	41.14
MBPP-1	0.47	7.37	0.74	20.23
BRIDGER1	0.47	9.12	0.29	7.50
CURRNTC1	0.47	7.90	0.18	9.09
EHUNTER1	0.47	5.69	0.08	11.05
RAWHIDE	0.47	1.83	0.04	-118.07
MBPP-1	0.49	0.56	0.01	141.34
SLHWKG1	0.54	29.58	1.00	0.00
JDA_0304	0.55	23.40	0.92	165.48
CRAIG_1	0.54	14.27	0.25	173.77
VALMY_G2	0.57	8.72	0.10	-146.77
HAYNES1G	0.55	8.30	0.05	40.90
EHUNTER1	0.57	7.13	0.04	-173.55
DIABLO_1	0.68	16.08	1.00	0.00
REV_13G1	0.66	13.96	0.81	138.14
CGS	0.65	13.14	0.76	-110.14
KMO_13G1	0.67	8.61	0.63	28.40
COLSTP_2	0.67	11.78	0.56	-154.20
BRWNL_5	0.66	11.48	0.50	-127.38
BRIDGER1	0.69	11.32	0.38	169.75
JDA_0304	0.68	11.21	0.36	-116.32
EHUNTER1	0.69	9.61	0.35	164.22
SHEER_1	0.66	13.43	0.30	139.41
CURRNTC1	0.68	8.80	0.25	-175.13
CRAIG_1	0.65	12.42	0.16	75.56
RAWHIDE	0.69	8.32	0.13	-68.47
SUND#5GN	0.67	14.37	0.10	-43.64
MBPP-1	0.68	8.97	0.09	-16.60
HAYNES1G	0.68	6.42	0.06	43.91
VALMY_G2	0.68	5.91	0.04	-127.39
REV_13G1	0.29	13.06	1.00	0.00
SLHWKG1	0.31	13.74	0.90	6.29
KMO_13G1	0.30	10.80	0.60	-37.78
CURRNTC1	0.32	12.90	0.56	-33.87
HAYNES1G	0.32	9.83	0.21	-96.27
CGS	0.30	7.74	0.13	25.18
COLSTP_2	0.30	6.12	0.08	-26.34
CURRNTC1	0.36	11.73	1.00	0.00
SJUAN_G1	0.34	7.33	0.38	-152.22
CGS	0.36	7.34	0.30	0.95
NAVAJO_1	0.34	8.22	0.25	-146.72
BRIDGER1	0.34	4.77	0.17	154.99
RAWHIDE	0.34	2.42	0.12	126.98
MBPP-1	0.35	2.46	0.12	112.35
BRWNL_5	0.35	3.20	0.10	87.59
JDA_0304	0.35	2.48	0.08	95.09

Table 80: 2022 light spring (Note 4), double Palo Verde trip

Gen ID	**Freq**	**Damping**	**Residue**	**Angle**
SHEER_1	0.36	2.45	0.07	-136.22
SUND#5GN	0.37	0.08	0.05	-158.26
CRAIG_1	0.34	-0.39	0.03	144.43
EHUNTER1	0.78	8.04	1.00	0.00
JDA_0304	0.82	9.33	0.51	108.04
BRIDGER1	0.80	7.87	0.46	-38.38
COULEE22	0.79	5.66	0.38	145.17
KMO_13G1	0.81	4.81	0.36	132.54
CGS	0.80	4.05	0.15	96.01
COLSTP_2	0.79	3.26	0.14	137.80
BRWNL_5	0.83	2.38	0.05	-91.31
VALMY_G2	0.13	23.81	1.00	0.00
SHEER_1	0.10	28.84	0.70	152.40
RAWHIDE	0.14	27.02	0.70	-43.55
SUND#5GN	0.13	28.35	0.48	34.80
EHUNTER1	0.15	19.64	0.43	-79.50
NAVAJO_1	0.13	12.19	0.24	19.47
BRIDGER1	0.15	16.37	0.24	-53.38
HAYNES1G	0.13	14.73	0.23	41.56
BRWNL_5	0.14	17.79	0.20	7.58
JDA_0304	0.13	14.79	0.18	24.90
HYATT_1	0.14	9.96	0.12	-25.39
SLHWKG1	0.92	13.56	1.00	0.00
HYATT_1	0.94	11.35	0.98	132.56
SUND#5GN	0.95	6.26	0.10	118.24

Appendix E - Prony Analysis, Low Damping Signals

Note 1: For this case, type 3/4 wind turbines were replaced with **genrou** models with governors

Note 2: For this case, type 3/4 wind turbines were replaced with **genrou** models without governors

Note 3: For this case, all wind turbines were replaced with **genrou** models with governors

Note 4: For this case, all wind turbines were replaced with **genrou** models without governors

Table 81: Summary of low damping signals

Gen ID	**Freq**	**Damping**	**Rel E**	**Energy**
2012 heavy summer, 1.4 GW at Chief Joseph brake, 0.5 sec				
HAYNES1G	0.87	4.84	1.00	0.000000002
CURRNTC1	0.85	5.21	0.83	0.000000001
SHEER_1	0.85	3.48	0.50	0.000000001
KMO_13G1	0.72	7.36	0.62	0.000003072
NAVAJO_1	0.55	8.64	0.23	0.000000015
BRWNL_5	0.78	8.38	0.11	0.000000287
RAWHIDE	0.36	8.57	0.27	0.000002803
HYATT_1	0.81	8.12	0.28	0.000000011
2012 heavy winter, 1.4 GW at Chief Joseph brake, 0.5 sec				
CRAIG_1	0.72	8.68	0.12	0.000000183
COLSTP_2	0.87	7.93	1.00	0.000000869
SHEER_1	0.90	7.25	0.14	0.000000017
MBPP-1	0.74	7.57	0.25	0.000000106
HYATT_1	0.76	6.68	0.18	0.000000053
PALOVRD2	0.55	8.74	0.11	0.000000123
2012 light summer, 1.4 GW at Chief Joseph brake, 0.5 sec				
BRIDGER1	0.41	8.95	0.22	0.000002927
RAWHIDE	0.41	4.28	0.17	0.000003682
CRAIG_1	0.41	6.65	0.16	0.000002075
CURRNTC1	0.41	8.84	0.12	0.000000851
HAYNES1G	0.40	7.51	0.11	0.000000971
MBPP-1	0.92	8.52	0.48	0.000000420
RAWHIDE	0.45	3.12	0.23	0.000000747
CGS	0.90	6.84	0.55	0.000000196
HAYNES1G	0.86	8.76	0.50	0.000000134
DIABLO_1	0.88	7.25	0.32	0.000000064
VALMY_G2	0.85	6.95	0.32	0.000000068
PALOVRD2	0.89	7.98	0.17	0.000000016
REV_13G1	0.88	3.06	0.15	0.000000031
KMO_13G1	0.90	3.61	0.14	0.000000026
SLHWKG1	0.89	7.33	0.14	0.000000013
NAVAJO_1	0.86	8.06	0.13	0.000000011
2022 heavy winter, 1.4 GW at Chief Joseph brake, 0.5 sec				
CURRNTC1	0.79	8.18	0.53	0.000000661
KMO_13G1	0.79	6.83	0.18	0.000000091
REV_13G1	0.57	8.62	0.24	0.000000080
2022 light summer, 1.4 GW at Chief Joseph brake, 0.5 sec				
REV_13G1	0.85	8.21	0.13	0.000000232

Table 81: Summary of low damping signals

Gen ID	Freq	Damping	Rel E	Energy
2022 light spring, 1.4 GW at Chief Joseph brake, 0.5 sec				
MBPP-1	0.97	7.77	1.00	0.000000165
SLHWKG1	0.94	7.10	0.21	0.000000008
DIABLO_1	0.89	7.39	0.50	0.000000515
HAYNES1G	0.88	5.35	0.15	0.000000058
2022 light spring (Note 1), 1.4 GW at Chief Joseph brake, 0.5 sec				
HYATT_1	0.64	8.49	0.44	0.000000298
REV_13G1	0.64	8.31	0.42	0.000000274
JDA_0304	0.64	7.61	0.28	0.000000127
DIABLO_1	0.89	7.28	0.23	0.000000351
RAWHIDE	0.53	8.98	0.21	0.000000147
2022 light spring (Note 2), 1.4 GW at Chief Joseph brake, 0.5 sec				
RAWHIDE	0.73	7.34	0.11	0.000000100
COLSTP_2	0.74	6.58	0.10	0.000000098
MBPP-1	0.46	8.83	0.17	0.000001943
DIABLO_1	0.90	7.14	0.11	0.000000298
KMO_13G1	0.65	7.09	0.11	0.000003421
2022 light spring (Note 3), 1.4 GW at Chief Joseph brake, 0.5 sec				
KMO_13G1	0.62	8.62	0.98	0.000003887
JDA_0304	0.63	8.01	0.19	0.000000155
REV_13G1	0.63	6.94	0.17	0.000000149
DIABLO_1	0.89	6.97	1.00	0.000000237
CURRNTC1	0.94	7.54	0.70	0.000000108
CRAIG_1	0.89	6.90	0.21	0.000000012
SLHWKG1	0.92	5.65	0.19	0.000000011
CURRNTC1	0.86	8.91	0.23	0.000001242
2022 light spring (Note 4), 1.4 GW at Chief Joseph brake, 0.5 sec				
KMO_13G1	0.66	7.95	0.20	0.000007585
BRIDGER1	0.59	6.68	0.13	0.000000012
RAWHIDE	0.73	7.31	0.13	0.000000128
DIABLO_1	0.90	8.01	0.76	0.000000389
2012 heavy summer, 1.4 GW at El Dorado bus, 0.5 sec				
SJUAN_G1	0.55	8.12	0.62	0.000000046
BRIDGER1	0.77	8.29	0.16	0.000000023
DIABLO_1	0.99	8.40	1.00	0.000000167
COLSTP_2	0.79	7.00	0.89	0.000000020
CURRNTC1	0.58	8.39	0.25	0.000000010
EHUNTER1	0.58	7.51	0.19	0.000000006
2012 heavy winter, 1.4 GW at El Dorado bus, 0.5 sec				
KMO_13G1	0.69	8.90	0.91	0.000001526
VALMY_G2	0.17	6.29	0.52	0.000000024
VALMY_G2	0.63	6.79	0.11	0.000000015
PALOVRD2	0.89	8.73	1.00	0.000000029
BRIDGER1	0.87	8.11	0.53	0.000000009
SJUAN_G1	0.96	6.80	0.58	0.000000010
2012 light summer, 1.4 GW at El Dorado bus, 0.5 sec				
KMO_13G1	0.72	8.58	0.76	0.000001035

Table 81: Summary of low damping signals

Gen ID	Freq	Damping	Rel E	Energy
MBPP-1	0.71	8.33	0.11	0.000000020
CURRNTC1	0.72	6.90	0.10	0.000000023
COLSTP_2	0.79	7.89	0.86	0.000001901
MBPP-1	0.86	6.46	0.46	0.000000047
CRAIG_1	0.88	7.39	0.26	0.000000012
CGS	0.87	6.33	0.21	0.000000010
EHUNTER1	0.89	4.91	0.20	0.000000011
BRWNL_5	0.85	4.69	0.17	0.000000009
CURRNTC1	0.89	3.38	0.11	0.000000005
2022 heavy winter, 1.4 GW at El Dorado bus, 0.5 sec				
CRAIG_1	0.96	8.62	0.29	0.000000002
EHUNTER1	0.96	2.34	0.11	0.000000001
2022 light summer, 1.4 GW at El Dorado bus, 0.5 sec				
COLSTP_2	0.84	8.99	0.16	0.000000005
2022 light spring, 1.4 GW at El Dorado bus, 0.5 sec				
HYATT_1	0.95	5.73	0.92	0.000000117
COLSTP_2	0.96	6.69	0.87	0.000000091
COULEE22	0.95	8.06	0.69	0.000000049
JDA_0304	0.95	7.32	0.32	0.000000011
MBPP-1	0.96	8.35	0.24	0.000000005
SHEER_1	0.94	5.06	0.15	0.000000003
CRAIG_1	0.51	6.56	0.33	0.000005093
CURRNTC1	0.53	7.49	0.10	0.000000377
PALOVRD2	0.60	7.58	0.40	0.000000384
BRIDGER1	0.56	6.60	0.26	0.000000220
REV_13G1	0.45	8.10	0.36	0.000004505
REV_13G1	0.42	8.60	0.16	0.000000879
2022 light spring (Note 1), 1.4 GW at El Dorado bus, 0.5 sec				
HYATT_1	0.95	5.03	0.24	0.000000073
COULEE22	0.95	6.90	0.19	0.000000035
COLSTP_2	0.96	5.09	0.16	0.000000034
MBPP-1	0.78	8.91	0.47	0.000000023
DIABLO_1	0.76	4.83	0.18	0.000000006
HYATT_1	0.85	6.22	0.26	0.000000158
COLSTP_2	0.86	6.60	0.25	0.000000124
COULEE22	0.86	5.71	0.20	0.000000095
SJUAN_G1	0.83	3.34	0.10	0.000000045
2022 light spring (Note 2), 1.4 GW at El Dorado bus, 0.5 sec				
KMO_13G1	0.79	5.11	0.13	0.000000020
HYATT_1	0.96	5.37	0.64	0.000000086
COLSTP_2	0.96	5.95	0.54	0.000000054
COULEE22	0.95	7.07	0.54	0.000000047
BRWNL_5	0.95	7.90	0.32	0.000000015
CGS	0.95	7.23	0.24	0.000000009
MBPP-1	0.94	6.68	0.14	0.000000004
2022 light spring (Note 3), 1.4 GW at El Dorado bus, 0.5 sec				
SJUAN_G1	0.83	4.74	0.25	0.000000122
COLSTP_2	0.86	6.85	0.27	0.000000127

Table 81: Summary of low damping signals

Gen ID	Freq	Damping	Rel E	Energy
HYATT_1	0.86	5.59	0.26	0.000000150
COULEE22	0.87	5.61	0.20	0.000000084
2022 light spring (Note 4), 1.4 GW at El Dorado bus, 0.5 sec				
HYATT_1	0.96	6.23	1.00	0.000000143
COLSTP_2	0.95	6.08	0.71	0.000000075
COULEE22	0.96	7.83	0.52	0.000000031
BRWNL_5	0.96	8.14	0.36	0.000000015
MBPP-1	0.95	6.50	0.16	0.000000003
JDA_0304	0.97	4.80	0.12	0.000000002
DIABLO_1	0.91	3.76	0.12	0.000000064
2012 heavy summer, 1.4 GW at Hemingway Bus, 0.5 sec				
KMO_13G1	0.74	7.87	0.61	0.000001044
REV_13G1	0.49	8.00	0.10	0.000000494
CGS	0.33	8.41	0.29	0.000000557
COULEE22	0.33	6.19	0.18	0.000000285
SJUAN_G1	0.36	4.99	0.16	0.000000242
2012 heavy winter, 1.4 GW at Hemingway Bus, 0.5 sec				
SLHWKG1	0.89	8.39	0.70	0.000000004
RAWHIDE	0.91	8.40	0.52	0.000000002
CGS	0.89	5.46	0.29	0.000000001
SHEER_1	0.91	6.24	0.23	0.000000001
KMO_13G1	0.72	6.15	0.12	0.000001075
MBPP-1	0.31	8.31	0.28	0.000000019
NAVAJO_1	0.27	8.02	0.20	0.000000012
COLSTP_2	0.85	8.39	0.31	0.000000190
2012 light summer, 1.4 GW at Hemingway Bus, 0.5 sec				
KMO_13G1	0.88	6.59	0.10	0.000000219
MBPP-1	0.39	7.57	0.20	0.000000814
RAWHIDE	0.40	6.58	0.19	0.000000846
CRAIG_1	0.40	6.70	0.12	0.000000343
COLSTP_2	0.78	7.69	0.21	0.000003615
2022 heavy winter, 1.4 GW at Hemingway Bus, 0.5 sec				
MBPP-1	0.43	8.58	0.16	0.000000009
COLSTP_2	0.39	8.61	0.12	0.000000066
2022 light summer, 1.4 GW at Hemingway Bus, 0.5 sec				
RAWHIDE	0.21	5.77	0.48	0.000000002
CGS	0.91	6.38	0.11	0.000000019
CURRNTC1	0.85	6.30	0.88	0.000000053
EHUNTER1	0.85	5.70	0.69	0.000000037
HAYNES1G	0.85	9.00	0.40	0.000000007
2022 light spring, 1.4 GW at Hemingway Bus, 0.5 sec				
SUND#5GN	1.00	8.06	0.16	0.000000019
HAYNES1G	0.99	7.14	0.14	0.000000016
KMO_13G1	0.74	7.80	0.12	0.000001569
CRAIG_1	0.49	8.59	0.55	0.000000575
EHUNTER1	0.51	8.29	0.25	0.000000133

Table 81: Summary of low damping signals

Gen ID	Freq	Damping	Rel E	Energy
2022 light spring (Note 1), 1.4 GW at Hemingway Bus, 0.5 sec				
KMO_13G1	0.74	7.65	0.31	0.000003201
EHUNTER1	0.73	7.67	0.17	0.000000805
SHEER_1	0.76	8.89	0.12	0.000000352
HYATT_1	0.95	5.26	0.62	0.000000058
DIABLO_1	0.95	4.12	0.33	0.000000021
2022 light spring (Note 2), 1.4 GW at Hemingway Bus, 0.5 sec				
REV_13G1	0.64	7.69	0.12	0.000000535
SHEER_1	0.71	6.08	0.21	0.000000052
EHUNTER1	0.73	8.11	0.11	0.000001258
CURRNTC1	0.72	8.18	0.11	0.000001141
EHUNTER1	0.94	2.50	0.20	0.000000017
2022 light spring (Note 3), 1.4 GW at Hemingway Bus, 0.5 sec				
EHUNTER1	0.76	7.05	0.20	0.000000947
CURRNTC1	0.74	6.22	0.12	0.000000417
RAWHIDE	0.48	6.18	0.19	0.000000172
CRAIG_1	0.51	3.20	0.14	0.000000154
DIABLO_1	0.94	4.39	0.17	0.000000030
KMO_13G1	0.73	8.99	0.25	0.000007172
REV_13G1	0.62	8.22	0.12	0.000000635
CRAIG_1	0.54	5.15	0.11	0.000000144
2022 light spring (Note 4), 1.4 GW at Hemingway Bus, 0.5 sec				
EHUNTER1	0.93	4.65	0.70	0.000000082
SUND#5GN	0.91	6.97	0.10	0.000000001
HAYNES1G	0.25	7.62	0.13	0.000000082
DIABLO_1	0.97	6.75	1.00	0.000000090
HYATT_1	0.95	5.00	0.66	0.000000058
SJUAN_G1	0.95	3.97	0.15	0.000000004
2012 heavy summer, 1.4 GW at Midway bus, 0.5 sec				
BRIDGER1	0.54	8.72	0.17	0.000000430
KMO_13G1	0.59	7.43	0.40	0.000007010
SJUAN_G1	0.51	8.74	0.13	0.000000156
KMO_13G1	0.68	6.64	0.86	0.000002099
BRIDGER1	0.82	7.68	1.00	0.000000008
COULEE22	0.80	6.24	0.94	0.000000010
CGS	0.80	5.24	0.60	0.000000005
CURRNTC1	0.84	3.43	0.19	0.000000001
KMO_13G1	0.22	5.48	0.12	0.000000406
2012 heavy winter, 1.4 GW at Midway bus, 0.5 sec				
COLSTP_2	0.87	5.92	0.42	0.000000038
JDA_0304	0.84	7.13	0.26	0.000000013
SUND#5GN	0.91	9.00	0.21	0.000000006
SHEER_1	0.68	6.77	0.11	0.000000061
KMO_13G1	0.67	7.65	1.00	0.000010435
BRWNL_5	0.66	8.66	0.11	0.000000105
CRAIG_1	0.76	7.12	0.19	0.000000042
EHUNTER1	0.81	7.18	0.19	0.000000037
BRIDGER1	0.79	8.88	0.13	0.000000016
CURRNTC1	0.81	5.71	0.12	0.000000019

Table 81: Summary of low damping signals

Gen ID	Freq	Damping	Rel E	Energy
2012 light summer, 1.4 GW at Midway bus, 0.5 sec				
MBPP-1	0.86	6.77	0.17	0.000000102
COULEE22	0.90	7.49	0.17	0.000000093
BRIDGER1	0.85	8.94	0.10	0.000000029
VALMY_G2	0.19	6.73	0.12	0.000000012
COLSTP_2	0.80	6.35	0.26	0.000000688
2022 heavy winter, 1.4 GW at Midway bus, 0.5 sec				
CGS	0.85	7.77	0.32	0.000000005
KMO_13G1	0.66	5.50	0.36	0.000001553
KMO_13G1	0.73	5.60	0.28	0.000000218
CURRNTC1	0.75	7.25	0.13	0.000000037
EHUNTER1	0.74	6.80	0.12	0.000000035
KMO_13G1	0.58	8.26	0.78	0.000003553
SLHWKG1	0.92	8.05	0.17	0.000000005
2022 light summer, 1.4 GW at Midway bus, 0.5 sec				
COULEE22	0.84	7.76	0.27	0.000000029
CURRNTC1	0.85	7.76	0.26	0.000000025
MBPP-1	0.84	8.88	0.12	0.000000005
BRIDGER1	0.76	8.07	0.10	0.000000005
KMO_13G1	0.70	8.71	0.52	0.000003586
2022 light spring, 1.4 GW at Midway bus, 0.5 sec				
DIABLO_1	0.55	7.45	0.23	0.000000606
COLSTP_2	0.91	6.50	0.23	0.000000832
EHUNTER1	0.80	8.16	0.21	0.000000477
CURRNTC1	0.79	7.85	0.21	0.000000489
CGS	0.87	8.68	0.23	0.000000460
COLSTP_2	1.00	8.98	1.00	0.000001066
HYATT_1	0.94	5.21	0.57	0.000000642
JDA_0304	0.95	8.18	0.40	0.000000183
JDA_0304	0.46	8.31	0.12	0.000000220
2022 light spring (Note 1), 1.4 GW at Midway bus, 0.5 sec				
JDA_0304	0.95	8.40	0.15	0.000000251
CURRNTC1	0.79	8.41	0.54	0.000000433
BRIDGER1	0.77	8.86	0.46	0.000000312
HYATT_1	0.47	8.83	0.11	0.000000212
DIABLO_1	0.91	7.95	1.00	0.000003091
COLSTP_2	0.94	6.43	0.64	0.000001679
HYATT_1	0.93	4.89	0.30	0.000000505
COULEE22	0.88	8.66	1.00	0.000001366
KMO_13G1	0.87	8.92	0.25	0.000000087
REV_13G1	0.87	8.47	0.19	0.000000051
2022 light spring (Note 2), 1.4 GW at Midway bus, 0.5 sec				
BRWNL_5	0.71	8.91	0.20	0.000001203
DIABLO_1	0.91	8.65	1.00	0.000004546
COLSTP_2	0.91	7.36	0.55	0.000001802
HYATT_1	0.93	4.75	0.23	0.000000464
CURRNTC1	0.78	7.44	0.46	0.000000246
COLSTP_2	0.98	8.90	1.00	0.000002210

Table 81: Summary of low damping signals

Gen ID	Freq	Damping	Rel E	Energy
VALMY_G2	0.98	8.76	0.69	0.000001102
JDA_0304	0.95	8.62	0.36	0.000000278
BRWNL_5	0.99	8.85	0.13	0.000000036
COULEE22	0.88	8.86	1.00	0.000001691
CGS	0.86	7.40	0.31	0.000000216
VALMY_G2	0.87	5.91	0.15	0.000000061
2022 light spring (Note 3), 1.4 GW at Midway bus, 0.5 sec				
VALMY_G2	0.97	5.94	1.00	0.000000150
BRWNL_5	0.97	8.59	0.69	0.000000052
CURRNTC1	0.98	6.73	0.23	0.000000007
SHEER_1	0.96	5.03	0.17	0.000000005
EHUNTER1	0.98	4.16	0.13	0.000000003
CURRNTC1	0.71	8.04	0.16	0.000001956
EHUNTER1	0.79	7.35	0.57	0.000000273
CURRNTC1	0.79	3.28	0.11	0.000000022
DIABLO_1	0.92	7.97	0.40	0.000003106
COLSTP_2	0.95	6.17	0.20	0.000000971
HYATT_1	0.93	4.86	0.12	0.000000529
2022 light spring (Note 4), 1.4 GW at Midway bus, 0.5 sec				
COLSTP_2	0.98	6.16	0.51	0.000000338
VALMY_G2	0.99	6.97	0.49	0.000000279
BRWNL_5	0.97	7.81	0.19	0.000000038
CGS	0.86	8.84	0.33	0.000000321
REV_13G1	0.86	8.54	0.11	0.000000036
DIABLO_1	0.91	8.47	1.00	0.000003962
HYATT_1	0.93	5.16	0.30	0.000000626
JDA_0304	0.95	7.62	0.17	0.000000135
EHUNTER1	0.78	7.49	0.20	0.000000423
CURRNTC1	0.78	6.76	0.15	0.000000275
KMO_13G1	0.72	8.94	0.67	0.000008400
EHUNTER1	0.69	8.73	0.31	0.000002238
CURRNTC1	0.69	8.20	0.27	0.000001712
SJUAN_G1	0.70	8.59	0.16	0.000000623
VALMY_G2	0.69	8.74	0.14	0.000000427
2012 heavy summer, double Palo Verde trip				
MBPP-1	0.35	8.98	0.14	0.000000310
CRAIG_1	0.35	8.50	0.10	0.000000173
BRWNL_5	0.93	8.58	0.15	0.000000004
EHUNTER1	0.92	7.65	0.13	0.000000003
VALMY_G2	0.60	8.49	0.16	0.000000046
REV_13G1	0.51	8.23	0.14	0.000000046
SHEER_1	0.70	8.70	0.12	0.000000003
2012 heavy winter, double Palo Verde trip				
COULEE22	0.96	8.38	0.28	0.000000010
KMO_13G1	0.71	8.44	0.44	0.000000116
VALMY_G2	0.69	8.48	0.37	0.000000093
HAYNES1G	0.70	7.92	0.17	0.000000021
REV_13G1	0.70	7.10	0.14	0.000000015
COLSTP_2	0.84	8.69	0.21	0.000000034
JDA_0304	0.80	8.53	0.13	0.000000016

Table 81: Summary of low damping signals

Gen ID	Freq	Damping	Rel E	Energy
COLSTP_2	0.75	8.44	0.56	0.000000127
CURRNTC1	0.75	8.69	0.40	0.000000074
EHUNTER1	0.73	7.95	0.38	0.000000063
MBPP-1	0.72	6.68	0.28	0.000000041
BRWNL_5	0.72	8.63	0.27	0.000000032
COULEE22	0.76	5.87	0.11	0.000000007
2012 light summer, double Palo Verde trip				
SHEER_1	0.39	8.60	0.24	0.000001583
VALMY_G2	0.38	8.93	0.16	0.000000669
NAVAJO_1	0.39	7.87	0.12	0.000000396
DIABLO_1	0.90	8.94	0.22	0.000000030
HYATT_1	0.66	8.73	0.13	0.000000065
CRAIG_1	0.16	8.82	0.11	0.000000003
HAYNES1G	0.78	7.42	0.30	0.000000032
SLHWKG1	0.79	7.60	0.26	0.000000022
DIABLO_1	0.78	7.46	0.19	0.000000012
VALMY_G2	0.77	7.04	0.18	0.000000013
EHUNTER1	0.78	6.10	0.17	0.000000014
BRWNL_5	0.75	6.34	0.12	0.000000007
2022 heavy winter, double Palo Verde trip				
EHUNTER1	0.61	7.25	0.12	0.000000013
HAYNES1G	0.65	8.70	0.11	0.000000016
JDA_0304	0.74	6.75	0.14	0.000000002
DIABLO_1	0.94	8.66	0.28	0.000000052
SJUAN_G1	0.90	8.33	0.16	0.000000019
2022 light summer, double Palo Verde trip				
REV_13G1	0.93	8.98	0.21	0.000000069
SHEER_1	0.96	6.65	0.11	0.000000022
SJUAN_G1	0.60	8.86	0.19	0.000000133
SLHWKG1	0.59	8.72	0.11	0.000000044
COLSTP_2	0.80	7.85	1.00	0.000000798
REV_13G1	0.81	8.15	0.95	0.000000717
KMO_13G1	0.79	7.66	0.75	0.000000422
CGS	0.80	6.58	0.20	0.000000039
CURRNTC1	0.81	4.80	0.10	0.000000013
KMO_13G1	0.67	7.24	0.12	0.000000142
CGS	0.91	8.52	0.18	0.000000117
COULEE22	0.89	7.67	0.12	0.000000063
KMO_13G1	0.90	7.93	0.10	0.000000052
CURRNTC1	0.73	8.71	0.74	0.000000160
2022 light spring, double Palo Verde trip				
NAVAJO_1	0.16	7.02	0.43	0.000000003
RAWHIDE	0.16	5.18	0.18	0.000000001
MBPP-1	0.51	8.68	1.00	0.000007640
RAWHIDE	0.50	7.66	0.80	0.000005710
CRAIG_1	0.49	7.08	0.32	0.000001126
CRAIG_1	0.52	6.28	0.29	0.000000895
BRIDGER1	0.52	7.87	0.20	0.000000346
RAWHIDE	0.53	4.81	0.15	0.000000326
JDA_0304	0.49	8.62	0.11	0.000000124

Table 81: Summary of low damping signals

Gen ID	Freq	Damping	Rel E	Energy
REV_13G1	0.52	8.75	0.11	0.000000084
HYATT_1	0.71	8.42	0.12	0.000000072
REV_13G1	0.73	8.83	0.12	0.000000073
EHUNTER1	0.71	7.78	0.11	0.000000069
CURRNTC1	0.81	8.97	0.46	0.000000126
KMO_13G1	0.84	6.60	0.35	0.000000103
CGS	0.82	6.23	0.19	0.000000033
COLSTP_2	0.82	4.90	0.19	0.000000039
COULEE22	0.82	4.97	0.13	0.000000020
HYATT_1	0.91	4.98	1.00	0.000000011
COLSTP_2	0.92	3.66	0.72	0.000000008
HAYNES1G	0.94	6.57	0.68	0.000000004
2022 light spring (Note 1), double Palo Verde trip				
CURRNTC1	0.73	7.84	0.17	0.000000686
KMO_13G1	0.44	8.67	0.22	0.000005893
RAWHIDE	0.47	6.42	0.15	0.000003601
MBPP-1	0.48	7.11	0.14	0.000002891
SJUAN_G1	0.45	8.73	0.10	0.000001203
COULEE22	0.90	5.92	1.00	0.000000015
COLSTP_2	0.92	4.86	0.72	0.000000010
HYATT_1	0.92	3.76	0.47	0.000000005
KMO_13G1	0.39	8.29	0.14	0.000000924
BRIDGER1	0.67	8.70	0.20	0.000000330
RAWHIDE	0.68	8.71	0.15	0.000000164
BRWNL_5	0.66	6.10	0.11	0.000000145
NAVAJO_1	0.64	8.66	0.11	0.000000093
VALMY_G2	0.83	8.04	1.00	0.000000033
COLSTP_2	0.82	3.11	0.21	0.000000003
2022 light spring (Note 2), double Palo Verde trip				
BRWNL_5	0.67	7.54	0.22	0.000000187
HYATT_1	0.90	8.41	0.50	0.000000045
DIABLO_1	0.88	5.37	0.40	0.000000045
COULEE22	0.89	5.46	0.20	0.000000012
KMO_13G1	0.30	7.74	0.50	0.000000122
REV_13G1	0.30	8.04	0.44	0.000000099
CRAIG_1	0.32	8.79	0.40	0.000000062
SJUAN_G1	0.34	8.55	0.34	0.000000046
RAWHIDE	0.32	5.67	0.21	0.000000027
EHUNTER1	0.34	7.20	0.18	0.000000016
NAVAJO_1	0.35	7.30	0.14	0.000000010
SHEER_1	0.36	5.78	0.14	0.000000011
HYATT_1	0.34	5.71	0.12	0.000000010
COLSTP_2	0.30	4.49	0.11	0.000000010
KMO_13G1	0.94	7.01	1.00	0.000000012
SHEER_1	0.92	5.05	0.28	0.000000001
SUND#5GN	0.93	3.63	0.12	0.000000000
RAWHIDE	0.45	8.79	0.77	0.000014122
KMO_13G1	0.44	7.68	0.42	0.000004940
REV_13G1	0.44	8.42	0.29	0.000002015
CRAIG_1	0.46	7.31	0.26	0.000001882
RAWHIDE	0.43	7.82	0.20	0.000001203
COULEE22	0.82	5.19	0.53	0.000000039

Table 81: Summary of low damping signals

Gen ID	Freq	Damping	Rel E	Energy
REV_13G1	0.84	5.58	0.39	0.000000019
KMO_13G1	0.83	4.96	0.38	0.000000020
COLSTP_2	0.81	3.65	0.24	0.000000011
DIABLO_1	0.86	2.68	0.16	0.000000007
2022 light spring (Note 3), double Palo Verde trip				
COLSTP_2	0.30	8.72	1.00	0.000000070
COULEE22	0.31	6.56	0.71	0.000000041
BRWNL_5	0.30	6.46	0.55	0.000000027
HYATT_1	0.34	5.42	0.47	0.000000021
SUND#5GN	0.33	1.83	0.39	0.000000036
CGS	0.30	4.12	0.35	0.000000017
SHEER_1	0.32	1.89	0.25	0.000000014
EHUNTER1	0.31	2.57	0.22	0.000000009
CRAIG_1	0.30	0.79	0.16	0.000000010
CURRNTC1	0.32	2.89	0.14	0.000000003
RAWHIDE	0.30	-0.53	0.12	0.000000010
KMO_13G1	0.44	8.95	0.42	0.000008728
SJUAN_G1	0.45	7.90	0.11	0.000000620
EHUNTER1	0.75	7.63	0.59	0.000000443
CURRNTC1	0.75	7.76	0.58	0.000000410
BRWNL_5	0.73	7.18	0.36	0.000000165
SHEER_1	0.73	7.58	0.25	0.000000076
DIABLO_1	0.72	4.58	0.21	0.000000087
HAYNES1G	0.72	5.62	0.16	0.000000045
KMO_13G1	0.40	5.86	0.26	0.000000464
REV_13G1	0.39	5.41	0.11	0.000000099
VALMY_G2	0.37	6.19	0.11	0.000000092
DIABLO_1	0.94	3.81	0.61	0.000000045
HAYNES1G	0.93	5.32	0.60	0.000000030
COULEE22	0.91	6.12	0.42	0.000000013
RAWHIDE	0.48	6.74	1.00	0.000003715
MBPP-1	0.48	7.68	0.94	0.000002876
CRAIG_1	0.47	6.48	0.60	0.000001444
JDA_0304	0.48	8.50	0.40	0.000000486
EHUNTER1	0.48	8.62	0.29	0.000000234
CURRNTC1	0.49	8.03	0.25	0.000000185
SJUAN_G1	0.52	8.38	0.18	0.000000091
KMO_13G1	0.69	8.91	1.00	0.000006745
COLSTP_2	0.67	8.56	0.35	0.000001016
VALMY_G2	0.68	5.88	0.13	0.000000199
2022 light spring (Note 4), double Palo Verde trip				
COULEE22	0.44	7.45	0.36	0.000002371
COULEE22	0.42	6.97	0.25	0.000001142
KMO_13G1	0.72	8.28	0.53	0.000000371
COULEE22	0.70	7.90	0.21	0.000000066
KMO_13G1	0.39	8.18	0.10	0.000000167
SHEER_1	0.75	8.11	0.12	0.000000102
COULEE22	0.61	6.91	0.13	0.000000339
RAWHIDE	0.48	7.46	1.00	0.000005713
MBPP-1	0.47	7.37	0.74	0.000003104
CURRNTC1	0.47	7.90	0.18	0.000000176
VALMY_G2	0.57	8.72	0.10	0.000000089

Table 81: Summary of low damping signals

Gen ID	Freq	Damping	Rel E	Energy
KMO_13G1	0.67	8.61	0.63	0.000002916
CURRNTC1	0.68	8.80	0.25	0.000000435
RAWHIDE	0.69	8.32	0.13	0.000000112
CGS	0.30	7.74	0.13	0.000000024
SJUAN_G1	0.34	7.33	0.38	0.000000039
CGS	0.36	7.34	0.30	0.000000024
NAVAJO_1	0.34	8.22	0.25	0.000000015
BRIDGER1	0.34	4.77	0.17	0.000000012
RAWHIDE	0.34	2.42	0.12	0.000000012
MBPP-1	0.35	2.46	0.12	0.000000010
EHUNTER1	0.78	8.04	1.00	0.000000139
BRIDGER1	0.80	7.87	0.46	0.000000029
COULEE22	0.79	5.66	0.38	0.000000028
KMO_13G1	0.81	4.81	0.36	0.000000029
CGS	0.80	4.05	0.15	0.000000007
COLSTP_2	0.79	3.26	0.14	0.000000007

Appendix F - Frequency Nadir

Table 82: Frequency Nadir for Different Stimulus

WECC Case	Freq Nadir	Time
2012 heavy summer, 1.4 GW at Chief Joseph brake, 0.5 sec	59.97711	10.50
2012 heavy winter, 1.4 GW at Chief Joseph brake, 0.5 sec	59.97334	10.50
2012 light summer, 1.4 GW at Chief Joseph brake, 0.5 sec	59.97354	10.50
2022 heavy winter, 1.4 GW at Chief Joseph brake, 0.5 sec	59.97948	10.50
2022 light summer, 1.4 GW at Chief Joseph brake, 0.5 sec	59.97385	10.50
2022 light spring, 1.4 GW at Chief Joseph brake, 0.5 sec	59.96781	10.50
2022 light spring (Note 1), 1.4 GW at Chief Joseph brake, 0.5 sec	59.97005	10.50
2022 light spring (Note 2), 1.4 GW at Chief Joseph brake, 0.5 sec	59.96953	10.50
2022 light spring (Note 3), 1.4 GW at Chief Joseph brake, 0.5 sec	59.96932	10.50
2022 light spring (Note 4), 1.4 GW at Chief Joseph brake, 0.5 sec	59.96929	10.50
2012 heavy summer, 1.4 GW at El Dorado bus, 0.5 sec	59.98266	10.50
2012 heavy winter, 1.4 GW at El Dorado bus, 0.5 sec	59.97915	10.50
2012 light summer, 1.4 GW at El Dorado bus, 0.5 sec	59.97422	10.50
2022 heavy winter, 1.4 GW at El Dorado bus, 0.5 sec	59.98123	10.50
2022 light summer, 1.4 GW at El Dorado bus, 0.5 sec	59.97573	10.50
2022 light spring, 1.4 GW at El Dorado bus, 0.5 sec	59.96976	10.50
2022 light spring (Note 1), 1.4 GW at El Dorado bus, 0.5 sec	59.97321	10.50
2022 light spring (Note 2), 1.4 GW at El Dorado bus, 0.5 sec	59.97238	10.50
2022 light spring (Note 3), 1.4 GW at El Dorado bus, 0.5 sec	59.97306	10.50
2022 light spring (Note 4), 1.4 GW at El Dorado bus, 0.5 sec	59.97292	10.50
2012 heavy summer, 1.4 GW at Hemingway Bus, 0.5 sec	59.98289	10.50
2012 heavy winter, 1.4 GW at Hemingway Bus, 0.5 sec	59.98105	10.50
2012 light summer, 1.4 GW at Hemingway Bus, 0.5 sec	59.97445	10.50
2022 heavy winter, 1.4 GW at Hemingway Bus, 0.5 sec	59.97974	10.50
2022 light summer, 1.4 GW at Hemingway Bus, 0.5 sec	59.97317	10.50
2022 light spring, 1.4 GW at Hemingway Bus, 0.5 sec	59.96713	10.50
2022 light spring (Note 1), 1.4 GW at Hemingway Bus, 0.5 sec	59.96988	10.50
2022 light spring (Note 2), 1.4 GW at Hemingway Bus, 0.5 sec	59.96945	10.50
2022 light spring (Note 3), 1.4 GW at Hemingway Bus, 0.5 sec	59.96931	10.50
2022 light spring (Note 4), 1.4 GW at Hemingway Bus, 0.5 sec	59.96934	10.50
2012 heavy summer, 1.4 GW at Midway bus, 0.5 sec	59.98408	10.50
2012 heavy winter, 1.4 GW at Midway bus, 0.5 sec	59.98117	10.50
2012 light summer, 1.4 GW at Midway bus, 0.5 sec	59.97737	10.50
2022 heavy winter, 1.4 GW at Midway bus, 0.5 sec	59.98254	10.50
2022 light summer, 1.4 GW at Midway bus, 0.5 sec	59.97739	10.50
2022 light spring, 1.4 GW at Midway bus, 0.5 sec	59.96964	10.95
2022 light spring (Note 1), 1.4 GW at Midway bus, 0.5 sec	59.97460	10.88
2022 light spring (Note 2), 1.4 GW at Midway bus, 0.5 sec	59.97344	10.95
2022 light spring (Note 3), 1.4 GW at Midway bus, 0.5 sec	59.97445	10.97
2022 light spring (Note 4), 1.4 GW at Midway bus, 0.5 sec	59.97355	10.97
2012 heavy summer, double Palo Verde trip	59.81658	19.40
2012 heavy winter, double Palo Verde trip	59.77482	18.86
2012 light summer, double Palo Verde trip	59.71314	20.16
2022 heavy winter, double Palo Verde trip	59.82865	18.19
2022 light summer, double Palo Verde trip	59.74212	19.83
2022 light spring, double Palo Verde trip	59.69335	17.65
2022 light spring (Note 1), double Palo Verde trip	59.74912	17.58
2022 light spring (Note 2), double Palo Verde trip	59.69532	18.81
2022 light spring (Note 3), double Palo Verde trip	59.74408	17.88
2022 light spring (Note 4), double Palo Verde trip	59.68789	18.95

Appendix G - Transient Stability: Generator Speeds

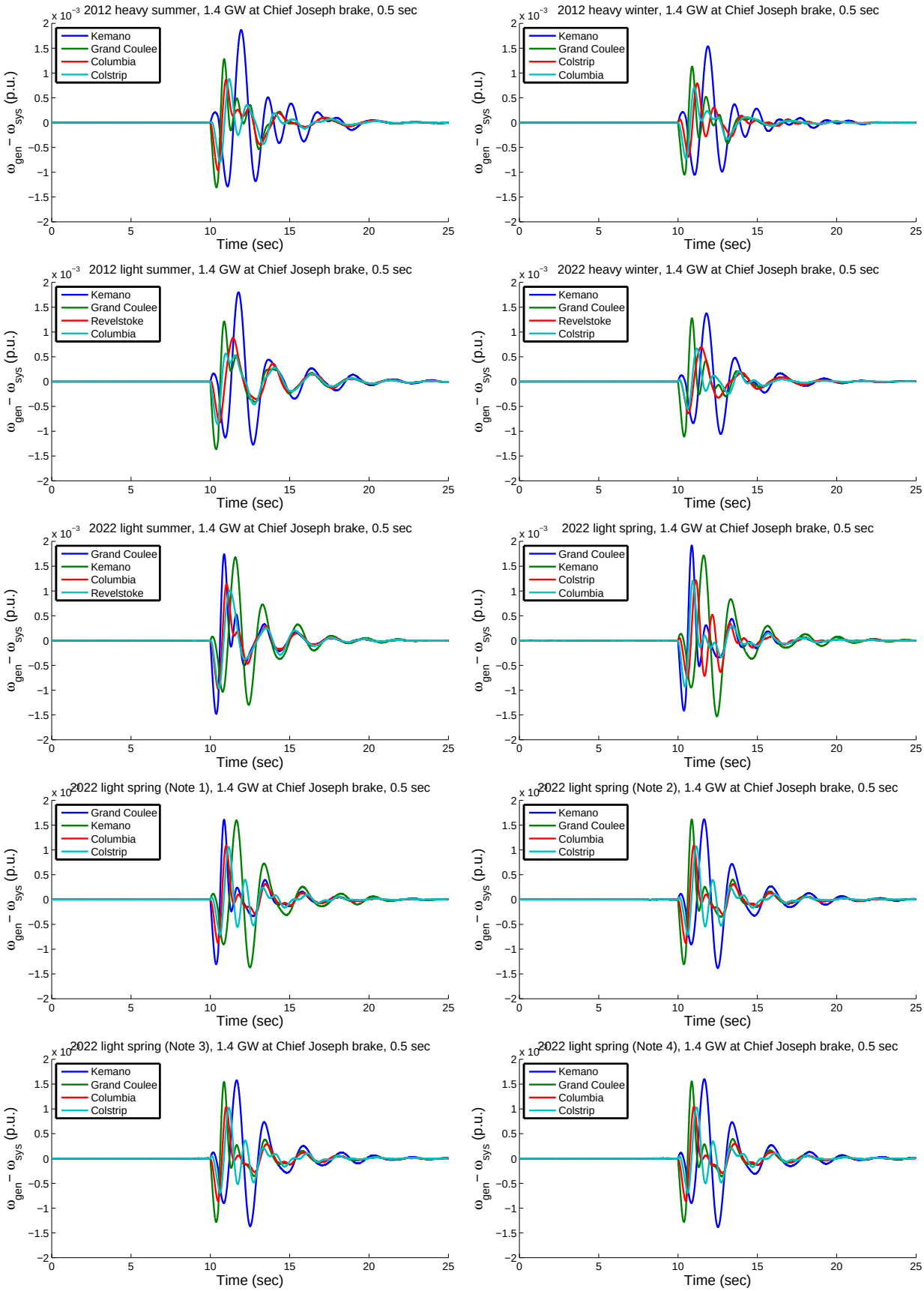

Figure 45: Maximum speed error relative to system speed. 1.4 GW Chief Joseph brake insertion for 0.5 seconds.

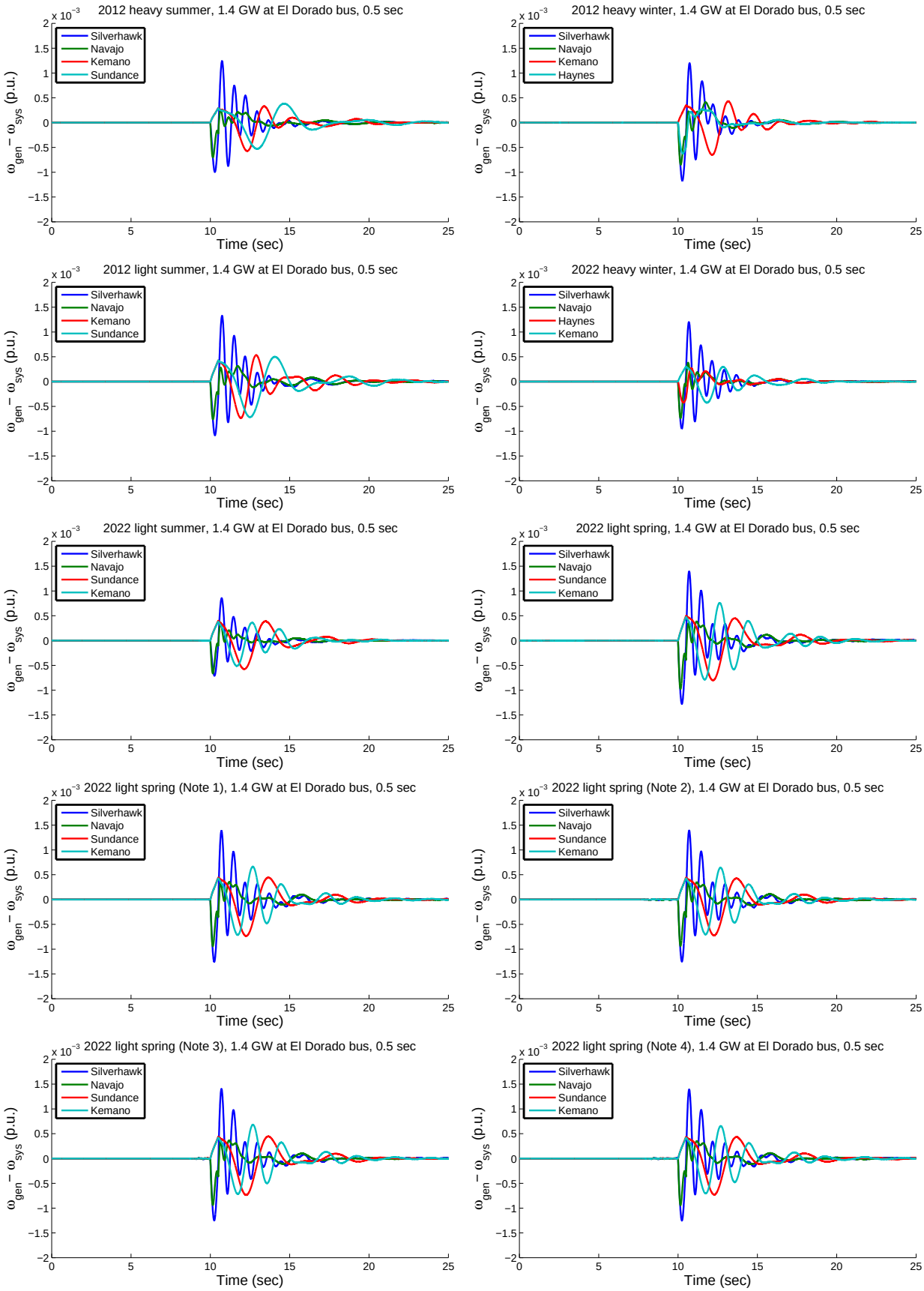

Figure 46: Maximum speed error relative to system speed. 1.4 GW brake insertion on the El Dorado bus for 0.5 seconds.

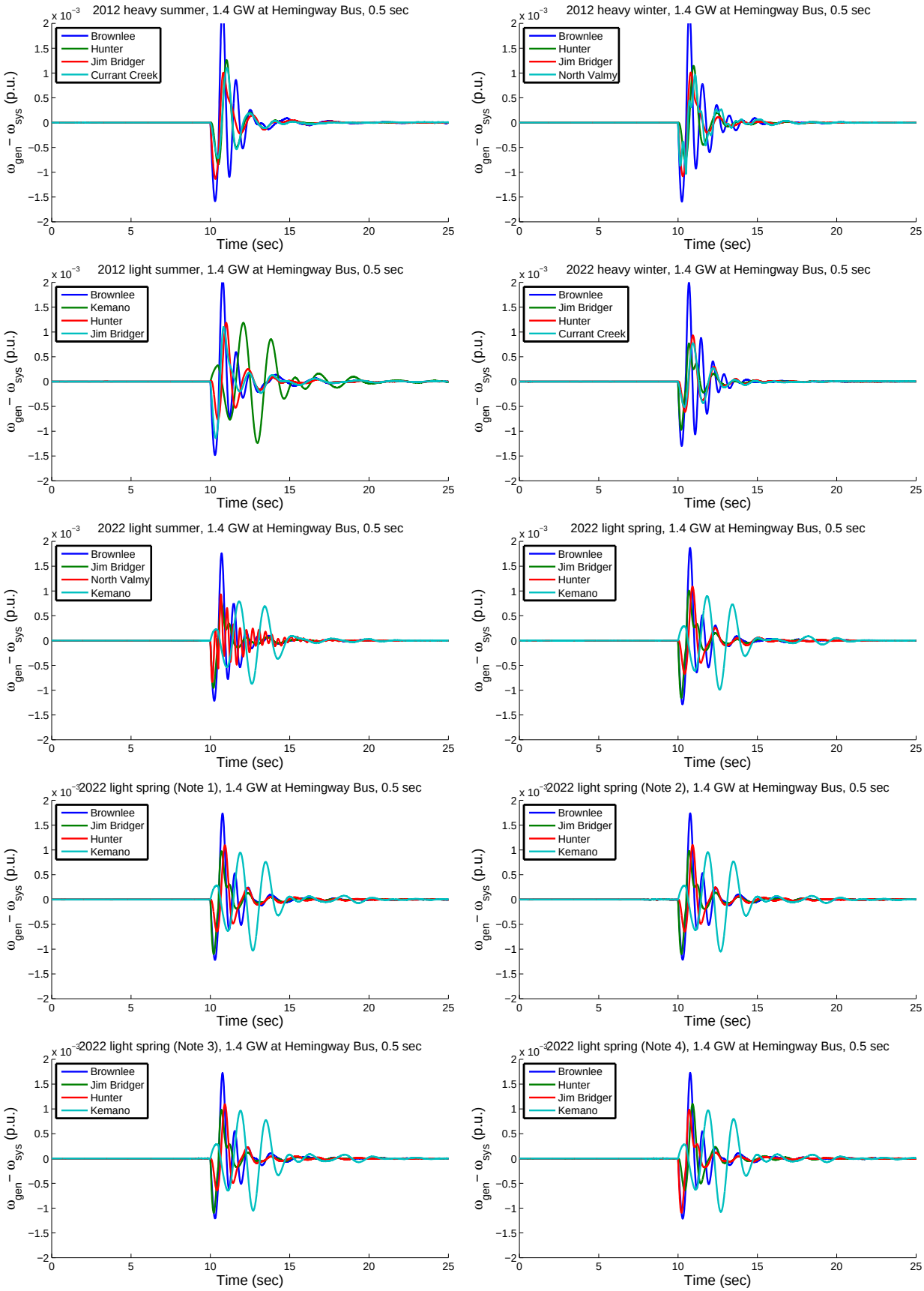

Figure 47: Maximum speed error relative to system speed. 1.4 GW brake insertion on the Hemingway bus for 0.5 seconds.

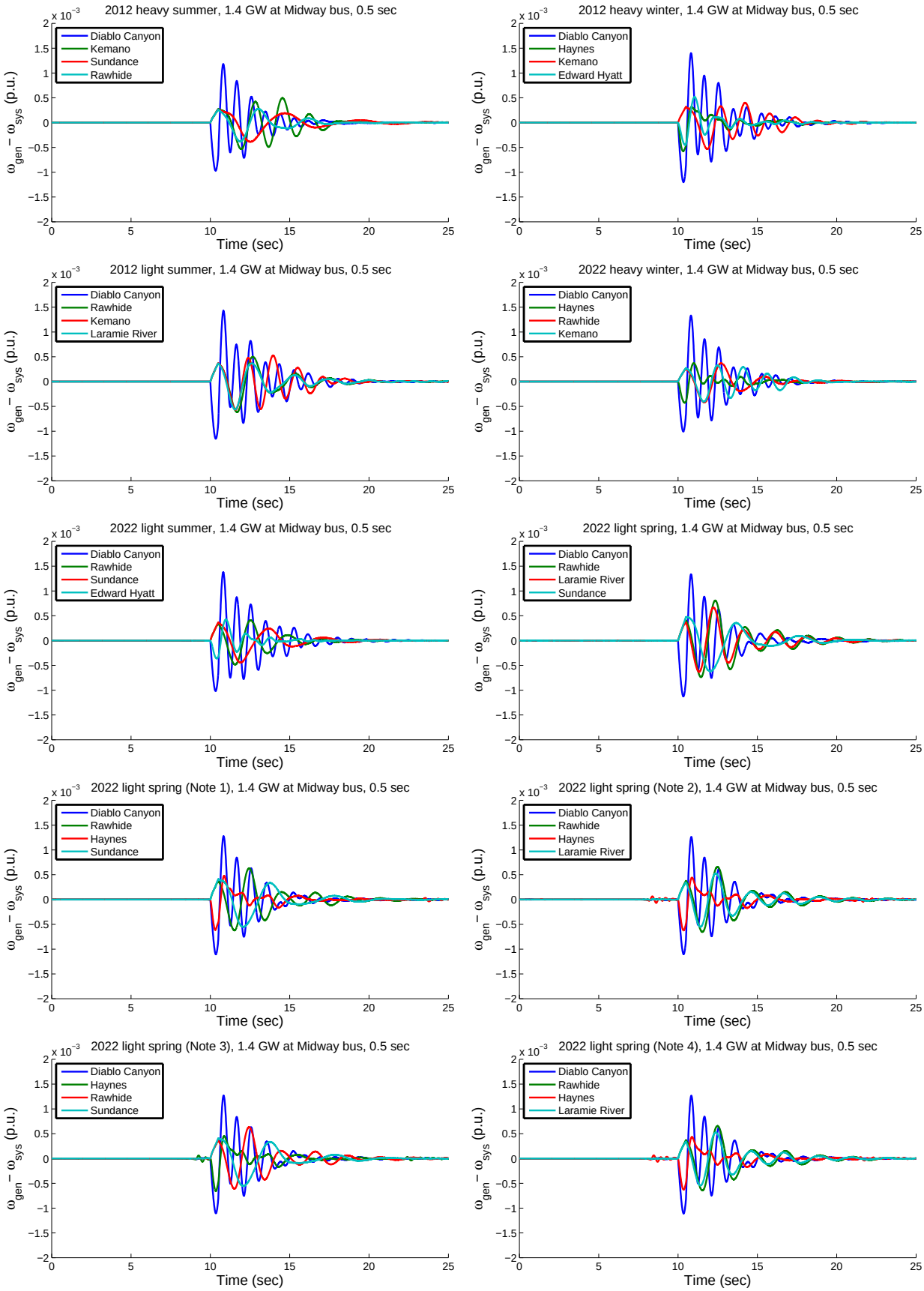

Figure 48: Maximum speed error relative to system speed. 1.4 GW brake insertion on the Midway bus for 0.5 seconds.

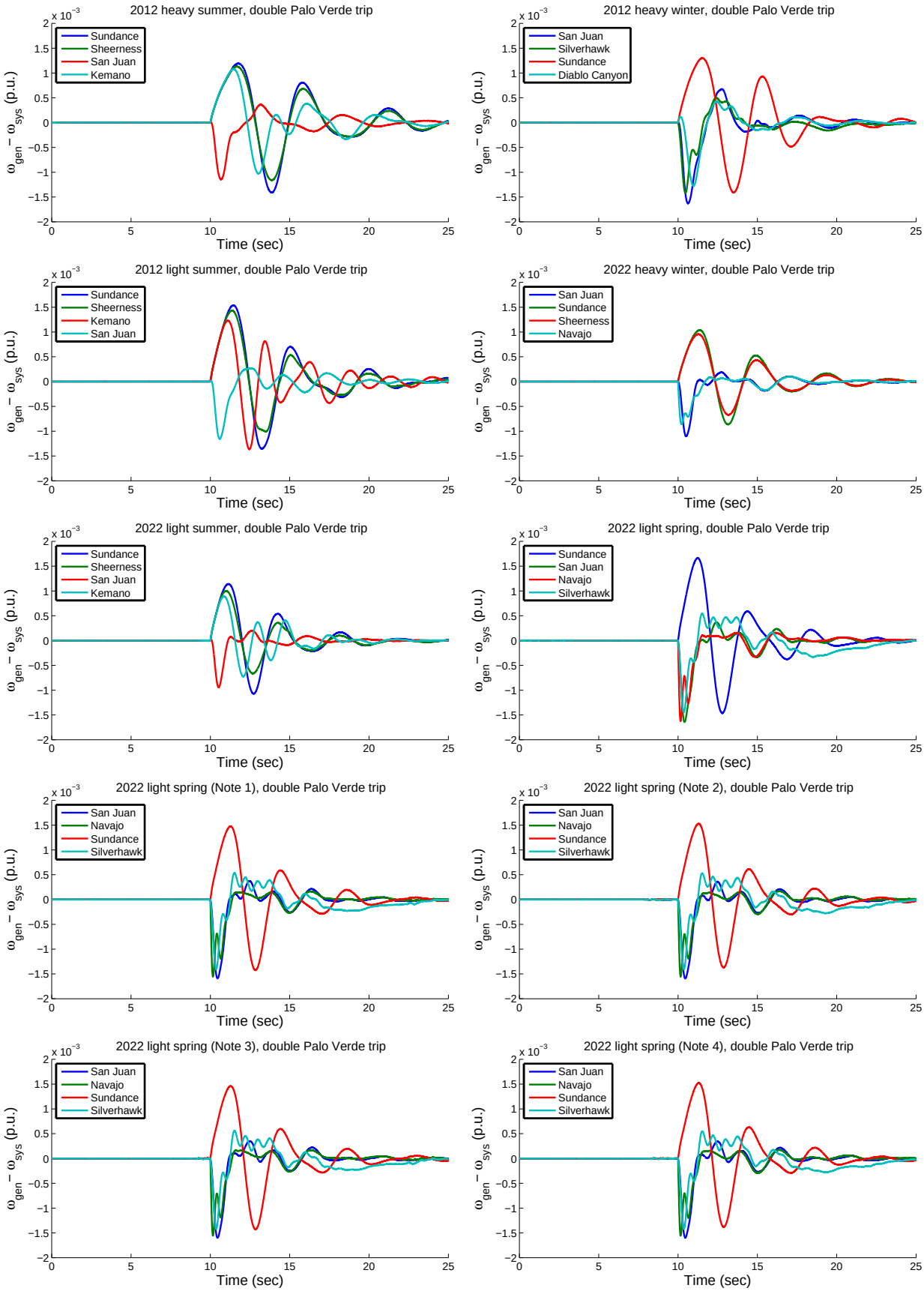

Figure 49: Maximum speed error relative to system speed. Double Palo Verde trip. Note that the remaining Palo Verde generator was not considered because of the close proximity to the contingency.

DISTRIBUTION:

1 Gil Bindewald
Office of Electricity Delivery and Energy Reliability
U.S. Dept. of Energy
Washington, DC 20585

1 Phil Overholt
Office of Electricity Delivery and Energy Reliability
U.S. Dept. of Energy
Washington, DC 20585

1 Dr. Dan Trudnowksi
Montana Tech University
Electrical Engineering Department
1300 W. Park Street
Butte, MT 59701

1 Dr. Matt Donnelly
Montana Tech University
Electrical Engineering Department
1300 W. Park Street
Butte, MT 59701

1 Dr. Dmitry Kosterev
Bonneville Power Administration
P.O. Box 3621
Portland, OR 97208-3621

1 MS 1104 Rush D. Robinett, 6110
1 MS 0124 Robert Q. Hwang, 8004
1 MS 1140 Ross Guttromson, 6113
1 MS 1152 Steven F. Glover, 1654
1 MS 1033 Charles J. Hanley, 6112
1 MS 1152 Jason C. Neely, 1654
1 MS 1140 Raymond H. Byrne, 6113
1 MS 1140 César A. Silva-Monroy, 6113
1 MS 1140 David A. Schoenwald, 6113
1 MS 1140 Georgianne Huff, 6113
1 MS 1140 Ryan T. Elliott, 6113
1 MS 1108 Dan R. Borneo, 6111
1 MS 1124 David G. Wilson, 6122
1 MS 1033 Abraham Ellis, 6112

1 MS 0899 Technical Library, 9536 (electronic copy)

Sandia National Laboratories